Lecture Notes in Control and Information Sciences

409

Yuanqing Xia
Mengyin Fu
Guo-Ping Liu

Analysis and Synthesis of Networked Control Systems

Lecture Notes
in Control and Information Sciences 409

Editors: M. Thoma, F. Allgöwer, M. Morari

Yuanqing Xia, Mengyin Fu, and Guo-Ping Liu

Analysis and Synthesis of Networked Control Systems

Springer

Authors

Prof. Dr. Yuanqing Xia

Beijing Institute of Technology
Department of Automatic Control
100086 Beijing
China
E-mail: xia_yuanqing@bit.edu.cn

Prof. Dr. Guo-Ping Liu

University of Glamorgan
Faculty of Advanced Technology
Cardiff CF 37 1DL
Pontypridd
UK
E-mail: gpliu@glam.ac.uk

Prof. Dr. Mengyin Fu

Beijing Institute of Technology
Department of Automatic Control
100086 Beijing
China
E-mail: fumy@bit.edu.cn

ISBN 978-3-642-17924-2 e-ISBN 978-3-642-17925-9

DOI 10.1007/978-3-642-17925-9

Lecture Notes in Control and Information Sciences ISSN 0170-8643

Typeset & Cover Design: Scientific Publishing Services Pvt. Ltd., Chennai, India.

Printed in acid-free paper

5 4 3 2 1 0

springer.com

The Internet is changing the way of life

The Internet will change the way of control

For researchers devoted to Networked Control Systems

Preface

In the last decade, network technology has dramatically been developed. Recently, more and more network technologies have been applied to control systems. Now, networked control is a new area in control systems. Particularly, Internet based control systems allow remote monitoring and adjustment of plants over the Internet, which makes the control systems benefit from the ways of retrieving data and reacting to plant fluctuations from anywhere around the world at any time. The networked control has also opened up a complete new range of real-world applications, namely tele-manufacturing, tele-surgery, museum guidance, traffic control, space exploration, disaster rescue, and health care. In recent years, the techniques of Internet of Things are developed rapidly, the research of networked control systems (NCSs) plays a key role in Internet of Things.

In NCSs, the plant, controller, sensor, actuator and reference command are connected through networks. As the structure of NCSs is different from that of tradition control systems, there exist various specific problems in NCSs, for example, quantization, network delay, loss of data packets, network security and safety. Therefore, analysis and synthesis of NCSs are of great importance.

The first chapter of this book is an overview of recent development of NCSs, which is concluded in Chapter 1.

Then, this book will present four parts:

Part I: Some development of quantization has been introduced and new results on quantization over networks are given. In Chapter 2, a simple quantization strategy is proposed and the feedback control is designed based on quantized estimated states sent through network. In Chapter 3, the problem of the mean square stability of linear discrete systems with quantization and packet dropout is considered. The quantizer used in this chapter is uniform quantizer and the packet dropout rate is important to the performance of system. The Lyapunov method and "zoom" strategy are used to guarantee the mean square stability of the discrete linear systems. In Chapter 4, the stability of a quantized system is considered, which is based on a quantized input computed from quantized measurements. The problem of globally

asymptotic stability of the system is transferred to the one of an equivalent system depending on a multiplier which is nonnegative and boundness. It is the focus of this chapter to discuss the nonnegative and boundness of multiplier. A sufficient condition is given for the globally asymptotic stability of the system.

Part II: New results on data fusion over networks are presented. In Chapter 5, the method of the state estimation algorithm in single channel is extended to multi-channel. Each channel is with a different packet arrival statistics. The arrival process via a random variable is modeled and two different data fusion architectures with finite buffer are proposed. The optimal state estimation for a kind of linear dynamic systems with the observations obtained asynchronously with multiple rates is concerned in Chapter 6, where the observations may lose randomly. For each sensor, a rule is proposed to check out whether the measurement is missing. With the help of the modified Kalman filter, the multiscale system theory and the federated square root filter, the optimal state estimate is obtained at the highest sampling rate given.

Part III: Most work have ignored another important feature of NCSs. This feature is that the communication networks can transmit a packet of data at the same time, which is not done in traditional control systems. Therefore, in Chapter 7, the network feature is made full use of and a new networked predictive control scheme is proposed, which can overcome the effects caused by network data dropout modeled as Markov chain. In Chapter 8, an optimal estimation method is proposed to overcome the time delay and data dropout in the feedback channel. There is a buffer to store the data from the sensor and the length of the buffer can be set to store the data in this step and before.

Part IV: With the development of NCSs, the research of fault detection over networks is of great interest. In Chapter 9, a more general case that the fault detection center is neither located at the controller node nor located at the plant node is considered, all the input data and measurement data are transmitted from the actuator node and the sensor node to the fault detection center, respectively, over unreliable networks with bounded packet loss. The bounded packet loss is modeled in two ways: arbitrary packet loss process and Markovian packet loss process. The stability analysis of the error system and the design of fault detection filter (FDF) gains are given to satisfy some performance constraints. In Chapter 10, a fault detection and compensation scheme based likelihood ratios for networked predictive control systems with random time delay and clock asynchronism is considered. A predictive control scheme based on state observer is designed to compensate the network-induced time delay. The measured outputs of plant are sent back to the local node with a buffer. The likelihood ratios of fault are computed, and if a fault is detected and identified, the estimate of the fault is sent to the controller to compensate the fault.

We would like to acknowledge the collaborations with Dr. Liping Yan on the work of multisensor data fusion reported in the monograph and PH.D

candidates: Jizong Shang, Jingjing Yan, Cui Zhu, Ge Wang, Xiaoyun Wang, Bo Liu, Hongjiu Yang and Li Li for their great contribution in this monograph. The supports from the National Natural Science Foundation of China under Grant (60974011), Program for New Century Excellent Talents in University of Peoples Republic of China (NCET-08-0047), the Ph.D. Programs Foundation of Ministry of Education of China (20091101110023), and Program for Changjiang Scholars and Innovative Research Team in University, and Beijing Municipal Natural Science Foundation (4102053), respectively, are gratefully acknowledged.

July 2010

Haidian District, Beijing, China, Yuanqing Xia
Haidian District, Beijing, China, Mengyin Fu
Trefforest, Glamorgan, UK, Guo-Ping Liu

Symbols and Acronyms

A	system matrix
A^{-1}	inverse of matrix A
A^T	transpose of matrix A
$A \geq 0$	symmetric positive semi-definite
$A > 0$	symmetric positive definite
$A \leq 0$	symmetric negative semi-definite
$A < 0$	symmetric negative definite
C	field of complex numbers
C_i	measurement matrix
$\det(A)$	determinant of matrix A
$\text{diag}(X_1, X_2, \cdots, X_m)$	diagonal matrix with X_i as its ith diagonal element
I	identity matrix
lim	limit
LMI	linear matrix inequality
$P(k\|k)$	the covariance of $\tilde{x}(k\|k)$
$P_i(k\|k)$	the covariance of $\tilde{x}_i(k\|k)$
$P_N(k\|k)$	the estimation error covariance of $x(k)$ based on Sensor N under the ideal assumption that without any measurements missing.
$P_{N\|i}(k\|k)$	the covariance of $\tilde{x}_{N\|i}(k\|k)$
$P_{N\|ij}(k\|k)$	the cross-covariance between $\tilde{x}_{N\|i}(k\|k)$ and $\tilde{x}_{N\|j}(k\|k)$
$\text{rank}(A)$	rank of matrix A
R	field of real numbers
R^n	n-dimensional real Euclidean space
$R^{n\times m}$	space of $n \times m$ real matrices
$\text{sgn}(x)$	the sign of x
S_i	the sampling rate of Sensor i
$\text{tr}(A)$	trace of matrix A
T	the sampling interval of Sensor N
$0_{n\times m}$	zero matrix of dimension $n \times m$
$\lambda(A)$	eigenvalue of matrix A
$\lambda_{\min}(A)$	minimum eigenvalue of matrix A

$\lambda_{\max}(A)$	maximum eigenvalue of matrix A
$\sigma(A)$	singular value of matrix A
$\sigma_{\min}(A)$	minimum singular value of matrix A
$\sigma_{\max}(A)$	maximum singular value of matrix A
$\|x\|$	absolute value (or modulus) of x
$\|\|x\|\|$	Euclidean norm
$\|\|P\|\|$	induced norm $\sup_{\|\|x\|\|=1} \|\|Px\|\|$
$\forall$	for all
$\in$	belong to
$\rightarrow$	tend to, or mapping to (case sensitive)
$\otimes$	matrix Kronecker product
$\sum$	sum
$\mathcal{E}\{\cdot\}$	mathematical expectation operator
$\Sigma(k)$	an $nN \times nN$ matrix, whose ij-th block is $P_{N\|ij}(k\|k)$
sup	supremum
inf	infimum
$A \perp B$	$E\{AB^T\} = 0$
δ_{kj}	Kronecker delta function
$x(k)$	the state variable vector at time kT
$w(k)$	process noise, meet $N(0, Q)$
$x_i(k)$	the state variable vector at Scale i
$y_i(k)$	the k-th measurement observed by Sensor i
$\gamma_i(k)$	a stochastic sequence that takes values on 1 and 0 with Bernoulli distribution, which is used to describe the missing of measurements of Sensor i
$v_i(k)$	measurement noise, meet $N(0, R_i)$
$\hat{x}(k\|k)$	the estimation of $x(k)$ based on the measurements observed by all the sensors before time kT
$\hat{x}_i(k\|k)$	the estimation of $x_i(k)$ based on the first to the k-th measurements of Sensor i
$\hat{x}_{N\|i}(k\|k)$	the estimation of $x(k)$ based on the measurements of Sensor i observed before time kT
$\tilde{x}(k\|k)$	the estimation error of $\hat{x}(k\|k)$
$\tilde{x}_i(k\|k)$	the estimation error of $\hat{x}_i(k\|k)$
$\tilde{x}_{N\|i}(k\|k)$	the estimation error of $\hat{x}_{N\|i}(k\|k)$

Contents

Chapter 1
Introduction

1.1 Background

With the emergence of high speed network technology that allows a cluster of devices to be linked together economically to form distributed networks which are capable of remote data transmission and data exchanges, distributed control systems based on networks are increasing rapidly in various applications([83, 84]). Due to the use of networks, the complexity and the cost of distributed control systems are reduced greatly and the maintenance of the systems becomes much easier ([229]). Because of these attractive benefits, many industrial companies and institutes have shown great interest in applying various networks to remote control systems and manufacturing automation. As a result of extensive research and development, several network protocols for industrial control have been released, such as industrial Ethernet, ControlNet, and DeviceNet.

The further expansion of the Internet and rapid development of wireless network technology will no doubt lead to even wider applications of control systems through networks. Through a real-time network, a feedback control system can be seen as a NCSs ([189]) which includes fieldbus control systems constructed on the basis of bus technology (e.g., DeviceNet, ControlNet and LonWorks) and Internet based on control systems using general computer networks. NCSs are completely distributed real-time feedback control systems, which are integration of sensors, controllers, actuators and communication networks. The frame diagram of NCSs can be shown as Fig. 1.1.

The NCSs provide data transmission between devices to ensure that the users of different sites can realize resource sharing and coordinating manipulation, reduce system wiring, make system diagnosis and increase system flexibility. But, the insertion of the communication network in the feedback control loop makes the analysis and design of NCSs complex. Conventional control theories with many ideal assumptions, such as synchronized control and non-delayed sensing and actuation, must be re-evaluated before they are applied to NCSs.

Y. Xia, M. Fu, and G.-P. Liu: Analysis and Synthesis of NCSs, LNCIS 409, pp. 1–11.
springerlink.com

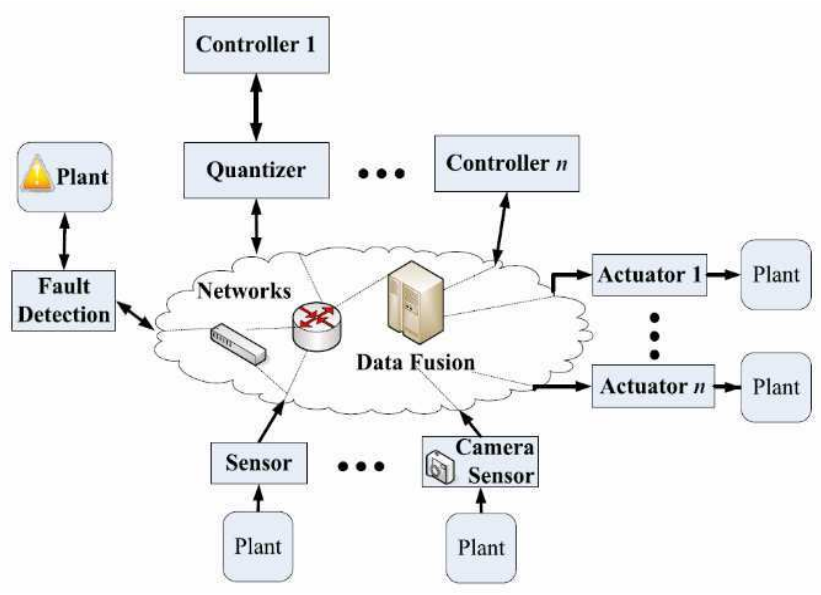

Fig. 1.1 Networked control system.

1.2 Internet of Things

In recent years, the Internet of Things is a hot research area. It is a technological revolution that represents the future of computing and communications, and its development depends on dynamic technical innovation in a number of important fields, from wireless sensors to nano-technology. NCSs play a key role in the Internet of Things.

1.2.1 The Origin of Internet of Things

Over a decade ago, the late Mark Weiser developed a seminal vision of future technological ubiquity-one in which the increasing "availability" of processing power would be accompanied by its decreasing "visibility". As he observed, "the most profound technologies are those that disappear...they weave themselves into the fabric of everyday life until they are indistinguishable from it". Early forms of ubiquitous information and communication networks are evident in the widespread use of mobile phones: the number of mobile phones worldwide surpassed 2 billion in mid-2005. These little gadgets have become an integral and intimate part of everyday life for many millions of people. Today, developments are rapidly under way to take this phenomenon an important step further, by embedding short-range mobile transceivers into a wide array of additional gadgets and everyday items, enabling new forms of

communication between people and things, and between things themselves. A new dimension has been added to the world of information and communication technologies: from anytime, any place connectivity for anyone, we will now have connectivity for anything.

1.2.2 The Definition of Internet of Things

Connections will multiply and create an entirely new dynamic network of networks-an Internet of Things. The Internet of Things is neither science fiction nor industry hype, but is based on solid technological advances and visions of network ubiquity that are zealously being realized. Furthermore, the technologies of the Internet of Things offer immense potential to consumers, manufacturers and firms. The Internet of Things refers to a network of objects, such as household appliances. It is often a self-configuring wireless network. The concept of the Internet of Things is attributed to the original Auto-ID Center, founded in 1999 and based at the time in Massachusetts Institute of Technology. If all cans, books, shoes or parts of cars are equipped with minuscule identifying devices, daily life on our planet will undergo a transformation. Things like running out of stock or wasted products will no longer exist as we will know exactly what is being consumed on the other side of the globe. Theft will be a thing of the past as we will know where a product is at all times. The same applies to parcels lost in the post.

1.2.3 The Meaning of Internet of Things

In Internet of Things, NCSs play a key role. First, in order to connect everyday objects and devices to large databases and networks- and indeed to the network of networks (the internet)-a simple, unobtrusive and cost-effective system of item identification is crucial. Only then can data about things be collected and processed. Radio-frequency identification offers this functionality. Second, data collection will benefit from the ability to detect changes in the physical status of things, using sensor technologies. Embedded intelligence in the things themselves can further enhance the power of the network by devolving information processing capabilities to the edges of the network. Finally, advances in miniaturization and nano-technology mean that smaller and smaller things will have the ability to interact and connect. A combination of all of these developments will create an Internet of Things that connects the world's objects in both a sensory and an intelligent manner. The Internet of Things will draw on the functionality offered by all of these technologies to realize the vision of a fully interactive and responsive network environment. Fig. 1.2 shows the future applications of the Internet of Things.

Fig. 1.2 Internet of Things.

1.3 Main Issues

Specifically, the following issues need to be addressed ([130, 188, 225]).

1) The network-induced delay (sensor-to-controller delay and controller-to-actuator delay) occurs while exchanging data among devices connected to the shared network, which will be either constant (up to jitter) or time varying, can degrade the performance of control systems designed without considering the delay and can even destabilize the system([201, 117, 200]).

2) The network can be viewed as a web of unreliable transmission paths. Some packets not only suffer transmission delay but, even worse, can be lost during transmission. Thus, how such packet dropouts affect the performance of a NCS is an issue that must be considered([224, 207]).

3) The plant outputs may be transmitted using multiple network packets (so-called multiple packet transmission) due to the bandwidth and packet size constraints of the network. Only a part or none of the packets could arrive on the controller side because of the arbitrariness of the network medium with other nodes on the network([138, 77]).

4) Stability and robustness analysis for NCSs is challenging since the network delay varies with network topology, network protocol, network load, network bandwidth and package size and its value may be bounded, unbounded, time-varying, constant or random([116, 107, 112, 199, 111]). There also exist several uncertainties in NCSs, e.g., external disturbance, modeling

error, system dynamics change. Up to date, some research results have been obtained in stability and robustness analysis of systems.

The problem of robust stabilization for uncertain systems with time-delay has been dealt using a number of different approaches, for example, the Riccati equation approaches, linear matrix inequality (LMI) approaches, and the Lyapunov min-max approaches. In particular, several approaches are applied to solve the problems arising in networked linear control systems.

1.4 Methods

Generally speaking, there are three types of NCS methods:

Type 1 – scheduling methods that guarantee network QoS (quality of service);

Type 2 – control methods that guarantee system QoP(quality of performance);

Type 3 – integrating scheduling and control methods that consider both QoS and QoP.

For Type 1, the following scheduling methods have been developed: scheduling method MEF (Maximum-Error-First) based on MATI (Maximal-Allowable-Transfer-Interval) ([189]), a scheduling protocol P-CSMA/CA (Prioritized -CSMA-CA) based on IEEE 802.11 wireless standard ([216]), and a sampling time scheduling method of network bandwidth allocation and sampling period decision for multi-loop NCSs in virtue of the notion "window", namely the service window of each transmission data in network ([73]).

For Type 2, there are many control methods developed for NCS, for example, augmented deterministic discrete-time model method ([64]), Queuing method ([114]), optimal control method ([130, 113]), perturbation method ([189]), robust control method ([60, 220]), fuzzy logic modulation method ([3]), event-based method ([177]), end-user control adaptation method ([183]), control under data rate constrains method([41, 126]).

For Type 3, the following problems have been studied: the optimal sampling period selection problem for a set of digital controllers ([162]), the sampling period optimization problem under the schedulability constraints ([147]), the optimal scheduling problem under both RM-schedulability constraints and NCS stability constraints ([229]), and the NCS analysis and simulation problem solved by two Matlab-based toolboxes: Jitterbug and TrueTime (http://www.control.lth.se/ anton/, 2003).

In addition, the stability problem of closed-loop NCS in the presence of network delays and data packet drops has been addressed in ([229]). The stability problem of NCSs with stochastic protocols and channels has been studied in ([175]). The problem of observer and robust state estimation has been

addressed in ([153, 151]). To reduce network traffic load, a sampled-data NCS scheme has been presented and some necessary and sufficient conditions for global exponential stability of the closed-loop systems via state/output feedback without/with network delays have been established in ([121]). Some issues related to network bandwidth constraints and network traffic congestion in NCSs have been studied in ([1, 65, 197]). Internet based control has also been considered for practical applications, for example, Internet-based process control ([148]), Internet-based control system as a control device ([34]), Internet robots ([179]), Internet based multimedia education ([129]), process monitoring and optimization via the web ([127]) and game-theoretic treatment of distributed power control in CDhlA wireless systems using outage probabilities([5]).

1.5 Problems Studied in This Book

The following four major issues for NCSs will be studied in this book: quantization, data fusion, predictive control and fault detection. In fact, because of the joint of network, the signals are necessary to be quantized before they are sent to the network. After the data are transmitted through network, the method of data fusion can be used to fuse the data to reduce the burden of respondents and avoid bias, then predictive control is adopted to deal with data losses and asynchronous measurement sampling in the control system, the last and necessary step is fault detection, which is used to detect fault and make a binary decision-either that something has gone wrong or that everything is fine. Therefore, quantization, data fusion, predictive control and fault detection are the main four issues in NCSs.

1.5.1 Quantization over Networks

Control using quantized feedback has been an important research area for a long time. A quantizer is a function that maps a real-valued function into a piecewise constant function taking on a finite set of values. At present, there exist two kinds of quantizers, which are uniform quantizers and logarithmic ones. As for uniform quantizer, which maps real-valued function to a finite number of quantization regions with rectilinear shape ([17]) or arbitrary shape ([100]). The study of system affected by uniform quantizer is always basing on "zoom" strategy , which is usually composed of two stages, i.e. "zooming-out" and "zooming-in". In first stage, the range of quantizer is increased to guarantee the states of system can be adequately measured. In second stage, the quantization error is decreased to drive the states to the origin. When system is affected by logarithmic quantizer, in which the quantization levels are linear in logarithmic scale, the simple classical approach to analysis and mitigation of quantization effects is to treat the quantization error as uncertainty or nonlinearity and bound it using a sector bound ([51]). The

main problem about quantization is to find a quantized feedback control law to stabilize the given system which can be stabilized by linear time-invariant feedback.

There is a new line of research on quantized feedback control where a quantizer is regarded as an information coder. The fundamental question of interest is how much information needs to be communicated by the quantizer in order to achieve a certain control objective. The problem of quadratic stabilization of discrete linear systems using quantized feedback is studied in [40]. It is proved that for a quadratically stabilizable system, the quantizer needs to be logarithmic, which means that the quantization levels are linear in logarithmic scale. Furthermore, the coarsest quantization density is given explicitly in terms of the system's unstable poles. Note that the required quantizer has an infinite number of quantization levels because of its time-invariance nature. When a finite number of quantization levels are available, the so-called practical stability is obtained where there is a region of attraction in the state and the steady state converges to a small limit cycle. In a different point of view ([17]), the number of quantized values is treated as being fixed a priori, but it allows to alter other quantization parameters while the system evolves. This approach enables to achieve asymptotic stability, which is a property that cannot be obtained with the schemes previously investigated. When the quantizer is allowed to be dynamic and time-varying, it is obviously advantageous to scale the quantization levels dynamically so that the region of attraction is increased and the steady state limit cycle is reduced. In addition, the minimum number of quantization levels is explicitly related to the unstable poles of the system under the assumption of noise free communications. In this setting, the dynamic quantizer effectively consists of two parts: an encoder at the output end and a decoder at the input end.

We do caution that many results on quantized feedback with dynamic quantizers may be impractical due to three problems: 1) Most results are for stabilization only rather than for performance control; 2) The transient response is typically very poor due to the lack of good control design algorithms; 3) The capacity results are in general not valid for practical communications channels which are not noise free. The section of quantization in this book attempts to solve these problems.

1.5.2 Data Fusion over Networks

Initial data fusion applications are predominant in the defense systems. Data fusion originates from market studies especially in media and consumption surveys, where it is often impossible to ask the same sample all the items when there are too many questions. There is an increasing interest in data fusion due to the availability of multiple sources in various fields. In order to reduce the burden of respondents and thus avoid bias, one proceeds with two different independent samples where the questions of interest are split two parts with a common set of descriptors. Numerous mathematical tools,

such as probability theory, Bayes analysis, evidence theory, possibility theory, fuzzy-logic, neural networks and evolutionary algorithms, are applied in solving data fusion problems. Currently, this field has expanded to cover many research topics in which data fusion is an essential component: combining and updating the mapping of gravitational anomalies and meteorological variables, target tracking, land mine detection, threat assessment, to name a few. Medicine, geoscience and industrial engineering are some other research fields which have vast applications of data fusion. With the rapid group of the internet and other electronic sources of information, the problem of the coherent merging of information from multiple sources has become an important issue. Unified fusion rules are proposed in the sense of best linear unbiased estimate and weighted least-square for all fusion architectures ([96]). A state estimation fusion algorithm which is optimal in the sense of maximum a posteriori is proposed in [24]. An algorithm accounting is provided in [19] for dynamically changing interconnections among sensors, unreliable communication links, and faults, where convergence of the estimates to the true values is proved, under suitable hypothesis of "dynamical" graph connectivity, while in [172] the authors propose a minimum variance estimator for distributed tracking of a noisy time-varying signal. The problem of distributed discrete-time state estimation over sensor networks has been considered in [165].

Some terms of the estimation fusion problem are defined in [168]. The term "raw measurement" refers to the measurement from any sensor at the end of its signal processing chain. The term "processed measurement" refers to the data after some transform of the raw measurement to be used for estimation. One of the purposes in processing the raw measurements is to compress the data and save communication bandwidth. The term "local estimate" refers to any estimate that uses measurements from the local platform. A local estimate may include data from a single sensor or multiple sensors, but all inputs must be from the local platform or the data processing unit. The fusion systems use three basic approaches of communication between a local platform and the fusion center, namely: i) sending raw measurements, ii) sending processed measurements, e.g., quantized measurements to satisfy the bandwidth constraint, iii) sending local posteriors, e.g., local estimates/covariances. The third approach is commonly used in the existing distributed tracking systems. To design a fusion system, one needs to choose the system architecture, develop an algorithm to perform the fusion based on certain optimality criterion, and find a way to compute the possible cross-correlations among the estimation errors from different sources. Apart from these three steps, another major component is to develop a data association algorithm when there is an association ambiguity among the local estimates from different sources. [9] presents an algorithm for the association of multiple estimates in target tracking. For brevity data association from different sources for estimation fusion will not be discussed further.

1.5.3 Predictive Control over Networks

In model predictive control, the current control action is obtained by solving a finite horizon open-loop optimal control problem on-line using the current state of the plant as the initial state at each sampling instant. The optimization yields an optimal control sequence, in which the first control is applied to the plant. This is its main difference from conventional control which uses a pre-computed control law. It can be seen that the raison d'être for model predictive control with the clarity gained by hindsight is able to handle control problems, where off-line computation of a control law is difficult or impossible although other features, such as its capability for controlling multi-variable plants, are initially deemed more important. Almost all applications impose constraints, for example, actuators are naturally limited in the force, safety limits states such as temperature, pressure, velocity and efficiency.

In the present work, the model-based control approach is adopted to deal with data losses and asynchronous measurement sampling in the control system. A Lyapunov-based model predictive controller is proposed for a broad class of nonlinear uncertain systems with both disturbances and data losses. Model predictive control is a popular control strategy based on a model to predict in the process of control at each sampling time, the future evolution of the system from the current state follows a given prediction horizon. Using these predictions, the input trajectory that minimizes a given performance index is computed by solving a suitable optimization problem. To solve finite dimensional optimization problems, MPC is used to optimize a family of piecewise constant trajectories with a fixed sampling time and a fixed prediction horizon. Once the optimal problem is solved, only the first input is implemented, the rest of the trajectory is discarded and the optimization is repeated at the next sampling step. In [136], MPC framework is particularly appropriate for controlling systems subject to data losses because the actuator can profit from the predicted evolution of the system. In recent years, a wide class of MPC algorithms have been documented many times, for examples [94, 76, 158], and the references therein. Furthermore, a suboptimal model predictive control algorithm is proposed to reduce the severe computational problems [159]. By using a parameter dependent Lyapunov functional, a MPC law for linear parameter varying systems is proposed in [187]. For nonlinear system, a robust MPC algorithm is developed by using a contractive formulation [157]. Moreover, a MPC algorithm is presented for nonlinear sampled data control systems [115]. Another MPC of nonlinear systems subject to data losses is considered in [35]. A MPC for constrained linear systems to track piecewise constant references is presented in [102]. A solution to a finite-horizon MPC problem for max-plus-linear systems is derived in [128]. The problem of robust MPC satisfying hard constraints on inputs and outputs of a closed-loop system with polytopic type uncertainties is investigated in [204]. Other researches about MPC can be shown as [198, 203, 109, 202, 105, 78].

1.5.4 Fault Detection over Networks

Observer based fault detection and isolation technology has attracted much attention from many researchers because of the increasing demand for reliability and safety in industrial processes. Generally speaking, an observer based fault detection system consists of an observer based residual generator and a residual evaluator. The basic idea of fault detection is to construct a residual signal and compare it with a predefined threshold. If the residual exceeds the threshold, an alarm is generated. Because noises and disturbances may result in significant changes in the residual and lead to false alarms, fault detection observers have to be robust, namely, it is insensitive or even invariant to noise and disturbances. A residual generator for fault detection based on multirate sampled data is designed in [87]. Moreover, some results on fault detection and isolation by using frequency domain approach have been reported in literature, such as [150, 228]. Problems related to the integrated design of robust fault detection systems in time-frequency domain are studied in [215].

Usually, H_∞ norm optimization technique is used to design the robust fault detection observers, the way of this technique is to introduce a performance index and formulate the fault detection as an optimization problem. But the technique may result in significant changes in the residual and lead to false alarms, and it is contrary to main objective of fault detection because the H_- norm measures the maximum effect of an input on an output. Based on H_-, which is defined as the smallest nonzero singular value of the transfer function matrix from fault to residual at the particular frequency, the study on minimum singular value aiming to maximize the minimum effect of faults on the residual output of a fault detection observer has gained much attention. On the one hand, the linear matrix inequality methodology has been under intensive research and widely used for various kinds of robust control and filtering problems. One advantage of the LMI approach is the relative ease in incorporating additional design objectives into the formulation. Hence, LMI formulations for the H_- and mixed H_-/H_∞ problems are of interest. Based on these performance evaluation criteria, multiple objective optimal filter problems such as H_-/H_∞ have attracted a great deal of research interests in the recent years, for examples [97, 75, 88]. There are also some results on fault finite frequency ranges detection filters with H_∞ and H_- performance indices for discrete systems [190] and continuous systems [191], respectively. In view of the wide usage of network cables in today's world, a seemingly natural research problem is to study fault detection problems for networked systems in the presence of network-induced delays or/with data missing [138].

1.6 Summary

As there are more and more applications of NCSs in industry, such as traffic, communication, aviation and spaceflight, more attention in this area has been

paid to design and analysis of NCSs. The main problems about NCSs are quantization, data fusion, predictive control and fault detection. In this book, these four issues are discussed on NCSs affected by network-induced delay, packet dropout, which are the significant factors in NCSs. The results in this book will no doubt advance the study of NCSs and potential applications in the area of Internet of Things.

Part I
Quantization over Networks

Chapter 2
Stability Analysis of Quantized Systems over Networks

2.1 Introduction

Recently there have been many of interests in NCSs, that is, control systems closed via possibly shared communication links with delay/bandwidth constraints. Particularly, Internet based control systems allow remote monitoring and adjustment of plants over the Internet. This enables the control system to benefit from the way it retrieves data and reacts to plant fluctuations from anywhere around the world at any time, see for example [56, 78], and references therein. The main advantages of NCSs are low cost, simple installation and maintenance, and potentially high reliability. As the structure of NCSs is different from that of traditional control systems, there exist various specific problems in NCSs, for example, quantization, network delay, loss of data packets, network security and safety [148]. In recent years, more and more network techniques have been applied to control systems [133], much attention has been paid to the study of control design and stability analysis of NCSs ([29, 131, 229, 221, 106, 122]). A state estimation problem involving bit-rate communication capacity constraints is studied in [119]. A current survey of the emerging field of NCSs is provided in [7] and Hespanha, et. al review several recent results on estimation, analysis, and controller synthesis for NCSs in [70]. In [206], a practical architecture and some algorithms for the networked data fusion system with packet losses and variable delays are given, in which optimal state estimates through network are presented. However, one important issue is not considered in [206], that is, the measurement or estimated states have to be quantized before they are sent through network.

Many research results on quantization have been obtained. For example, the problem of detectability and stabilization of nonlinear systems via limited capacity digital communication channels is considered in [152], state estimation and stabilization with coder-decoder and coder-decoder-controller procedures are studied in [238] and the controllability condition under the discrete-valued input in [144]. The characterizations of the minimum data

Y. Xia, M. Fu, and G.-P. Liu: Analysis and Synthesis of NCSs, LNCIS 409, pp. 15–34.
springerlink.com

rate and the quantization level for stabilizing feedback control systems are considered in [40, 125, 178], and the optimal quantizer for the identification and control is discussed in [18]. An optimal dynamic quantizer is proposed for control of linear time-invariant plants whose inputs are constrained to be discrete-valued in [6]. In [17], Brockett and Liberzon consider the problems of quantized feedback stabilization of linear system and propose a new control design methodology which yields globally asymptotic stability of the systems. [100] and [101] conduct a deeper study based on [17]. Although fruitful results on quantization can be found in recent publications, there are still a lot of space for further investigation such as quantization problems under network conditions.

In fact, there are some works about quantized systems over network. For example, the problem of output feedback control for NCSs with limited communication capacity is considered by Engang Tian, Dong Yue, Chen Peng in [181]. Very recently, [137], [182]and [223] propose some new results about the guaranteed cost control and H_∞ control of continuous systems over network with quantization, where the effect of both network conditions and data quantization are taken into consideration. Yue et al. [223] considers the guaranteed cost control of continuous systems over networks with state and input quantization based on the sector bound condition of quantizer given in [51]. Gao et al. [56] combines the transformation method similar to [223] with a technique of two successive delay components, and investigates problems of H_∞ stability and stabilization for continuous-time NCSs with only quantized state feedback. The problems of H_∞ stability and stabilization for NCSs with both sensor-to-controller and controller-to-actuator quantizations are considered in [239]. The issue of designing quantizers in order to reduce a remote control system, where the plant and the controller are connected by a network cable, to be stable has been studied in [86].

In this chapter, the problem of quantized feedback under network conditions is considered. It is known that the quantized feedback problem has been considered in [17] and globally asymptotic stability is achieved. This chapter has many different points from [17]. First, the network is considered in this chapter. Second, the stability discussed in this chapter is not the same as globally asymptotic stability. Third, Kalman filter is adopted in this chapter to estimate states from measurements on the sensor side. So, this chapter has its own significance. In this chapter, a simple quantization strategy is proposed and the feedback control is designed based on quantized estimated states sent through network. Sufficient condition is given to guarantee the stability of the closed-loop systems. Finally, a numerical simulation is presented to show the effectiveness of the main results.

This chapter is organized as follows: Section 2.2 gives the problem formulation. Quantization strategy is proposed in Section 2.3. Section 2.4 presents the results of the stability of the closed-loop systems. A numerical example is designed in Section 2.5. Some conclusions are given in Section 2.6.

2.2 State Estimation Based on Kalman Filter

In this section, we will consider the following system:

$$\begin{aligned} x(k+1) &= Ax(k) + Bu(k) + \omega(k) \\ y(k) &= Cx(k) + v(k) \end{aligned} \tag{2.1}$$

where $x(k) \in R^n$ is the state variable, $u(k) \in R^p$ is the control variable, $y(k) \in R^m$ is the measurement output, $A \in R^{n\times n}$ is the system matrix, $B \in R^{n\times p}$ is the input matrix, $C \in R^{m\times n}$ is the measurement matrix, $\omega(k) \in R^n$ is the input noise, $v(k) \in R^m$ is the measurement noise. The following assumptions are standard.

Assumption 2.1. *A is unstable and (A, B) is controllable.*

Assumption 2.2. *$\omega(k) \in R^n$ and $v(k) \in R^m$ are the uncorrelated white noises with zero mean and*

$$\begin{aligned} E[\omega(k)\omega^T(j)] &= Q\delta_{kj} \\ E[v(k)v^T(l)] &= R\delta_{kl} \\ E[\omega(k)v^T(j)] &= 0 \end{aligned} \tag{2.2}$$

Assumption 2.3. *The initial state $x(0)$ is independent of $\omega(k)$ and $v(k), k = 1, 2, \cdots M$ and*

$$\begin{aligned} E[x(0)] &= \mu_0 \\ E[(x(0) - \mu_0)(x(0) - \mu_0)^T] &= P_0 \end{aligned} \tag{2.3}$$

The following lemmas will be used to prove our main results in this chapter.

Lemma 2.1. *[49] Assume $A \in R^{n\times n}$, $\rho(A)$ denotes spectral radius of matrix A. Then for any $\epsilon > 0$, there exists a kind of norm $\|\cdot\|_M$ satisfying:*

$$\|A\|_M \le \rho(A) + \epsilon \tag{2.4}$$

Lemma 2.2. *[49] The norms are equal to each other in finite normed linear space, that is, for any two kinds of norm $\|\cdot\|_1$ and $\|\cdot\|_2$, there exist positive constants c_1, c_2, c_3 and c_4 satisfying:*

$$c_1\|\cdot\|_1 \le \|\cdot\|_2 \le c_2\|\cdot\|_1 \tag{2.5}$$

$$c_3\|\cdot\|_2 \le \|\cdot\|_1 \le c_4\|\cdot\|_2 \tag{2.6}$$

Some notations are defined as follows:

$$\begin{aligned} Y(k) &= [y(1), \cdots, y(k)]^T \\ \hat{x}(k|k) &= E[x(k)|Y(k)] \\ \bar{P}(k|k) &= E[(x(k) - \hat{x}(k|k))(x(k) - \hat{x}(k|k))^T|Y(k)] \\ \hat{x}(k+1|k) &= E[x(k+1)|Y(k)] \\ \bar{P}(k+1|k) &= E[(x(k+1) - \hat{x}(k+1|k))^T|Y(k)] \end{aligned} \tag{2.7}$$

The purpose of this chapter is to propose a quantization strategy and design a quantized feedback controller $u(k)$ which depends on estimated value $\hat{x}(k|k)$ basing on Kalman filtering ([206]) such that system (2.1) is stable.

The Kalman filter based state observer is designed as

$$\begin{aligned} \hat{x}(k|k-1) &= A\hat{x}(k-1|k-1) + Bu(k-1) \\ \hat{x}(k|k) &= \hat{x}(k|k-1) + \bar{K}(k)(y(k) - C\hat{x}(k|k-1)) \\ \bar{P}(k|k) &= \bar{P}(k|k-1) - \bar{K}(k)C\bar{P}(k|k-1) \\ \bar{K}(k) &= \bar{P}(k|k-1)C^T(C\bar{P}(k|k-1)C^T + R)^{-1} \end{aligned} \tag{2.8}$$

where $\hat{x}(k+1|k) \in R^n$ and $u(k-1) \in R^m$ are the one-step ahead state prediction and the input of the observer at time k, $\bar{P}(k|k-1)$ is the solution of the following Riccati equation [167]

$$\begin{aligned} \bar{P}(k|k-1) = A\bar{P}(k-1|k-2)A^T + \bar{Q} - \bar{P}(k-1|k-2)C^T \\ (C\bar{P}(k-1|k-2)C^T + R)^{-1}C\bar{P}(k-1|k-2)A^T \end{aligned} \tag{2.9}$$

Due to the insertion of network, the estimated states have to be quantized before being sent through network, the control strategy proposed in this chapter is shown as Fig. 2.1:

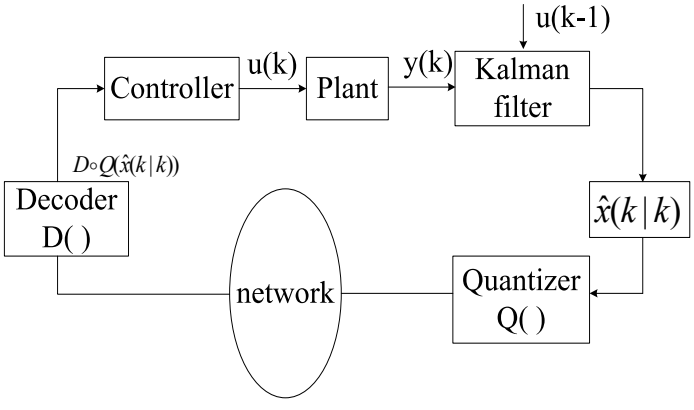

Fig. 2.1 Control based on quantized states.

It is assumed that the input of the plant at last time can be used as an input of Kalman filter, which is reasonable in some cases. The estimated states $\hat{x}(k|k)$ are quantized before sent through network, as is shown in Fig. 2.1, the quantizer $Q(\cdot)$ is introduced to quantize $\hat{x}(k|k)$. At the other side of the network, $Q(\hat{x}(k|k))$ is decoded by decoder $D(\cdot)$ such that the closed-loop system (2.1) is stable with quantized feedback.

2.3 Quantization Strategy

Let us consider the quantizer $Q(\cdot)$. First, the 2-dimensional state quantization is considered to show the method proposed in this chapter, and then we extend it to the n-dimensional case. As is shown in Fig. 2.2, the quantization regions are squares with length L and the quantized value is a sequence.

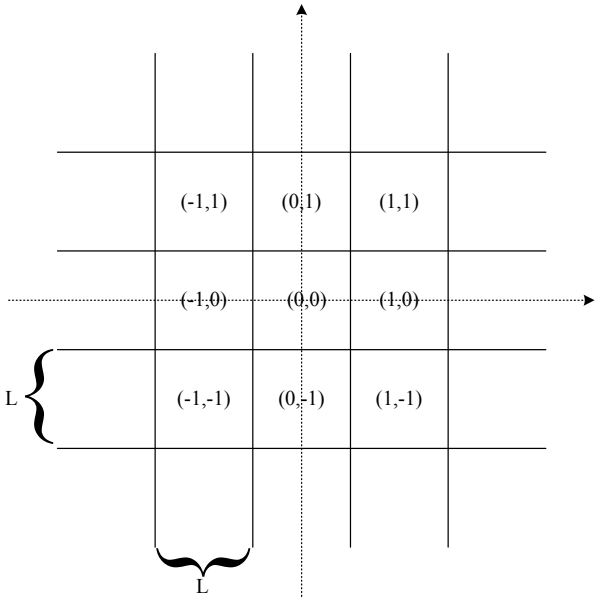

Fig. 2.2 2-dimensional state quantization.

If $x = [x_1\ x_2]^T$ with $x_1 \in (-L/2, L/2)$ and $x_2 \in (-L/2, L/2)$, then x will be quantized to $(0,0)$ by quantizer $Q(\cdot)$, that is, $Q(x) = (0,0)$. In other words, as to $x = [x_1\ x_2]^T$, we will ensure the components' sequence according to the interval which components belong to. Indicated by Fig. 2.2, we can see that the quantization rule of quantizer $Q : R^2 \to Z \times Z$ is:

$$Q([x_1\ x_2]^T) = (i, j) \tag{2.10}$$

where Z denotes integer set, $x_1 \in (iL - L/2, iL + L/2)$, $x_2 \in (jL - L/2, jL + L/2)$.

Decoder $D(\cdot) : Z \times Z \to R^2$ decodes the sequence (i, j) to the center of the square, that is

$$D((i, j)) = [iL\ jL]^T \tag{2.11}$$

where $i, j \in Z$.

As to the vector x on the edge of square, we quantize it according to the principle of the smallest vector norm after decoding the quantization sequence. For example, we choose $(0, 0)$ as the quantized value of the $*$ point on the edge of square. That is obtained according to the principle of the smallest vector norm after decoding the quantization sequence. After decoded by decoder $D(\cdot)$, $(0, 0)$ is transferred to $[0, 0]^T$ and $(-1, 0)$ is to $[-L\ 0]^T$. It is obvious that vector norm after decoding is smaller by selecting $(0, 0)$, which is shown in Fig. 2.3.

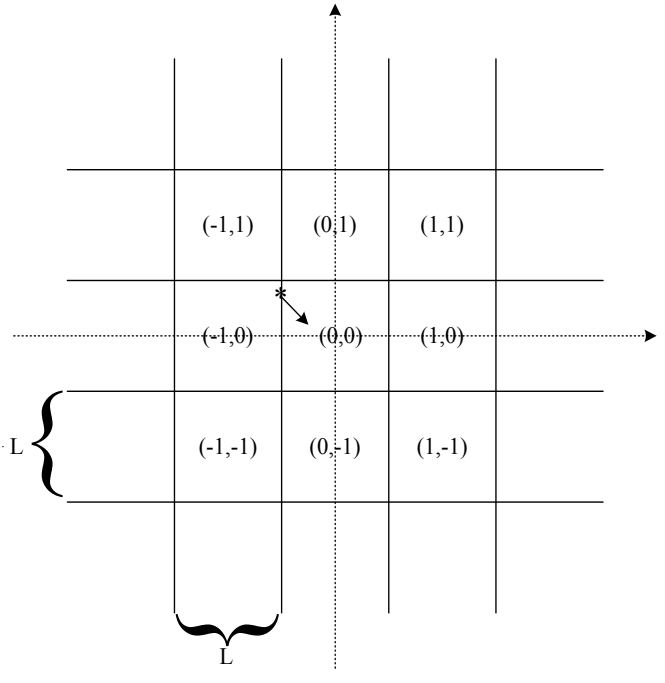

Fig. 2.3 Indication for edge point's quantization.

According to the quantization rule, it can be shown that the components of vectors on the edge of squares can be quantized to $-iL/2$ or $iL/2$, where i is a positive odd number. The sequence numbers of $-iL/2$ and $iL/2$ are ensured by the following rule:

$$\begin{cases} -iL/2 \to -(i-1)/2 \\ iL/2 \to (i-1)/2 \end{cases} \tag{2.12}$$

where i is a positive odd number.

As to n-dimensional vector, 2-dimensional square in Fig. 2.2 is changed to n-dimensional super square box without an intuitive geometric figure to represent it.

The quantization rule of n-dimensional quantizer $Q : R^n \to Z^n$ is obtained easily by extending the 2-dimensional case:

$$Q([x_1\ x_2\ \cdots x_n]^T) = (i_1, i_2, \cdots i_n) \tag{2.13}$$

where, Z denotes integer set, $x_k \in (i_k L - L/2, i_k L + L/2), k = 1, 2, \cdots n$.

The decode rule of decoder $D : Z^n \to R^n$ is:

$$D((i_1, i_2, \cdots i_n)) = [i_1 L\ i_2 L\ \cdots i_n L]^T \tag{2.14}$$

where $i_1, i_2, \cdots, i_n \in Z$.

The quantized value of the point on the edge of the n-dimensional super square box is ensured by rule (2.12).

Then, we can obtain a general equation for quantization from the previous analysis:

$$\begin{cases} i_k = \lceil \frac{x_k}{L} - \frac{1}{2} \rceil & x_k \geq 0 \\ i_k = \lfloor \frac{x_k}{L} + \frac{1}{2} \rfloor & x_k \leq 0 \end{cases} \tag{2.15}$$

where, x_k is the kth component of the n-dimensional vector and i_k is the quantized value of x_k, $\lceil \cdot \rceil$ and $\lfloor \cdot \rfloor$ indicate the integer function upward and downward, respectively, which can be described as follows:

$$\begin{cases} \lceil x \rceil = m + 1 & m < x \leq m + 1 \\ \lfloor x \rfloor = m & m \leq x < m + 1 \end{cases} \tag{2.16}$$

where $m \in Z$.

From Assumption 2.1, it follows that there exit a positive definite matrix P and matrix K satisfying the following equation:

$$(A + BK)^T P(A + BK) - P = -I \tag{2.17}$$

It is obvious that $A+BK$ is a Schur stable matrix based on Lyapunov stability theory and (2.17). We design $u(k) = KD \circ Q(\hat{x}(k|k))$, system (2.1) can be written as

$$x(k + 1) = Ax(k) + BKD \circ Q(\hat{x}(k|k)) + \omega(k) \tag{2.18}$$

Then the following equation is obtained from (2.18)

$$\bar{x}(k + 1) = A\bar{x}(k) + BKE[D \circ Q(\hat{x}(k|k))] \tag{2.19}$$

Definition 2.3. Let $\bar{x}(k) = E[x(k)]$ and $P(k) = E[(x(k) - \bar{x}(k))(x(k) - \bar{x}(k))^T]$, system (2.1) is said to be stable, if $\lim_{k\to\infty} \bar{x}(k) = 0$ and there is a constant $M > 0$ such that $\|P(k)\|_2 < M$.

2.4 Stability Analysis

In this section, a quantization control strategy is given based on quantization strategy presented in previous section and the stability of system is discussed.

System (2.18) can be written as:

$$\begin{aligned} x(k+1) &= Ax(k) + BKD \circ Q(\hat{x}(k|k)) + \omega(k) \\ &= (A+BK)x(k) - BK(x(k) - \hat{x}(k|k)) - BK((\hat{x}(k|k) \\ &\quad -D \circ Q(\hat{x}(k|k))) + \omega(k) \\ &= (A+BK)x(k) - BK(x(k) - \hat{x}(k|k)) - BKs(k) + \omega(k) \end{aligned} \tag{2.20}$$

where $s(k) = \hat{x}(k|k) - D \circ Q(\hat{x}(k|k))$.

Since the estimate $\hat{x}(k|k)$ is unbiased, take the expectation at both sides of (2.20), the following equation is achieved:

$$\bar{x}(k+1) = (A+BK)\bar{x} - BKE[s(k)] \tag{2.21}$$

In fact, equation (2.21) is equal to (2.19).

The inequality $\|s(k)\|_2 \leq \sqrt{n}L/2$ can be obtained by the former quantization strategy. Let $\bar{s}(k) = E[s(k)]$, the following inequality can be derived according to the above inequality:

$$\|\bar{s}(k)\|_2 = \|E[s(k)]\|_2 \leq E[\|s(k)\|_2] \leq \sqrt{n}L/2 \tag{2.22}$$

In the sequel, a quantization control strategy depending on Lyapunov stability theory is presented. Lyapunov function can be chosen as $V(\bar{x}(k)) = \bar{x}^T(k)P\bar{x}(k)(P > 0)$ by quantization rule (2.15) and equation (2.17). Let $\bar{\lambda}$ and $\underline{\lambda}$ indicate the maximum and minimum eigenvalue of the symmetric positive definite matrix P, then $\bar{\lambda} > 0$ and $\underline{\lambda} > 0$.

Let $\Delta V(\bar{x}(k)) = V(\bar{x}(k+1)) - V(\bar{x}(k))$, then

$$\begin{aligned} \Delta V(\bar{x}(k)) &= \bar{x}^T(k)(A+BK)^T P(A+BK)\bar{x}(k) - \bar{x}^T(k)P\bar{x}(k) \\ &\quad -2\bar{x}^T(k)(A+BK)^T PBKE[s(k)] + E^T[s(k)]K^T B^T BKE[s(k)] \\ &= -\|\bar{x}(k)\|_2^2 - 2\bar{x}^T(k)(A+BK)^T PBK\bar{s}(k) \\ &\quad +\bar{s}^T(k)K^T B^T BK\bar{s}(k) \\ &\leq -\|\bar{x}(k)\|_2^2 + 2\|(A+BK)^T PBK\|_2\|\bar{x}(k)\|_2\|\bar{s}(k)\|_2 \\ &\quad +\|BK\|_2^2\|\bar{s}(k)\|_2^2 \\ &\leq -(1-\theta)\|\bar{x}(k)\|_2^2 - (\theta\|\bar{x}(k)\|_2^2 \\ &\quad -\sqrt{n}\|(A+BK)^T PBK\|_2 L\|\bar{x}(k)\|_2 - nL^2\|BK\|_2^2/4) \\ &\leq -(1-\theta)\|\bar{x}(k)\|_2^2 \end{aligned} \tag{2.23}$$

when

$$\begin{aligned} \|\bar{x}(k)\|_2 \geq (\sqrt{n}L/2\theta)(\|(A+BK)^T PBK\|_2 \\ +\sqrt{\|(A+BK)^T PBK\|_2^2 + \theta\|BK\|_2^2}), \theta \in (0,1) \end{aligned}$$

For simplicity, let

$$\Pi = (\|(A+BK)^T PBK\|_2 + \sqrt{\|(A+BK)^T PBK\|_2^2 + \theta\|BK\|_2^2}) \quad (2.24)$$

then $\Delta V(\bar{x}(k)) \leq -(1-\theta)\|\bar{x}(k)\|_2^2$ can be guaranteed by (2.23) when $\|\bar{x}(k)\|_2 \geq (\sqrt{n}L/2\theta)\Pi$.

Let

$$\Omega_0 = \{\bar{x}(k) \in R^n : \|\bar{x}(k)\|_2 < (\sqrt{n}L/2\theta)\Pi\} \quad (2.25)$$

From the above discussion, it can be concluded that if there is a time $\bar{t}$ such that $\|\bar{x}(k)(\bar{t})\|_2 \geq (\sqrt{n}L/2\theta)\Pi$, there exists a finite time T such that $\bar{x}(k) \in \Omega_0$ when $k > T$, that is, the track of $\bar{x}(k)$ is in Ω_0 after T. Observing the variability of parameter L, if L is decreased, a new smaller sphere can be defined similar to (2.25) to make $\bar{x}(k)$ arrive at it in finite time and never leave it thereafter. In the ideal case, when L is reduced infinitely small, the sphere reduces infinitely small correspondingly. From (2.23), it can be shown that $\Omega_0 \to 0$ when $L \to 0$, that is, $\bar{x}(k) \to 0$ when $k \to \infty$.

Let a constant $\zeta \in (0,1)$ represent the decay factor of L, that is, take $L_i = \zeta^i L$ to represent the length of super square box after the ith decay, where $i = 0, 1, \cdots$. The spheroid is defined as:

$$\Omega_i = \{\bar{x}(k) \in R^n : \|\bar{x}(k)\|_2 < (\sqrt{n}L_i/2\theta)\Pi\} \quad (2.26)$$

Let τ_i be the time when $\bar{x}(k)$ enters the spheroid Ω_i and decreases L for the ith time. Define T_{i+1} as the time when $\bar{x}(k)$ enters the spheroid Ω_{i+1}. Let $\Delta T(i, i+1) = T_{i+1} - \tau_i$, then a time interval is defined by ΔT. Generally speaking, it is difficult to get the time interval precisely, but the upper bound which is enough in practice can be obtained.

Assume $\bar{x}(k) \in \Omega_i$, $\bar{x}(k) \notin \Omega_{i+1}$ and L is decreased $(i+1)$th at time instant k. From (2.23), it can be shown that

$$V(\bar{x}(k+1)) - V(\bar{x}(k)) \leq -(1-\theta)\|\bar{x}(k)\|_2^2 \leq -(1-\theta)V(\bar{x}(k))/\bar{\lambda} \quad (2.27)$$

Then

$$V(\bar{x}(k+1)) \leq (1-(1-\theta)/\bar{\lambda})V(\bar{x}(k)) \quad (2.28)$$

Suppose that $(1-(1-\theta)/\bar{\lambda}) < 1$ or $(1-(1-\theta)/\bar{\lambda}) \leq 0$. In the later situation, it follows that $\bar{x}(\cdot)$ is able to reach zero at time instant $k+1$ according to (2.28). But an upper bound is needed, thus, a general case is assumed, that is, $0 < (1-(1-\theta)/\bar{\lambda}) < 1$. From (2.28), it results in

$$V(\bar{x}(k+p)) \leq (1-(1-\theta)/\bar{\lambda})^p V(\bar{x}(k)) \quad (2.29)$$

And then

$$\begin{aligned}\|\bar{x}(k+p)\|_2 &\leq \sqrt{(1-(1-\theta)/\bar{\lambda})^p V(\bar{x}(k))/\underline{\lambda}} \\ &\leq \sqrt{\bar{\lambda}(1-(1-\theta)/\bar{\lambda})^p/\underline{\lambda}}\|\bar{x}(k)\|_2 \\ &\leq \sqrt{\bar{\lambda}(1-(1-\theta)/\bar{\lambda})^p/\underline{\lambda}}(\sqrt{n}L_i/2\theta)\Pi\end{aligned} \tag{2.30}$$

In order to get the upper bound of time interval, let the last line of (2.30) be smaller than the radius of sphere Ω_{i+1}, then

$$\sqrt{\bar{\lambda}(1-(1-\theta)/\bar{\lambda})^p/\underline{\lambda}}(\zeta^i\sqrt{n}L/2\theta)\Pi \leq (\sqrt{n}L_{i+1}/2\theta)\Pi \tag{2.31}$$

Let $a = 1-(1-\theta)/\bar{\lambda}$, then

$$p \leq \log_a(\underline{\lambda}\zeta^2/\bar{\lambda}) \tag{2.32}$$

and then,

$$\Delta T(i,i+1) \leq \log_a(\underline{\lambda}\zeta^2/\bar{\lambda}) \tag{2.33}$$

It is obvious that the right side of inequality (2.33) is a constant. Let $\Delta T(i,i+1) = \Delta T$, it results in

$$\Delta T \leq \log_a(\underline{\lambda}\zeta^2/\bar{\lambda}) \tag{2.34}$$

Then an upper bound of time interval between reduced time and arrival time is obtained.

Let $\tilde{e}(k) = x(k) - \hat{x}(k|k)$ and $\tilde{P}(k) = E[\tilde{e}(k)\tilde{e}^T(k)]$, then there exists a positive definite matrix $\bar{M} > 0$ such that $E[\|\tilde{e}(k)\|_2^2] < \bar{M}$. Considering $\tilde{s}(k) = s(k) - \bar{s}(k)$ and above discussion, the following inequality can be obtained:

$$\|\tilde{s}(k)\|_2 \leq \|s(k)\|_2 + \|\bar{s(k)}\|_2 \leq \sqrt{n}L_i = \sqrt{S_i} \tag{2.35}$$

Then

$$E[\|\tilde{s}(k)\|_2^2] \leq S_i \tag{2.36}$$

Let $e(k) = x(k) - \bar{x}(k)$, it follows from (2.20) and (2.21) that

$$e(k+1) = (A+BK)e(k) - BK\tilde{e}(k) - BK\tilde{s}(k) + \omega(k) \tag{2.37}$$

Then

$$\begin{aligned}P(k+1) &= E[e(k+1)e^T(k+1)] \\ &= (A+BK)E[e(k)e^T(k)](A+BK)^T \\ &\quad -(A+BK)E[e(k)\tilde{e}^T(k)]K^TB^T \\ &\quad -(A+BK)E[e(k)\tilde{s}^T(k)]K^TB^T - BKE[\tilde{e}(k)e^T(k)](A+BK)^T \\ &\quad +BKE[\tilde{e}(k)\tilde{e}^T(k)]K^TB^T + BKE[\tilde{e}(k)\tilde{s}^T(k)]K^TB^T \\ &\quad -BKE[\tilde{s}(k)e^T(k)](A+BK)^T + BKE[\tilde{s}(k)\tilde{e}^T(k)]K^TB^T \\ &\quad +BKE[\tilde{s}(k)\tilde{s}^T(k)]K^TB^T + Q\end{aligned} \tag{2.38}$$

From the above discussion, the following inequality can be obtained:

$$\begin{aligned}
P(k+1) \leq\ & 2(A+BK)P(k)(A+BK)^T - (A+BK)\tilde{P}(k)K^TB^T \\
& -BK\tilde{P}(k)(A+BK)^T + 2BKE[\tilde{s}(k)\tilde{s}^T(k)]K^TB^T \\
& +BK\tilde{P}(k)K^TB^T + BKE[\tilde{e}(k)\tilde{s}^T(k)]K^TB^T \\
& +BKE[\tilde{s}(k)\tilde{e}^T(k)]K^TB^T + Q \\
=\ & 2(A+BK)P(k)(A+BK)^T + A\tilde{P}(k)A^T \\
& -(A+BK)\tilde{P}(k)(A+BK)^T + 2BKE[\tilde{s}(k)\tilde{s}^T(k)]K^TB^T \\
& +BKE[\tilde{e}(k)\tilde{s}^T(k)]K^TB^T + BKE[\tilde{s}(k)\tilde{e}^T(k)]K^TB^T + Q
\end{aligned} \tag{2.39}$$

where $AA^T + BB^T \geq -AB^T - A^TB$ and the following equality are useful

$$\begin{aligned}
E[e(k)\tilde{e}^T(k)] &= E[(x(k)-\bar{x}(k))\tilde{e}^T(k)] \\
&= E[(x(k)-\hat{x}(k|k)+\hat{x}(k|k)-\bar{x}(k))\tilde{e}^T(k)] \\
&= \tilde{P}(k) + E[\hat{x}(k|k)\tilde{e}^T(k)] - \bar{x}(k)E[\tilde{e}^T(k)] \\
&= \tilde{P}(k)
\end{aligned} \tag{2.40}$$

Let L_i be the length of super square box, the boundedness of $P(k)$ can be guaranteed by Lemma 2.2. For the norm discussed in Lemma 2.2, it is assumed that there exist constants $\tilde{c} > 0$ and $c > 0$ satisfying $\tilde{c}\|\cdot\|_2 \leq \|\cdot\|_M \leq c\|\cdot\|_2$, where $\|\cdot\|_2$ denotes 2 norm in Euclid space.

Basing on above analysis and observing that A, $A+BK$, $P(k)$, $\tilde{P}(k)$, BK, $\tilde{s}(k)\tilde{s}^T(k)$, $\tilde{e}(k)\tilde{s}^T(k)$ are all square matrices, we have

$$\begin{aligned}
\|P(k+1)\|_M \leq\ & 2\|A+BK\|_M^2\|P(k)\|_M + \|A\|_M^2\|\tilde{P}(k)\|_M \\
& +\|A+BK\|_M^2\|\tilde{P}(k)\|_M + 2\|BK\|_M^2\|E[\tilde{s}(k)\tilde{s}^T(k)]\|_M \\
& +\|BK\|_M^2\|E[\tilde{e}(k)\tilde{s}^T(k)]\|_M + \|BK\|_M^2\|E[\tilde{s}(k)\tilde{e}^T(k)]\|_M \\
& +\|Q\|_M \\
\leq\ & 2\|A+BK\|_M^2\|P(k)\|_M + c^3\|A\|_2^2\|\tilde{P}(k)\|_2 \\
& +c^3\|A+BK\|_2^2\|\tilde{P}(k)\|_2 + 2c^3\|BK\|_2^2\|E[\tilde{s}(k)\tilde{s}^T(k)]\|_2 \\
& +c^3\|BK\|_2^2\|E[\tilde{e}(k)\tilde{s}^T(k)]\|_2 + c^3\|BK\|_2^2\|E[\tilde{s}(k)\tilde{e}^T(k)]\|_2 \\
& +c\|Q\|_2 \\
\leq\ & 2\|A+BK\|_M^2\|P(k)\|_M + c^3\|A\|_2^2\|\tilde{P}(k)\|_2 \\
& +c^3\|A+BK\|_2^2\|\tilde{P}(k)\|_2 + 2c^3\|BK\|_2^2E[\|\tilde{s}(k)\|_2^2] \\
& +2c^3\|BK\|_2^2E[\|\tilde{e}(k)\|_2\|\tilde{s}(k)\|_2] + c\|Q\|_2 \\
\leq\ & 2\|A+BK\|_M^2\|P(k)\|_M + c^3\|A\|_2^2\|\tilde{P}(k)\|_2 \\
& +c^3\|A+BK\|_2^2\|\tilde{P}(k)\|_2 + 2c^3\|BK\|_2^2E[\|\tilde{s}(k)\|_2^2] \\
& +2c^3\|BK\|_2^2\{E[\|\tilde{e}(k)\|_2^2]\}^{\frac{1}{2}}\{E[\|\tilde{s}(k)\|_2^2]\}^{\frac{1}{2}} + c\|Q\|_2 \\
\leq\ & 2\|A+BK\|_M^2\|P(k)\|_M + c^3(\|A\|_2^2 + \|A+BK\|_2^2)\bar{M} \\
& +2c^3\|BK\|_2^2S_i + 2c^3\|BK\|_2^2\sqrt{\bar{M}}\sqrt{S_i} + c\|Q\|_2 \\
\leq\ & 2\|A+BK\|_M^2\|P(k)\|_M + c^3(\|A\|_2^2 + \|A+BK\|_2^2)\bar{M} \\
& +2c^3\|BK\|_2^2S_0 + 2c^3\|BK\|_2^2\sqrt{\bar{M}}\sqrt{S_0} + c\|Q\|_2
\end{aligned} \tag{2.41}$$

Let

$$\Xi = c^3[(\|A\|_2^2 + \|A+BK\|_2^2)\bar{M} + 2\|BK\|_2^2 S_0 + 2\|BK\|_2^2\sqrt{\bar{M}}\sqrt{S_0}] + c\|Q\|_2,$$

it is obvious that $\Xi > 0$, then (2.41) can be written as

$$\|P(k+1)\|_M \leq 2\|A+BK\|_M^2\|P(k)\|_M + \Xi \tag{2.42}$$

Theorem 2.4. *If $\rho(A+BK) < \sqrt{2}/2$, there exists a kind of quantization control strategy such that system (2.1) is stable in the sense of Definition 2.3.*

Proof. The quantization control strategy which make $\lim_{k\to\infty} \bar{x}(k) = 0$ is discussed above. In the following part, inequality (2.42) is used to prove that there exists a constant $\tilde{M} > 0$ such that $\|P(k)\|_2 < \tilde{M}$.

A sequence is defined as

$$m(k+1) = 2\|A+BK\|_M^2 m(k) + \Xi,\ m(0) = \|P(0)\|_M \tag{2.43}$$

It is obvious that $\|P(k)\|_M \leq m(k)$. From Lemma 2.1 and $\rho(A+BK) < \sqrt{2}/2$, $\|\cdot\|_M$ satisfying $\|A+BK\|_M < \sqrt{2}/2$, then $2\|A+BK\|_M^2 < 1$ can be obtained. For any finite initial value which is larger than zero, the sequence $\{m(k)\}_{k=1}^{\infty}$ is convergent to a positive constant $\Xi/(1-2\|A+BK\|_M^2)$, that is,

$$\lim_{k\to\infty} m(k) = \Xi/(1-2\|A+BK\|_M^2) \tag{2.44}$$

Because of the boundedness of convergence sequence, it can be seen that there exists a constant $M > 0$ such that $0 < m(k) < \tilde{M}$, then $\|P(k)\|_M < \tilde{M}$ and $\|P(k)\|_2 < \tilde{M}/\tilde{c}$.

Therefore, system (2.1) is stable in the sense of Definition 2.3 based on the quantization control strategy proposed above.

Remark 2.5. Because of the controllable of (A, B), the poles of $A+BK$ can be assigned arbitrarily, therefore, the condition $\rho(A+BK) < \sqrt{2}/2$ in Theorem 2.4 can be satisfied.

2.5 Numerical Example

Simulation is given in this section to demonstrate the performance of the quantization strategy designed above comparing with the conventional state feedback control $u = Kx$. The model is taken from [81], which is specified by $A = \begin{bmatrix} 1.3 & 0.3 \\ 0 & 1.2 \end{bmatrix}$, $B = \begin{bmatrix} 1 \\ 0.5 \end{bmatrix}$, $C = \begin{bmatrix} 1 & 1 \end{bmatrix}$, $w(k)$ and $v(k)$ are white noises with covariance matrices $Q = \begin{bmatrix} 0.01 & 0 \\ 0 & 0.01 \end{bmatrix}$ and $R = 0.01$. The feedback gain is selected as $K = \begin{bmatrix} -5.28 & 6.16 \end{bmatrix}$ which satisfies the condition in Theorem 2.4.

The system performances under the two control strategies are depicted in Fig. 2.4-Fig. 2.12 when $L = 0.01$. It is apparent that the system behavior under the quantization scheme is almost the same as conventional state feedback control approach (see Fig. 2.10 and Fig. 2.11), and the norm of estimated error covariance is finite (see Fig. 2.12).

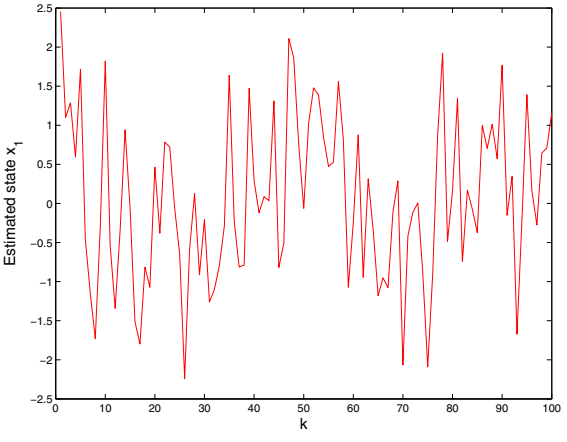

Fig. 2.4 Estimated state x_1 when L=0.01.

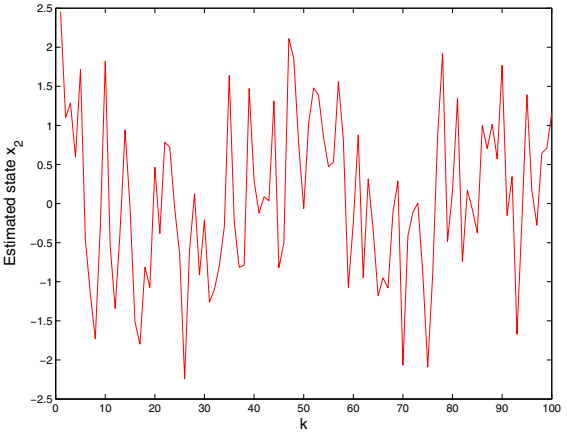

Fig. 2.5 Estimated state x_2 when L=0.01.

The system states are depicted in Fig. 2.13-Fig. 2.14 when parameter L is selected as $L = 1$. It is clear that the system performance under the quantization scheme is inferior than the state feedback control method. The norm of

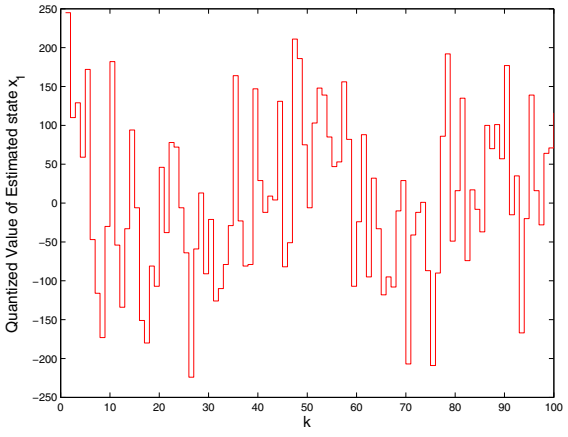

Fig. 2.6 Quantized value of estimated state x_1 when L=0.01.

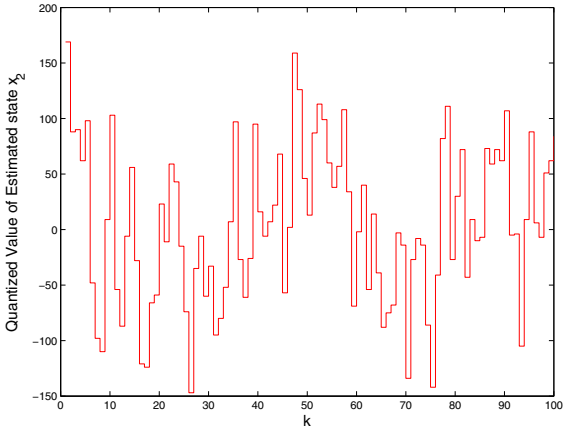

Fig. 2.7 Quantized value of estimated state x_2 when L=0.01.

estimated error covariance is given in Fig. 2.15, which shows the boundness of the norm of estimated error covariance.

The system trajectories are depicted in Fig. 2.16-Fig. 2.17 when parameter L is select as $L = 1000$. It is obvious that the system performance under the quantization scheme works badly. However, we can still guarantee the finiteness of the norm for the estimated error covariance although it is very large (see Fig. 2.18).

In the above simulations, it is clear that L is an essential factor in the performance of the closed-loop systems. When L is very small, such as $L = 0.01$, the performance of the closed-loop system with quantized feedback control is almost the same as the one with conventional feedback control (see Fig. 2.10 and Fig. 2.11). When $L = 1$, the norm of covariance of estimated error,

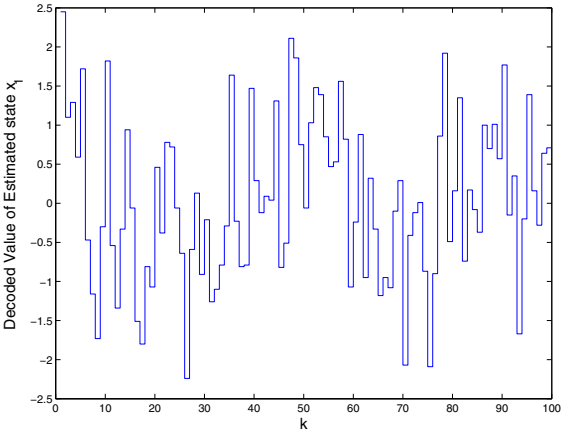

Fig. 2.8 Decoded value of estimated state x_1 when L=0.01.

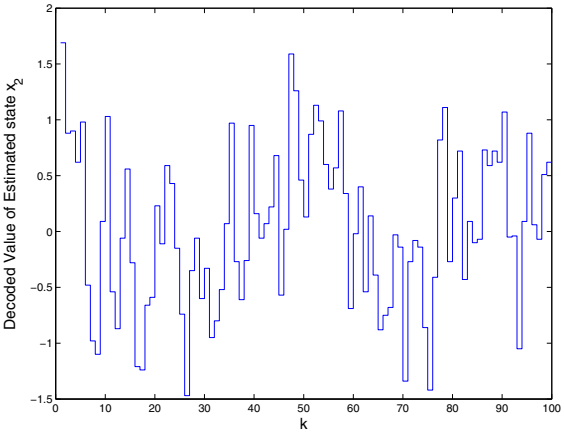

Fig. 2.9 Decoded value of estimated state x_2 when L=0.01.

$P(k)$, increases (see Fig. 2.15). While $L = 1000$, the norm of covariance of estimated error, $P(k)$, increases remarkably (see Fig. 2.18). It is worth to say that even if L is very large, for example $L = 1000$, the states of system are bounded although the bound is very large. This is reasonable, because if L is small, in this example, $L = 0.01$, the error induced by quantization is small, and it is helpful to decrease the bound of estimated state $\hat{x}(k|k)$ after quantizing. If L increases, however, the decoder performs is not so well. In fact, when $L > 1$, the bound of quantized estimated state $\hat{x}(k|k)$ becomes larger after quantizing, which brings the negative effect to the system. Therefore, it is very important to choose a suitable L for implementation in practice.

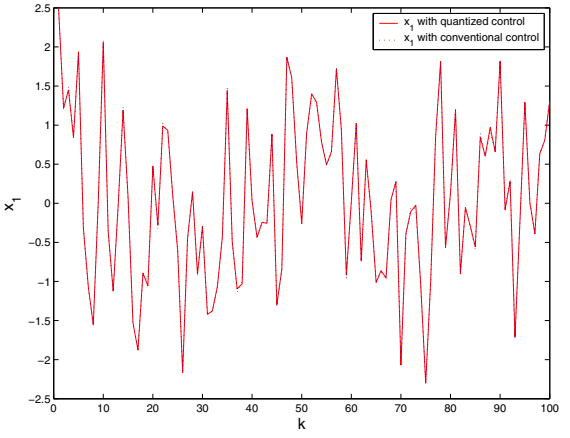

Fig. 2.10 x_1 with quantized control when L=0.01.

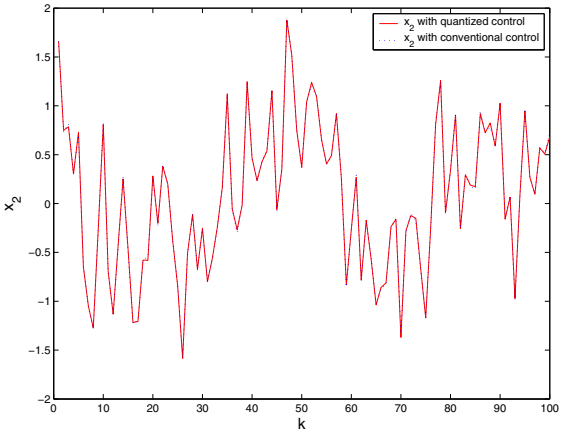

Fig. 2.11 x_2 with quantized control when L=0.01.

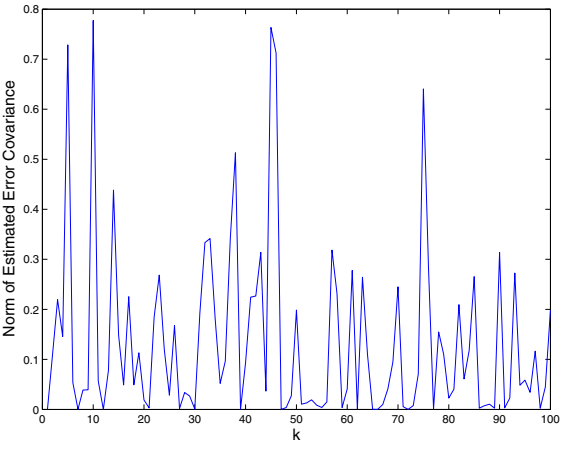

Fig. 2.12 Norm of estimated error covariance when L=0.01.

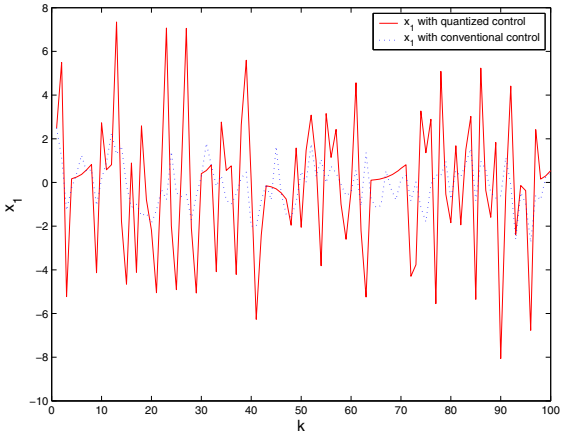

Fig. 2.13 x_1 with quantized control when L=1.

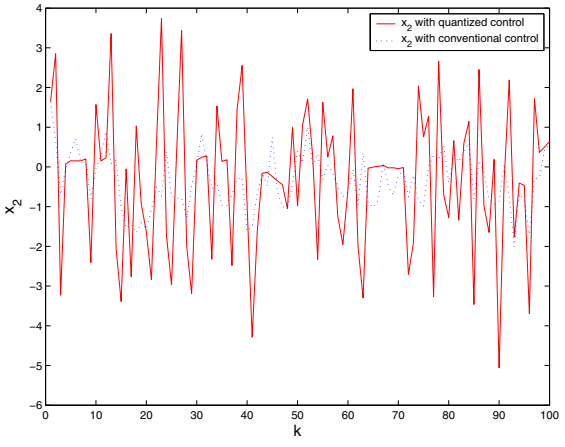

Fig. 2.14 x_2 with quantized control when L=1.

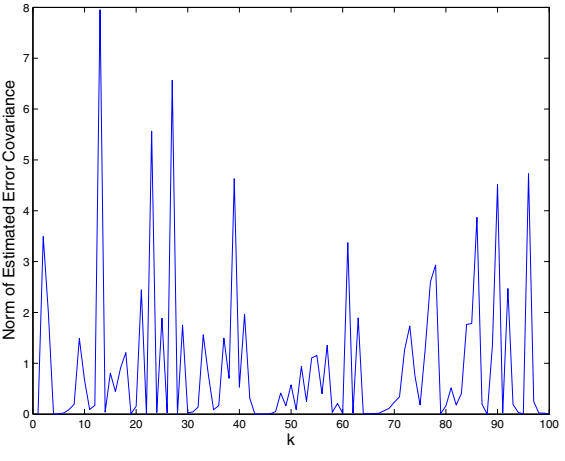

Fig. 2.15 Norm of estimated error covariance when L=1.

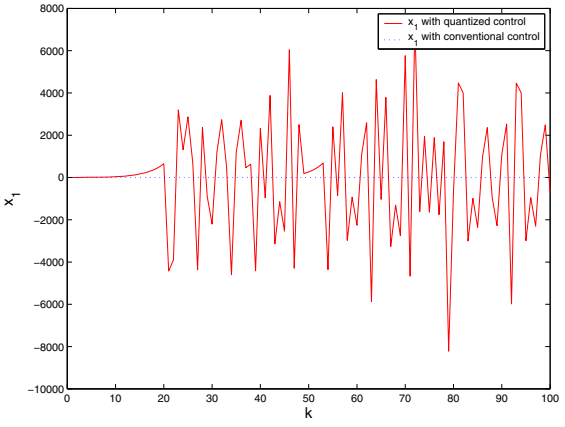

Fig. 2.16 x_1 with quantized control when L=1000.

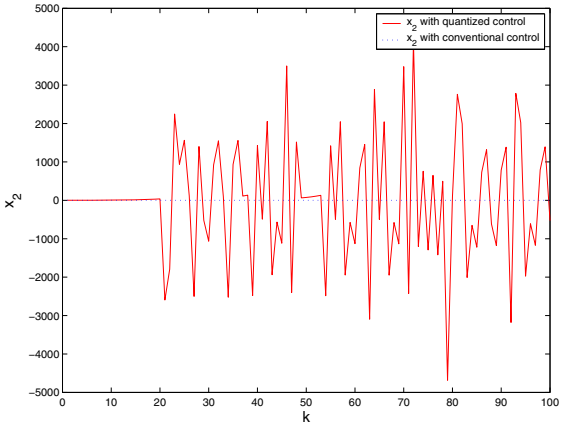

Fig. 2.17 x_2 with quantized control when L=1000.

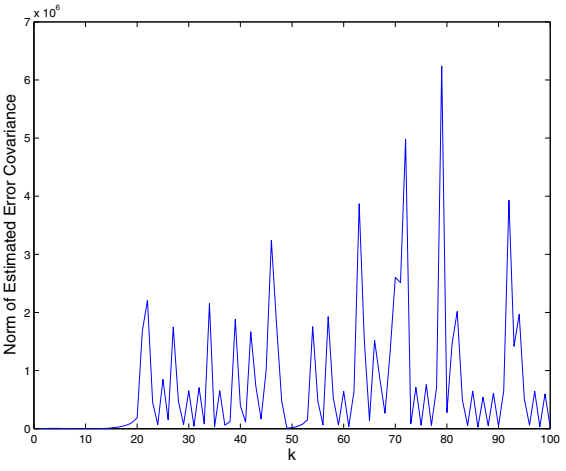

Fig. 2.18 Norm of estimated error covariance when L=1000.

2.6 Summary

In this chapter, the stability of closed-loop systems based on quantization feedback has been investigated. The Kalman filter is employed in this chapter to estimate states from noisy measurements on the sensor side. A simple quantization strategy is proposed to quantize the estimated states. The feedback control is designed based on quantized estimated states sent through network. Sufficient condition has been given to guarantee the stability of the closed-loop systems.

Chapter 3
Stabilization of Quantized Systems with Packet Dropout

3.1 Introduction

In recent years, NCSs have been actively investigated ([229, 236, 221, 161, 107, 198, 170, 210, 230, 58, 193, 202, 219, 206]). Due to the limited transmission capacity of the network and some devices in the closed-loop systems, data transmitted in practical NCSs should be quantized before they are sent to the next network node. Therefore, to achieve better performance of the considered systems, the effect of data quantization on the system should be taken into consideration. Furthermore, the network can be viewed as a web of unreliable transmission paths. Some packets not only suffer transmission delay but, even worse, can be lost during transmission. Thus, how such packet dropouts affect the performance of a NCS is an issue that must be studied.

Nowadays, there are two quantizers used frequently, one is logarithmic quantizer and another is uniform quantizer. Comparing logarithmic quantizer with the uniform one, it is not hard to see that the former one holds more advanced performance around origin and the later one is more easily to operate. Each quantizer has advantages and disadvantages. Some of the recent works about logarithmic quantizer include [40, 51, 86, 66, 67] and some ones relating to uniform quantizer are [17, 100, 43, 46, 101, 50].

The purpose of this chapter is to consider the quantization issue and packet dropout issue simultaneously. Some papers have already studied the two problems at the same time ([142, 61, 62, 132, 222, 182, 137, 181, 185, 14, 233, 212, 143, 25, 218]). The quantizers used in [142, 61, 62, 132, 222, 182, 137, 181, 185] are logarithmic ones. As to uniform quantizer, the problem of stabilizing linear systems by taking quantization and packet dropout together is studied in [14, 233, 212, 143, 25, 218]. Most of existing works considering quantization and packet dropout simultaneously do not study the effect of packet dropout rate on system performance. Reference [218] provid a sufficient and necessary condition to ensure the system to be asymptotically stabilizable in the mean square sense via quantized feedback. In [218], the relationship between packet dropout rate and eigenvalues of system matrix plays an important

Y. Xia, M. Fu, and G.-P. Liu: Analysis and Synthesis of NCSs, LNCIS 409, pp. 35–48.
springerlink.com

role. However, there is a strong assumption in [218], that is, all the eigenvalues of system matrix lie outside or on the unit circle. In fact, if the system is unstable, it can only ensure that there is at least one eigenvalue outside the unit circle. Furthermore, the quantization regions of uniform quantizer used in [218] hold rectangular shapes, which is not in general.

In this chapter, we will consider the mean square stability of linear discrete system affected by uniform quantization and packet dropout simultaneously and show that the packet dropout rate is important to the performance of system. The shapes of quantization regions considered here are arbitrary and there is no limit to the eigenvalues of system matrix. The Lyapunov method and "zoom" strategy which involved in [17] and [100] are used to guarantee the mean square stability of the discrete linear system. The "zoom" strategy is composed of two stages, i.e. "zooming-out" and "zooming-in". In the first stage, the range of quantizer is increased to guarantee that the states of system can be adequately measured, at this stage, the system is open-loop. In the second stage, the quantization error is decreased to drive the states to the origin, at this stage, the system is closed-loop. Because the quantization regions in [17] are rectilinear and the quantization regions with arbitrary shapes are considered in [100], the uniform quantizer used in this chapter will adopt the one introduced in [100]. Although the "zoom" strategy used here is the same as [17] and [100], the analysis process is more complex than [17] and [100] because of the consideration of packet dropout in this chapter.

The contents of this chapter are as follows. In Section 3.2 we introduce the quantizer used in this chapter. In Section 3.3 the problem considered here is given and the main result is shown in section 3.4. A numerical simulation is presented in section 3.5 to show the effectiveness of the main result. In section 3.6 we draw the conclusion.

Notations: R^n denotes the n-dimensional Euclidean space. The superscript "T" stands for matrix transposition. The notation $P > 0$ (≥ 0) means that P is a real symmetric positive definitive matrix (positive semi-definite). In symmetric block matrices, asterisk $*$ is used to represent a term that is induced by symmetry. We denote by $|\cdot|$ the standard Euclidean norm in R^n and by $\|\cdot\|$ the corresponding induced matrix norm in $R^{n\times n}$. $E\{x\}$ stands for the expectation of x. M_n denotes the set of all $n \times n$ matrices over C which represents the complex field.

3.2 Quantizer

Let $x(k)$ be the variable being quantized. A quantizer can be described by a piecewise constant function $q : R^n \to \Gamma$, where Γ is a finite subset of R^n with a fixed number of elements N. This leads to a partition of R^n into a finite number of quantization regions of the form $\{x(k) \in R^n : q(x(k)) = i, i \in \Gamma\}$. The quantization regions can be shown as Fig. 3.1

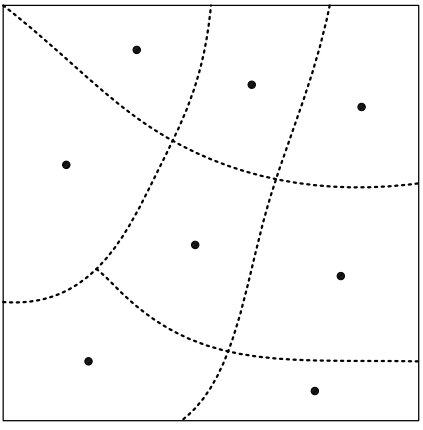

Fig. 3.1 The square domain denotes the set of states being quantized. Quantization regions are denoted by closed domains surrounding by dotted line. Every quantization region has a quantized value represented by a dot.

We assume that there exist positive real number M and $\triangle$ such that

I. If $|x(k)| \leq M$, then $|q(x(k)) - x(k)| \leq \triangle$;
II. If $|x(k)| > M$, then $|q(x(k))| > M - \triangle$.

Then the quantizer above is called a uniform quantizer, where M is saturation value and $\triangle$ means sensitivity. When $x(k)$ does not belong to the union of quantization regions of finite size, the quantizer saturates. So Condition I gives a bound on the quantization error when the quantizer does not saturate. Condition II provides a way to detect the possibility of saturation.

Remark 3.1. Generally speaking, quantizer $q : \mathbb{R} \to \mathbb{Z}$ with sensitivity $\triangle$ and saturation value M is defined as

$$q(x) = \begin{cases} M, & if\ x > (M - \frac{1}{2})\triangle, \\ -M, & if\ x \leq -(M - \frac{1}{2})\triangle, \\ \lfloor \frac{x}{\triangle} + \frac{1}{2} \rfloor, & if\ -(M - \frac{1}{2})\triangle < x \leq (M - \frac{1}{2})\triangle \end{cases} \tag{3.1}$$

It is obvious that the quantizer defined above satisfys Condition I and II and the quantization regions of the quantizer (3.1) are rectangular [100]. Because the quantization regions of uniform quantizer with Condition I and II have arbitrary shapes, the uniform quantizer is more useful and worthy to be considered.

Remark 3.2. Note the quantizer defined as (3.1) has some differences with the one in [17]. In fact, based on the analysis process of system performance, $(M + \frac{1}{2})\triangle$ should be changed to $(M - \frac{1}{2})\triangle$ in the definition of quantizer in [17].

In this chapter, we use quantized measurements of the form in [100], i.e.

$$q_\mu(x(k)) = \mu(k)q\left(\frac{x(k)}{\mu(k)}\right) \tag{3.2}$$

where $\mu(k) > 0$.

It is obvious that the following conditions about $q_\mu(\cdot)$ can be given:

III. If $|x(k)| \leq M\mu(k)$, then $|q_\mu(x(k)) - x(k)| \leq \triangle\mu(k)$;
IV. If $|x(k)| > M\mu(k)$, then $|q_\mu(x(k))| > M\mu(k) - \triangle\mu(k)$.

Remark 3.3. The role of $\mu(k)$ is to simply the analysis. In fact, for the quantizer satisfying the Condition I and II, the process of "zooming-out" stage is increasing M such that $|q(x(k))| \leq M - \triangle$, then the quantizer does not saturate, that is, $|x(k)| \leq M$, according to Condition II. Based on Condition I, we have $|q(x(k)) - x(k)| \leq \triangle$. In the stage of "zooming-in", $\triangle$ is decreased to ensure the stability of the system. When $\mu(k)$ is introduced, we just need to increase or decrease $\mu(k)$ rather than M and $\triangle$ in "zoom" strategy.

3.3 Problem Formulation

In this chapter, we will consider the following discrete-time linear system:

$$G : x(k+1) = Ax(k) + Bu(k). \tag{3.3}$$

where $x(k) \in R^n$ is the state vector, $u(k) \in R^n$ is the control input, A and B are matrices of suitable dimensions. Assume that A is unstable and (A, B) is stabilizable.

The following control law will be considered

$$u(k) = \theta(k)Kq_\mu(x(k)) \tag{3.4}$$

where $q_\mu(\cdot)$ is defined as (3.2) and $\theta(k)$ is a 0-1 random variable with probability distribution given by

$$Pr(\theta(k) = i) = \begin{cases} \alpha, & i = 0, \\ 1 - \alpha, & i = 1, \end{cases} \quad 0 \leq \alpha < 1. \tag{3.5}$$

when $\theta(k) = 0$, the packet dropout occurs and the control law $u(k) = 0$, otherwise $u(k) = Kq_\mu(x(k))$, that is

$$\begin{aligned} &Pr(u(k) = 0) = \alpha \\ &Pr(u(k) = Kq_\mu(x(k))) = 1 - \alpha \end{aligned} \tag{3.6}$$

Then system (3.3) with control law (3.2) can be given as

$$x(k+1) = Ax(k) + B\theta(k)Kq_\mu(x(k)) \tag{3.7}$$

We explain how the control signal is processed when it is transmitted from a controller to the input side of G according to Fig. 3.2.

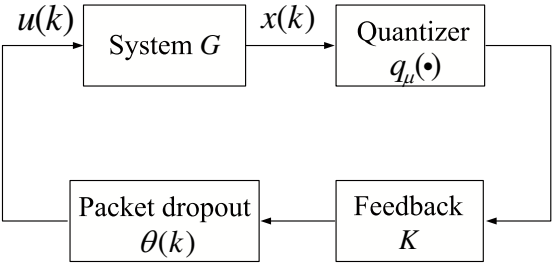

Fig. 3.2 Stabilization via quantized signals with stochastic losses.

Definition 3.4. System (3.7) is said to be mean square stable if

$$lim_{k\to\infty} E\{|x(k)|^2\} = 0 \tag{3.8}$$

for any initial state $x(0) \in R^n$.

As we can see, system (3.7) is affected by quantization and packet dropout simultaneously, then we will consider the problem of which conditions the packet dropout rate α should satisfy to ensure that the states of the closed-loop system (3.7) is mean square stable.

Lemma 3.5. *The following inequality holds for any positive matrix P and matrices E and F:*

$$E^T PF + F^T PE \leq E^T PE + F^T PF. \tag{3.9}$$

Definition 3.6. [74] The spectral radius $\rho(A)$ of a matrix $A \in M_n$ is

$$\rho(A) \equiv max\{|\lambda| : \lambda \; is \; an \; eigenvalue \; of \; A\} \tag{3.10}$$

where $|\lambda|$ denotes the amplitude of λ.

Lemma 3.7. *[74] If $\|\cdot\|_*$ is any matrix norm and if $A \in M_n$, then $\| A \|_* \geq \rho(A)$.*

Remark 3.8. If the following system

$$x(k+1) = Ax(k) \tag{3.11}$$

is unstable, then there is at least one eigenvalue $\tilde{\lambda}$ for which $|\tilde{\lambda}| > 1$. Based on Definition 3.6 and Lemma 3.7, we have $\| A \|_* \geq \rho(A) > 1$, especially, $\| A \| > 1$.

3.4 Main Results

In this section, the main result is given as Theorem 3.9.

Theorem 3.9. *Consider system (3.7), for a given packet dropout rate α, if there exist a matrix Ψ and a positive matrix Ξ satisfying*

$$\begin{bmatrix} -\Xi & (A\Xi + B\Psi)^T & (B\Psi)^T \\ * & -\frac{1}{2}\Xi & 0 \\ * & * & -\frac{1}{2\alpha}\Xi \end{bmatrix} < 0 \tag{3.12}$$

then we let $K = \Psi\Xi^{-1}$, the closed-loop system (3.7) is mean square stable.

Proof: The system (3.7) can be rewritten as

$$x(k+1) = (A + BK)x(k) - BKx(k)(1 - \theta(k)) + BK\theta(k)s(x(k)) \tag{3.13}$$

where the "error" vector $s(x(k)) = q_\mu(x(k)) - x(k)$.

In the following, we will use "zoom" strategy in [17] and [100] to prove the mean square stability of system (3.7).

The "zooming-out" stage: If we let $u(k) = 0$ and increase $\mu(k)$ fast enough to dominate the rate of growth of $\|A\|^k$, that is, $\mu(0) = 1$ and $\mu(k) = \|A\|^k$, then based on $\| A \| > 1$, there exists a positive integer k such that

$$\left|\frac{x(k)}{\mu(k)}\right| \leq M\sqrt{\frac{\lambda_{min}(P)}{\lambda_{max}(P)}} - 2\triangle \tag{3.14}$$

hence

$$\left|q(\frac{x(k)}{\mu(k)})\right| \leq \left|\frac{x(k)}{\mu(k)}\right| + \triangle \leq M\sqrt{\frac{\lambda_{min}(P)}{\lambda_{max}(P)}} - \triangle \tag{3.15}$$

Thus, we can define

$$k_0 = min\left\{k \geq 1 : \left|q(\frac{x(k)}{\mu(k)})\right| \leq M\sqrt{\frac{\lambda_{min}(P)}{\lambda_{max}(P)}} - \triangle\right\} \tag{3.16}$$

It is obvious that

$$\left|q(\frac{x(k_0)}{\mu(k_0)})\right| \leq M\sqrt{\frac{\lambda_{min}(P)}{\lambda_{max}(P)}} - \triangle \tag{3.17}$$

hence

$$\left|\frac{x(k_0)}{\mu(k_0)}\right| \leq \left|q(\frac{x(k_0)}{\mu(k_0)})\right| + \triangle \leq M\sqrt{\frac{\lambda_{min}(P)}{\lambda_{max}(P)}} \tag{3.18}$$

that is

$$|x(k_0)| \leq M\mu(k_0)\sqrt{\frac{\lambda_{min}(P)}{\lambda_{max}(P)}} \tag{3.19}$$

Therefore, $x(k_0)$ belongs to the ellipsoid

$$R_1 = \{x(k) : x^T(k)Px(k) \leq M^2\mu^2(k_0)\lambda_{min}(P)\} \tag{3.20}$$

In the following part, we will prove that R_1 is a invariant region, that is, if we let $u(k) = \theta(k)Kq_{\mu(k)}x(k)$ with $\mu(k) = \mu(k_0)$ for $k \geq k_0$, then $x(k)$ will not leave R_1.

Based on (3.20), it is obvious that

$$|x(k)| \leq M\mu(k) \tag{3.21}$$

holds with $\mu(k) = \mu(k_0)$ for all $x(k) \in R_1$, which means the quantizer does not saturate, then based on the Condition III, we have

$$|s(x(k))| \leq \triangle\mu(k) \tag{3.22}$$

for all $x(k) \in R_1$.

Let $V(x(k)) = x^T(k)Px(k)$, where $P = \Xi^{-1}$, it is obvious that P is a positive matrix.

Based on (3.5) and $E\{(\theta(k))^2\} = E\{\theta(k)\} = 1 - \alpha$, we have

$$\begin{aligned}
&\Delta V(x(k)) \\
&= E\{x^T(k+1)Px(k+1)\} - x^T(k)Px(k) \\
&= x^T(k)[(A+BK)^TP(A+BK) - P + \alpha K^TB^TPBK \\
&\quad -\alpha K^TB^TP(A+BK) - \alpha(A+BK)^TPBK]x(k) \\
&\quad +(1-\alpha)s^T(x(k))K^TB^TPBKs(x(k)) \\
&\quad +(1-\alpha)s^T(x(k))K^TB^TP(A+BK)x(k) \\
&\quad +(1-\alpha)x^T(k)(A+BK)^TPBKs(x(k))
\end{aligned} \tag{3.23}$$

Let $E = -BK$, $F = (A+BK)$, $M = BKs(x(k))$ and $N = (A+BK)x(k)$, the following inequalities can be given by Lemma 3.5:

$$\begin{aligned}
&-\alpha K^TB^TP(A+BK) - \alpha(A+BK)^TPBK \\
&< \alpha K^TB^TPBK + \alpha(A+BK)^TP(A+BK)
\end{aligned} \tag{3.24}$$

$$\begin{aligned}
&(1-\alpha)s^T(x(k))K^TB^TP(A+BK)x(k) \\
&\quad +(1-\alpha)x^T(k)(A+BK)^TPBKS(x(k)) \\
&< (1-\alpha)s^T(x(k))K^TB^TPBKs(x(k)) \\
&\quad +(1-\alpha)x^T(k)(A+BK)^TP(A+BK)x(k)
\end{aligned} \tag{3.25}$$

Based on (3.23), (3.24) and (3.25), it is obvious that

$$\begin{aligned}
\Delta V(x(k)) \leq\ & x^T(k)[2(A+BK)^TP(A+BK) - P + 2\alpha K^TB^TPBK]x(k) \\
& +2(1-\alpha)s^T(x(k))K^TB^TPBKs(x(k))
\end{aligned} \tag{3.26}$$

Define $\Lambda = diag\{P, I, I\}$ and pre–multiplying and post-multiplying (3.12) by Λ give

$$\begin{bmatrix} -P & (A+BK)^T & (BK)^T \\ * & -\frac{1}{2}P^{-1} & 0 \\ * & * & -\frac{1}{2\alpha}P^{-1} \end{bmatrix} < 0 \tag{3.27}$$

Then based on Schur complement and (3.27), we can see that

$$2(A+BK)^T P(A+BK) - P + 2\alpha K^T B^T PBK < 0, \tag{3.28}$$

which means that there exists a positive matrix $\tilde{Q}$, such that

$$2(A+BK)^T P(A+BK) - P + 2\alpha K^T B^T PBK = -\tilde{Q} < 0 \tag{3.29}$$

Then

$$\begin{aligned} &\Delta(V(x(k))) \\ &\leq -x^T(k)(\tilde{Q})x(k) + 2(1-\alpha)s^T(x(k))K^T B^T PBKs(x(k)) \\ &\leq -\lambda_{min}(\tilde{Q})|x(k)|^2 + 2(1-\alpha) \parallel K^T B^T PBK \parallel \triangle^2 \mu^2(k) \end{aligned} \tag{3.30}$$

The last expression is negative outside the ball $\mathbf{B} = \{x(k) : |x(k)| \leq \Phi \triangle \mu(k)\}$, where

$$\Phi = \left(\frac{2(1-\alpha)}{\lambda_{min}(\tilde{Q})} \parallel K^T B^T PBK \parallel \right)^{\frac{1}{2}} \tag{3.31}$$

Define the scaling factor Ω by the formula

$$\Omega = \sqrt{\frac{\lambda_{max}(P)}{\lambda_{min}(P)}} \sqrt{\Phi^2 + \epsilon} \triangle M^{-1} \tag{3.32}$$

for some fixed $\epsilon > 0$, and take M of $\triangle$ to be large enough such that $\Omega < 1$, we have $R_1 \supset \mathbf{B}$ and R_1 is a invariant region. It follows that if we let $u(k) = \theta(k)Kq_{\mu(k)}x(k)$ with $\mu(k) = \mu(k_0)$ for $k \geq k_0$, then $x(k)$ will not leave R_1.

The "zooming-in" stage:

Define

$$\tilde{\tau} = \frac{M^2 \lambda_{min}(P) - \triangle^2 \Phi^2 \lambda_{max}(P)}{\lambda_{min}(\tilde{Q}) \triangle^2 \epsilon}. \tag{3.33}$$

Since $\Omega < 1$, it is easy to see that $\tilde{\tau} > 0$. Define $\tau = \lceil \tilde{\tau} \rceil$, where $\lceil \cdot \rceil$ denotes the smallest integer which satisfying $\tau \geq \tilde{\tau}$, it is obvious that $\tau \in Z_{\geq 0}$.

We claim that the following inequality can be given for the τ defined above,

$$E\{x^T(k_0+\tau)Px(k_0+\tau)\} \leq \triangle^2 \mu^2(k_0)(\Phi^2 + \epsilon)\lambda_{max}(P) \tag{3.34}$$

where ϵ is defined in (3.32).

Define

$$\tilde{R}_2 = \{x(k) : E\{x^T(k)Px(k)\} \leq \triangle^2 \mu^2(k_0)(\Phi^2 + \epsilon)\lambda_{max}(P)\} \tag{3.35}$$

It is obvious that $\tilde{R}_2$ is a invariant region based on $\tilde{R}_2 \supset B$ for all $k_0 \leq k \leq k_0 + \tau$. Suppose that (3.34) is not true. Then for $\tau \in Z_{\geq 0}$, we have

$$E\{x^T(k_0+\tau)Px(k_0+\tau)\} > \triangle^2\mu^2(k_0)(\Phi^2+\epsilon)\lambda_{max}(P) \tag{3.36}$$

Therefore

$$E\{|x(k)|^2\} > \triangle^2\mu^2(k_0)(\Phi^2+\epsilon) \tag{3.37}$$

for all $k_0 \leq k \leq k_0 + \tau$. Based on (3.30) and $\Omega < 1$, we can see that

$$\begin{aligned} &\Delta V(x(k_0+\tau-1)) \\ &= E\{x^T(k_0+\tau)Px(k_0+\tau)\} - E\{x^T(k_0+\tau-1)Px(k_0+\tau-1)\} \\ &\leq -\lambda_{min}(\tilde{Q})E\{|x(k_0+\tau-1)|^2\} + \lambda_{min}(\tilde{Q})\Phi^2\triangle^2\mu^2(k_0) \\ &< -\lambda_{min}(\tilde{Q})\triangle^2\mu^2(k_0)(\Phi^2+\epsilon) + \lambda_{min}(\tilde{Q})\Phi^2\triangle^2\mu^2(k_0) \\ &= -\lambda_{min}(\tilde{Q})\triangle^2\mu^2(k_0)\epsilon \end{aligned} \tag{3.38}$$

Similarly, we have

$$\begin{aligned} &\Delta V(x(k_0+\tau-i)) \\ &= E\{x^T(k_0+\tau-i+1)Px(k_0+\tau-i+1)\} \\ &\quad -E\{x^T(k_0+\tau-i)Px(k_0+\tau-i)\} \\ &\leq -\lambda_{min}(\tilde{Q})E\{|x(k_0+\tau-i)|^2\} + \lambda_{min}(\tilde{Q})\Phi^2\triangle^2\mu^2(k_0) \\ &< -\lambda_{min}(\tilde{Q})\triangle^2\mu^2(k_0)\epsilon \end{aligned} \tag{3.39}$$

where $i \in \{1, 2, 3, \cdots, \tau\}$.
Then the following inequality can be given

$$\begin{aligned} &E\{x^T(k_0+\tau)Px(k_0+\tau)\} - x^T(k_0)Px(k_0) \\ &< -\lambda_{min}(\tilde{Q})\triangle^2\mu^2(k_0)\epsilon\cdot\tau \\ &\leq -\lambda_{min}(\tilde{Q})\triangle^2\mu^2(k_0)\epsilon\cdot\tilde{\tau} \\ &= \triangle^2\Phi^2\lambda_{max}(P)\mu^2(k_0) - M^2\lambda_{min}(P)\mu^2(k_0) \end{aligned} \tag{3.40}$$

But (3.20), (3.36) imply that

$$\begin{aligned} \Delta V(x(k_0)) &= E\{x^T(k_0+\tau)Px(k_0+\tau)\} - x^T(k_0)Px(k_0) \\ &> \triangle^2\mu^2(k_0)(\Phi^2+\epsilon)\lambda_{max}(P) - \mu^2(k_0)M^2\lambda_{min}(P) \\ &> \triangle^2\Phi^2\lambda_{max}(P)\mu^2(k_0) - M^2\lambda_{min}(P)\mu^2(k_0) \end{aligned} \tag{3.41}$$

Comparing (3.40) and (3.41), we arrive at a contradiction, which establishes the validity of (3.34).
Based on $\Omega < 1$, for the $\tau \in Z_{\geq 0}$, we have

$$\begin{aligned} E\{x^T(k_0+\tau)Px(k_0+\tau)\} &\leq \triangle^2\mu^2(k_0)(\Phi^2+\epsilon)\lambda_{max}(P) \\ &< (\Omega\mu(k_0))^2M^2\lambda_{min}(P) \end{aligned} \tag{3.42}$$

that is

$$E\{x^T(k_0+\tau)Px(k_0+\tau)\} < (\Omega\mu(k_0))^2M^2\lambda_{min}(P) \tag{3.43}$$

Then $x(k_0+\tau)$ belongs to

$$R_2 = \{x(k) : E\{x^T(k)Px(k)\} \leq (\Omega\mu(k_0))^2 M^2 \lambda_{min}(P)\} \tag{3.44}$$

Thus we let $u(k) = K\theta q_\mu(x(k))$ with $\mu(k) = \Omega\mu(k_0)$ for $k_0+\tau \leq k < k_0+2\tau$, similar to above analysis, we have

$$E\{x^T(k_0+2\tau)Px(k_0+2\tau)\} < (\Omega^2\mu(k_0))^2 M^2 \lambda_{min}(P) \tag{3.45}$$

Similarly, let $\mu(k) = \Omega^{i-1}\mu(k_0)$ for $k_0+(i-1)\tau \leq k < k_0+i\tau$, we have

$$E\{x^T(k_0+i\tau)Px(k_0+i\tau)\} < (\Omega^i\mu(k_0))^2 M^2 \lambda_{min}(P) \tag{3.46}$$

Repeating this procedure, it is obvious that $\mu(k) \to 0$ as $k \to \infty$ which means $i \to \infty$, and the closed-loop system (3.7) is mean square stable, that is, $lim_{k\to\infty} E\{|x(k)|^2\} = 0$. ■

Remark 3.10. According the proof of Theorem 3.9, if the initial state $x(0)$ is not saturate, then we can omit "zooming-out" strategy and select $k_0 = 1$.

Remark 3.11. As we can see, the packet dropout just occurs at the input side in the above analysis. Then what will happen if the packet dropout exists at the both sides of the input and output? In the following, we will consider the system shown as Fig.3.3.

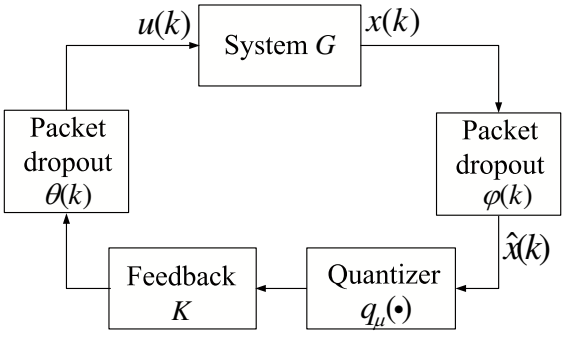

Fig. 3.3 Stabilization via quantized signals with stochastic losses occurred at the both sides.

Where $q_\mu(\cdot)$ and $\theta(\cdot)$ are defined as above and $\hat{x}(k) = \varphi(k)x(k)$, where $\varphi(\cdot)$ is a 0-1 random variable with probability distribution given by

$$Pr(\varphi(k) = i) = \begin{cases} \beta, & i = 0, \\ 1-\beta, & i = 1, \end{cases} \quad 0 \leq \beta < 1. \tag{3.47}$$

When $\varphi(k) = 0$, the packet dropout occurs and $\hat{x}(k) = 0$, otherwise $\hat{x}(k) = x(k)$.

It is easily to see that the control law $u(k) = \theta(k)Kq_\mu(\varphi(k)x(k))$ has the following property:

$$u(k) = \begin{cases} 0 & when\ \theta(k) = 0, \varphi(k) = 0 \\ 0 & when\ \theta(k) = 1, \varphi(k) = 0 \\ 0 & when\ \theta(k) = 0, \varphi(k) = 1 \\ Kq_\mu(x(k)) & when\ \theta(k) = 1, \varphi(k) = 1 \end{cases} \tag{3.48}$$

that is

$$\begin{aligned} &Pr(u(k) = 0) = \alpha + \beta - \alpha\beta \\ &Pr(u(k) = Kq_\mu(x(k))) = 1 - \alpha - \beta + \alpha\beta \end{aligned} \tag{3.49}$$

Comparing (3.49) with (3.6) and based on Theorem 3.9, it is obvious that for the given packet dropout rate α and β, if there exist a matrix $\tilde{\Psi}$ and a positive matrix $\tilde{\Xi}$ satisfying

$$\begin{bmatrix} -\tilde{\Xi} & (A\tilde{\Xi} + B\tilde{\Psi})^T & (B\tilde{\Psi})^T \\ * & -\frac{1}{2}\tilde{\Xi} & 0 \\ * & * & -\frac{1}{2(\alpha+\beta-\alpha\beta)}\tilde{\Xi} \end{bmatrix} < 0 \tag{3.50}$$

let $K = \tilde{\Psi}\tilde{\Xi}^{-1}$, system (3.3) under control law $u(k) = \theta(k)Kq_\mu(\varphi(k)x(k))$ is mean square stable.

3.5 Numerical Example

Example 3.12. In this example, we consider an application of the method proposed in this chapter to the following discrete-time system

$$x(k+1) = Ax(k) + Bu(k) \tag{3.51}$$

where

$$A = \begin{bmatrix} 0.1 & -0.4 & -0.2 \\ 0 & 1.5 & -0.1 \\ 0.1 & 0.1 & -0.1 \end{bmatrix} \quad B = \begin{bmatrix} 0.5 & 0 \\ 0.5 & 1 \\ 1 & 0.5 \end{bmatrix} \tag{3.52}$$

The eigenvalues of A are 0.0022+0.1156i, 0.0022-0.1156i and 1.4956, it is obvious that the system (3.51) is unstable. The system is stabilizable since $rank[B\ AB\ A^2B] = 3$.

If packet dropout rate $\alpha = 0.2$, there exist positive matrics

$$\Xi = \begin{bmatrix} 0.7244 & -0.0287 & 0.0020 \\ -0.0287 & 0.5054 & 0.0223 \\ 0.0020 & 0.0223 & 0.7033 \end{bmatrix} \tag{3.53}$$

and

$$\Psi = \begin{bmatrix} -0.1119 & 0.3407 & 0.1232 \\ 0.0893 & -0.7548 & -0.0481 \end{bmatrix} \tag{3.54}$$

satisfying (3.12), then system (3.51) under control $u(k) = \theta(k)Kq_\mu(\varphi(k)x(k))$ is mean square stable based on Theorem 3.9 and K is defined as

$$K = \begin{bmatrix} -0.1288 & 0.6600 & 0.1546 \\ 0.0643 & -1.4889 & -0.0213 \end{bmatrix} \tag{3.55}$$

Here, the quantizer is selected as

$$q_\mu(x_i(k)) = \begin{cases} 3\mu(k)sgn\{x_i(k)\}, \ if \ |x_i(k)| > 3\mu(k), \\ \left\lfloor x_i(k) + \frac{1}{2}\mu(k) \right\rfloor, \ if \ |x_i(k)| \leq 3\mu(k). \end{cases} \tag{3.56}$$

where $x_i(k)$ is the ith component of $x(k)$ and $sgn\{x_i(k)\}$ is a symbolic function. It is obvious that Condition III and IV are satisfied with $M = 3$ and $\triangle = 0.5$.

When $\epsilon = 0.1$, we have $\Omega = 0.6660 < 1$. Let initial state $x(0) = [7\ 8\ 7]^T$ and $\mu(k) = \| A \|^k$, it is obvious that $x(0)$ is saturate, that is, $|x(0)| > M\mu(0)$. Then based on "zooming-out" strategy, a unsaturate time k_0 which satisfying (3.19) can be shown as Fig. 3.4.

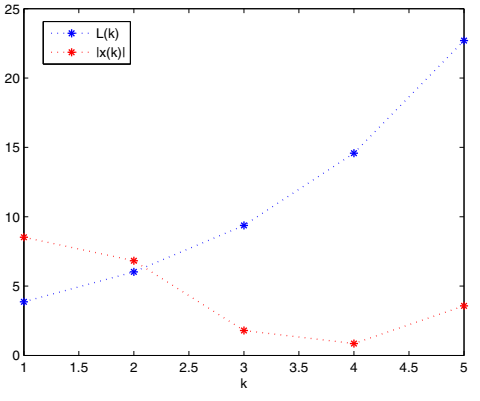

Fig. 3.4 The selection of k_0.

In Fig. 3.4, $L(k) = M\mu(k)\sqrt{\frac{\lambda_{min}(P)}{\lambda_{max}(p)}}$ and $k_0 = 3$ is the smallest k satisfying (3.19). Then based on "zoom" strategy, $\mu(k)$ can be shown as Fig. 3.5 according to $k_0 = 3$ and $\tau = 1$.

Then the mean square of $x(k)$ can be shown as Fig. 3.6 and system (3.51) is mean square stable.

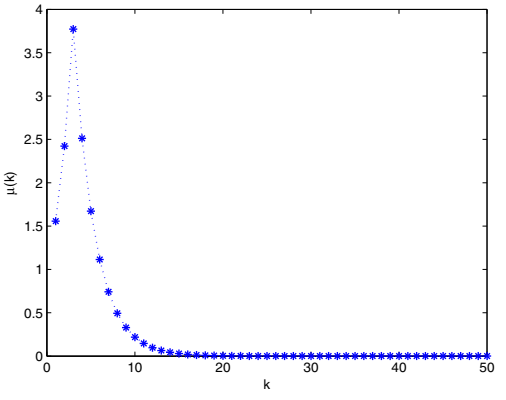

Fig. 3.5 $\mu(k)$ in "zoom" strategy.

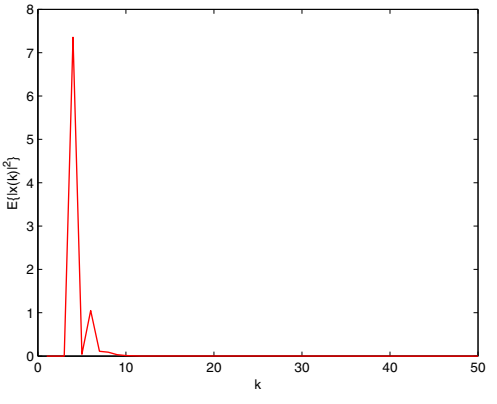

Fig. 3.6 The mean square of $x(k)$.

Remark 3.13. Note that when $u(k)=\theta(k)Kq_\mu(\varphi(k)x(k))$, the states of closed-loop will be influenced by random variable $\theta(k)$, then the states trajectory will be random. Therefore, the k_0 selected is random and $\mu(k)$ must be adjusted according to k_0.

Remark 3.14. If the initial state is selected as $x(0) = [1\ 2\ 1]^T$, then based on Fig. 3.7, k_0 is selected as 1 and the "zooming-out" strategy can be omitted.

If packet dropout rate $\alpha = 0.3$, we have

$$\begin{bmatrix} -\Xi & (A\Xi + B\Psi)^T & (B\Psi)^T \\ * & -\frac{1}{2}\Xi & 0 \\ * & * & -\frac{1}{2\alpha}\Xi \end{bmatrix} > 0 \tag{3.57}$$

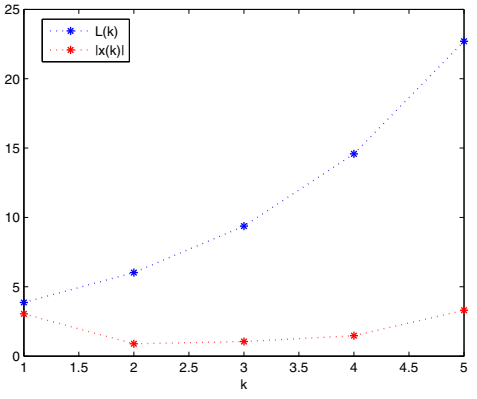

Fig. 3.7 The selection of k_0.

for all matrices Ψ and positive matrices Ξ, so Theorem 3.9 is not useful to verify the mean square stability of system (3.51).

Remark 3.15. In fact, when initial state $x(0) = [7\ 8\ 7]^T$, we can solve the largest packet dropout $\alpha \approx 0.2741$ to ensure the mean square stability of the closed-loop system (3.51), that is, if the packet dropout rate $\alpha \leq 0.2741$, the closed-loop system (3.51) is mean square stable, otherwise, Theorem 1 is invalid to verify the mean square stability of system (3.51).

3.6 Summary

In this chapter, the problem of mean square stability of linear discrete system with quantization and packet dropout is considered. For a given packet dropout rate, a sufficient condition is given to ensure that the closed loop system is mean square stable. The "zoom" strategy is used here, which was based on the hypothesis that it is possible to change the sensitivity $\triangle\mu(k)$ and saturation value $M\mu(k)$ of the quantizer. Based on (3.12) and (3.50), the largest packet dropout rate can be given to ensure the mean square stability of closed-loop system. However, the condition given in main Theorem is a sufficient one, the sufficient and necessary is worthy to be considered in future. Because the form of packet dropout considered in this chapter is simple, some "representation complexity" of packet dropout needs to be developed and taken into account. The system considered here is linear discrete, so the nonlinear systems can be studied in future.

Chapter 4
Stabilization of Systems with Quantized Feedback and Measurements

4.1 Introduction

As we know, two quantizers are used frequently. The uniform quantizer is introduced in above chapter, as for logarithmic quantizer, wonderful results have been obtained. In [40], a logarithmic quantizer is firstly presented for stabilization of a linear discrete-time system. Ref. [51] shows an alternative proof for the optimal design and extends the results to quantized output feedback and quantized quadratic performance control using the sector bound method. Output feedback control of discrete-time linear systems using a finite-level quantizer is studied in [52]. A new approach based on sector bound method is used to analyze the stability of quantized feedback control systems in [237]. Remote control system affected by quantized signal is considered in [86]. Based on a quantization dependent Lyapunov function, the study on stability analysis of quantized feedback control system is given in [55]. The problems of discontinuous stabilization and robust stabilization of nonlinear systems are discussed in [21] and [139], respectively. Ref. [57] considers the problem of dynamic out-feedback stabilization of NCSs. In [66] and [67], the adaptive quantized control is considered and an adaptive feedback control law is given to ensure Lyapunov stable and $x(k) \to 0$ as $k \to \infty$. In [185], quantization and packet dropout are considered simultaneously, packet losses rate and unstable poles of the plant are considered to ensure different stability of the system, such as stochastically quadratically stable and mean square practically stable.

Note that most of results just considered the network exists at one side of systems, i.e. input inside or output side. In fact, the network always exists at the both sides in practice. So a quantized input computed from quantized measurements (QIQM) system in accordance with network exists at both sides is necessary to be considered.

In Ref. [223], the guaranteed cost control design (GCCD) problem of linear system, which is affected by both quantized input and quantized output, is considered. Based on linear matrix inequation, a sufficient condition is given

Y. Xia, M. Fu, and G.-P. Liu: Analysis and Synthesis of NCSs, LNCIS 409, pp. 49–71.
springerlink.com

to ensure the GCCD problem for system with a network-based quantized controller is solvable. Ref. [33] investigates the case of feedback control systems subject to both input and output quantization. Based on sector bound approach, a sufficient and necessary condition for quadratic stabilization of closed-loop system is given. But the condition given in [33] is hard to verified because of the uncertainty of variables. So, in this chapter, another method, which is proposed in [146], is used to analyze the stability of closed-loop system. Note that quantizer used in [146] is a uniform one, which is simpler implement but holds lower performance compared to logarithmic quantizer. Therefore, in order to improve the performance of system, the logarithmic quantizer is more useful than uniform quantizer when network exists at the both sides of system.

In this chapter, the globally asymptotic stability of QIQM system is analyzed and a sufficient condition is given to ensure the stability. The quantizer used here is a logarithmic one and a nonnegative and bounded multiplier plays an important role in the process of stability analysis. Attention of this chapter is restricted to linear discrete-time system, which is open-loop stable and affected by network at both input and output sides. Note that network is necessary to be inserted although the open-loop is stable in some situations, such as remote control system. Therefore the problem considered here holds it's own practical meanings.

The contents of this chapter are as follows. In Section 4.2 we introduce QIQM system and quantizer used in this chapter. In Section 4.3 the stability of system is analyzed and a sufficient condition is given for globally asymptotically stable of closed-loop system. A numerical simulation is presented in Section 4.4 to show the effectiveness of the main results and the conclusion is drawn in Section 4.5.

4.2 QIQM System Description

In this chapter, we will consider the system with network exists at both input and output sides. Because of the existence of network, quantization is necessary to be considered and framework of system can be shown as Fig. 4.1.

The system shown as above can be seen as a QIQM system:

$$\Sigma_0 : \begin{cases} x(k+1) = Ax(k) + Bu(k) \\ u(k) = -Q(F\mathcal{Q}(x(k))) \end{cases} \tag{4.1}$$

where $x(k)$ is the n-dimensional state vector, A is a square matrix with eigenvalues inside the unit circle, B is an n-by-1 vector and $F \in R^{n\times 1}$ is a state feedback matrix. The mapping $Q : R \to R$ is a logarithmic quantizer

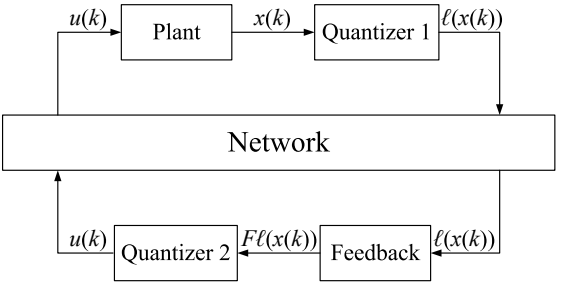

Fig. 4.1 System description.

with a dead-zone around origin. Similar to quantizer used in [185], $Q(\cdot)$ can be expressed as:

$$Q(z) = \begin{cases} v_i, & z \in [\frac{\rho+1}{2\rho}v_i, \frac{\rho+1}{2}v_i) \\ -v_i, & z \in (-\frac{\rho+1}{2}v_i, -\frac{\rho+1}{2\rho}v_i] \\ 0, & z \in (-v, v) \end{cases} \tag{4.2}$$

$v_i = \rho^i v_0, v_0 > 0, i \in Z_{\geq 0}$.

Where the coarseness $\rho > 1$ and $v = \frac{\rho+1}{2\rho}v_0$.

The logarithmic quantizer $Q(\cdot)$ can be shown as Fig. 4.2

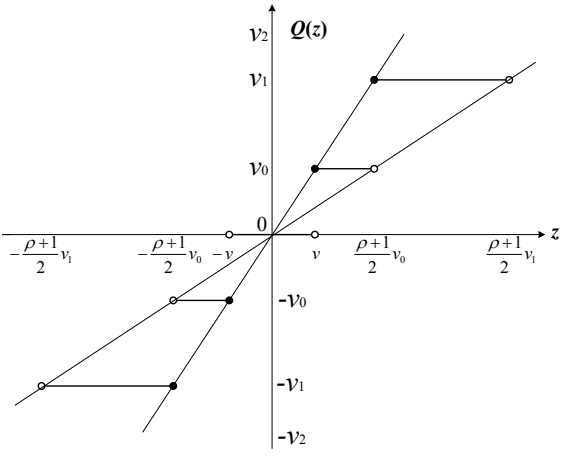

Fig. 4.2 Logarithmic quantizer with dead-zone.

The mapping $\mathcal{Q} : R^n \to R^n$ is the vector quantization function satisfying:

$$\mathcal{Q}(x) = \xi, where\ \xi_i = Q(x_i). \tag{4.3}$$

Remark 4.1. Note that the logarithmic quantizer considered here is different from traditional quantizer used in [40] and [51], where quantization coarseness $\rho < 1$ and quantization levels decrease monotonously. But in this chapter, quantization levels increase monotonously according to $\rho > 1$. In fact, the quantizer described as (4.2) is the same as traditional quantizer essentially and ρ considered here is equal to $\frac{1}{\rho}$ in [40] and [51]. Comparing to [185], quantization regions are different from each other, but the changes do not influence the performance of quantizer. The changes here are just to facilitate the discussion.

4.3 Stability of QIQM System

4.3.1 Construction of an Equivalent System and a Multiplier

Define the following system:

$$L_1 : \begin{cases} x(k+1) = Ax(k) + B\tilde{u}(k) \\ y(k) = Fx(k) + d\tilde{u}(k) \end{cases} \tag{4.4}$$

where $\tilde{u}(k)$ is the same as $u(k)$ defined in (4.1) and d is a parameter to be determined, it is obvious that the state trajectory of (4.4) is equal to the one of (4.1) according to the same initial state.

Then we have the following Lemma.

Lemma 4.2. *There exists a mapping $\alpha : R^n \to R$, called multiplier, such that*

$$\tilde{u}(k) = -Q[\alpha(x(k))y(k)] = u(k), \ \forall k \tag{4.5}$$

Proof: Let

$$\begin{aligned} \Omega_{v_i} &= \{x(k) \in R^n | \mathcal{Q}(x(k)) = v_i\} \\ F_0 &= \{x(k) \in R^n | Fx(k) = 0\} \\ \Lambda &= \Omega_0 \cap F_0 \end{aligned} \tag{4.6}$$

We will show that there exists a mapping $\alpha(x(k))$ satisfying $Q[\alpha(x(k))y(k)] = Q[F\mathcal{Q}(x(k))]$, then the result is satisfied.

If $Q(F\mathcal{Q}(x(k))) > 0$, all we should do is to illustrate that there exists a mapping $\alpha(\cdot)$ such that

$$\frac{\rho+1}{2\rho} Q(F\mathcal{Q}(x(k))) \leq \alpha(x(k))y(k) < \frac{\rho+1}{2} Q(F\mathcal{Q}(x(k))) \tag{4.7}$$

In fact, if $x \notin \Lambda$, then there exists an appropriate d, such that

$$y(k) = Fx(k) - dQ(F\mathcal{Q}(x(k))) > 0 \ (or < 0) \tag{4.8}$$

Then (4.7) is equal to

$$\frac{\rho+1}{2\rho}\frac{Q(F\mathcal{Q}(x(k)))}{Fx(k)-dQ(F\mathcal{Q}(x(k)))} \leq (or \geq)\ \alpha(x(k)) < (or >)\ \frac{\rho+1}{2}\frac{Q(F\mathcal{Q}(x(k)))}{Fx(k)-dQ(F\mathcal{Q}(x(k)))} \tag{4.9}$$

Let

$$\alpha(x(k)) = \frac{Q(F\mathcal{Q}(x(k)))}{Fx(k) - dQ(F\mathcal{Q}(x(k)))} \tag{4.10}$$

It is obvious that $\alpha(x(k))$ defined above satisfies (4.5).

If $x \in \Lambda$, then $Q[\alpha(x(k))y(k)]$ is equal to $Q[F\mathcal{Q}(x(k))]$ for any $\alpha(x(k))$, we let $\alpha(x(k)) = 0$ for simplicity.

If $Q(F\mathcal{Q}(x(k))) < 0$, the proof is the same as $Q(F\mathcal{Q}(x(k))) > 0$ and $\alpha(x(k))$ is defined as (4.10).

Last, $\alpha(x(k))$ can be chosen as 0 when $Q(F\mathcal{Q}(x(k))) = 0$.

Based on the proof of Lemma 4.2, the *multiplier* $\alpha(x(k))$ is defined as:

$$\alpha(x(k)) = \begin{cases} \frac{Q(F\mathcal{Q}(x(k)))}{Fx(k)-dQ(F\mathcal{Q}(x(k)))}, & if\ x \notin \Lambda \\ 0, & if\ x \in \Lambda \end{cases} \tag{4.11}$$

4.3.2 Well-Defined Multiplier

Note that the selection of d should be considered in the proof of Lemma 4.2, now we will show that there exists a suitable d such that $Fx(k) - dQ(F\mathcal{Q}(x(k))) = 0$ if and only if $x \in \Lambda$.

In the following, two-dimensional system is discussed for simplicity. Firstly, we consider $\sup_{x\in\Omega_\eta} Fx$ and $\inf_{x\in\Omega_\eta} Fx$, where $\eta = [\eta_1\ \eta_2]^T$ and $\eta_1, \eta_2 \in \{\pm v_i, i \in Z_{\geq 0}\}$.

Because Fx is linear, $\sup_{x\in\Omega_\eta} Fx$ and $\inf_{x\in\Omega_\eta} Fx$ should happen on the edge of Ω_η.

For $\eta_j = v_i > 0$, $j = 1, 2$ and $i \in Z_{\geq 0}$, we have

$$\max_{x_j\in\Omega_{\eta_j}} x_j = \begin{cases} \frac{(\rho+1)^2}{4\rho}\eta_j + \frac{\rho^2-1}{4\rho}\eta_j & if\ f_i > 0 \\ \frac{(\rho+1)^2}{4\rho}\eta_j - \frac{\rho^2-1}{4\rho}\eta_j & if\ f_i < 0 \end{cases} \tag{4.12}$$

Otherwise, if $\eta_j = -v_i < 0$,

$$\max_{x_j\in\Omega_\eta} x_j = \begin{cases} \frac{(\rho+1)^2}{4\rho}\eta_j - \frac{\rho^2-1}{4\rho}\eta_j & if\ f_i > 0 \\ \frac{(\rho+1)^2}{4\rho}\eta_j + \frac{\rho^2-1}{4\rho}\eta_j & if\ f_i < 0 \end{cases} \tag{4.13}$$

where $\frac{(\rho+1)^2}{4\rho}\eta_j$ is the middle point between $\frac{\rho+1}{2\rho}\eta_j$ and $\frac{\rho+1}{2}\eta_j$ and $\frac{\rho^2-1}{4\rho}|\eta_j|$ is the distance between the middle point and boundary points.

Then based on (4.12) and (4.13), we have

$$\max_{x_j\in\Omega_\eta} x_j = \frac{(\rho+1)^2}{4\rho}\eta_j + sgn(f_j)\frac{\rho^2-1}{4\rho}|\eta_j| \tag{4.14}$$

for any f_j and η_j, where $sgn(\cdot)$ is a symbolic function. Then

$$\sup_{x\in\Omega_\eta} Fx = \frac{(\rho+1)^2}{4\rho}F\eta + \frac{\rho^2-1}{4\rho}\|F\eta\|_1 \tag{4.15}$$

Note that $Q(F\mathcal{Q}(x(k))) = Q(F\eta)$ when $x \in \Omega_\eta$. In the following, we will show that there exists a suitable d such that

$$F_d \triangleq \{x(k)|Fx(k) = dQ(F\eta)\} \cap \Omega_\eta = \emptyset \tag{4.16}$$

That is, the denominator of $\alpha(x(k))$ can not be zero in Ω_η and it can not be zero for all $x(k)$ except for Ω_0 according to the arbitrary of η.

To verify (4.16), we discuss the value of $\| F\eta \|_1$ for sub-four cases:

i) When $\eta_1 = v_i > 0$ and $\eta_2 = v_j > 0$, the quantization region Ω_η can be shown as Fig. 4.3. Note that $\sup_{x\in\Omega_\eta} Fx$ can be realized at a_1, b_1, c_1 or d_1. Assume that $\sup_{x\in\Omega_\eta} Fx$ is achieved at a_1 and there exists a suitable d such that the distance between F_η and F_d is larger than the one between F_η and $\sup_{x\in\Omega_\eta} Fx$, then (4.16) is satisfied. It is obvious that if $\sup_{x\in\Omega_\eta} Fx$ is achieved at b_1, c_1 or d_1 rather than a_1, d selected above can also ensure (4.16). So, the case, $\sup_{x\in\Omega_\eta} Fx$ is achieved at a_1, is only considered.

When $\sup_{x\in\Omega_\eta} Fx$ is achieved at a_1, $f_1 > 0, f_2 > 0$ should be satisfied. Then

$$\|F\eta\|_1 = |f_1\eta_1| + |f_2\eta_2| = F\eta \tag{4.17}$$

ii) For $\eta_1 = v_i > 0$ and $\eta_2 = -v_j < 0$, the quantization region is illustrated as Fig. 4.4. The same as above analysis, we only consider the case that $\sup_{x\in\Omega_\eta} Fx$ is achieved at d_2 and then $f_1 > 0, f_2 < 0$. Again, we have

$$\|F\eta\|_1 = F\eta \tag{4.18}$$

As for $\eta = [-v_i\ v_j]^T$ and $\eta = [-v_i\ -v_j]^T$, the case, $\sup_{x\in\Omega_\eta} Fx$ is achieved at b_3 and c_4, is considered respectively and $\|F\eta\|_1 = F\eta$.

Above all, we can see that the case, $\|F\eta\|_1 = F\eta$, is only discussed whatever η chooses. Then there is no point of intersection between Ω_η and F_d, that is (4.16) is satisfied, is equal to

$$\begin{aligned} &|F\eta - \sup_{x\in\Omega_\eta} Fx| < |F\eta - dQ(F\eta)| \\ \Leftrightarrow\ &|F\eta - \tfrac{(\rho+1)^2}{4\rho}F\eta - \tfrac{\rho^2-1}{4\rho}\|F\eta\|_1| < |F\eta - dQ(F\eta)| \\ \Leftrightarrow\ &|F\eta - \tfrac{(\rho+1)^2}{4\rho}F\eta - \tfrac{\rho^2-1}{4\rho}F\eta| < |F\eta - dQ(F\eta)| \end{aligned} \tag{4.19}$$

Let $\rho = \frac{1+\delta}{1-\delta}$, (4.19) is changed to

$$|-\frac{\delta}{1-\delta}F\eta| < |F\eta - dQ(F\eta)| \tag{4.20}$$

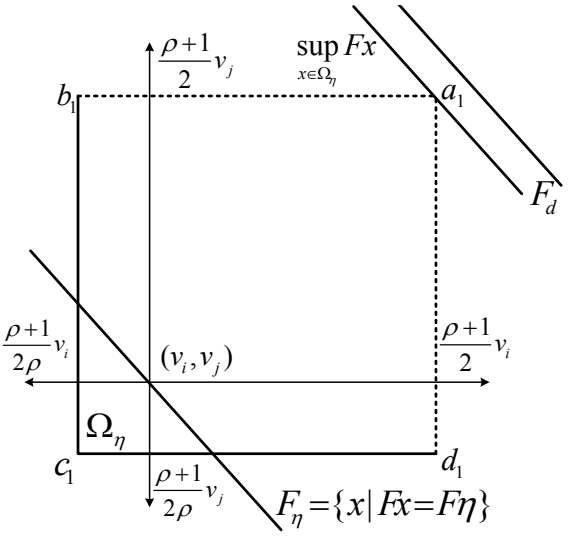

Fig. 4.3 Quantization region.

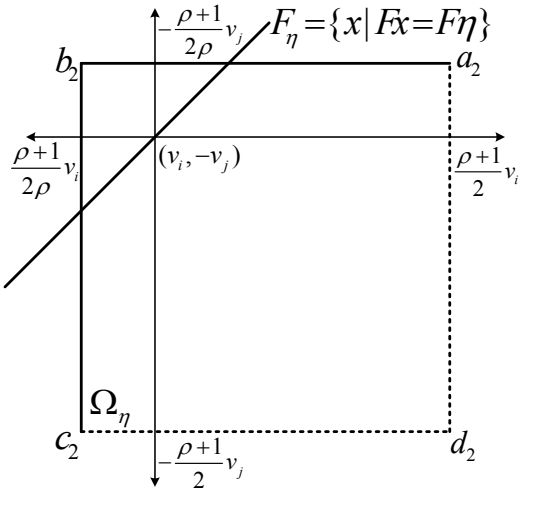

Fig. 4.4 Quantization region.

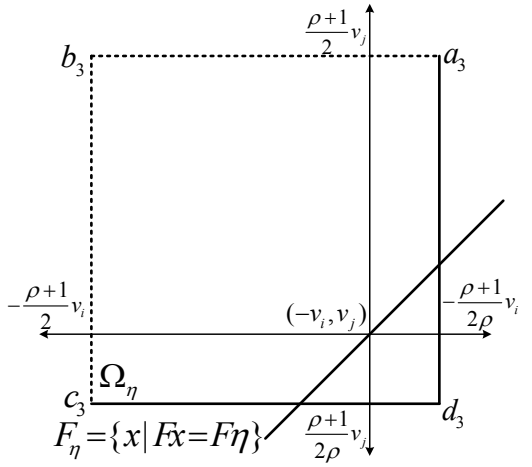

Fig. 4.5 Quantization region.

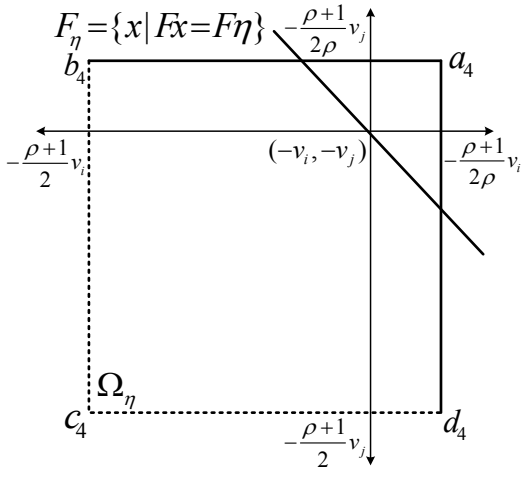

Fig. 4.6 Quantization region.

According to $0 < \delta < 1$ and there exists an uncertain variable $\triangle$ such that $Q(F\eta) = (1 + \triangle)F\eta$, where $|\triangle| < \delta$ [51], (4.20) is equivalent to

$$\tfrac{\delta}{1-\delta}|F\eta| < |1 - d(1 + \triangle)||F\eta| \Leftrightarrow \tfrac{\delta}{1-\delta} < |1 - d(1 + \triangle)| \tag{4.21}$$

Assume $d < 0$, it is obvious that $1 - d(1 + \triangle) > 0$ and the inequation above is equal to

$$d < \frac{1 - 2\delta}{(1 - \delta)(1 + \triangle)} \tag{4.22}$$

When $1-2\delta \geq 0$, that is $0 < \delta \leq \frac{1}{2}$, $\frac{1-2\delta}{(1-\delta)(1+\triangle)}$ decreases when $\triangle$ increases. Then (4.22) is satisfied if and only if

$$d < \frac{1-2\delta}{1-\delta^2} \tag{4.23}$$

Otherwise, if $1-2\delta \leq 0$, that is $\frac{1}{2} \leq \delta < 1$, $\frac{1-2\delta}{(1-\delta)(1+\triangle)}$ increases as long as $\triangle$ increases. Then (4.22) is equivalent to

$$d < \frac{1-2\delta}{(1-\delta)^2} \tag{4.24}$$

Summarized above, it is obvious that (4.22) is equal to

$$d < f(\delta) \triangleq \begin{cases} \frac{1-2\delta}{1-\delta^2} & if \;\; 0 < \delta \leq \frac{1}{2} \\ \frac{1-2\delta}{(1-\delta)^2} & if \;\; \frac{1}{2} \leq \delta < 1 \end{cases} \tag{4.25}$$

Note that $d < 0$ is assumed, d has to satisfy

$$d < min(0, f(\delta)) \triangleq g(\delta) = \begin{cases} 0 & if \;\; 0 < \delta \leq \frac{1}{2} \\ \frac{1-2\delta}{(1-\delta)^2} & if \;\; \frac{1}{2} \leq \delta < 1 \end{cases} \tag{4.26}$$

In the above, $\sup_{x\in\Omega_\eta} Fx$ is considered. As for $\inf_{x\in\Omega_\eta} Fx$, if $\eta_j = v_i > 0$, $j = 1, 2$ and $i \in Z_{\geq 0}$, we have

$$\min_{x_j\in\Omega_{\eta_j}} x_j = \begin{cases} \frac{(\rho+1)^2}{4\rho}\eta_j - \frac{\rho^2-1}{4\rho}\eta_j & if \;\; f_i > 0 \\ \frac{(\rho+1)^2}{4\rho}\eta_j + \frac{\rho^2-1}{4\rho}\eta_j & if \;\; f_i < 0 \end{cases} \tag{4.27}$$

Otherwise, if $\eta_j = -v_i < 0$,

$$\min_{x_j\in\Omega_\eta} x_j = \begin{cases} \frac{(\rho+1)^2}{4\rho}\eta_j + \frac{\rho^2-1}{4\rho}\eta_j & if \;\; f_i > 0 \\ \frac{(\rho+1)^2}{4\rho}\eta_j - \frac{\rho^2-1}{4\rho}\eta_j & if \;\; f_i < 0 \end{cases} \tag{4.28}$$

Combining (4.27) with (4.28), we have

$$\min_{x_j\in\Omega_\eta} x_j = \frac{(\rho+1)^2}{4\rho}\eta_j - sign(f_j)\frac{\rho^2-1}{4\rho}|\eta_j| \tag{4.29}$$

for any f_j and η_j. Then

$$\inf_{x\in\Omega_\eta} Fx = \frac{(\rho+1)^2}{4\rho}F\eta - \frac{\rho^2-1}{4\rho}\|F\eta\|_1 \tag{4.30}$$

In the following, we discuss the value of $\| F\eta \|_1$ for sub-four cases:

i) When $\eta_1 = v_i > 0$ and $\eta_2 = v_j > 0$, the quantization region Ω_η can be shown as Fig. 4.3. Note that $\inf_{x\in\Omega_\eta} Fx$ can be realized at a_1, b_1, c_1 or d_1. The same as the above analysis, the case, $\inf_{x\in\Omega_\eta} Fx$ is achieved at a_1, is just discussed.

When $\inf_{x\in\Omega_\eta} Fx$ is achieved at a_1, $f_1 < 0, f_2 < 0$ must be satisfied. Then

$$\|F\eta\|_1 = |f_1\eta_1| + |f_2\eta_2| = -F\eta \tag{4.31}$$

ii) For $\eta_1 = v_i > 0$ and $\eta_2 = -v_j < 0$, the quantization region is shown as Fig. 4.4. Then we only consider the case that $\inf_{x\in\Omega_\eta} Fx$ is achieved at d_2 and then $f_1 < 0, f_2 > 0$. Again, we have

$$\|F\eta\|_1 = -F\eta \tag{4.32}$$

As for $\eta = [-v_i \ v_j]^T$ and $\eta = [-v_i \ -v_j]^T$, the case, $\inf_{x\in\Omega_\eta} Fx$ is achieved at b_3 and c_4, is considered respectively and $\|F\eta\|_1 = -F\eta$.

Above all, we can see that the case, $\|F\eta\|_1 = -F\eta$, only need to be considered whatever η chooses when $\inf_{x\in\Omega_\eta} Fx$ is discussed. Then there is no common point of intersection between Ω_η and F_d, which means

$$\begin{aligned} & |F\eta - \inf_{x\in\Omega_\eta} Fx| < |F\eta - dQ(F\eta)| \\ \Leftrightarrow\ & |F\eta - \tfrac{(\rho+1)^2}{4\rho} F\eta + \tfrac{\rho^2-1}{4\rho}\|F\eta\|_1| < |F\eta - dQ(F\eta)| \\ \Leftrightarrow\ & |F\eta - \tfrac{(\rho+1)^2}{4\rho} F\eta - \tfrac{\rho^2-1}{4\rho} F\eta| < |F\eta - dQ(F\eta)| \\ \Leftrightarrow\ & (4.19) \end{aligned} \tag{4.33}$$

Then the same as above analysis, d defined as (4.26) can ensure (4.16).

Therefore, the following condition can be given.

Corollary 4.3. *The multiplier $\alpha(x(k))$ in (4.11) is well-defined if*

$$d < g(\delta) = \begin{cases} 0 & if \quad 0 < \delta \le \frac{1}{2} \\ \frac{1-2\delta}{(1-\delta)^2} & if \quad \frac{1}{2} \le \delta < 1 \end{cases} \tag{4.34}$$

Remark 4.4. Note that all analysis above just shows that if $x \notin \Omega_0$, then $a(x(k))$ is well-defined when $d < g(\delta)$. Comparing to $\alpha(x(k))$ defined in (4.11), we should also prove that $a(x(k))$ is well-defined if $x(k) \in \Omega_0 \backslash F_0$. In fact, the result is obvious. If $x(k) \in \Omega_0 \backslash F_0$, it is easy to see that $Q(F\mathcal{Q}(x(k))) = 0$ and $Fx(k) \neq 0$, then $Fx(k) - dQ(F\mathcal{Q}(x(k))) = Fx(k) \neq 0$ for any d.

4.3.3 Nonnegativity of Multiplier

In this section, nonnegativity of $\alpha(x(k))$ is discussed and one Lemma is given.

Let $x(k) \in \Omega_\eta$, then $Q(F\mathcal{Q}(x(k)))$ is equal to $Q(F\eta)$ and

$$\alpha(x(k)) = \frac{Q(F\eta)}{Fx(k) - dQ(F\eta)} \tag{4.35}$$

is a function of $Fx(k)$. Note that $\alpha(x(k))$ has singular points satisfying $Fx(k) = dQ(F\eta)$. When $d < g(\delta)$, these singular points are not in Ω_η and $\alpha(x(k))$ is monotonic in Ω_η based on

$$\frac{d\alpha(x(k))}{dFx(k)} = -\frac{Q(F\eta)}{(Fx(k) - dQ(F\eta))^2} \tag{4.36}$$

It is obvious that $\alpha(x(k))$ increases monotonously when $Q(F\eta) \leq 0$ and $\alpha(x(k))$ decreases monotonously when $Q(F\eta) \geq 0$.

Lemma 4.5. *Suppose d is chosen such that $d < g(\delta)$, then $\alpha(x(k)) \geq 0$ for all $x(k) \in R^n$.*

Proof: Suppose $x(k) \in \Omega_\eta$, where $\eta = \{\pm v_i, i \in Z_{\geq 0}\}$. When $d < g(\delta)$, the multiplier $\alpha(x(k))$ is well-defined and $\alpha(x(k)) \geq 0$ if and only if $\inf_{x(k)\in\Omega_\eta} \alpha(x(k)) \geq 0$. Three cases are considered to verify the result.

Case 1: $F\eta \geq v$
It is obvious that $\alpha(x(k))$ decreases monotonously with $Fx(k)$ and denominator of $\alpha(x(k))$ is a positive definite constant within Ω_η.

Then $\inf_{x(k)\in\Omega_\eta} \alpha(x(k)) \geq 0$ is equal to

$$\sup_{x(k)\in\Omega_\eta} F(x(k)) - dQ(F\eta) \geq 0 \tag{4.37}$$

In fact,

$$\begin{aligned} &\sup_{x(k)\in\Omega_\eta} F(x(k)) - dQ(F\eta) \\ &= \tfrac{(\rho+1)^2}{4\rho} F\eta + \tfrac{\rho^2-1}{4\rho} \parallel F\eta \parallel_1 - dQ(F\eta) \\ &\geq \tfrac{(\rho+1)^2}{4\rho} F\eta + \tfrac{\rho^2-1}{4\rho} F\eta - dQ(F\eta) \\ &= [\tfrac{1}{1-\delta} - d(1+\triangle)]F\eta \\ &\geq 0 \end{aligned} \tag{4.38}$$

where $|\triangle| < \delta < 1$. The last inequation is based on $d < 0$ and $F\eta > 0$. Then, (4.37) is satisfied and $\alpha(x(k)) \geq 0$ in Ω_η.

Case 2: $F\eta \leq -v$
In this case, $Q(F\eta)$ is negative definite and $\alpha(x(k))$ increases monotonously with $Fx(k)$. In order to verify $\alpha(x(k)) \geq 0$, the following inequation should be satisfied:

$$\inf_{x(k)\in\Omega_\eta} F(x(k)) - dQ(F\eta) \leq 0 \tag{4.39}$$

In fact,

$$\begin{aligned} &\inf_{x(k)\in\Omega_\eta} F(x(k)) - dQ(F\eta) \\ &= \tfrac{(\rho+1)^2}{4\rho} F\eta - \tfrac{\rho^2-1}{4\rho} \parallel F\eta \parallel_1 - dQ(F\eta) \\ &\le \tfrac{(\rho+1)^2}{4\rho} F\eta - \tfrac{\rho^2-1}{4\rho} F\eta - dQ(F\eta) \\ &= [\tfrac{1}{1+\delta} - d(1+\triangle)]F\eta \\ &\le 0 \end{aligned} \tag{4.40}$$

where $|\triangle| < \delta < 1$. The last inequation is based on $d < 0$ and $F\eta < 0$. Then, (4.39) is satisfied and $\alpha(x(k)) \ge 0$ in Ω_η.

Case 3: $-v < F\eta < v$
It is obvious that $\alpha(x(k)) = 0$ in this case.

Above all, we have $\alpha(x(k)) \ge 0$ for $x(k) \in \Omega_\eta$. Then for any $x(k) \in R^n$, $\alpha(x(k))$ is nonnegative based on the arbitrary of η. ■

4.3.4 Boundedness of Multiplier

In the following, we discuss the boundedness of multiplier $\alpha(\cdot)$ and show that the least upper bound of $\alpha(\cdot)$ exists.

If $F\eta \ge 0$, then $Q(F\eta) \ge 0$ and $\alpha(\cdot)$ decreases monotonously in Ω_η. Therefore

$$\begin{aligned} \sup_{x(k)\in\Omega_\eta} \alpha(x(k)) &= \tfrac{Q(F\eta)}{\inf_{x(k)\in\Omega_\eta} Fx - dQ(F\eta)} \\ &= \tfrac{Q(F\eta)}{\frac{(\rho+1)^2}{4\rho} F\eta - \frac{\rho^2-1}{4\rho}\|F\eta\|_1 - dQ(F\eta)} \end{aligned} \tag{4.41}$$

can be seen as a function of $F\eta$.

Let $\bar{\alpha} = \sup_\eta \sup_{x\in\Omega_\eta} \alpha(x(k))$, the boundedness of $\bar{\alpha}$ is discussed based on graphic method.

Select $v_0 = 1 > 0$, $\rho = 1.5 > 1$ and $d = -0.5 < 0$, then $v = \frac{\rho+1}{2\rho} v_0 = 0.8333$ and the following graphic, Fig. 4.7, can be given

Then, we can see that the supremum of $\alpha(\cdot)$ is achieved at $F\eta = v$ and $\bar{\alpha}$ can be given as

$$\begin{aligned} \bar{\alpha} &= \sup_\eta \sup_{x(k)\in\Omega_\eta} \alpha(x(k)) \\ &= \sup_\eta \tfrac{Q(F\eta)}{\inf_{x(k)\in\Omega_\eta} Fx - dQ(F\eta)} \\ &= \sup_\eta \tfrac{Q(F\eta)}{\frac{(\rho+1)^2}{4\rho} F\eta - \frac{\rho^2-1}{4\rho}\|F\eta\|_1 - dQ(F\eta)} \\ &= \tfrac{v_0}{\frac{(\rho+1)^2}{4\rho} v - \frac{\rho^2-1}{4\rho} v - dv_0} \\ &= \tfrac{4\rho^2}{(\rho+1)^2 - 4d\rho^2} \end{aligned} \tag{4.42}$$

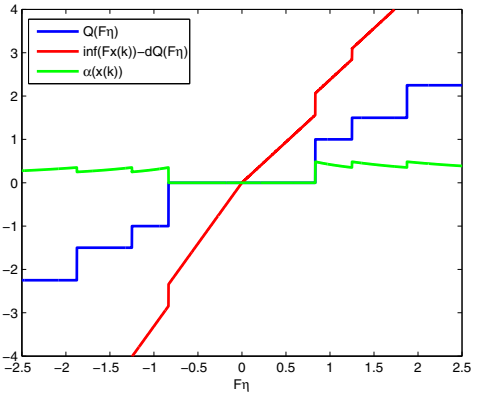

Fig. 4.7 Variations of Multiplier.

As for $F\eta \leq 0$, $Q(F\eta) \leq 0$ and $\alpha(\cdot)$ increases monotonously in Ω_η. Then

$$\begin{aligned} \sup_{x(k)\in\Omega_\eta} \alpha(x(k)) &= \frac{Q(F\eta)}{\sup_{x(k)\in\Omega_\eta} Fx - dQ(F\eta)} \\ &= \frac{Q(F\eta)}{\frac{(\rho+1)^2}{4\rho} F\eta + \frac{\rho^2-1}{4\rho}\|F\eta\|_1 - dQ(F\eta)} \end{aligned} \tag{4.43}$$

Note that $\sup_{x(k)\in\Omega_\eta} \alpha(x(k))$ can be seen as a function of $F\eta$ also. Let

$$\underline{\alpha} = \sup_{\eta} \sup_{x(k)\in\Omega_\eta} \alpha(x(k)) \tag{4.44}$$

and variations of multiplier selected as above, Fig. 4.8 can be shown as follows

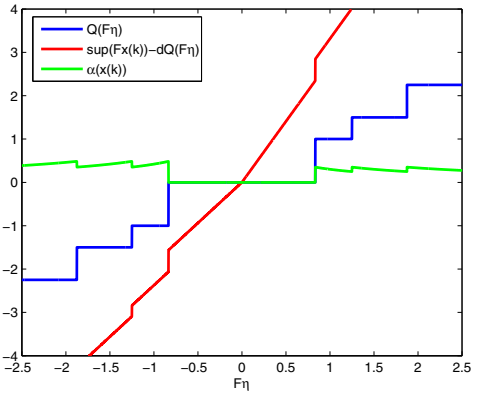

Fig. 4.8 Variations of Multiplier.

Then, when $F\eta = -v$, $\underline{\alpha}$ can be achieved and shown as

$$\begin{aligned}\underline{\alpha} &= \sup_{\eta} \sup_{x(k)\in\Omega_\eta} \alpha(x(k)) \\ &= \frac{-v_0}{-\frac{(\rho+1)^2}{4\rho}v+\frac{\rho^2-1}{4\rho}v+dv_0} \\ &= \frac{4\rho^2}{(\rho+1)^2-4d\rho^2} \\ &= \bar{\alpha}\end{aligned} \tag{4.45}$$

Above all, if there exists η such that $F\eta = v$ or $F\eta = -v$, then the least upper bound of $\alpha(\cdot)$ exists and equals to $\frac{4\rho^2}{(\rho+1)^2-4d\rho^2}$.

But, what will happen if there does not exist η such that $F\eta = v$ or $F\eta = -v$? We will explain that the least upper bound of $\alpha(\cdot)$ exists although the η, which satisfies $F\eta = v$ or $F\eta = -v$, does not exist.

If there does not exist η such that $F\eta = v$ or $F\eta = -v$, we will find the node $\eta \in \{\pm v_i, i \in Z_{\geq 0}\}$, for which the contour approaches the value v or $-v$. Mathematically, define the set

$$\tilde{F} = \{F\eta | \eta \in Z_\eta = \pm\rho^i v_o, i \in Z_{\geq 0}, F\eta \geq v = \frac{\rho+1}{2\rho}v_0\} \tag{4.46}$$

and

$$\bar{F} = \{F\eta | \eta \in Z_\eta = \pm\rho^i v_o, i \in Z_{\geq 0}, F\eta \leq -v = -\frac{\rho+1}{2\rho}v_0\} \tag{4.47}$$

We claim that the infimum of $\tilde{F}$ exists for any F. In the following, $\eta_j \geq 0, j = 1, 2$ is considered only and other cases can be analyzed similarly.

Case 1: If $f_1 > 0$ and $f_2 > 0$, then $F\eta \geq \frac{\rho+1}{2\rho}v_0$ is equal to

$$f_1\rho^i v_0 + f_2\rho^j v_0 \geq \frac{\rho+1}{2\rho}v_0 \tag{4.48}$$

If i, j are selected large enough, then the above inequation is satisfied and it is obvious that there exist suitable $\tilde{i}$, $\tilde{j}$ such that

$$f_1\rho^{\tilde{i}}v_0 + f_2\rho^{\tilde{j}}v_0 = \inf\{f_1\rho^i v_0 + f_2\rho^j v_0\} = \inf \tilde{F} \tag{4.49}$$

Case 2: If $f_1 > 0$ and $f_2 < 0$, then $F\eta \geq \frac{\rho+1}{2\rho}v_0$ is equal to (4.48). If i and j are selected large enough and small enough respectively, then (4.48) is satisfied and there exist suitable $\tilde{i}$ and $\tilde{j}$ such that

$$f_1\rho^{\tilde{i}}v_0 + f_2\rho^{\tilde{j}}v_0 = \inf \tilde{F} \tag{4.50}$$

Case 3: As for $f_1 < 0$ and $f_2 > 0$, the analysis is the same as case 2.

Case 4: If $f_1 < 0$ and $f_2 < 0$, then $F\eta \leq -\frac{\rho+1}{2\rho}v_0$ can be changed to

$$(-f_1)\rho^i v_0 + (-f_2)\rho^j v_0 \geq \frac{\rho+1}{2\rho}v_0 \tag{4.51}$$

and i, j selected large enough can ensure the above inequation. Therefore there exists suitable $\tilde{i}$, $\tilde{j}$ such that

$$(-f_1)\rho^{\tilde{i}} v_0 + (-f_2)\rho^{\tilde{j}} v_0 = \inf\{(-f_1)\rho^i v_0 + (-f_2)\rho^j v_0\} = -\sup \bar{F} \tag{4.52}$$

that is the supremum of $\bar{F}$ exists and can be shown as

$$\sup \bar{F} = -[(-f_1)\rho^{\tilde{i}} v_0 + (-f_2)\rho^{\tilde{j}} v_0] \tag{4.53}$$

and

$$\inf \tilde{F} = -\sup \bar{F} = (-f_1)\rho^{\tilde{i}} v_0 + (-f_2)\rho^{\tilde{j}} v_0 \tag{4.54}$$

Then the claim above is satisfied. To show analysis above clearly, a graph is given as follows.

In Fig. 4.9, $v_0 = 1$, $\rho = 1.5$, $f_1 = -0.4$ and $f_2 = 0.3$, based on the definition of $\tilde{F}$ and $F\eta \geq \frac{\rho+1}{2\rho}v_0$ which is equivalent to

$$f_1\rho^i v_0 + f_2\rho^j v_0 \geq \frac{\rho+1}{2\rho}v_0 \tag{4.55}$$

there exist i, j such that (4.55) is satisfied, such as i and j chosen as 2 and 10 respectively. Also, $\tilde{i}$ and $\tilde{j}$, which satisfy (4.50), exist. If there exist $i, j \in Z_{\geq 0}$ such that

$$-0.4\rho^i v_0 + 0.3\rho^j v_0 = \frac{\rho+1}{2\rho}v_0 \tag{4.56}$$

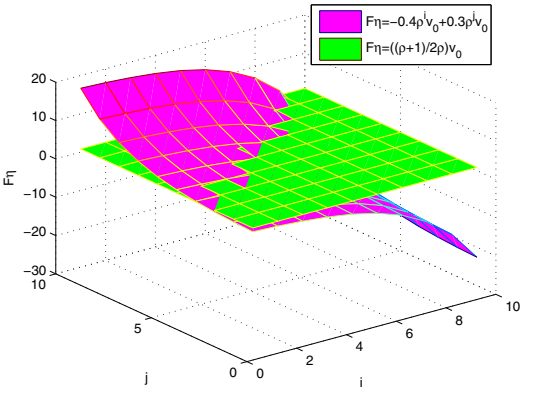

Fig. 4.9 Existence of the infimum of $\tilde{F}$.

then $\tilde{i}$ and $\tilde{j}$, which satisfy (4.50), exist and the infimum of $\tilde{F}$ is equal to $\frac{\rho+1}{2\rho}v_0$. Otherwise, $\tilde{i}$ and $\tilde{j}$ are chosen such that $-0.4\rho^i v_0 + 0.3\rho^j v_0$ is larger than and closed to $\frac{\rho+1}{2\rho}v_0$. In this case, the optimal $\tilde{i}$ and $\tilde{j}$ can be chosen as 8 and 7 respectively and the infimum of $\tilde{F}$ is 0.8543 approximately. Then select $F_q = \inf \tilde{F} = 0.8543 > 0$, we have

$$\begin{aligned} \bar{\alpha} &= \sup_\eta \sup_{x(k)\in\Omega_\eta} \alpha(x(k)) \\ &= \frac{Q(F_q)}{\frac{(\rho+1)^2}{4\rho}F_q - \frac{\rho^2-1}{4\rho}\|F_q\|_1 - dQ(F_q)} \\ &= \frac{1}{\frac{(\rho+1)^2}{4\rho}\times 0.8543 - \frac{\rho^2-1}{4\rho}\times 0.8543 - d} \\ &\approx 0.8252 \end{aligned} \tag{4.57}$$

where $d = -0.5$ and $Q(F_q) = v_0 = 1$ based on

$$\frac{\rho+1}{2\rho}v_0 \le F_q = 0.8543 \le \frac{\rho+1}{2}v_0 \tag{4.58}$$

Above all, the supremum of multiplier $\alpha(x(k))$ can be given as

$$\bar{\alpha} = \sup_\eta \sup_{x(k)\in\Omega_\eta} \alpha(x(k)) = \frac{Q(F_q)}{\frac{(\rho+1)^2}{4\rho}F_q - \frac{\rho^2-1}{4\rho}\|F_q\|_1 - dQ(F_q)} \tag{4.59}$$

where

$$F_q = \inf \tilde{F} = \inf\{F\eta | \eta \in Z_\eta = \pm\rho^i v_o, i \in Z_{\ge 0}, F\eta \ge v = \tfrac{\rho+1}{2\rho}v_0\} \tag{4.60}$$

Note that if $F_q < 0$, it is easy to see that $\underline{\alpha}$ is equal to $\bar{\alpha}$ defined in (4.59).

Remark 4.6. In the above, all of analysis are based on two-dimensional system, as to n-dimensional system, the analysis process is the same as above but more complex than it. The results according to two-dimensional system are satisfied for n-dimensional system.

4.3.5 Expression of Multiplier

The multiplier $\alpha(x(k))$ is given as (4.11). If

$$d < g(\delta) = \begin{cases} 0 & if \quad 0 < \delta \le \frac{1}{2} \\ \frac{1-2\delta}{(1-\delta)^2} & if \quad \frac{1}{2} \le \delta < 1 \end{cases} \tag{4.61}$$

then $\alpha(x(k))$ is well-defined and satisfies

$$0 \le \alpha(x(k)) \le \bar{\alpha} \quad \forall x(k) \in R^n \tag{4.62}$$

where

$$\bar{\alpha} = \frac{Q(F_q)}{\frac{(\rho+1)^2}{4\rho}F_q - \frac{\rho^2-1}{4\rho} \parallel F_q \parallel_1 - dQ(F_q)} \tag{4.63}$$

and

$$F_q = \inf \tilde{F} = \inf \{F\eta | \eta \in Z_\eta = \pm\rho^i v_o, i \in Z_{\geq 0}, F\eta \geq v = \tfrac{\rho+1}{2\rho} v_0\} \tag{4.64}$$

4.3.6 A Useful Lemma

Definition 4.7. [146] Let a class of function be defined by

$$\mathcal{S}(K_1, K_2) = \left\{\sigma : R \to R \middle| K_1 < \frac{\sigma(y)}{y} < K_2\right\} \tag{4.65}$$

A function ϕ is said to be of the sector type with sector bounds $K_1 < K_2$ if $\phi \in \mathcal{S}(K_1, K_2)$. If equality is allowed in either side, the notations $\mathcal{S}[K_1, K_2)$, $\mathcal{S}(K_1, K_2]$, and $\mathcal{S}[K_1, K_2]$ are used.

Definition 4.8. [146][71] Let A have eigenvalues inside the open unit circle and let $\bar{K}$ be a constant. Define the transfer matrix

$$W(z) = \frac{1}{\bar{K}} = C(zI - A)^{-1}B. \tag{4.66}$$

We say that $W(z)$ is DPR (discrete positive real) if

$$Re\{W(e^{j\omega})\} \geq -\frac{1}{\bar{K}} \quad \forall \omega \in R. \tag{4.67}$$

Lemma 4.9. *[146] Let L_1 be a stable discrete-time system represented by*

$$\begin{cases} x(k+1) = Ax(k) + Bu(k) \\ y(k) = Fx(k) + Du(k) \end{cases} \tag{4.68}$$

Let $\alpha : R^n \to R$ be a mapping such that there exists a finite constant $\bar{\alpha}$ satisfying $0 \leq \alpha(x) < \bar{\alpha}$ for all $x \in R^n$. Let $\mathcal{N} : R \to R$ be a sector nonlinearity $\mathcal{N} \in \mathcal{S}[0, \bar{n}]$. Assume that a unique solution to the above system exists when $u(k) = -\mathcal{N}[\alpha(x(k))y(k)]$. Then, if the transfer matrix

$$H(z) = F(zI - A)^{-1}B + D + \frac{1}{\bar{K}} \tag{4.69}$$

is DPR, and $\bar{\alpha}\bar{n} < \bar{K}$*, the closed-loop system formed by applying the feedback* $u(k) = -\mathcal{N}[\alpha(x(k))y(k)]$ *is stable in the large.*

4.3.7 Stability Theorem for QIQM Systems

Theorem 4.10. *Let a linear time-invariant system under quantized feedback with QIQM described by*

$$\begin{cases} x(k+1) = Ax(k) + Bu(k) \\ u(k) = -Q(F\mathcal{Q}(x(k))). \end{cases} \tag{4.70}$$

Suppose A has eigenvalues inside the open unit circle. Define the transfer function

$$G(z) = F(zI - A)^{-1}B \tag{4.71}$$

Then, the closed-loop system is globally asymptotically stable about origin if

$$\inf_{\omega \in R} Re\{G(e^{j\omega})\} > \varepsilon \tag{4.72}$$

where

$$\varepsilon = \begin{cases} \frac{1}{(\delta-1)(\delta+1)^2}\left(\frac{F_q}{Q(F_q)} - \delta\frac{\|F_q\|_1}{Q(F_q)}\right) & if\ 0 < \delta \le \frac{1}{2} \\ \frac{(2\delta-1)\delta}{(1-\delta)^2(1+\delta)} + \frac{1}{(\delta-1)(\delta+1)^2}\left(\frac{F_q}{Q(F_q)} - \delta\frac{\|F_q\|_1}{Q(F_q)}\right) & if\ \frac{1}{2} \le \delta < 1. \end{cases} \tag{4.73}$$

Proof: The outline of the proof is similar to that of Richter and Misawa (2003). We focus on the difference in the following, but also refer to some parts of the proof of Richter and Misawa (2003) in order to make the proof in a self-contained form.

At first, change system (4.70) to the equivalent form

$$\begin{cases} x(k+1) = Ax(k) + Bu(k) \\ y(k) = Fx(k) + du(k) \\ u(k) = -Q(\alpha(x(k))y(k)) \end{cases} \tag{4.74}$$

where $\alpha(x(k))$ is defined in (4.11) and the state of this system is identical to that of original system based on Lemma 4.2. A unique solution sequence exists for every initial condition. Assume a suitable d is selected to guarantee that $\alpha(x(k))$ is nonnegative and upper-bounded by $\bar{\alpha}$. Note that quantizer in (4.2) is a nonlinear function with $Q \in \mathcal{S}(0, \frac{2\rho}{\rho+1}]$, that is, $\bar{n} = \frac{2\rho}{\rho+1}$. Based on Lemma 4.9, global stability is obtained if the transfer function

$$H(z) = F(zI - A)^{-1}B + d + \frac{1}{\bar{K}} \tag{4.75}$$

is DPR with $\frac{2\rho}{\rho+1}\bar{\alpha} < \bar{K}$, that is

$$Re\{G(e^{j\omega})\} \geq -d - \frac{1}{\bar{K}} \tag{4.76}$$

for all frequencies ω. The maximum of $\bar{K}$ can be chosen as

$$\bar{K}_{max} = \frac{1}{-d - \inf Re\{G(e^{j\omega})\}} \tag{4.77}$$

and the following inequation must be satisfied

$$\bar{K}_{max} > \frac{2\rho}{\rho+1}\bar{\alpha} \tag{4.78}$$

where $\bar{\alpha}$ defined in (4.63). Then (4.78) is equal to

$$d > \frac{1}{\delta(\delta^2-1)}\frac{F_q}{Q(F_q)} + \frac{1}{1-\delta^2}\frac{\parallel F_q \parallel_1}{Q(F_q)} - \frac{1+\delta}{\delta}\inf Re\{G(e^{j\omega})\} \tag{4.79}$$

It is obvious that $\bar{K}_{max}$ is positive based on $\inf_{\omega\in R} Re\{G(e^{j\omega})\} \leq 0$ and $d < 0$. Take Condition 1 into consideration, the following inequation is obtained:

$$\begin{array}{l} \frac{1}{\delta(\delta^2-1)}\frac{F_q}{Q(F_q)} + \frac{1}{1-\delta^2}\frac{\|F_q\|_1}{Q(F_q)} - \frac{1+\delta}{\delta}\inf Re\{G(e^{j\omega})\} \\ < d < \left\{ \begin{array}{ll} 0 & if \quad 0 < \delta \leq \frac{1}{2} \\ \frac{1-2\delta}{(1-\delta)^2} & if \quad \frac{1}{2} \leq \delta < 1 \end{array} \right. \end{array} \tag{4.80}$$

Then (4.72) is given. Based on Lemma 4.9, stability of closed-loop system is satisfied. As for asymptotic stability, $\triangle V(x(k))$ is given as [146]

$$\begin{array}{l} \triangle V(x(k)) = -[L^T x(k) - WQ(\alpha(x(k))y)]^T[L^T x(k) - WQ(\alpha(x(k))y)] \\ \quad -2Q(\alpha(x(k))y)[y - \frac{Q(\alpha(x(k))y)}{\bar{K}}] \end{array} \tag{4.81}$$

where P, L, W satisfies

$$\begin{array}{l} A^T PA - P = -LL^T \\ B^T PA = F - W^T L^T \\ W^T W = 2D + \frac{2}{\bar{K}} - B^T PB \end{array} \tag{4.82}$$

The first term and second term of (4.81) have to be zero for $\triangle V(x(k))$ to be zero. It can be seen that the second term is zero if and only if $Q(\alpha(x(k))y) = 0$ or $y = 0$. Then the first term of (4.81) is changed to $-x^T(k)LL^T x(k)$.

Note that $Q(\alpha(x(k))y) = 0$ is equal to $|F\mathcal{Q}(x(k))| < v$ based on $Q(\alpha(x(k))y) = Q(F\mathcal{Q}(x(k)))$, and $y = Fx(k) - dQ(F\mathcal{Q}(k)) = 0$ only happens in $\Lambda \in \Omega_0$, where $\Omega_0 = \{x(k)|\mathcal{Q}(x(k)) = 0\}$, we have

$$\begin{aligned}\Theta &= \{x|\triangle V(x(k)) = 0\} \\ &= [\{x\big||F\mathcal{Q}(x(k))| < v\}\bigcup\{x|\mathcal{Q}(x(k)) = 0\}]\bigcap null(LL^T)\} \\ &= \{x\big||F\mathcal{Q}(x(k))| < v\}\bigcap null(LL^T)\end{aligned} \tag{4.83}$$

where $null(LL^T) = \{x|x^T LL^T x = 0\}$. It is obvious that no information is available about $null(LL^T)$, therefore, the left set is taken into consideration. Let Ω be an arbitrary bounded region of state-space, in which $\triangle V(x(k)) \leq 0$. It can be seen that Θ is the largest invariant set in Ω, therefore, the trajectories of system must stay within Θ. Note that system equation in Θ is

$$x(k+1) = Ax(k) \tag{4.84}$$

Then the trajectories of system must converge asymptotically to the origin based on the eigenvalues of A are inside the open unit circle. Also, the globally asymptotic stability is proved according to the arbitrarily large of Ω.

4.4 Numerical Example

Example 4.11. In this example, we consider an application of the method proposed in this chapter to system (4.1), where

$$A = \begin{bmatrix} -\frac{1}{2} & -\frac{1}{4} \\ 1 & \frac{3}{4} \end{bmatrix}, \quad B = \begin{bmatrix} 1 \\ 2 \end{bmatrix} \tag{4.85}$$

It is obvious that A has eigenvalues inside the unit circle, therefore Theorem 4.10 can be applied. Select $v_0 = 1$, $\rho = 1.5$, $f_1 = -0.4$ and $f_2 = 0.3$ as above, let $x_0 = [38\ 40]^T$, we have $\tilde{i} = 8, \tilde{j} = 7, F_q = 0.8543$ and $Q(F_q) = v_0 = 1$, then $\delta = 0.2$ and $\varepsilon \approx -0.5933$, the graph of $G(e^{jw})$ and state trajectories of system can be shown as

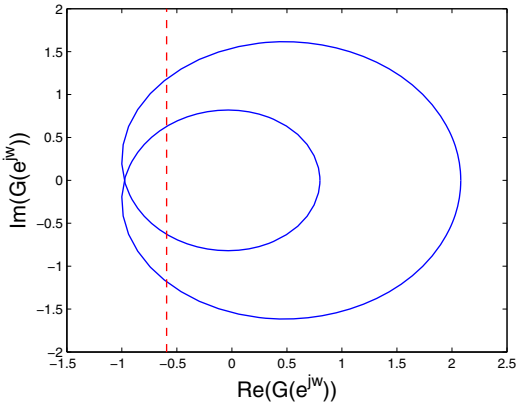

Fig. 4.10 Nyquist curve of QIQM system.

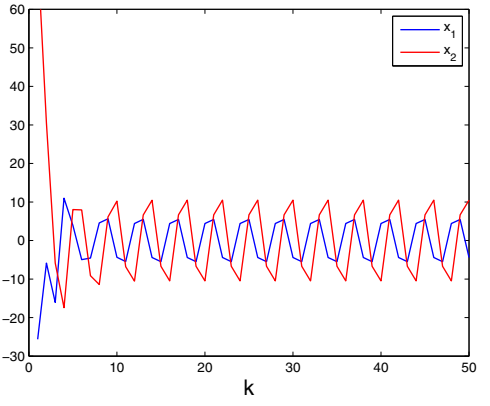

Fig. 4.11 Limit Cycle of QIQM system.

The top figure shows stability condition being violated and resulting in limit cycle. If $F = [-0.4 \ -0.4]$, we have $F_q = -1.2, \varepsilon \approx -1.25$ and $Q(F_q) = -v_0 = -1$. The Nyquist curve and state trajectories of system can be shown as Fig. 4.12 and Fig. 4.13.

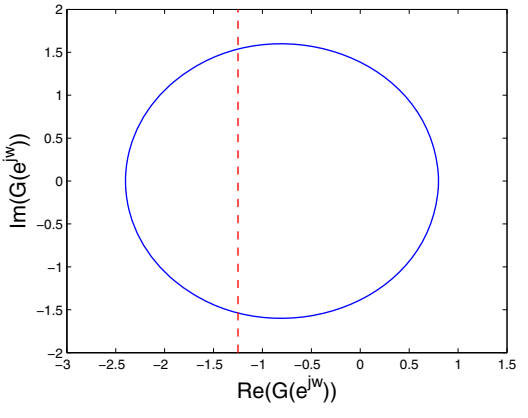

Fig. 4.12 Nyquist curve of QIQM system.

It is obvious that the sufficient condition in Theorem 4.10 is not satisfied and a state trajectory shown as limit cycle and the other converge to a nonzero equilibrium. If $F = [0.2 \ 0.2]$, then $F_q = 0.9, \varepsilon \approx -0.6250$ and the states of the system asymptotically convergence to zero.

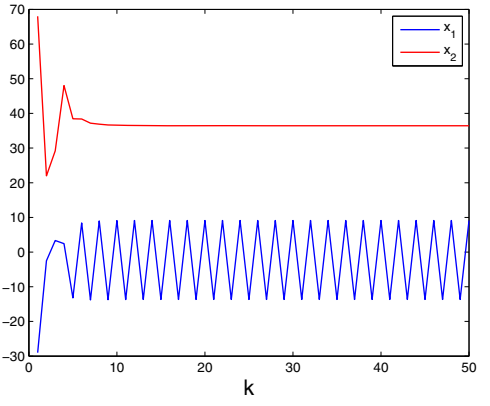

Fig. 4.13 State trajectories of QIQM system.

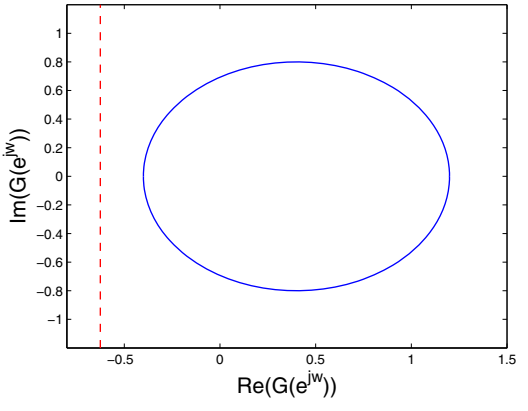

Fig. 4.14 Nyquist curve of QIQM system.

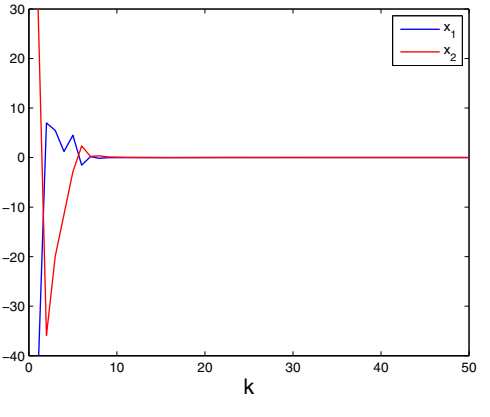

Fig. 4.15 Asymptotic stability of QIQM system.

4.5 Summary

Asymptotic stability of QIQM system is analyzed in this chapter. In the process of analysis, a multiplier, which is well-defined, nonnegative and bounded, plays an important role. The stability analysis of QIQM system is transferred into the one of an equivalent system by the multiplier. A sufficient condition is given for asymptotic stability of QIQM system. Note that the open-closed system considered in this chapter is restrict to be stable, that is, the system matrix A has eigenvalues inside the unit circle. As to unstable open-closed system, the stability analysis of closed-loop system is more challenging and will be considered in future.

Part II
Data Fusion over Networks

Chapter 5
Data Fusion over Networks with Measurement Delay

5.1 Introduction

Data fusion, one of the key technologies of NCSs, has been served as an interesting benchmark in the past decades. The fusion center deals with the information from the local sensors to improve the performance of the system. It has been applied in both military and nonmilitary fields. Military applications include: automated target recognition, guidance for autonomous vehicles, remote sensing, battlefield surveillance, and automated threat recognition systems, such as identification-friend-foe-neutral (IFFN) systems. Nonmilitary applications include: monitoring of manufacturing processes, condition-based maintenance of complex machinery, robotics, and medical applications.

The popularization of network technology promotes the development of the data fusion. It can implement remote transmission and real-time monitoring and so on. However, because of the property of the network, it also exist some challenges such as data transmission delay and loss. A significant work is to model the arrival process and then to find an optimal algorithm to update the current estimate through the delayed measurements.

The measurement arrival process is modeled as different forms and the relationship between the process and the stability is studied in many researches. [169] addresses Kalman filtering with i.i.d. Bernoulli losses and shows that depending on the eigenvalues of the state matrix and the structure of the observation matrix, there exists a critical value λ_c which is related to the stability. Meanwhile, [169] gives explicit upper and lower bounds on λ_c, and shows that they are tight in some special cases. [209] proposes a sufficient stability condition for time-varying Kalman filter with finite consecutive packet losses driven by a Markovian chain. [81] introduces the notion of peak covariance and gives the upper envelope of the actual covariance process in an unstable scalar model and a sufficient condition for peak covariance stability for the general vector model. A related problem has been studied in [140], which further shows the known lower bound on λ_c is the exact critical probability. However, in the above two papers, the number of consecutive packet

Y. Xia, M. Fu, and G.-P. Liu: Analysis and Synthesis of NCSs, LNCIS 409, pp. 75–88.
springerlink.com

losses can be infinite, which may not be practical and can lead to conservative results. [171] develops a suboptimal jump linear estimator for complexity reduction in computing the corrector gain using finite loss history where the loss process is modeled by a two-state Markovian chain. [45] considers the state estimation with lost measurements resulting from time-varying channel conditions and introduces a more general multiple state Markovian chain to model the loss and non-loss channel states, and the asymptotic mean squares estimation error for a suboptimal linear estimator is analyzed and optimized by a LMI approach. [37] shows that the expected (with respect to the fading process) estimation error covariance at the fusion center remains bounded and converges to a steady state value and provides exact deterministic bounding sequences on the average error covariance for the system models with scalar measurements (per sensor) and specific fading distributions.

Recently, many researches on state estimation both in centralized and in distributed architectures with intermittent measurements have been carried out, such as in [118, 205, 206, 123, 13, 124, 8, 164, 163, 180, 155, 166]. [118] presents an optimal algorithm for updating with out-of-sequence measurements, however, the method is referring to one-step-lag measurements. [206] presents a practical architecture and some algorithms for the networked data fusion systems with packet losses and variable delays. It's main contribution is proposing an optimal solution for one-step and multi-step out-of-sequence measurements (OOSM) problem and proving it's stability. However, the assumption that all the measurements for the different Local Filters are compressed in the same packets is not realistic. [123] shows the impact of the stochastic communication noise on the estimation process and proves that in order to maximize the stability range, the receiver should keep all the packets independent of the quality of the link or availability of a cross-layer path. [13] presents two streamlined algorithms. One is IFAsyn which is optimal for the linear system and avoids to recalculate the information of the already received measurements, the other is EIFAsyn which is suboptimal solution for nonlinear systems. [8] also considers the optimal update algorithm with single one-step-lag OOSM, which is called "algorithm A", and the optimal update algorithm, which are called algorithm Al1 and algorithm Bl1. [164] extends the optimal update algorithm with single one-step-lag and l-step-lag OOSMs algorithms in [8] to some optimal centralized update algorithms with multiple asynchronous (different lag time) OOSMs. Based on [164], [163] further presents the optimal distributed fusion update algorithm with multiple local asynchronous (1-step-lag) OOSM updates, which is proved, under some regularity conditions, to be equivalent to the corresponding optimal centralized update algorithm with all-sensor 1-step-lag OOSMs, and an optimal distributed fusion update algorithm with multiple local arbitrary-step-lag OOSM updates is also developed. A related problem has been studied by [180], in which the transmission time from each radar to the fusion center is assumed to be known only statistically but not exactly, that is, no time tag is appended to the measurement. [155] studies optimal estimation design

for sampled linear systems where the sensors measurements are transmitted to the estimator site via a generic digital communication network. Sensor measurements are subject to random delay or might even be completely lost. But the assumption in this paper which the arrival process should satisfy, is too strict. A parallel work is studied in [166], in which a probabilistic approach of state estimation for two different architectures is developed, and the assumption in it is more realistic.

In this chapter, based on the state estimation algorithm in single channel in [166], we further extends the method to multi-channel, each with a different packet arrival statistics. We first model the arrival process via a random variable. Then, we propose two different data fusion architectures with finite buffer. In the first architecture, we consider the multi-channel system as a single one with random variables through a stacked equation, then solve the state estimation problem through the Modified Kalman Filter, see Fig. 5.1. In the second architecture, we combine the Local Filter (LF) and the Master Filter (MF) as a data fusion system. The measurements are transmitted to the Local Filter with certain data delay probability, then the local state estimates are sent to the Master Filter faultlessly to be fused through a fusion criteria, see Fig. 5.2. Meanwhile, the stability of the two fusion architectures is analyzed straightforward.

The rest of this chapter is organized as follows: The problem of state estimation with intermittent measurements is formalized in Section 5.2. The centralized and distributed fusion architectures and the corresponding fusion criteria are proposed in Section 5.3 and Section 5.4. In Section 5.5 two numerical examples are given to illustrate the effectiveness of the proposed algorithms. Finally, Section 5.6 gives the conclusions and directions of the future study.

5.2 Description of Multi-sensors

Consider the following discrete time linear stochastic system with local sensors:

$$x(k+1) = Ax(k) + w(k) \tag{5.1}$$

$$y_i(k) = C_i x(k) + v_i(k), \qquad i = 1, 2, ..., N \tag{5.2}$$

where N is the total local sensors number, $x(k) \in R^n$ is the state vector, $y_i(k) \in R^{m_i}, i = 1, 2, ..., N$, are measurements, $w(k) \in R^n$ is the input noise, and $v_i(k) \in R^{m_i}, i = 1, 2, ..., N$, are measurement noises, and A, C_i are system matrices with compatible dimensions.

Assumption 5.1. *$w(k)$, $v(k)$, $k = 1, 2, ..., N$, are the uncorrelated white noises with zero mean and*

$$E\{w(k)w(j)^T\} = Q(k)\delta_{kj}$$
$$E\{v(k)v(j)^T\} = R(k)\delta_{kj}$$
$$E\{w(k)v(j)^T\} = 0$$

where $E\{\cdot\}$ is the expectation, $Q(k) \geq 0$ and $R(k) > 0$ are covariances respectively.

$$\delta_{kj} = \begin{cases} 1 & if \quad k = j \ , \\ 0 & if \quad k \neq j \ . \end{cases}$$

Assumption 5.2. *The initial state $x(0)$ is independent of $w(k)$, $v_i(k)$, $i = 1, 2, ..., N$, and*

$$E\{x(0)\} = \mu(0)$$
$$E\{[x(0) - \mu(0)][x(0) - \mu(0)]^T\} = P(0)$$

Assumption 5.3. *(A, C_i) is observable, $(A, Q^{1/2})$ is controllable.*

The stacked equation is defined as

$$y(k) = Cx(k) + v(k) \tag{5.3}$$

where

$$y(k) = [\ (y_1(k))^T\ ,\ (y_2(k))^T\ ,\ ...\ ,\ (y_N(k))^T\ ]^T$$
$$C = [\ C_1^T\ ,\ C_2^T\ ,\ ...\ ,\ C_N^T\ ]^T$$
$$v(k) = [\ (v_1(k))^T\ ,\ (v_2(k))^T\ ,\ ...\ ,\ (v_N(k))^T\ ]^T$$

There are two forms of sending information to the Fusion Center (FC). One is that the measurements of local sensors are time-stamped and transmitted through network to the Fusion Center directly. The other is that the measurements are sent to the Local Filters, then the state estimates of the Local Filters are delivered to the Master Filter. Time-stamping is necessary to reorder measurements at the filter as they can arrive out of sequence or even be lost due to the unreliability of the transmission through network. For the model in this chapter, each $y_i(k)$ is delayed by $d_i(k)$ times, where $d_i(k)$ is a random variable described by a probability mass function f_i:

$$f_i(j) = Pr[d_i(k) = j], \quad j = 0, 1, 2, ...\ ,\ i = 1, 2, ..., N \tag{5.4}$$

For simplicity, we assume that f_{i_1} and f_{i_2} are independent and identical distribution (i.i.d) if $i_1 \neq i_2$, and $d(k_1)$ and $d(k_2)$ are independent if $k_1 \neq k_2$. We further assume that $d_i(k)$ is independent of $w(k)$, $v_i(k)$ and the initial state $x(0)$.

In this chapter, similar to [166], we assume that all observation packets correctly delivered to the Fusion Center are stored in a buffer with length

of L. If $y_i(k-L)$ is not received by the FC before or at k, then it will be considered to be lost, the arrival process is modeled via the random variable $\gamma_i(t,k)$:

$$\gamma_i(t,k) = \begin{cases} 1 & if\ y_i(t)\ arrived\ before\ or\ at\ time\ k, k \geq t \\ 0 & otherwise. \end{cases} \tag{5.5}$$

From this definition, it follows that if $\gamma_i(t,k) = 1$, then $\gamma_i(t,k+l) = 1$ for $\forall l \in \mathbf{N}$, which indicates that if $y_i(t)$ is received by the filter before or at time k, then it will be present for all future times. More formally, the value stored in the t-slot of the buffer at time k can be written as

$$y_i(t,k) = \gamma_i(t,k)y_i(t) = \gamma_i(t,k)C_i x(t) + \gamma_i(t,k)v_i(t) \tag{5.6}$$

The optimal update problem is as follows:

$$\hat{x}(k|k) = E\{x(k)|Y_k, \gamma_k\} \tag{5.7}$$
$$\hat{x}(k|k-1) = E\{x(k)|Y_{k-1}, \gamma_{k-1}\} \tag{5.8}$$

where

$$\begin{aligned} Y_k &= [y(1,k), y(2,k), ..., y(k,k)] \\ y(t,k) &= [(y_1(t,k))^T, (y_2(t,k))^T, ..., (y_N(t,k))^T]^T \\ \gamma_k &= [\gamma(1,k), \gamma(2,k), ..., \gamma(k,k)] \\ \gamma(t,k) &= [\gamma_1(t,k), \gamma_2(t,k), ..., \gamma_N(t,k)]^T \end{aligned}$$

Without loss of generality, the error and error covariance are defined as

$$e(k|k) = x(k) - \hat{x}(k|k) \tag{5.9}$$
$$P(k|k) = E\{e(k|k)(e(k|k))^T|Y_k, \gamma_k\} \tag{5.10}$$
$$e(k|k-1) = x(k) - \hat{x}(k|k-1) \tag{5.11}$$
$$P(k|k-1) = E\{e(k|k-1)(e(k|k-1))^T|Y_{k-1}, \gamma_{k-1}\} \tag{5.12}$$

For convenience, we define the following variables:

$$\begin{aligned} \hat{x}(t|h,k) &= E\{x(t)|y(1,k), y(2,k), ..., y(h,k), \gamma(1,k), \gamma(2,k), ..., \gamma(h,k)\} \\ e(t|h,k) &= x(t) - \hat{x}(t|h,k) \\ P(t|h,k) &= E\{e(t|h,k)(e(t|h,k))^T|y(1,k), y(2,k), ..., y(h,k), \\ &\qquad \gamma(1,k), \gamma(2,k), ..., \gamma(h,k)\} \end{aligned}$$

Obviously, $\hat{x}(k|k) = \hat{x}(k|k,k)$ and $P(k|k) = P(k|k,k)$.

In the following, two different architectures and methods of computing the optimal estimate and the error covariance by utilizing the delayed observations will be considered.

5.3 A Centralized Fusion Method of Multi-channel Estimation with Measurement Delay

In this part, we assume that all the measurements are sent to the Fusion Center directly through the communication channels, then a centralized method of computing the optimal estimate and the error covariance by using all the information including the delayed observation will be presented.

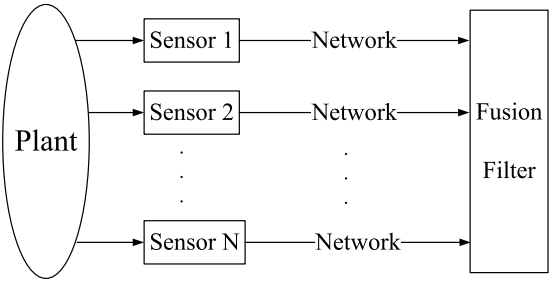

Fig. 5.1 Centralized fusion system.

Similar to (5.3) , the observation equation can be written as

$$y(t,k) = C(t,k)x(t) + v(t,k) \tag{5.13}$$

where

$$y(t,k) = \begin{pmatrix} y_1(t,k) \\ y_2(t,k) \\ \vdots \\ y_N(t,k) \end{pmatrix}, C(t,k) = \begin{pmatrix} \gamma_1(t,k)C_1 \\ \gamma_2(t,k)C_2 \\ \vdots \\ \gamma_N(t,k)C_N \end{pmatrix},$$
$$v(t,k) = \begin{pmatrix} \gamma_1(t,k)v_1(t,k) \\ \gamma_2(t,k)v_2(t,k) \\ \vdots \\ \gamma_N(t,k)v_N(t,k) \end{pmatrix} \tag{5.14}$$

and the covariance of the vector $v(t,k)$ is given as

$$R(t,k) = E\{v(t,k)(v(t,k))^T\} = \begin{bmatrix} \tilde{R}_1 & 0 & \cdots & 0 \\ 0 & \tilde{R}_2 & \cdots & 0 \\ \vdots & \vdots & \ddots & \vdots \\ 0 & 0 & \cdots & \tilde{R}_N \end{bmatrix}$$

where

$$\tilde{R}_i = \begin{cases} R_i & if \quad \gamma_i(t,k) = 1 \\ \sigma^2 I & if \quad \gamma_i(t,k) = 0 \end{cases}$$

In reality, the absence of observation corresponds to the limiting case of $\sigma \to \infty$, i.e., the measurement noise can be seen as infinite if the observation is not received, see [169].

The length of the buffer in multi-channel will be described as

$$L = \begin{cases} max\{L_i |\ if\ \exists L_i\ s.t.\ Pr[P_i(k|k)(L_i, f_i) \leq M] \geq 1 - \epsilon\} \\ \infty \qquad otherwise \end{cases} \tag{5.15}$$

where L_i is the length of the given buffer in single channel and the computation of it can be seen in [166], f_i was defined in (5.4) and $\Pr[P_i(k|k)(L_i, f_i) \leq M]$ is the probability of $P_i(k|k) \leq M$ under the condition of L_i, f_i. The received measurements are stored in the buffer which the length is L, i.e., $y(t,k) = [(y_1(t,k))^T, (y_2(t,k))^T, ..., (y_N(t,k))^T]^T,\ t = k - L + 1, ..., k,$ are stored in the t-slot of the buffer at time k, meanwhile, if the measurement $y_i(t,k),\ t = k - L + 1, ..., k,\ i = 1, 2, ..., N$ has not been received until time k, then the dummy variable zero would be stored in the corresponding slot.

$$\tau = \begin{cases} min\{t | \sum_{i=1}^{N} \gamma_i(t,k) > \sum_{i=1}^{N} \gamma_i(t,k), k - L + 1 \leq t < k\} \\ k \qquad otherwise \end{cases} \tag{5.16}$$

From the definition of τ, it can be seen that $y(\tau, k)$ is the oldest measurement vector, in which at least one measurement $y_i(\tau, k)$ is received by the FC at time k.

Now we can give the main results of this section:

Theorem 5.1. *Consider the stochastic linear system given in equations (5.1) - (5.2), the optimal estimate $\hat{x}(k|k,k)$ can be computed as follows:*

(1) when $1 \leq k \leq L$, we have:

$$\hat{x}(t|t-1,k) = A\hat{x}(t-1|t-1,k) \tag{5.17}$$

$$P(t|t-1,k) = AP(t-1|t-1,k)A^T + Q \tag{5.18}$$

$$K(t,k) = P(t|t-1,k)C(t,k)^T(C(t,k)P(t|t-1,k)C(t,k)^T + R(t,k))^{-1} \tag{5.19}$$

$$\hat{x}(t|t,k) = \hat{x}(t|t-1,k) + K(t,k)(y(t,k) - C(t,k)x(t|t-1,k)) \tag{5.20}$$

$$P(t|t,k) = (I - K(t,k)C(t,k))P(t|t-1,k) \tag{5.21}$$

for $t = 1, 2, ..., k$ and $\hat{x}(0|0,k) = x(0)$, $P(0|0,k) = P(0)$.

(2) when $k > L$, from the definition of τ, we have:

$$\hat{x}(\tau-1|\tau-1,k) = \hat{x}(\tau-1|\tau-1,k-1) \tag{5.22}$$

$$P(\tau-1|\tau-1,k) = P(\tau-1|\tau-1,k-1) \tag{5.23}$$

then as equations (5.17)-(5.21), for $t = \tau, ..., k$, the optimal estimate $\hat{x}(k|k)$ and the error covariance $P(k|k)$ can be easily obtained by iterating $k-\tau+1$ times from $\hat{x}(\tau-1|\tau-1,k)$.

Proof:

(1) Substituting $y(t,k)$, $C(t,k)$, $v(t,k)$ and $R(t,k)$ into the standard Kalman filter, then (5.17)-(5.21) can be gotten.

(2) From the definition of τ in equation (5.16), it can be known: τ is the oldest time when the measurement of one communication channel was updated, i.e., no new information in observation vector $y(t), t = k-L+1, ..., \tau-1$ in equation (5.3) was received at time k, therefore, $\hat{x}(\tau-1|\tau-1,k) = \hat{x}(\tau-1|\tau-1,k-1)$, and $P(\tau-1|\tau-1,k) = P(\tau-1|\tau-1,k-1)$, the optimal estimate $x(k|k)$ and error covariance $P(k|k)$ can be obtained by iterating $k-\tau+1$ times from $\hat{x}(\tau-1|\tau-1,k)$.

Remark 5.2. If there is no observation delay or loss, i.e., $\gamma_i(t,k) = 1$ for $\forall t \le k$ *and* $\forall i = 1, 2, ..., N$, then the method in Theorem 5.1 can be seen as the standard Kalman Filter. If there is only one communication channel, i.e., $N = 1$, then the method is similar to the Modified Kalman Filter in [169] and [166].

Remark 5.3. [154] also presented a method of state estimation with buffer, but the assumption $\hat{x}(k-L+1|k-L+1,k) = \hat{x}(k-L+1|k-L+1,k-1)$, $P(k-L+1|k-L+1,k) = P(k-L+1|k-L+1,k-1)$ is unrealistic. Compared with [154], there is no such constraint on the arrival process, so the method in this chapter is not necessary to iterate L times from the beginning of the buffer, but just $k-\tau+1$ times from $\tau-1 (k-L+1 \le \tau \le k)$ when one new measurement $y^i(\tau,k)$ is received by the FC at time k. In particular, if $\tau = k-L+1$, then the method of Theorem 5.1 is similar to that of [154], i.e., the result in [154] is a special case of this chapter.

Note that the data fusion method with buffer in Theorem 5.1 always includes more information than that without buffer, then another result can be given as follows:

Theorem 5.4. *Consider the stochastic linear system given in equations (5.1)-(5.2), and the data arrival process in equation (5.5). Let the optimal estimate $\hat{x}(k|k)$ computed by Theorem 5.1 with buffer be $\hat{x}(k|k,k)$, and without buffer be $\tilde{x}(k|k)$ if $P(k|k,k) = E\{(x(k)-\hat{x}(k|k,k))(x(k)-\hat{x}(k|k,k))^T\}$, and $\tilde{P}(k|k) = E\{(x(k)-\tilde{x}(k|k))(x(k)-\tilde{x}(k|k))^T\}$, then*

$$P(k|k,k) \le \tilde{P}(k|k) \tag{5.24}$$

Proof: According to the computation of $\hat{x}(k|k,k) = E\{x(k)|Y_k, \gamma_k\}$, we know that Y_k includes both the measurements arrived on time and that delayed not more than $L-1$ times. Meanwhile, $\tilde{x}(k|k) = E\{x(k)|\tilde{Y}_k, \tilde{\gamma}_k\}$, $\tilde{Y}_k$ only includes the measurements arrived on time. Obviously, Y_k contains more information than $\tilde{Y}_k$, i.e., $Y_k \supseteq \tilde{Y}_k$. Therefore, the error covariance of $\hat{x}(k|k,k)$ with buffer is always smaller than that of $\tilde{x}(k|k)$.

5.4 A Distributed Fusion Method of Multi-channel with Measurement Delay

In this section, we assume that all the measurements are sent to the local fusion filter through the communication channels, then the local optimal estimates are delivered to the Fusion Center directly. We also assume that the Fusion Center received the optimal estimates without data loss or delay, then based on [166], in which a single channel optimal estimate method was proposed, a distributed fusion theorem of computing the optimal estimate and the error covariance by using all the information including the delayed observation will be presented.

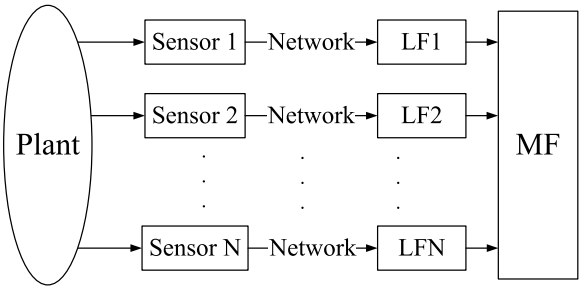

Fig. 5.2 Distributed fusion system.

First, we will introduce a well-known distributed fusion architecture: Federated Filter. In this fusion architecture, the Local Filters sent their state estimates to the Master Filter, then the Master Filter fused the estimates according to the following criteria to get the global state estimate:

$$P_g = [\sum_{i=1}^{N} (P_i)^{-1}]^{-1}$$

$$\hat{x}_g = P_g \sum_{i=1}^{N} (P_i)^{-1} \hat{x}_i$$

where $\hat{x}_i(k|k)$ and $P_i(k|k)$ are the state estimate and the error covariance of the ith Local Filter, respectively, $\hat{x}_g(k|k)$ and $P_g(k|k)$ are the global optimal state estimate and its error covariance.

As aforementioned, for the model in this chapter, each $y_i(k)$ is delayed by $d_i(k)$ times, where $d_i(k)$ is a random variable described by a probability mass function f_i:

$$f_i(j) = Pr[d_i(k) = j], \quad j = 0, 1, 2, \dots, \ i = 1, 2, ..., N$$

where f_{i_1} and f_{i_2} are independent and identical distribution (i.i.d) if $i_1 \neq i_2$, and $d(k_1)$ and $d(k_2)$ are independent if $k_1 \neq k_2$.

Based on the single channel fusion method in [166], it is easy to find a sufficient and necessary L_i such that $E\{P_i(k|k)\}$ is stable, i.e., $E\{P_i(k|k)\} \leq M$. We also define

$$\tau_i = \begin{cases} min\{t| \ \ if \ \exists \ t \ s.t. \ \gamma_i(t,k) = 1 \ and \ \gamma_i(t,k-1) = 0, \\ \qquad\qquad 0 < k - L_i + 1 \leq t < k\}, \\ k \qquad otherwise. \end{cases} \tag{5.25}$$

for the ith channel.

Then the global state estimate can be computed as follows:

Theorem 5.5. *Consider the stochastic linear system given in equations (5.1)-(5.2), and the data arrival process in equation (5.5), the optimal estimate $\hat{x}(k|k,k)$ can be yielded by two steps:*

Step 1: Computing the state estimate and the corresponding error covariance of the ith Local Filter as in [166]:

$$\hat{x}_i(\tau_i - 1|\tau_i - 1, k) = \hat{x}_i(\tau_i - 1|\tau_i - 1, k - 1) \tag{5.26}$$

$$P_i(\tau_i - 1|\tau_i - 1, k) = P_i(\tau_i - 1|\tau_i - 1, k - 1) \tag{5.27}$$

$$K_i(\tau_i, k) = P_i(\tau_i|\tau_i - 1, k)C_i^T(C_iP_i(\tau_i|\tau_i - 1, k)C_i^T + R_i)^{-1} \tag{5.28}$$

$$\hat{x}_i(\tau_i|\tau_i, k) = A\hat{x}_i(\tau_i|\tau_i, k) + \gamma_i(\tau_i, k)K_i(\tau_i, k)(y_i(\tau_i) - C_ix_i(\tau_i|\tau_i, k)) \tag{5.29}$$

$$P_i(\tau_i|\tau_i, k) = (I - \gamma_i(\tau_i, k)K_i(\tau_i, k)C_i)P_i(\tau_i|\tau_i - 1, k) \tag{5.30}$$

where $\hat{x}(0|0,k) = x(0), P(0|0,k) = P(0)$.

Then the optimal estimate $\hat{x}_i(k|k)$ and the corresponding error covariance $P_i(k|k)$ can be yielded by iterating $k - \tau$ times from $\hat{x}(\tau|\tau,k)$.

Step 2: After receiving the state estimates from the Local Filters, the global estimate can be obtained according to the Federated Filter criteria as

$$P_g(k|k) = [\sum_{i=1}^{N}(P_i(k|k))^{-1}]^{-1} \tag{5.31}$$

$$\hat{x}_g(k|k) = P_g(k|k) \sum_{i=1}^{N} (P_g(k|k))^{-1} \hat{x}_i(k|k) \tag{5.32}$$

Proof: The proof is similar to the proof of Theorem 5.1.

Theorem 5.6. *Consider the stochastic linear system given in equations (5.1)-(5.2), and the data arrival process in equation (5.5), the sufficient and necessary minimum* L_i, $i = 1, 2, ..., N$, *can be always found such that:*

$$P_g(k|k) \leq M$$

Proof: For the ith ($i = 1, 2, ..., N$) Local Filter, [166] has proved that there must be sufficient and necessary minimum L_i, $i = 1, 2, ..., N$, such that $P_i(k|k) \leq M$, and it is obvious that $P_g(k|k) \leq P_i(k|k)$ according to equation (5.31), therefore, we have $P_g(k|k) \leq M$.

5.5 Numerical Examples

In this section, we illustrate some examples of different parameters to support the results in this chapter.

Consider the following discrete time linear stochastic system with local sensors in equation (5.1) and equation (5.2):

$$A = \begin{bmatrix} 1.01 & 0.3 \\ 0 & 1.01 \end{bmatrix}, \quad C_1 = [\,1\ 1\,], \quad C_2 = [\,1\ 1.5\,],$$
$$Q = \begin{bmatrix} 1 & 0 \\ 0 & 1 \end{bmatrix}, \quad R_1 = 1, \quad R_2 = 1.5,$$

Similar to [166], we model the packet delay as a Poisson distribution with mean d_i, i.e., the probability density function satisfies:

$$f_i(j) = \frac{(d_i)^j e^{-d_i}}{j!}, \quad j = 0, 1, ...$$

where $d_i = E\{d_k^i\}$ denotes the mean value of the packet delay in the ith channel, and in this chapter suppose $d_1 = 3$ and $d_2 = 2$.

5.5.1 A Centralized Example

In this example, from the centralized filter architecture, we can obtain corresponding $D_1 = 5$ and $D_2 = 3$ by utilizing the same method as shown in [166] such that single channel keep stable. Then we choose $D = max\{D_1, D_2\} = 5$ to illustrate Theorem 5.1 as shown in Fig. 5.3-Fig. 5.5.

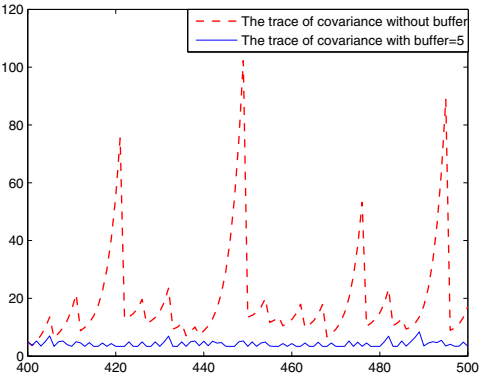

Fig. 5.3 The trace of the covariance of filter with buffer=5 and without buffer in centralized system.

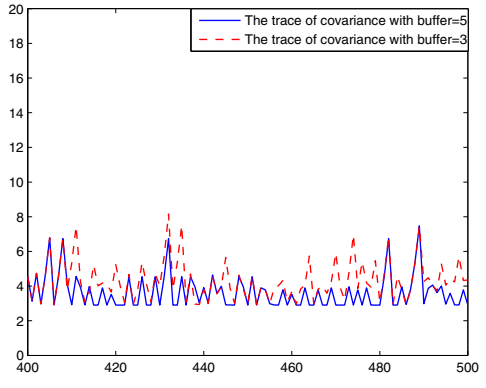

Fig. 5.4 The trace of the covariance of filter with buffer=5 and buffer=3 in centralized system.

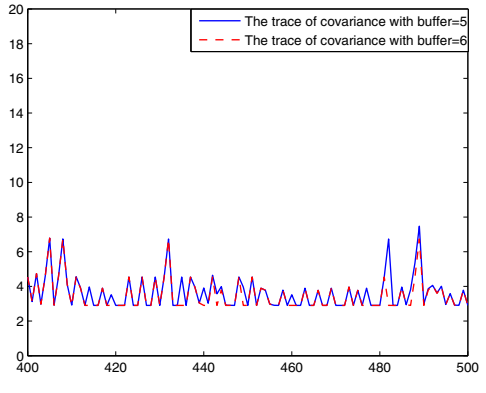

Fig. 5.5 The trace of the covariance of filter with buffer=5 and buffer=6 in centralized system.

From Fig. 5.1, it is clear that the trace of the error covariance with buffer $D = 5$ is much smaller than that without buffer. However, if $D = 3$ as shown in Fig. 5.2, the performance of the filter become worse than $D = 5$. Meanwhile, from Fig. 5.3 we also notice that $D = 6$ leads to little difference on the filter, but increases burden of calculations.

5.5.2 A Distributed Example

In this example, a distributed filter architecture is considered and we also choose $D_1 = 5$ and $D_2 = 3$ to estimate the Local Filters states, then send them to Master Filter. Fig. 5.6 and Fig. 5.7 show the simulation results as follows:

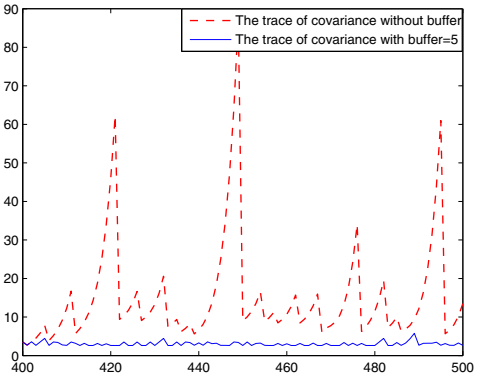

Fig. 5.6 The trace of the covariance of filter with buffer=5 and without buffer in distributed system.

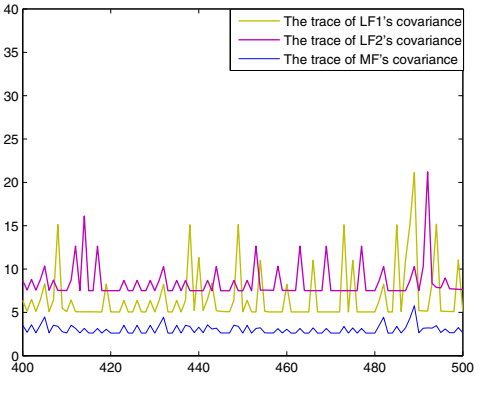

Fig. 5.7 The trace of the covariance of the Local Filters and the Master Filter with buffer=5 in distributed system.

From Fig. 5.6 and Fig. 5.7, we can see that the trace of the error covariance of the Master Filter is smaller than that of local filters and that without buffer.

Actually, there have been proved that under the assumption of cross-uncorrelated sensor noises, the centralized Kalman Filter is equivalent to the distributed Kalman Filter when all the measurements information are received.

5.6 Summary

In this chapter, we have presented two different architectures for networked data fusion-a centralized architecture and a distributed architecture with finite buffer. It is shown that the performance of the fusion filter with buffer is much better than that without it. The results obtained are useful for the practical applications. Finally, two numerical examples are given to show the theorem proposed in this chapter. An important future study is to consider the relationship between the local sensors, it is interesting to extend the work in this chapter to that aspect.

Chapter 6
Networked Data Fusion with the Asynchronous Observations at Multiple Rates

6.1 Introduction

Most of the earlier works are based on the measurements observed by sensors with synchronous samples at the same sampling rate [10, 20, 23, 28, 39]. Only a few pieces of work deal with asynchronous multirate multisensor data fusion. Based on continuous time systems, Alouani with his group [4] and Bar-Shalom et al. [10, 8] present some effective algorithms for asynchronous multisensor systems. As far as the discrete time systems are concerned, the related researches include the approaches based on multiscale system theory [72, 11, 12, 195, 211, 226], the batch process methods [104], and the algorithms based on the designing of multirate filter banks [42], etc. In the literature listed above, the missing of observations is rarely concerned, which is inclined to encounter in many application fields including communication, navigation, etc. For filtering of incomplete measurements, there are some interesting results. Among these, the algorithms presented by the team of Wang are promising that it has proper computation complexity and can generate nearly optimal state estimate [194]. Based on a discrete-time linear dynamic system, Kalman filtering with intermittent observations is studied in [169], where the arrival of the observations is modeled as a random process, and the statistical convergence property of Kalman filter is given. The modified Riccati equation is studied by Boers and his group [15]. Some useful results are presented as far as a single sensor observing a single target which is described by a linear state space model is concerned. Kalman filtering with faded measurements is studied in [173]. By use of peak covariance as an estimate of filtering deterioration caused by packet losses, the stability of Kalman filtering with Markovian packet losses is studied in [81] based on a linear time-invariant system. Bar-Shalom studies the state estimation with out of sequence measurements based on a time-invariant dynamic system [8]. Xia, Shang, Chen and Liu study the networked data fusion with packet losses and variable delays, and an optimal state estimate is generated [206]. However, in all these interesting papers, multirate systems are not concerned.

Y. Xia, M. Fu, and G.-P. Liu: Analysis and Synthesis of NCSs, LNCIS 409, pp. 89–105.
springerlink.com

The multi-rate linear minimum mean squared error state estimation problem is solved by use of the lifting technique [99]. While, asynchronous sampling and data losses are not concerned in this reference. To sum up, there are few results on the fusion of multirate sensors that sample asynchronously with measurements randomly missing. This motivates us for the present study.

In this chapter, the optimal state estimation for a kind of linear dynamic systems with the observations obtained asynchronously with multiple rates will be concerned, where the observations may lose randomly. For each sensor, a rule is proposed to check out whether the measurement is missing. With the help of the modified Kalman filter, the multiscale system theory and the federated square root filter, the optimal state estimate is obtained at the highest sampling rate.

This chapter is organized as follows: Section 6.2 is the problem formulation. In Section 6.3, the state estimation algorithm is presented. Section 6.4 is the numerical simulation and Section 6.5 reaches the conclusion.

6.2 Description of Multi-sensors with Different Sampling Rates

A class of dynamic system that is observed by multiple sensors will be considered in this chapter. These sensors sample asynchronously at different sampling rates with measurements randomly missing [211, 104, 194, 103]

$$x(k+1) = Ax(k) + w(k) \tag{6.1}$$

$$y_i(k) = \gamma_i(k)C_i x_i(k) + v_i(k),\ i = 1, 2, ..., N \tag{6.2}$$

where $x(k) \in R^n$ is the state variable vector at time kT, where T is the sampling interval of sensor N. $A \in R^{n\times n}$ is the system matrix. The process noise $w(k) \in R^{n\times 1}$ is zero-mean white Gaussian sequence, whose variance is Q.

The system state vector $x(k)$ is observed by N sensors, and each sensor i observes the same single target independently with different sampling rates. The measurements $y_i(k),\ i = 1, 2, \cdots, N$ are obtained asynchronously. $y_i(k) \in R^{q_i\times 1}(q_i \leq n)$ is the kth measurement observed by sensor i with sampling rate S_i. The sampling rates of the sensors meet

$$S_i = S_N/n_i, 1 \leq i \leq N-1 \tag{6.3}$$

where n_i are known positive integers. For $i = 1, 2, \cdots, N$, $C_i \in R^{q_i\times n}$ is the measurement matrix. The measurement noise $v_i(k) \in R^{q_i\times 1}$ is supposed to be a zero-mean white Gaussian noise with variance $R_i, i = 1, 2, \cdots, N$.

The initial value of the state vector $x(0)$ is a random vector, whose mean and estimation error covariance are x_0 and P_0, respectively. It is assumed that $x(0)$, $w(k)$ and $v_i(k)$ are mutually independent.

The variable $\gamma_i(k) \in R$ is a stochastic sequence that takes values on 1 and 0 with Bernoulli distribution, which is used to describe the missing of measurements. It is assumed that $\gamma_i(k)$ is independent of $w(k)$, $v_i(k)$ and $x(0)$, $i = 1, 2, \cdots, N$.

The objective of this chapter is to develop an algorithm, which can effectively fuse the measurements observed by different sensors with asynchronous sampling at multiple rates in case of measurements randomly missing, in order to generate the optimal estimate of state $x(k)$.

Remark 6.1. The asynchronous multirate multisensor dynamic system is described at different scales, where the sensors that observe the target with higher sampling rates are at finer scales, and the sensors that observe with lower sampling rates are at lower scales.

Remark 6.2. For simplification, time delay and out of sequence measurements are not concerned in this chapter. The measurements of sensor N are divided into blocks, and the length of per block $m(n_1, n_2, \cdots, n_{N-1})$ is the least common multiple of $n_1, n_2, \cdots$, and n_{N-1}. It is assumed that sensor N (at the highest sampling rate) should sample uniformly. While, any other sensor $i(1 \leq i \leq N-1)$ does not need to sample uniformly but should sample $p_i = m(n_1, n_2, \cdots, n_{N-1})/n_i$ times per block. This means $y_i(k)$ can be obtained at any time between $(p_i(k-1)+1)T$ and $(p_i k)T$, and the sampling of different sensors can be asynchronous. For example, in Fig. 6.1, sensor 3 at the highest sampling rate samples uniformly, i.e., $y_3(k)$ is obtained at time kT. As to sensors 2 and 1, whose sampling rates are half and one third of sensor 3, respectively, may sample non-uniformly. $y_2(k)$ is obtained at any time between $(2k-1)T$ and $(2k)T$. $y_1(k)$ is obtained between $(3k-2)T$ and $(3k)T$. We refer the readers to [211] or [104] for more detail.

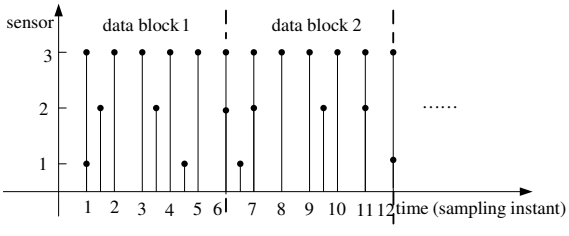

Fig. 6.1 Time (sampling instant) vs. sensor.

6.3 The Data Fusion State Estimation Algorithm

When there is no any prior information, the state variable vector $x_i(k)$ at scale i may be established by the state vector $x(n_i k)$ at scale N through the following linear transformation [11, 12, 211, 226, 104]:

$$x_i(k) = \frac{1}{n_i}[\sum_{m=0}^{n_i-1} A^{-m}]x(n_i k) \tag{6.4}$$

where n_i is the sampling ratio of sensor N to sensor i, $i = 1, 2, \cdots, N$.

In the sequel, we will first establish the state space model at scale $i(1 \leq i \leq N)$. Then, using the modified Kalman filter at scale i to estimate $x_i(k)$. Finally, by regressing the estimate from scale i to N, and then by fusing them, the optimal state estimate of $x(k)$ will be generated.

Theorem 6.3. *The dynamic system models can be described at scale* $i(1 \leq i \leq N)$ *by the following formulas:*

$$x_i(k+1) = A_i x_i(k) + w_i(k) \tag{6.5}$$
$$y_i(k) = \gamma_i(k) C_i x_i(k) + v_i(k) \tag{6.6}$$

where $w_i(k)$ *and* $v_i(k)$ *are zero-mean Gaussian white noises that satisfy*

$$E\{w_i(k) w_i^T(l)\} = Q_i \delta_{kl} \tag{6.7}$$
$$E\{v_i(k) v_j^T(l)\} = Q_i \delta_{ij} \delta_{kl} \tag{6.8}$$
$$E\{w_i(k) v_j^T(l)\} = 0,\ i, j = 1, 2, \cdots, N-1;\ k, l = 1, 2, \cdots \tag{6.9}$$

and

$$A_i = A^{n_i} \tag{6.10}$$

$$Q_i = \frac{1}{n_i^2}[\sum_{m=0}^{n_i-1} A^{-m}][\sum_{m=0}^{n_i-1} A^m Q A^{m,T}][\sum_{m=0}^{n_i-1} A^{-m}]^T \tag{6.11}$$

where $E\{\cdot\}$ is the expectation function, δ_{kl} is the Kronecker δ function, and $A^{m,T}$ denotes the transpose of A^m that is the mth power of matrix A.

Proof. When $i = N, n_N = 1$, we have $A_N = A^{n_N} = A$. Therefore, from (6.1) and (6.2), we have Theorem 1 in the case of $N = 1$. Generally speaking, from (6.4), we have

$$\begin{aligned} x_i(k+1) &= \frac{1}{n_i}[\sum_{m=0}^{n_i-1} A^{-m}]x(n_i(k+1)) \\ &= \frac{1}{n_i}[\sum_{m=0}^{n_i-1} A^{-m}][Ax(n_i k + n_i - 1) + w(n_i k + n_i - 1)] \\ &= \frac{1}{n_i}[\sum_{m=0}^{n_i-1} A^{-m}][A^{n_i} x(n_i k) + \sum_{m=0}^{n_i-1} A^m w(n_i k + n_i - 1 - m)] \\ &= A_i x_i(k) + w_i(k) \end{aligned} \tag{6.12}$$

where

$$A_i = A^{n_i} \tag{6.13}$$

and

$$w_i(k) = \frac{1}{n_i}[\sum_{m=0}^{n_i-1} A^{-m}] \sum_{m=0}^{n_i-1} A^m w(n_i k + n_i - 1 - m) \tag{6.14}$$

For the stochastic sequence $w_i(k)$, by use of the linear property of the mathematical expectation, we have

$$E\{w_i(k)\} = \frac{1}{n_i}[\sum_{m=0}^{n_i-1} A^{-m}] \sum_{m=0}^{n_i-1} A^m E\{w(n_i k + n_i - 1 - m)\} \tag{6.15}$$

and

$$E\{w_i(k) w_i^T(l)\} = E[\{\frac{1}{n_i}[\sum_{m=0}^{n_i-1} A^{-m}] \tag{6.16}$$

$$\begin{aligned}
&\sum_{m=0}^{n_i-1} A^m w(n_i k + n_i - 1 - m)\}\{\frac{1}{n_i}[\sum_{m=0}^{n_i-1} A^{-m}] \sum_{m=0}^{n_i-1} A^m w(n_i k + n_i - 1 - m)\}^T] \\
&= \frac{1}{n_i^2}[\sum_{m=0}^{n_i-1} A^{-m}][\sum_{m=0}^{n_i-1} A^m Q A^{m,T}][\sum_{m=0}^{n_i-1} A^{-m}]^T \delta_{kl} \\
&= Q_i \delta_{kl}
\end{aligned} \tag{6.17}$$

where $A^{m,T}$ denotes the transpose of A^m, and where

$$Q_i = \frac{1}{n_i^2}[\sum_{m=0}^{n_i-1} A^{-m}][\sum_{m=0}^{n_i-1} A^m Q A^{m,T}][\sum_{m=0}^{n_i-1} A^{-m}]^T \tag{6.18}$$

In addition, by use of (6.14) and the independence of $w(k)$ and $v_i(k)$, for $i, j = 1, 2, \cdots, N-1$; $k, l = 1, 2, \cdots$, we have

$$E\{w_i(k) v_j^T(l)\} = E[\{\frac{1}{n_i}[\sum_{m=0}^{n_i-1} A^{-m}] \sum_{m=0}^{n_i-1} A^m w(n_i k + n_i - 1 - m)\} v_j^T(l)] = 0$$

□

For $i = 1, 2, \cdots, N$, denote

$$\hat{x}_i(k|k) \equiv E\{x_i(k)|Y_1^k(i)\} \tag{6.19}$$

$$\hat{x}_{N|i}(k|k) \equiv E\{x(k)|Y_1^{[\frac{k}{n_i}]}(i)\} \tag{6.20}$$

$$\hat{x}(k|k) \equiv E\{x(k)|Y_1^k(N), Y_1^{[\frac{k}{n_{N-1}}]}(N-1), \cdots, Y_1^{[\frac{k}{n_1}]}(1)\} \tag{6.21}$$

where

$$Y_1^k(i) \equiv \{y_i(1), y_i(2), \cdots, y_i(k)\} \tag{6.22}$$

In the sequel, $\hat{x}(k|k)$ is to be generated.

It should be noted that $Y_1^k(i)$ is the first to the k-th measurements observed by sensor i. $\hat{x}_i(k|k)$ means the expectation (the estimation) of $x_i(k)$ based on information from $Y_1^k(i)$. $\hat{x}_{N|i}(k|k)$ means the expectation of $x(k)$ based on the information from sensor i obtained till time kT. $\hat{x}(k|k)$ means the expectation of $x(k)$ based on the information from all the sensors up to time kT. $'[\cdot]'$ in (6.20) and (6.21) means the minimum integer that is not less than $'\cdot'$.

Based on the results in [20, 169, 30], we have the following theorem.

Theorem 6.4. *For any $k = 1, 2, \cdots$, the estimate and the estimation error covariance of $x(k)$ based on all the observations before time kT are denoted by $\hat{x}(k|k)$ and $P(k|k)$, then they can be generated by use of the following formulas:*

$$\hat{x}(k|k) = \sum_{i=1}^{N} \alpha_i(k)\hat{x}_{N|i}(k|k) \tag{6.23}$$

$$P(k|k) = (\sum_{i=1}^{N} P_{N|i}^{-1}(k|k))^{-1} \tag{6.24}$$

where

$$\alpha_i(k) = P(k|k)P_{N|i}^{-1}(k|k) \tag{6.25}$$

$$\hat{x}_{N|i}(k|k) = \begin{cases} n_i[\sum\limits_{m=0}^{n_i-1} A^{-m}]^{-1}\hat{x}_i(l|l), & \text{if } k = n_i l \\ n_i A^p[\sum\limits_{m=0}^{n_i-1} A^{-m}]^{-1}\hat{x}_i(l|l), \text{ if } k = n_i l + p, \quad p = 1, 2, \cdots, n_i - 1 \end{cases} \tag{6.26}$$

$$P_{N|i}(k|k) = \begin{cases} n_i^2[\sum\limits_{m=0}^{n_i-1} A^{-m}]^{-1}P_i(l|l)[\sum\limits_{m=0}^{n_i-1} A^{-m}]^{-T}, & \text{if } k = n_i l \\ n_i^2 A^p[\sum\limits_{m=0}^{n_i-1} A^{-m}]^{-1}P_i(l|l)[\sum\limits_{m=0}^{n_i-1} A^{-m}]^{-T}A^{p,T} \\ \qquad + \sum\limits_{l=0}^{p-1} A^l Q A^{l,T}, \\ \text{if } k = n_i l + p, \ p = 1, 2, \cdots, n_i - 1 \end{cases} \tag{6.27}$$

and for $l = k/n_i$,

$$\hat{x}_i(l|l) = \begin{cases} \hat{x}_i(l|l-1) + K_i(l)[y_i(l) - C_i\hat{x}_i(l|l-1)], & \text{if } y_i(l) \in \mathcal{Y}(i,l) \\ \hat{x}_i(l|l-1), & \text{otherwise} \end{cases}$$

$$P_i(l|l) = \begin{cases} [I - K_i(l)C_i]P_i(l|l-1), & \text{if } y_i(l) \in \mathcal{Y}(i,l) \\ P_i(l|l-1), & \text{otherwise} \end{cases}$$

$$\hat{x}_i(l|l-1) = A_i\hat{x}_i(l-1|l-1)$$

$$P_i(l|l-1) = A_iP_i(l-1|l-1)A_i^T + Q_i$$

$$K_i(l) = P_i(l|l-1)C_i^T[C_iP_i(l|l-1)C_i^T + R_i]^{-1}$$

where

$$\mathcal{Y}(i,l) = \{y_i(l) \| [y_i(l) - C_i\hat{x}_i(l|l-1)][y_i(l) - C_i\hat{x}_i(l|l-1)]^T \leq \lambda R_i\} \quad (6.28)$$

where λ *could be any scalar larger than 4. The initial terms are,*

$$\hat{x}_i(0|0) = x_0, \qquad P_i(0|0) = P_0 \quad (6.29)$$

Proof. We will prove this theorem by use of the deduction method.

For $i = N$ and $k = 1$, from equation (6.1), it follows that

$$\hat{x}_N(1|0) = Ax_0 = A\hat{x}_N(0|0) \quad (6.30)$$

therefore,

$$\tilde{x}_N(1|0) = x(1) - \hat{x}_N(1|0) = A\tilde{x}_N(0|0) + w(0) \quad (6.31)$$

and

$$P_N(1|0) = E\{\tilde{x}_N(1|0)\tilde{x}_N(1|0)^T\} = AP_N(0|0)A^T + Q = A_NP_N(0|0)A_N^T + Q_N$$

If measurement $y_N(1)$ is missing or faulty, then it should be avoided. In this case, $\hat{x}_N(1|0)$ does not need to be updated. Then we have

$$\hat{x}_N(1|1) = \hat{x}_N(1|0), \quad P_N(1|1) = P_N(1|0) \quad (6.32)$$

If measurement $y_N(1)$ is normal, then by use of Kalman filter [30], it results in

$$\hat{x}_N(1|1) = \hat{x}_N(1|0) + K_N(1)[y_N(1) - C_N\hat{x}_N(1|0)] \quad (6.33)$$

$$P_N(1|1) = [I - K_N(1)C_N]P_N(1|0) \quad (6.34)$$

where

$$K_N(1) = P_N(1|0)C_N^T[C_NP_N(1|0)C_N^T + R_N]^{-1} \quad (6.35)$$

When $k = 1$, if there are no other observations, then

$$\hat{x}(1|1) = \hat{x}_N(1|1), P(1|1) = P_N(1|1) \tag{6.36}$$

Otherwise, if there exist $y_i(1)$ and $n_i = 1$, then $\hat{x}_i(1|1)$ and $P_i(1|1)$ can be generated in the same way as $\hat{x}_N(1|1)$ and $P_N(1|1)$. The fused state estimate $\hat{x}(1|1)$ and the error covariance $P(1|1)$ can be generated by use of the federated filter [20], and (23)-(24) can be obtained. For measurements $y_i(1)$ with $n_i \neq 1$, it is obvious that $y_i(1)$ should be obtained at time lT that meets uniform distribution between $[1, n_i]T$. Hence, the event "$y_i(1)$ *and* $y_N(1)$ *arrive at exactly the same time*" can be viewed as a small probability event. When $l \in (1, n_i]$, for simplification and consistency, $y_i(1)$ would not be dealt with until time n_iT.

It should be pointed out that one may use the following rule to judge whether measurement $y_i(1)$ is missing or not:

$$[y_i(l) - C_i\hat{x}_i(l|l-1)][y_i(l) - C_i\hat{x}_i(l|l-1)]^T \leq \lambda R_i \tag{6.37}$$

where λ could be any scalar larger than 4. The reason is that

$$E\{[y_i(1) - C_ix_i(1)][y_i(1) - C_ix_i(1)]^T\} = R_i \tag{6.38}$$

Briefly, the theorem is true when $k = 1$.

Suppose $\hat{x}(k-1|k-1)$ and $P(k-1|k-1)$ have been generated by use of Theorem 6.4, $\hat{x}(k|k)$ and $P(k|k)$ will be deduced in the sequel.

Denote

$$\begin{aligned}\mathcal{Y}(i,l) = \ & \{y_i(l) \| [y_i(l) - C_iA_i\hat{x}_i(l-1|l-1)] \\ & [y_i(l) - C_iA_i\hat{x}_i(l-1|l-1)]^T \leq \lambda R_i\}\end{aligned}$$

Then, $'y_i(l) \notin \mathcal{Y}(i,l)'$ means the l-th measurement from Sensor i is missing.

It follows from (6.5) and (6.19) that

$$\begin{aligned}&\hat{x}_i(l|l) \\ &= \begin{cases} E\{x_i(l)|Y_1^{l-1}(i)\} + K_i(l)[y_i(l) - C_iE\{x_i(l)|Y_1^{l-1}(i)\}], & \text{if } y_i(l) \in \mathcal{Y}(i,l) \\ E\{x_i(l)|Y_1^{l-1}(i)\}, & \text{else} \end{cases} \\ &= \begin{cases} \hat{x}_i(l|l-1) + K_i(l)[y_i(l) - C_i\hat{x}_i(l|l-1)], & \text{if } \ y_i(l) \in \mathcal{Y}(i,l) \\ \hat{x}_i(l|l-1), & \text{else} \end{cases}\end{aligned} \tag{6.39}$$

therefore, from (6.5), (6.6) and (6.39), we have

$$\begin{aligned}\tilde{x}_i(l|l) &= x_i(l) - \hat{x}_i(l) \\ &= \begin{cases} [I - K_i(l)C_i]\tilde{x}_i(l|l-1) + K_i(l)v_i(l), & \text{if } \ y_i(l) \in \mathcal{Y}(i,l) \\ \tilde{x}_i(l|l-1), & \text{else} \end{cases}\end{aligned} \tag{6.40}$$

and

$$P_i(l|l) = E\tilde{x}_i(l|l)\tilde{x}_i^T(l|l) \tag{6.41}$$
$$= \begin{cases} [I - K_i(l)C_i]P_i(l|l-1), & \text{if } y_i(l) \in \mathcal{Y}(i,l) \\ P_i(l|l-1), & \text{else} \end{cases}$$

where $K_i(l)$ is deduced by Kalman filter as follows,

$$K_i(l) = P_i(l|l-1)C_i^T[C_iP_i(l|l-1)C_i^T + R_i]^{-1} \tag{6.42}$$

Equation (6.4) can be rewritten as

$$x(n_il) = n_i[\sum_{m=0}^{n_i-1} A^{-m}]^{-1}x_i(l) \tag{6.43}$$

therefore,

$$\begin{aligned} \hat{x}_{N|i}(n_il|n_il) &= E\{x(n_il)|Y_1^l(i)\} \\ &= E\{n_i[\sum_{m=0}^{n_i-1} A^{-m}]^{-1}x_i(l)|Y_1^l(i)\} \\ &= n_i[\sum_{m=0}^{n_i-1} A^{-m}]^{-1}E\{x_i(l)|Y_1^l(i)\} \\ &= n_i[\sum_{m=0}^{n_i-1} A^{-m}]^{-1}\hat{x}_i(l|l) \end{aligned} \tag{6.44}$$

From (6.1), for $p = 1, 2, \cdots, n_i - 1$, we have

$$\begin{aligned} \hat{x}_{N|i}(n_il+p|n_il+p) &= E\{x(n_il+p)|Y_1^{[\frac{n_il+p}{n_i}]}(i)\} \\ &= E\{x(n_il+p)|Y_1^l(i)\} \\ &= E\{A^px(n_il) + \sum_{l=0}^{p-1} A^pw(n_il+p-1-l)|Y_1^l(i)\} \\ &= A^pE\{x(n_il)|Y_1^l(i)\} \\ &= n_iA^p[\sum_{m=0}^{n_i-1} A^{-m}]^{-1}\hat{x}_i(l|l) \end{aligned} \tag{6.45}$$

Equations (6.44) and (6.45) can be rewritten as

$$\hat{x}_{N|i}(k|k) = \begin{cases} n_i[\sum_{m=0}^{n_i-1} A^{-m}]^{-1}\hat{x}_i(l|l), & \text{if } k = n_il \\ n_iA^p[\sum_{m=0}^{n_i-1} A^{-m}]^{-1}\hat{x}_i(l|l), & \text{if } k = n_il+p, \quad p = 1, 2, \cdots, n_i - 1 \end{cases} \tag{6.46}$$

From (6.21), by use of the federated filter, we have

$$\begin{aligned}\hat{x}(k|k) &= E\{x(k)|Y_1^k(N), Y_1^{[\frac{k}{n_{N-1}}]}(N-1), Y_1^{[\frac{k}{n_1}]}(1)\} \\ &= \sum_{i=1}^{N} \alpha_i(k) E\{x(k)|Y_1^{[\frac{k}{n_i}]}(i)\} \\ &= \sum_{i=1}^{N} \alpha_i(k)\hat{x}_{N|i}(k|k)\end{aligned} \tag{6.47}$$

where

$$P(k|k) = (\sum_{i=1}^{N} P_{N|i}^{-1}(k|k))^{-1}, \quad \alpha_i(k) = P(k|k)P_{N|i}^{-1}(k|k) \tag{6.48}$$

and

$$P_{N|i}(k|k) = E\{[x(k) - \hat{x}_{N|i}(k|k)][x(k) - \hat{x}_{N|i}(k|k)]^T\} \tag{6.49}$$

which can be deduced by use of (6.50)-(6.53).
For $k = n_i l$, by use of (6.4) and (6.46), we have

$$\begin{aligned}\tilde{x}_{N|i}(k|k) &= x(k) - \hat{x}_{N|i}(k|k) \\ &= n_i[\sum_{m=0}^{n_i-1} A^{-m}]^{-1} x_i(l) - n_i[\sum_{m=0}^{n_i-1} A^{-m}]^{-1}\hat{x}_i(l|l) \\ &= n_i[\sum_{m=0}^{n_i-1} A^{-m}]^{-1}\tilde{x}_i(l|l)\end{aligned} \tag{6.50}$$

therefore,

$$\begin{aligned}P_{N|i}(k|k) &= E\{\tilde{x}_{N|i}(k|k)\tilde{x}_{N|i}^T(k|k)\} \\ &= n_i^2[\sum_{m=0}^{n_i-1} A^{-m}]^{-1} P_i(l|l)[\sum_{m=0}^{n_i-1} A^{-m}]^{-T}\end{aligned} \tag{6.51}$$

For $k = n_i l + p,\ p = 1, 2, \cdots, n_i - 1$, by use of (6.1), (6.4) and (6.46), we obtain

$$\begin{aligned}\tilde{x}_{N|i}(k|k) &= x(k) - \hat{x}_{N|i}(k|k) \\ &= x(n_i l + p) - \hat{x}_{N|i}(n_i l + p|n_i l + p) \\ &= A^p x(n_i l) + \sum_{l=0}^{p-1} A^l w(n_i l + p - 1 - l) - \hat{x}_{N|i}(n_i l + p|n_i l + p) \\ &= n_i A^p[\sum_{m=0}^{n_i-1} A^{-m}]^{-1}\tilde{x}_i(l|l) + \sum_{l=0}^{p-1} A^l w(n_i l + p - 1 - l)\end{aligned} \tag{6.52}$$

and

$$P_{N|i}(k|k) = E\{\tilde{x}_{N|i}(k|k)\tilde{x}_{N|i}^T(k|k)\}$$
$$= n_i^2[\sum_{m=0}^{n_i-1} A^{-m}]^{-1}P_i(l|l)[\sum_{m=0}^{n_i-1} A^{-m}]^{-T}A^{p,T} + \sum_{l=0}^{p-1} A^l Q A^{l,T}$$

(6.51) and (6.53) can be rewritten as (6.27). This concludes the proof of Theorem 2.

Remark 6.5. From (6.38) we could get (6.37), the reason is that from the problem formulation, we know that $y_i(1) - C_i x_i(1)$ is zero-mean white Gaussian sequence. Based on the property of the normal distribution, one has $P([y_i(1) - C_i\hat{x}_i(1)][y_i(1) - C_i\hat{x}_i(1)]^T < 4\sqrt{R_i}) = 0.9544$, where $P(A)$ means the probability of A. So, if we choose λ lager than 4, (6.37) is true in the probability of lager than 0.9544.

After Theorem 6.3 and Theorem 6.4, the following result could be obtained immediately.

Theorem 6.6. *The state fusion estimation algorithm generated by Theorem 6.4 is meaningful and convergent, and we have*

$$P(k|k) \leq P_{N|i}(k|k) \tag{6.53}$$

and

$$\lim_{k\to\infty} P(k|k) \leq P \tag{6.54}$$

where P is a constant positive matrix.

Proof. (6.53) can be drawn from (6.24) directly since for each $i = 1, 2, \cdots, N$, $P_{N|i}(k|k)$ is nonnegtive. In fact, $P_{N|i}(k|k)$ is generally positive, in this case, we have $P(k|k) < P_{N|i}(k|k)$. On the other hand, from Theorem 6.4, we have

$$\begin{aligned} P(k|k) &= (\sum_{i=1}^{N} P_{N|i}^{-1}(k|k))^{-1} \\ &\leq \max\{P_N(k|k), P_N(k|k-1)\} \\ &= \max\{P_N(k|k), A_N P_N(k-1|k-1)A_N^T + Q_i\} \end{aligned} \tag{6.55}$$

therefore

$$\begin{aligned} \lim_{k\to\infty} P(k|k) &\leq \lim_{k\to\infty}[\max\{P_N(k|k), A_N P_N(k-1|k-1)A_N^T + Q_i\}] \\ &= \max\{\lim_{k\to\infty} P_N(k|k), \lim_{k\to\infty}[A_N P_N(k-1|k-1)A_N^T + Q_N]\} \\ &= \max\{P_N, AP_N A^T + Q\} \end{aligned}$$

where $P_N(k|k)$ denotes the estimation error covariance of $x(k)$ based on Sensor N without measurements missing, and P_N denotes the steady value of $P_N(k|k)$.
Denote

$$P = \max\{P_N, AP_NA^T + Q\} \tag{6.56}$$

and (6.54) can be directly generated.

Remark 6.7. Theorem 6.6 indicates two facts: (1) The presented data fusion state estimation algorithm is effective. From (6.53), one can see that the fused state estimate error covariance is smaller than those from each single sensor's. (2) The presented algorithm is meaningful. From (6.54), one can see that the presented algorithm is convergent.

Remark 6.8. For simplicity and without lose of generality, in Theorem 6.4, the effects of the cross-covariances among the local state estimation errors were not considered. In considering of the estimation error cross-covariances, the global optimal fused state estimate could be obtained by generalizing the results given by [174] from single sampling rate synchronous data fusion to the formulated problem:

$$\hat{x}(k|k) = \sum_{i=1}^{N} \alpha_i(k)\hat{x}_{N|i}(k|k) \tag{6.57}$$

$$P(k|k) = (e^T(k)\Sigma^{-1}(k)e(k))^{-1} \tag{6.58}$$

where

$$(\,\alpha_1(k)\ \alpha_2(k)\ \cdots\ \alpha_N(k)\,)^T = \Sigma^{-1}(k)e(k)(e^T(k)\Sigma^{-1}(k)e(k))^{-1} \tag{6.59}$$

$$\begin{aligned} P_{N|ij}(k|k) &= E\{[x(k) - \hat{x}_{N|i}(k|k)][x(k) - \hat{x}_{N|j}(k|k)]^T\} \\ &\equiv E\{\tilde{x}_{N|i}(k|k)\tilde{x}^T_{N|j}(k|k)\} \end{aligned} \tag{6.60}$$

and where $e(k) = (\,I_n\ I_n\ \cdots\ I_n\,)^T$ is the $nN \times n$ matrix and I_n denotes the identity matrix of dimension n. $\Sigma(k) = (P_{N|ij}(k|k))$ is an $nN \times nN$ matrix whose ijth block is $P_{N|ij}(k|k)$, $i, j = 1, 2, \cdots, N$. $\tilde{x}^T_{N|i}(k|k)$ and $\tilde{x}^T_{N|j}(k|k)$ in (6.60) are given by (6.50) and (6.52), for $k \bmod n_i = 0$ and $k \bmod n_i \neq 0$, respectively, $i, j = 1, 2, \cdots, N$. In this case, similar as [174], by use of Schwartz matrix inequality, it can be easily proven that Theorem 6.6 also holds.

The sketch of the proposed algorithm is illustrated in Fig. 6.2, where two sensors are shown with the sampling ratio being 2. The legends of the blocks are:

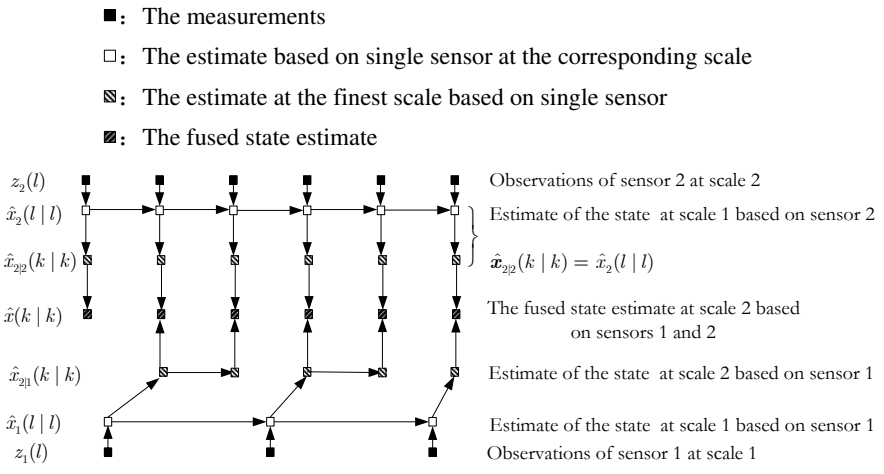

Fig. 6.2 The illustration of the presented state estimation algorithm.

6.4 Simulations

To demonstrate the performance of the proposed algorithm, an example is illustrated in this section. A radar tracking system with three sensors can be described by [104]

$$x(k+1) = \begin{bmatrix} 1 & T & T^2/2 \\ 0 & 1 & T \\ 0 & 0 & 1 \end{bmatrix} x(k) + w(k)$$
$$y_i(k) = \gamma_i(k) C_i x_i(k) + v_i(k), \ i = 1, 2, 3$$

where T is the sampling period. The state $x(k) = [s(k)\ \dot{s}(k)\ \ddot{s}(k)]^T$, where $s(k)$, $\dot{s}(k)$, and $\ddot{s}(k)$ are the position, velocity and acceleration, respectively, of the target at time kT. $y_i(k)(i = 1, 2, 3)$ are the measurements of three sensors, which observe the acceleration, the velocity and the position, respectively, i.e., $C_1 = [0\ 0\ 1]$, $C_2 = [0\ 1\ 0]$, $C_3 = [1\ 0\ 0]$. $v_i(k)$ are zero-mean Gaussian noises with variances R_i, and are independent of white Gaussian noise $w(k)$ with zero-mean and variance Q. In the sequel, one should generate the estimate of $x(k)$ by fusing the information from three sensors.

In this simulation, set $T = 0.01$s, $Q = 0.01, R_3 = 0.25, R_2 = 0.09$, and $R_1 = 0.01$. The stochastic variable $\gamma_i \in R$ is a Bernoulli distributed white sequence taking values on 0 and 1, whose mean is $\bar{\gamma}_i$. Here, we take $\bar{\gamma}_1 = 0.9$, $\bar{\gamma}_2 = 0.8$, and $\bar{\gamma}_3 = 0.8$. It means that the measurements are missing at the probability of 0.1, 0.2 and 0.2, respectively. The initial values are $x(0) = [10\ 0\ 0]^T$ and $P_0 = I_3$. Sensor 1, sensor 2, and sensor 3 sample 100, 150 and 300 data, respectively.

The Monte Carlo simulation results are shown in Table 1, and Figs. 6.3 to 6.6.

In Fig. 6.3, the measurements of the three sensors are shown, where (a), (c) and (e) denote the measurements from sensors 1, 2 and 3, respectively, under the assumption that all the measurements are normal. Figs. (b), (d) and (f) of Fig. 6.3 are the real measurements of sensors 1, 2 and 3, respectively, with the measurements randomly missing. From Fig. 6.3, one can see that the data missing of each sensor is obvious. In Fig. 6.4, the first dimension of the original signal (blue real line) and the estimate signals (the red dashed line) are illustrated, where the dashed lines in (a) through (d) denote: the Kalman filter of sensor 3, the estimate by use of the algorithm presented in [194], the estimate by use of the algorithm presented in [211], and the estimate by use of the presented method, respectively. The corresponding estimation error curves are drawn in Fig. 6.5. From Fig. 6.4 and Fig. 6.5, one can observe that the traditional Kalman filter and the algorithm proposed by [211] are divergent in the case of measurements randomly missing. However, the algorithm presented by [194] and the proposed algorithm are effective.

In Fig. 6.6, the Monte Carlo simulation curves of 100 runs are shown, where (a) through (d) are the statistical estimation errors of (i) the result based on Kalman filter of sensor 3, (ii) the result based on the algorithm presented in [194], (iii) the result based on the algorithm presented in [211], and (iv) the result by use of the proposed algorithm, respectively. From Fig. 6.6, one can see that the proposed algorithm is also effective in the sense of statistics. However, statistically, the algorithm in [194] is divergent.

The values listed in Table 6.1 are the means of the absolute values of the estimation errors, which is computed by $\frac{1}{KJ}\sum_{j=1}^{J}\sum_{k=1}^{K}|\tilde{x}_j(k|k)|$, where $K = 360$ denotes the number of the sampling points of sensor 3, $J = 100$ denotes the Monte Carlo simulation runs, while $\tilde{x}_j(k|k)$ denotes the estimation error of the state at the jth run. Six schemes are tested and listed in Table 6.1 for the proposed algorithm: (i) Kalman filter of sensor 1; (ii) Kalman filter of sensor 2; (iii) Kalman filter of sensor 3; (iv) by use of the algorithm presented by [194] to generate the state estimate by use of measurements from sensor 3; (v) by use of the algorithm presented by [211] to fuse three sensors and generate the state estimate; (vi) by use of the presented algorithm to fuse sensors 1, 2 and 3. The second to fourth rows of Table 6.1 denote the statistical means of the absolute values of the estimation errors of position, velocity, and acceleration, respectively.

From Table 6.1, one can notice that, because of the randomly missing of measurements, statistically, both Kalman filter (Observe the second to the fourth lines of Table 6.1 and algorithm in [194] and [211], Observe the fifth and the sixth line of Table 6.1) are divergent. The reasons are: (1) When there are measurements randomly missing, the measurement error variances became very large. In this case, Kalman filter still updates in the same way as the measurements are not missing, which results in divergence. (2) The algorithm of [211] is the generation of Kalman filter to multiple sensors. So,

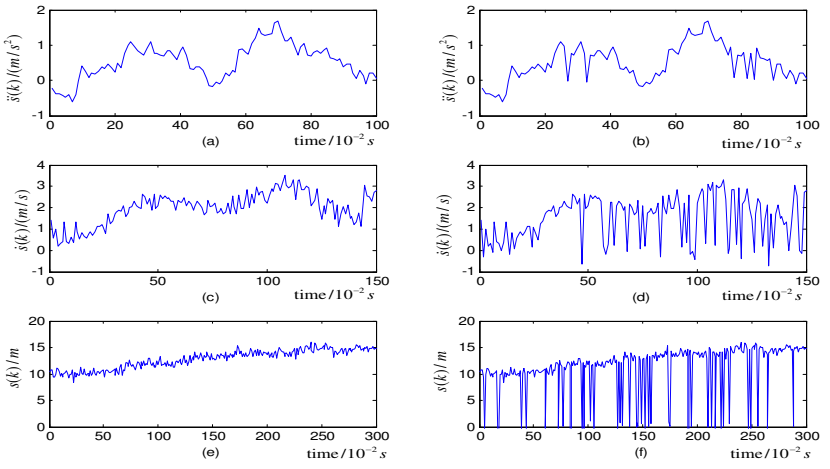

Fig. 6.3 Measurements with and without missing.

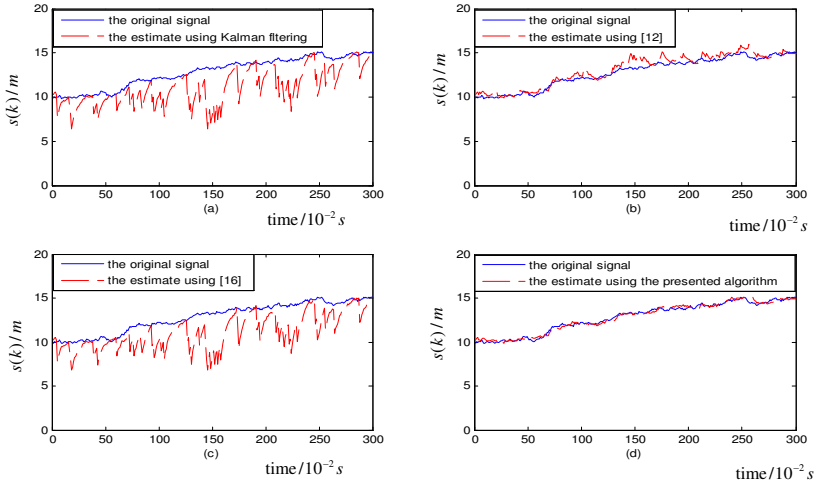

Fig. 6.4 The original signal and the estimate signals.

Table 6.1 The statistical means of the absolute values of the estimation errors

state	(i)	(ii)	(iii)	(iv)	(v)	(vi)
position	10.4958	13.3191	230.0571	46.7013	226.7272	2.1055
velocity	7.3700	22.2880	33.0451	9.6595	32.0598	1.9001
acceleration	2.5496	5.2736	9.5893	7.5492	5.5450	1.1923

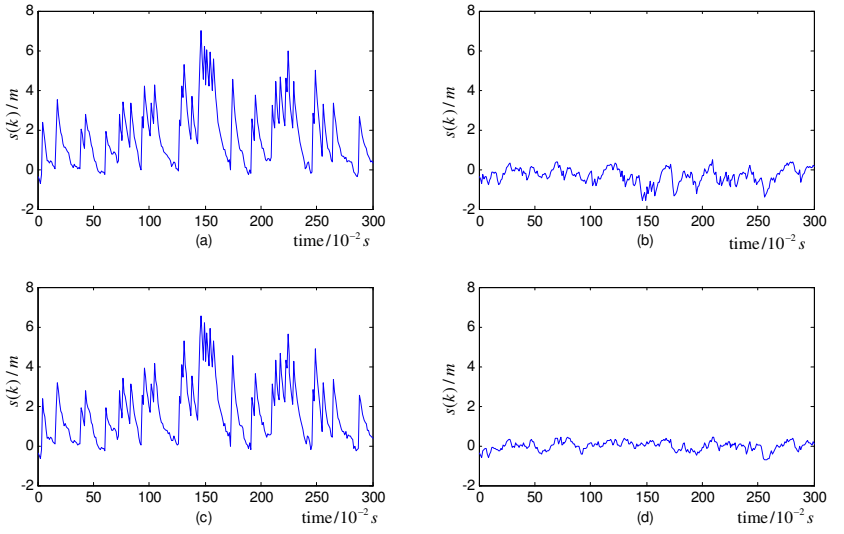

Fig. 6.5 The estimation errors corresponding to Fig. 6.4.

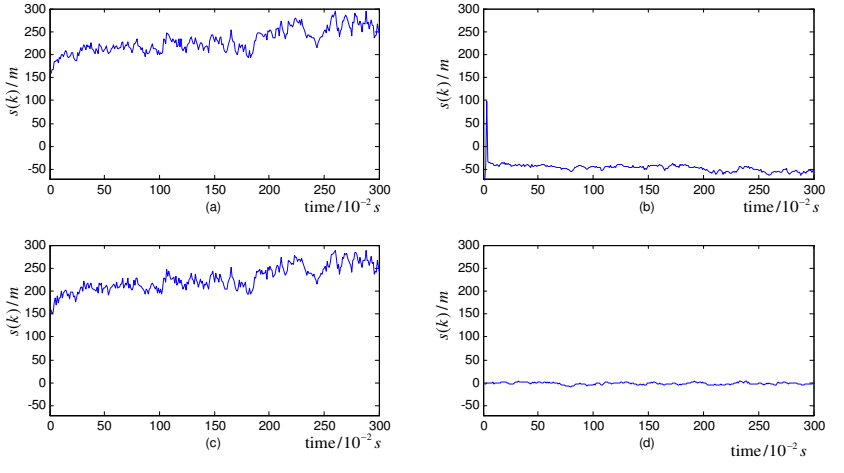

Fig. 6.6 The statistical estimation errors.

it has the same problem as Kalman filter. (3) The algorithm presented by [194], which takes measurements missing into consideration, is more effective than Kalman filter and even than the fusion algorithm proposed by [211]. From Fig. 6.4 and Fig. 6.5, one can observe that it is effective in simulation of randomly one run. However, stochastically, it is not so effective. It means the stability of algorithm [194] is not as good as the presented algorithm. (4) The bad measurements are checked out and properly dealt with in the presented algorithm, which result in the convergence of the results.

Briefly, the simulation results in this section illustrate the effectiveness of the presented algorithm.

6.5 Summary

When a target is observed by multiple sensors that sample asynchronously at different sampling rates with the measurements randomly missing, a state estimation algorithm has been presented in this chapter. From theoretical analysis and simulation results, it can be concluded that the proposed algorithm is effective and has potential value especially in some application fields, such as target tracking, integrated navigation, network transportation, and fault tolerance, etc.

Part III
Predictive Control over Networks

Chapter 7
Networked Predictive Control Systems with Data Dropout

7.1 Introduction

In recent years, networked control and data fusion technology have become popular control problems which have been extensively studied under various assumptions and scenarios [197, 235, 98, 145, 91, 2, 206]. There has been a growing interest in the design of controllers based on the network systems such as traffic, communication, aviation and spaceflight [236]. Particularly, the rapid rising of Internet makes Internet based control systems accomplish remote monitoring and adjustment over a long distance. This makes the control systems benefit from the ways of retrieving data and reacting to plant fluctuations from anywhere around the world at any time [34, 179, 129, 127]. In NCSs, the plant, controller, sensor, actuator and reference command are connected through a network. As the structure of NCSs is different from that of traditional control systems, there exist various specific problems in NCSs, for example, network delay, loss of data packets, network security and safety [213].

Several methodologies have been reported in the open literature to handle with the problems mentioned above in networked systems. Among these papers, two basic control strategies are applied when the packet dropping happens, they are zero-input schemes, by which the actuator input is set to zero when the control packet is lost, and hold-input scheme which implies the previous control input is used again when the control packet drops. The further research is proposed in [156] by directly comparing the two control methods. In [229], the stability problem of closed-loop NCSs in the presence of network delays and data packet drops has been addressed under an assumption that the network-induced delay is less than the sampling period. To reduce network traffic load, a sampled-data NCSs scheme combining the model-based control methods has been presented and some necessary and sufficient conditions for globally exponential stability of the closed-loop systems via state/output feedback without/with network delays have been

Y. Xia, M. Fu, and G.-P. Liu: Analysis and Synthesis of NCSs, LNCIS 409, pp. 109–125.
springerlink.com

established in [121]. In [221], a new model of NCSs is provided under consideration of both the network-induced delay and the data packet dropout in the transmission. State feedback stabilizing controller is proposed based on the delay-dependent approach and the maximum allowable value of the network-induced delay can be determined by solving a set of LMIs. Since H_∞ control can make a well established connection between the performance index being optimized and performance requirements encountered in practical situations, the method is proposed in [160] where the packet dropouts and channel delays are modeled as Markov Chains with the usual assumption, that is all the transition probabilities are completely accessible. The work of [106] present a novel control technique combining modified Model Predictive Control (MPC) and modified Smith predictor to guarantee the stability of NCSs. Especially, the key point in this paper is that the future control sequence is used to compensate for the forward communication time delay and predictor is responsible for compensating the time delay in the backward channel. In [110], a novel networked predictive control method is proposed to deal with NCSs with random time-delay existing in both feedback and forward channels. The dynamics of the plant is explicitly used to derive a sequence of forward control predictions, which are sent to the actuator simultaneously and the actuator chooses the appropriate one to compensate for the delays.

Although much research work have been done in NCSs, many of those results simply treat the NCSs as a system with time delay, which ignores NCSs' features, e.g., random network delay and data transmission in packets [200]. In order to solve the problem, Markovian jump system can be used to model the random time-delay. Moreover, most work have also ignored another important feature of NCSs. This feature is that the communication networks can transmit a packet of data at the same time, which is not done in traditional control systems. Therefore, in this chapter, we will make full use of this feature and propose a new networked predictive control scheme which can overcome the effects caused by network data dropout modeled as Markov chain.

This chapter is organized as follows. Section 7.2 presents a novel networked predictive control scheme such that the closed-loop system is asymptotically stable. Section 7.3 gives a review of other control methods for NCSs. The furuta pendulum of a NCSs is modeled with random packet dropouts in Section 7.4. Numerical simulations are presented in Section 7.5. Some conclusion remarks are given in Section 7.6.

7.2 Networked Predictive Control for Systems

To overcome unknown network transmission dropout, a networked predictive control scheme is proposed. It mainly consists of a control prediction generator and a network dropout compensator. The control prediction generator is designed to generate a set of future control predictions. The network

dropout compensator is used to compensate the unknown random network dropout. The structure of the networked predictive control system (NPCS) is shown as Fig. 7.1. This chapter mainly focus on the random transmission data dropout existing in both feedback and forward channels in NCSs. So, the network-induced time delay is not discussed here.

Consider a MIMO discrete system described as the following state space form

$$\begin{aligned} x(k+1) &= Ax(k) + Bu(k) + w(k) \\ y(k) &= Cx(k) + v(k) \end{aligned} \tag{7.1}$$

where $x(k) \in R^n$, $u(k) \in R^m$, and $y(k) \in R^l$ are the system state, input, and output vectors, respectively. The noise process $\{w(k)\}$ is a white, zero-mean, uncorrelated one with known covariance matrice Q_1. $A,\ B,\ C$ are matrices of appropriate dimensions. For the simplicity of stability analysis, it is assumed that the reference input of the system is zero and the following assumptions are hold.

The arrival of the observation at time k is a binary random variable $\gamma(k)$ with probability distribution $P(\gamma(k) = 1) = \lambda_k, \lambda_k \in (0, 1)$ and $\gamma(k)$ is independent of $\gamma(s)$ if $k \neq s$. The output noise is defined as

$$v(k) \sim \begin{cases} N(0, R_1),\ \gamma(k) = 1 \\ N(0, \sigma^2 I),\ \gamma(k) = 0 \end{cases} \tag{7.2}$$

for some σ^2.

Assumption 7.1. *(A, B) is completely controllable and (A, C) is completely observable.*

Assumption 7.2. *The number of consecutive data dropouts must be less than N (a positive integer).*

Remark 7.1. In a real NCS, if a data packet does not arrive at a destination in a certain transmission time, it means that the data packet is lost based on the commonly used network protocols. From the physical point of view, it is natural to assume that only a finite number of consecutive data dropouts can be tolerated in order to avoid the NCS to be an open-loop. Thus, the number of consecutive data dropouts should be less than a finite number N.

Some notations are defined as follows:

$$\begin{aligned} Y(k) &= [y(0), \cdots, y(k)]^T \\ \Gamma(k) &= [\gamma(0), \cdots, \gamma(k)]^T \\ \hat{x}(k|k) &= E[x(k)|Y(k), \Gamma(k)] \\ P(k|k) &= E[(x(k) - \hat{x}(k|k))(x(k) - \hat{x}(k|k))^T|Y(k), \Gamma(k)] \\ \hat{x}(k+1|k) &= E[x(k+1)|Y(k), \Gamma(k)] \\ P(k+1|k) &= E[(x(k+1) - \hat{x}(k+1|k))(x(k+1) - \hat{x}(k+1|k))^T|Y(k), \Gamma(k)] \\ \hat{y}(k+1|k) &= E[y(k+1)|Y(k), \Gamma(k)] \end{aligned} \tag{7.3}$$

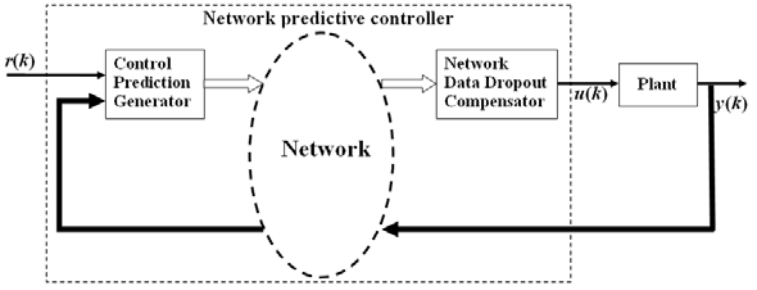

Fig. 7.1 The networked predictive control system.

The Kalman filter based state observer is designed as

$$\begin{aligned} \hat{x}(k|k-1) &= A\hat{x}(k-1|k-1) + Bu(k-1) \\ \hat{x}(k|k) &= \hat{x}(k|k-1) + \gamma(k)K(k)(y(k) - C\hat{x}(k|k-1)) \\ P(k|k) &= P(k|k-1) - \gamma(k)K(k)CP(k|k-1) \\ K(k) &= P(k|k-1)C^T(CP(k|k-1)C^T + R)^{-1} \end{aligned} \tag{7.4}$$

where $\hat{x}(k+1|k) \in R^n$ and $u(k|k) \in R^m$ are the one-step ahead state prediction and the input of the observer at time k, respectively. $P(k|k-1)$ is the solution of the following modified Riccati equation [169]

$$\begin{aligned} P(k|k-1) = AP(k-1|k-2)A^T + Q - \gamma(k)AP(k-1|k-2) \\ \times C^T(CP(k-1|k-2)C^T + R)^{-1}CP(k-1|k-2)A^T \end{aligned} \tag{7.5}$$

The state predictions at time k are constructed as

$$\begin{aligned} \hat{x}(k+1|k) &= A\hat{x}(k|k-1) + Bu(k) + \gamma(k)AK(k)(y(k) - C\hat{x}(k|k-1)) \\ \hat{x}(k+2|k) &= A\hat{x}(k+1|k) + Bu(k+1|k) \\ &\vdots \\ \hat{x}(k+N|k) &= A\hat{x}(k+N-1|k) + Bu(k+N-1|k) \end{aligned} \tag{7.6}$$

Assume that the controller is of the following form:

$$u(k) = u(k|k) = L(k)\hat{x}(k|k) \tag{7.7}$$

where $L(k) \in R^{m\times n}$ is the state feedback control matrix to be determined using modern control theory. Then, the control predictions are generated by

$$u(k+t|k) = L(k)\hat{x}(k+t|k), \text{for} \quad t = 0, 1, 2, \cdots, N \tag{7.8}$$

Thus, it follows from equation (7.6) that

$$\hat{x}(k+t|k) = (A + BL(k))^{t-1}\hat{x}(k+1|k) \tag{7.9}$$

Based on equations (7.4), (7.6) and (7.8), it can be shown that

$$\begin{aligned}
&\hat{x}(k+t|k)\\
&= (A+BL(k))^{t-1}[A\hat{x}(k|k-1)+Bu(k)+\gamma(k)AK(k)(y(k)-Cx(k|k-1))]\\
&= (A+BL(k))^{t-1}[(A+BL(k)-\gamma(k)(AK(k)-BL(k)K(k))C)\hat{x}(k|k-1)\\
&\quad +\gamma(k)(AK(k)+BL(k)K(k))Cx(k)]
\end{aligned}$$

and

$$\begin{aligned}
&u(k+t|k)\\
&= L(k)\hat{x}(k+t|k)\\
&= L(k)(A+BL(k))^{t-1}[(A+BL(k)-\gamma(k)(AK(k)-BL(k)K(k))C)\\
&\quad \times\hat{x}(k|k-1)+\gamma(k)(AK(k)+BL(k)K(k))Cx(k)]
\end{aligned} \tag{7.10}$$

In order to compensate the network transmission data loss, a network delay compensator is proposed. A very important characteristic of the network is that it can transmit a set of data at the same time. Thus, it is assumed that predictive control sequence at time k is packed and sent to the plant side through a network. The network delay compensator chooses the latest control value from the control prediction sequences available on the plant side. For example, if the following predictive control sequences are received on the plant side:

$$[u^T(k|k), u^T(k+1|k), \cdots, u^T(k+N-1|k), \cdots, u^T(k+N|k)]^T \tag{7.11}$$

then $u(k|k)$ is used as the input to the actuator. If new control package containing control predictive sequences is dropped at the next step, one step control prediction $u(k+1|k)$ will be used as control input to the actuator. Then, if new package of control predictive sequences are received, then the first control input will be used as the input to the actuator. Otherwise, $u(k+2|k)$ will be used as input to the actuator, ... and so on. Based on the assumption, it is reasonable that there are N times consecutive data dropout at least. The stochastic stability criteria of the closed-loop networked predictive control systems can be analytically derived based on the methods in previous work [110]. In fact, using the networked predictive control scheme presented in this section, the control performance of the closed-loop system with data dropout is very similar to the one without data dropout.

7.3 Previous Work for Networked Control Systems

Some strategies have been declared for dealing with NCSs. In this section, many of representative control schemes are reviewed.

7.3.1 Another Networked Predictive Control Based on State Observer

A predictive control scheme for NCSs with random network delay and packet dropout in both forward and feedback channels has been studied in [110]. The control method also utilizes the characteristic that it can transmit a set of data at the same time via networks. Similarly, control predictors and compensators are built to reduce the impact caused by time delay and data dropout. It is assumed that control predictions at time k are packed and sent to the plant side through a network. On the actuator side, only the control latest prediction sequence is kept. The network delay compensator chooses the control value from the control latest prediction sequence. The model considered here is similar to (7.1) but without considering system noise and measurement noise.

$$\begin{aligned} x(k+1) &= Ax(k) + Bu(k) \\ y(k) &= Cx(k) \end{aligned} \tag{7.12}$$

In particular, for NCSs without time delay and the state feedback control $u(k) = K_m\hat{x}(k|k-1)$ is considered and the state predictions at time k are finally constructed as follows:

$$\begin{aligned} \hat{x}(k+1|k) &= (A + BK_m - L_mC)\hat{x}(k|k-1) + L_mCx(k) \\ \hat{x}(k+2|k) &= A\hat{x}(k+1|k) + Bu(k+1|k) \\ &\vdots \\ \hat{x}(k+N|k) &= A\hat{x}(k+N-1|k) + Bu(k+N-1|k) \end{aligned} \tag{7.13}$$

The control predictions are calculated by

$$u(k+t|k) = K_m\hat{x}(k+t|k) \tag{7.14}$$

It should be noted that the control strategy proposed in [110] can be used in the NCSs with both time delay and data dropout. Here, the control approach is revised to deal with NCSs without time delay. It is shown that if the data is lost within the current sampling period, the control input should be taken as the ith-step ahead control prediction of the current time, which is received in the previous sampling period. In the same way, when the data dropout happens in the feedback channel, the observer will use the measurement output $y(k-1)$ received at the last sampling instant if the measurement output $y(k)$ is lost; otherwise, $y(k-j)$ will be used if $y(k-i)$ arrives after $y(k-j)$, where $j < i$. These methods play a very important role in compensating for data dropout in the proposed NPC implementation. When data dropout exists in both forward and feedback channels, the scheme proposed in this chapter can achieve the desired control performance, which is similar to that of the system without data dropout. Thus, on the sensor side, the measurement output is sent to the controller side through the feedback channel. On the controller side, the control prediction sequence at time k, which consists

of the future control predictions, is packed and sent to the plant side through the forward channel. The compensator chooses the latest control value from the latest control prediction sequence on the plant side.

7.3.2 Zero Control and Zero-Order Hold Control

In literature, two basic control strategies are applied when packet dropping happens. They are zero-input scheme, by which the actuator input is set to zero when the control packet is lost, and hold-input scheme, which implies the latest control input is used again when the control packet drops. Generally, the two methods are applied only in the forward channel concerning whether the control packet is obtained or not. Here, the methods are extended in both feedback and forward channels.

i) Zero-input method

Zero-input scheme can be described as follows. Consider the stochastic system [85]

$$\begin{aligned} x(k+1) &= Ax(k) + \alpha(k)Bu(k) \\ y(k) &= \beta(k)x(k) \end{aligned} \tag{7.15}$$

The plant is remotely controlled over a network containing random packet losses. The stochastic process $\alpha(k)$ and $\beta(k)$ depict the unreliable nature of the network. Basically, $\alpha(k) = 0$ when the transmission from the controller to the plant fails, i.e. the control packet is lost, and $\alpha(k) = 1$ when the control packet is successfully acquired in the forward channel. The link from the plant to the controller is unreliable as well, $\beta(k) = 0$ when the link from the sensor to the controller fails, and $\beta(k) = 1$ when the measurement packet is correctly obtained in the feedback channel.

ii) Hold-input method

Consider system (7.12), on the condition of hold-input scheme applied in both forward and feedback channels, the measure $y(k)$ is chosen as $y(k) = y(k-1)$ if dropout happens in the feedback channel, and in the forward channel, if the control packet is lost, the actuator could employ the previous control value $u(k) = u(k-1)$.

7.4 Digital Control Design of Furuta Pendulum

In this section, in order to construct the NCS, we will adopt a nonlinear furuta pendulum which can be linearized as a plant and introduce Markov process to depict the random packet dropout.

7.4.1 Furuta Pendulum Model

Consider a single inverted pendulum which contains two parts, a vertical level of the inverted pendulum and a horizontal arm. The structure of the furuta pendulum is shown in Fig. 7.2, where ϕ is the arm angle, θ denotes the pendulum angle, $\dot{\phi}$ and $\dot{\theta}$ present their angular velocity respectively.

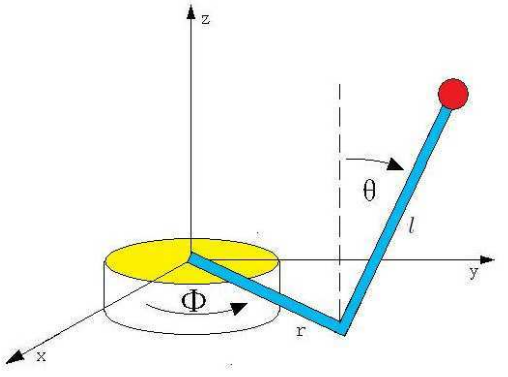

Fig. 7.2 Structure of the Furuta pendulum.

The nonlinear dynamics of the furuta pendulum using Euler-Lagrange equations has been researched in many reports, for example, in [53].

$$\begin{aligned}
&\tfrac{d}{dt}\theta = \dot{\theta} \\
&\tfrac{d}{dt}\dot{\theta} = \tfrac{1}{\alpha\beta-\gamma^2+(\beta^2+\gamma^2)\sin^2\theta}\{\beta(\alpha+\beta\sin^2\theta)\cos\theta\sin\theta\dot{\phi}^2 \\
&\quad +2\beta\gamma(1-\sin^2\theta)\sin\theta\dot{\phi}\dot{\theta} \\
&\quad -\gamma^2\cos\theta\sin\theta\dot{\theta}^2+\delta(\alpha+\beta\sin^2\theta)\sin\theta-\gamma\cos\theta\times\tau\} \\
&\tfrac{d}{dt}\phi = \dot{\phi} \\
&\tfrac{d}{dt}\dot{\phi} = \tfrac{1}{\alpha\beta-\gamma^2+(\beta^2+\gamma^2)\sin^2\theta}\{\beta\gamma(\sin^2\theta-1)\sin\theta\dot{\phi}^2-2\beta^2\cos\theta\sin\theta\dot{\phi}\dot{\theta}^2 \\
&\quad -\gamma\delta\cos\theta\sin\theta+\beta\times\tau\}
\end{aligned} \tag{7.16}$$

where

$$\alpha=(M+\frac{m}{3})l^2,\ \beta=J+(M+m)r^2,\ \gamma=(M+\frac{m}{2})rl,\ \delta=(M+\frac{m}{2})gl \tag{7.17}$$

The notation M, m, l, r, J, g denote the parameters used in the furuta pendulum model, which is shown in Table 7.1. $\tau \in R$ is the input torque which can be divided into a driving torque and its consumption of friction

$$\tau = \tau_u - \tau_F \tag{7.18}$$

where the friction τ_F can be modeled as coulomb friction with stiction

$$\tau_F = \begin{cases} \tau_c \text{sgn}\dot{\phi} & if\ \dot{\phi} \neq 0 \\ \tau_u & if\ \dot{\phi} = 0\ and\ |\tau_u| < \tau_s \\ \tau_s & otherwise \end{cases} \tag{7.19}$$

Table 7.1 Parameters used in the Furuta pendulum model

Symbol	Value	Meaning
m	0.025 Kg	Mass of pendulum rod
M	0.004 Kg	Mass of pendulum ball
l	0.241 m	Length of pendulum rod
r	0.152 m	Length of horizontal arm
J	$1.21e^{-3} Kg \cdot m^2$	Moment of inertia of central shaft
g	$9.81 m/s^2$	Gravitational constant

Introducing the state variable

$$x = \left(\theta\ \dot{\theta}\ \phi\ \dot{\phi}\right)^T,\ u = \tau \tag{7.20}$$

and linearized pendulum model [53]

$$\dot{x} = Ax + Bu = \begin{bmatrix} 0 & 1\ 0\ 0 \\ \frac{\alpha\delta}{\alpha\beta-\gamma^2} & 0\ 0\ 0 \\ 0 & 0\ 0\ 1 \\ \frac{-\gamma\delta}{\alpha\beta-\gamma^2} & 0\ 0\ 0 \end{bmatrix} x + \begin{bmatrix} 0 \\ \frac{-\gamma}{\alpha\beta-\gamma^2} \\ 0 \\ \frac{\beta}{\alpha\beta-\gamma^2} \end{bmatrix} u \tag{7.21}$$

7.4.2 Random Network Data Dropout Model

The problem of network data dropout over a network has been proposed in [141, 89], some types of model have been established. The networks can be described as having long periods of good performance and relatively short periods of bad performance. The two-state Markov chains are the simplest model to capture the behavior accurately, which are described in Fig. 7.2. The parameters $r_{i,j}$ and e_i are transition probability depicting the switching movement between two states.

The model explicitly switches between a good network state and a bad one with state-based transition probability. If the network is in a good state, it has a higher probability to move the good state in next stage to a bad one. Similarly, if the network is in a bad state, it has a higher probability to keep the bad state and a lower probability to switch to a good state. In addition, packet dropout appears for either states. The probability of individual packet

Table 7.2 Parameters in the 2-state Markov model

Symbol	Value	Meaning of Probability transition
$r_{0,1}$	0.005	Good state to Bad state of the network
$r_{0,0}$	0.995	Good state to Good state of the network
$r_{1,0}$	0.0027	Bad state to Good state of the network
$r_{1,1}$	0.9973	Bad state to Bad state of the network
e_0	0.01	Data drop out in the Good state
e_1	0.90	Data drop out in the Bad state

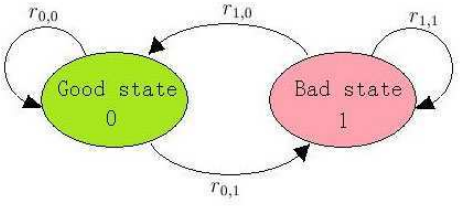

Fig. 7.3 Two-state Markov chain network model.

loss in the bad state is more significant while the probability is quite small in good state.

Based on above description, the data dropout can be modeled as follows. Consider $S(k)$, $\gamma(k)$ at any time $k > 0$, where $S(k) = 0$ denotes the good state and $S(k) = 1$ represents the bad state. The variable $\gamma(k)$ determines whether data dropout appears in the network. Here, $\gamma(k) = 0$ means that the dropout happens and $\gamma(k) = 1$ means not. Given $S(k)$, the chain's next move can be specified by:

$$S(k+1) = \begin{cases} 0, & if \quad U_1 \leq r(S(k), 0) \\ 1, & if \quad r(S(k), 0) < U_1 \leq 1 \end{cases} \tag{7.22}$$

$$\gamma(k+1) = \begin{cases} 0, & if \quad U_2 \leq e(S(k+1)) \\ 1, & if \quad e(S(k+1)) < U_2 \leq 1 \end{cases} \tag{7.23}$$

where U_1, U_2 are random variables following a uniform distribution on the interval [0, 1].

7.4.3 Structure of Controller

The optimal control of LQR scheme is adopted here for the control design. The objective is to design a discrete state feedback controller

$$\tau_u = -Lx \tag{7.24}$$

to stabilize the pendulum system (7.21) by minimizing the quadratic cost functional

$$J = \lim_{N\to\infty} \sum_{k=0}^{N} (x^T(k)Qx(k) + u^T(k)Ru(k)) \tag{7.25}$$

7.5 Simulation Results

In order to demonstrate the effectiveness of the proposed predictive control scheme (7.10), numerical simulations have been performed and presented comparing with another three kinds of control methods in this section. The plant is chosen as furuta pendulum model (7.21) with (7.17) and the pendulum parameter values are selected in Table 7.1. This section gives the trajectory curves of the arm angle ϕ and pendulum angle θ when the horizontal arm tracks the square-wave signals. The numerical simulations are discussed in three steps. We first consider the model of the furuta pendulum (7.21) and LQR state feedback control law (7.24) without data dropouts and noise. Then, four control methods are applied for NCSs with data dropout, and we will show that the two predictive control schemes are superior than zero-input and input-hold control approaches. Especially, in the high dropout rate condition, the predictive control methods can perform much better. Finally, the two predictive control methods are considered on the conditions of NCSs with packet loss and noise, and the simulation results indicate that the predictive control strategy we proposed in this chapter has the best performance when data dropout and noise appear in the network simultaneously.

7.5.1 Track a Square-Wave Signal without Network and Noise

Consider the model of the furuta pendulum (7.21) and LQR state feedback control law (7.24) without data dropouts and noises. The parameters in cost function (7.25) are selected as

$$Q = \begin{bmatrix} 300 & 0 & 0 & 0 \\ 0 & 100 & 0 & 0 \\ 0 & 0 & 30 & 0 \\ 0 & 0 & 0 & 3 \end{bmatrix}, \qquad R = 1000 \tag{7.26}$$

which yield the feedback gain

$$L = [-2.094 \ -0.378 \ -0.117 \ -0.092] \tag{7.27}$$

The horizontal arm tracking square-waves and the trajectory of pendulum angle are depicted in Fig. 7.4, which indicates that, without networks and noises, the arm tracking and pendulum stability can be guaranteed under the LQR state feedback control law.

7.5.2 Track a Square-Wave Signal with Network without Noise

In this part, we will consider the NCSs with data dropouts. In order to construct a NCS with random packet loss which is depicted by Markov chains, the transition probability in Markov model (7.22) is selected as Table 7.2. System performances of the four kind of control methods are shown when the data dropout happens in both the forward and feedback channels.

System performances for zero-input control approach with random data dropouts are shown in Fig. 7.5 and Fig. 7.6. When data dropout happens in the forward and feedback channels, the input of the actuator is set to be zero. Fig. 7.5 gives the result with 10% data dropouts and Fig. 7.6 presents the result with 18% data dropouts. It is obvious that the control loop will be instability as the data dropout rate raised. With the data dropout rate raised to 18%, the horizontal arm can not track the square-wave signal and the pendulum arm can not keep in the upright position, which means that this method can not control the system with high data dropout rate.

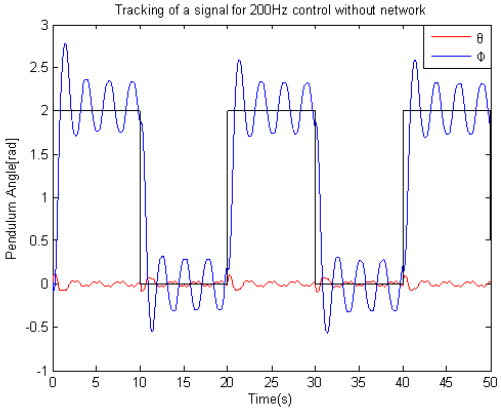

Fig. 7.4 Tracking of a square-wave for 200 Hz control without network and noise.

Simulation results for hold-input control scheme with data dropouts are shown in Fig. 7.7 and Fig. 7.8. As seen in Fig. 7.7, it can guarantee the stable tracking for the case of 40% data dropouts following a random distribution, but with the increased data dropout rate, the pendulum switches to be unstable, which is shown in the Fig. 7.8 with the data dropout rate of 48%. It is significant that the hold-input control scheme can maintain the trajectory tracking at an even higher data dropout rate than the zero-input control approach. However, the system becomes unstable when data dropout rate is larger than 48%.

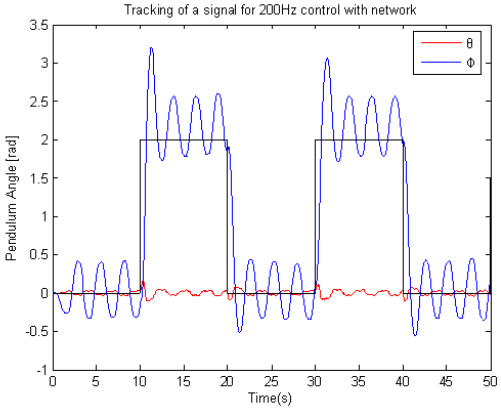

Fig. 7.5 Tracking of a square-wave for 200 Hz Zero control with 10% data dropouts.

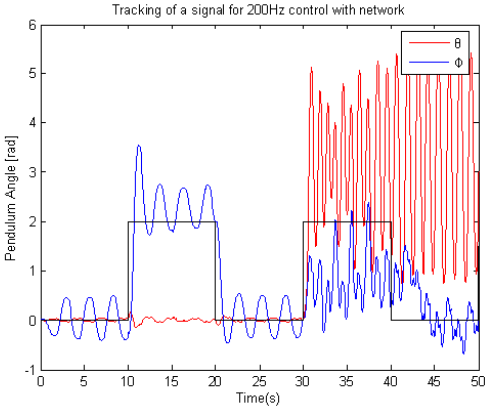

Fig. 7.6 Tracking of a square-wave for 200 Hz Zero control with 18% data dropouts.

The arm tracking and stability of pendulum for the two predictive control schemes are described in Fig. 7.9 and Fig. 7.10. It is clear that, for both predictive methods, when we put the prediction generator into the controller and the network data dropout compensator into the actuator, the stability of pendulum can be guaranteed with high data dropout rate. Fig. 7.9 shows the simulation result for network predictive control (7.13) based on the state observer with the 48% data dropouts and Fig. 7.10 shows the simulation result for network predictive control (7.10) based on the Kalman filter with the same data dropout rate. As seen in the two trajectories, the arm can track the square-wave signal well with the small overshoot and the pendulum also can be stabilized in the vertical position. As expected, the performance

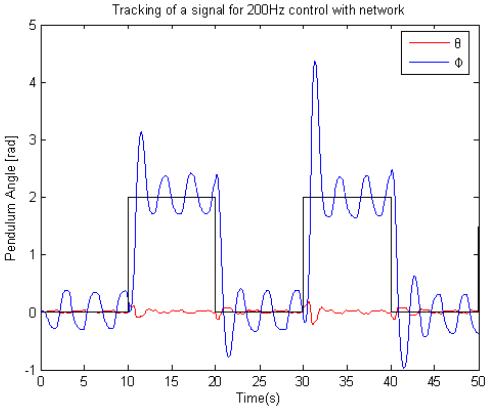

Fig. 7.7 Tracking of a square-wave for 200 Hz input-hold control with 40% data dropouts.

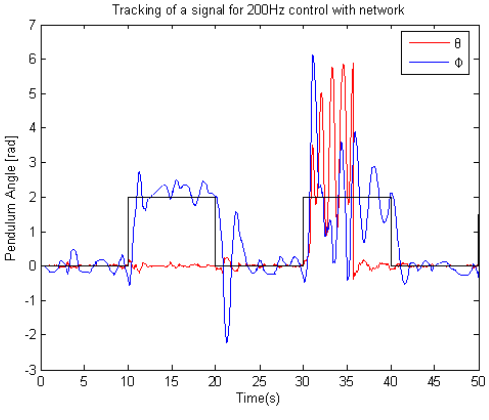

Fig. 7.8 Tracking of a square-wave for 200 Hz input-hold control with 48% data dropouts.

of the system is improved dramatically with the predictive control algorithms compared with the zero-input and input-hold control approaches.

7.5.3 Track a Square-Wave Signal with Network and Noise

It has been shown that the two predictive control methods perform much better than other control schemes for resisting the packet loss. On the other hand, noise is also an ingredient affecting the performance of the system. In

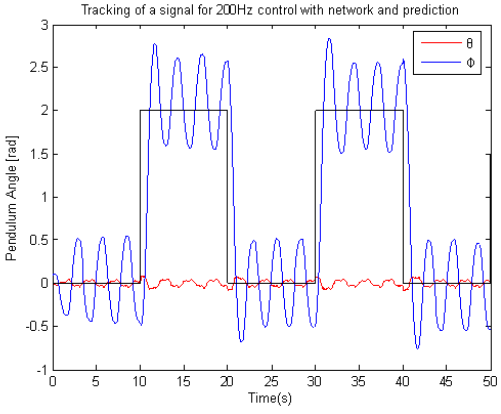

Fig. 7.9 Tracking of a square-wave for 200 Hz control based on the state observer with 48% data dropouts.

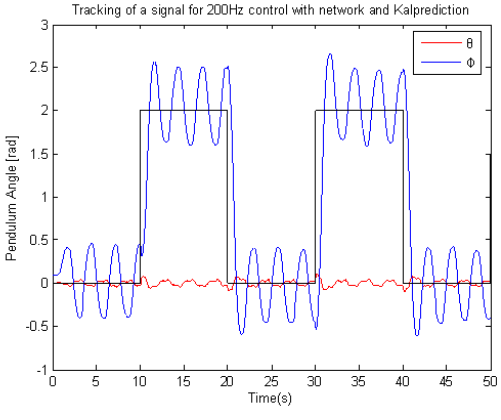

Fig. 7.10 Tracking of a square-wave for 200 Hz control based on the Kalman filter with 48% data dropouts.

this subsection, we concern about the NCS with both data dropout and noise under the two predictive control schemes.

Consider NCS (7.1) with noise and data dropout (7.22), the covariance of noise $\{w(k)\}$ and $\{v(k)\}$ are selected as

$$Q_1 = \begin{bmatrix} 0\,1\,0\,0 \\ 0\,1\,0\,0 \\ 0\,0\,1\,0 \\ 0\,0\,0\,1 \end{bmatrix} \times 10^{-3}, \quad R_1 = \begin{bmatrix} 0\,1\,0\,0 \\ 0\,1\,0\,0 \\ 0\,0\,1\,0 \\ 0\,0\,0\,1 \end{bmatrix} \tag{7.28}$$

The predictive control (7.13) based on state observer is shown in Fig. 7.11 and the predictive control (7.10) based on Kalman filter is depicted in Fig. 12. Due to the process noises, the performance of the system become worse than the system without noise at the same rate of the data dropouts. Compared Fig. 11 with Fig. 7.12, it is clear that the performance of the predictive control based on Kalman filter we proposed is better than the predictive control based on state observer. This indicates that the proposed predictive control based on Kalman filter can keep an outstanding system performance when the data dropout and noise exist in the network.

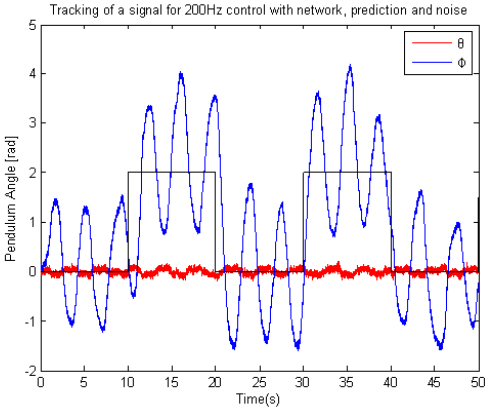

Fig. 7.11 Tracking of a square-wave for 200 Hz control based on the state observer with 40% data dropouts and processes noise.

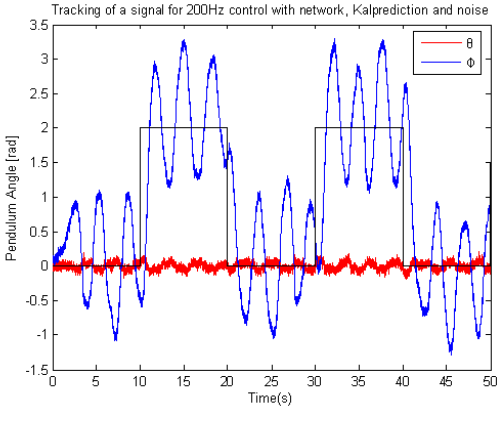

Fig. 7.12 Tracking of a square-wave for 200 Hz control based on the Kalman filter with 40% data dropouts and processes noise.

The control behaviors of zero-input and input-hold approaches have been discussed in many aspects [156]. The numerical result of the pendulum NCS shows that the input-hold control scheme performs better than zero-input control approach for resisting the data dropout. In this simulation, input-hold control approach can guarantee the system stable until the dropout rate reaches to 48% while zero-input control method with the data loss rate to 18% (see Fig. 7.6 and Fig. 7.8). However, both the two methods are not so excellent as predictive control approaches which can guarantee the stability of the pendulum and arm tracking at the 48% data dropout rate (see Fig. 7.9 and Fig. 7.10). Moveover, the proposed predictive control approach based on Kalman filter (7.10) performs better than the predictive controller (7.13)on noise attenuation since the advantage of Kalman filter over state observer is noise resistance (see Fig. 7.11 and Fig. 7.12).

7.6 Summary

A new networked predictive control scheme based on Kalman filter has been proposed for MIMO networked distributed control systems with random network data dropout. Based on the network feature of transmitting a set of data at each time, the proposed networked predictive controller consists of the control prediction generator and the network data loss compensator. The former one provides a set of future control predictions to satisfy the system performance requirements. The latter compensates for the random network transmission packet loss. Simulation results are presented to illustrate the effectiveness of the proposed predictive control strategy via comparing with other three existing control schemes.

Chapter 8
Networked Control of Systems with Predictive Compensator

8.1 Introduction

With the development of network technology, an increasing number of network technology has been applied to control systems. The networked control has became a new area in control systems. In this chapter, we will make full use of the network feature and propose a new networked predictive control scheme with the optimal estimation.

This chapter is organized as follows. Section 8.2 presents a novel networked predictive control scheme and an optimal estimation method for the state estimate such that the closed-loop system is asymptotically stable. The linear inverted pendulum of a NCS is modeled with random time delay and packet dropouts in Section 8.3. Numerical simulations are presented in Section 8.4. Some conclusion remarks are given in Section 8.5.

8.2 Networked Predictive Control for Systems

In this section, a networked predictive control scheme, which mainly consists of a control prediction generator and a network delay and data dropout compensator, is proposed to overcome unknown network transmission with time delay and data dropout. The control prediction generator is designed to generate a set of future control predictions with the optimal state estimate. The network time delay and data dropout compensator is used to compensate for the unknown random network dropout. This networked predictive control system (NPCS) structure is shown in Fig. 8.1.

Y. Xia, M. Fu, and G.-P. Liu: Analysis and Synthesis of NCSs, LNCIS 409, pp. 127–139.
springerlink.com

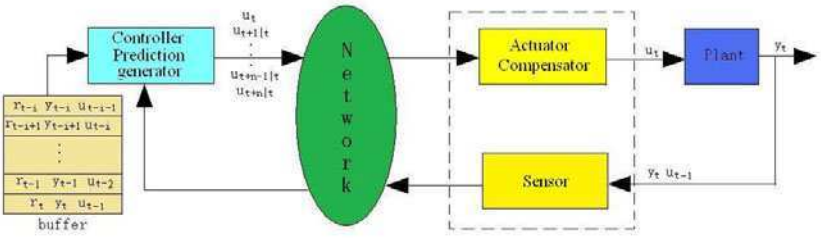

Fig. 8.1 The networked predictive control system.

8.2.1 System Model

Consider a MIMO discrete system described in the following state space form

$$\begin{aligned} x(k+1) &= Ax(k) + Bu(k) + w(k) \\ y(k) &= Cx(k) + v(k) \end{aligned} \tag{8.1}$$

where $x(k) \in R^n$, $u(k) \in R^m$, and $y(k) \in R^l$ are the system state, input, and output vectors, respectively. The noise process $\{w(k)\}$ is white, zero-mean, uncorrelated one with known covariance matrices Q_1. A, B, C are matrices of appropriate dimensions. The reference input of the system is assumed as zero and the following assumptions are made.

The arrival of the observation at time k is a binary random variable $\gamma(k)$, with probability distribution $P(\gamma(k) = 1) = \lambda_k, \lambda_k \in (0, 1)$ and $\gamma(k)$ is independent of $\gamma(s)$ if $k \neq s$. The output noise is defined in the following way:

$$v(k) \sim \begin{cases} N(0, R_1), & \gamma(k) = 1 \\ N(0, \sigma^2 I), & \gamma(k) = 0 \end{cases} \tag{8.2}$$

for some σ^2.

Assumption 8.1. *The pair, (A, B), is completely controllable, and the pair, (A, C), is completely observable.*

Assumption 8.2. *The number of consecutive data dropouts must be less than N_1 (a positive integer).*

Assumption 8.3. *The upper bound of the network delay is not greater than N (a positive integer).*

Some notations are defined as follows:

$$\begin{aligned} Y(k) &= [y(0), \cdots, y(k)]^T \\ \Gamma(k) &= [\gamma(0), \cdots, \gamma(k)]^T \\ \hat{x}(k|k) &= E[x(k)|Y(k), \Gamma(k)] \\ P(k|k) &= E[(x(k) - \hat{x}(k|k))(x(k) - \hat{x}(k|k))^T|Y(k), \Gamma(k)] \\ \hat{x}(k+1|k) &= E[x(k+1)|Y(k), \Gamma(k)] \\ P(k+1|k) &= E[(x(k+1) - \hat{x}(k+1|k))^T|Y(k), \Gamma(k)] \\ \hat{y}(k+1|k) &= E[y(k+1)|Y(k), \Gamma(k)] \end{aligned} \tag{8.3}$$

8.2.2 Network Delay and Data Dropout

As we know, more and more control systems use the network to transmit control signals. Because the network is used in control systems, there are various factors introduced as a consequence of the communication network, such as time delay and data dropout, which are considered for ensuring the desired performance of the NCS.

We assume that the measurement data $y(k)$ from the sensor is sent to the controller across a network with delay and data dropout. Time delays and data dropout occur in a NCS due to the addition of a network. This delay can destabilize a system designed or can degrade the system performance. Network delay can be further subdivided into sensor-to-controller delay, controller-to-actuator delay, and the computational delay. In this chapter, the sensor-to-controller delay and controller-to-actuator delay will be considered and the computational delay is not considered.

The problem of network time delay over a network has been proposed in [90, 92] and some types of the model have already been established. In this chapter, a simple approach of random time delay, which we set up as the Markov model for its accurate and sample is considered. To construct a Markov chain in discrete time, the time delay is a stochastic process with an upper bound N(N is a positive integer), which is a multiple of the sampling period of the system.

8.2.3 The Predictive Control Scheme to Compensate for Time Delay and Data Dropout in the Forward Channel

The Kalman Filter(**KF**) based state observer is designed as

$$\begin{aligned} \hat{x}(k|k-1) &= A\hat{x}(k-1|k-1) + Bu(t-1) \\ \hat{x}(k|k) &= \hat{x}(k|k-1) + \gamma(k)K(k)(y(k) - C\hat{x}(k|k-1)) \\ P(k|k) &= P(k|k-1) - \gamma(k)K(k)CP(k|k-1) \\ K(k) &= P(k|k-1)C^T(CP(k|k-1)C^T + R)^{-1} \end{aligned} \tag{8.4}$$

where $\hat{x}(k|k-1) \in R^n$ and $u(k-1) \in R^m$ are the one-step ahead state prediction and the input of the observer at time $k-1$, respectively, and $\gamma(k)$ indicate the signal is received or not by controller at time k. If the $\gamma(k) = 1$, it means that the signal is received by the controller at time k, otherwise $\gamma(k) = 0$ means the signal is not received. $P(k|k-1)$ is the solution of the following modified Riccati equation [169]

$$\begin{aligned} P(k|k-1) = {} & AP(k-1|k-2)A^T + Q - \gamma(k)AP(k-1|k-2)C^T \\ & \times(CP(k-1|k-2)C^T + R)^{-1}CP(k-1|k-2)A^T \end{aligned} \tag{8.5}$$

The state predictions at time k are constructed as

$$\begin{aligned} \hat{x}(k+1|k) &= A\hat{x}(k|k-1) + Bu(k) + \gamma(k)AK(k)(y(k) - C\hat{x}(k|k-1)) \\ \hat{x}(k+2|k) &= A\hat{x}(k+1|k) + Bu(k+1|k) \\ &\vdots \\ \hat{x}(k+N|k) &= A\hat{x}(k+N-1|k) + Bu(k+N-1|k) \end{aligned} \tag{8.6}$$

Assume that the controller is of the following form:

$$u(k) = u(k|k) = L(k)\hat{x}(k|k) \tag{8.7}$$

where $L(k) \in R^{m\times n}$ is the state feedback control matrix to be determined using modern control theory. Then, the control predictions are generated by

$$u(k+t|k) = L(k)\hat{x}(k+t|k), \text{for} \quad t = 0, 1, 2, \cdots, N \tag{8.8}$$

Thus, it follows from equation (8.6) that

$$\hat{x}(k+t|k) = (A + BL(k))^{t-1}\hat{x}(k+1|k) \tag{8.9}$$

Based on equations (8.4), (8.6) and (8.8), it can be shown that

$$\begin{aligned} & \hat{x}(k+t|k) \\ &= (A + BL(k))^{t-1}[A\hat{x}(k|k-1) + Bu(k) + \gamma(k)AK(k)(y(k) - Cx(k|k-1))] \\ &= (A + BL(k))^{t-1}[(A + BL(k) - \gamma(k)(AK(k) \\ & \quad -BL(k)K(k))C)\hat{x}(k|k-1) + \gamma(k)(AK(k) + BL(k)K(k))Cx(k)] \end{aligned} \tag{8.10}$$

and

$$\begin{aligned} & u(k+t|k) \\ &= L(k)\hat{x}(k+t|k) \\ &= L(k)(A + BL(k))^{t-1}[(A + BL(k) - \gamma(k)(AK(k) \\ & \quad -BL(k)K(k))C)\hat{x}(k|k-1) + \gamma(k)(AK(k) + BL(k)K(k))Cx(k)] \end{aligned} \tag{8.11}$$

In order to compensate for the network transmission delay and data loss, a network delay compensator is proposed. A very important characteristic of the network is that it can transmit a set of data at the same time. Thus, it is assumed that predictive control sequence at time k is packed and sent

to the plant side through a network. The network delay compensator chooses the latest control value from the control prediction sequences available on the plant side. For example, if the following predictive control sequences are received on the plant side:

$$[u^T(k|k), u^T(k+1|k), \cdots, u^T(k+N-1|k), \cdots, u^T(k+N|k)]^T \quad (8.12)$$

On the side of the actuator, $u(k|k)$ is used as the input to the actuator. If a new control package containing control predictive sequences, which are delayed or dropped at the next step, is dropped, one step control prediction $u(k+1|k)$ will be used as control input to the actuator. If the new package of control predictive sequences are received, then the first control input will be used as the input to the actuator. Otherwise, $u(k+2|k)$ will be used as input to the actuator, ... and so on. Based on the assumption, it is reasonable that there are at least N times consecutive time delay or data dropout. The stochastic stability criteria of the closed-loop networked predictive control systems can be analytically derived based on the methods in previous work [110, 198]. In fact, using the networked predictive control scheme presented in this section, the control performance of the closed-loop system with delay and data dropout is very similar to that of the closed-loop system without delay and data dropout.

8.2.4 The Optimal Estimation Method to Compensate for Time Delay and Data Dropout in the Feedback Channel

In this part, we will propose an optimal estimation method, which is modified from the method presented in [166], to overcome the time delay and data dropout in the feedback channel. There is a buffer to store the data from the sensor and the length of the buffer can be set to store the data in this step and before.

We assume that the length of the buffer is set to be D, so the controller discards the data, which are delayed by D times or more, from the sensor. For example, if $y(k-D)$ is not received by the controller before k, then even if $y(k-D)$ arrives at k or at a later time, it will be discarded by the controller. In 8.2.3, We have given the form of the Kalman Filter, which is shown in (8.4). Let $\gamma(k)$ be the indicator function for $y(k)$ at time $t, k \leq t$. i.e.,$\gamma(k) = 1$ if $y(k)$ arrives at t and $\gamma(k) = 0$ otherwise. Depending on whether $y(k)$ is received or not, i.e., $\gamma(k) = 1$ or 0. $(\hat{x}(k|k), P(k|k))$ is known to be computed by a Kalman Filter(**KF**) through equation (8.4). We write the $(\hat{x}(k|k), P(k|k))$ in the compact form as

$$(\hat{x}(k|k), P(k|k)) = \mathbf{KF}(\hat{x}(k-1|k-1), P(k-1|k-1), \gamma(k), y(k), u(k-1)) \quad (8.13)$$

which represents the equation (8.4).

A method to optimal the control with time delay in the feedback channel will be presented in this part. As $y(k-i)$ may arrive at time k due to the delays introduced by the network, we can improve the control quality by recalculating $\hat{x}(k-i|k-i)$ utilizing the new available measurement $y(k-i)$. Once $\hat{x}(k-i|k-i)$ is updated, we can update $\hat{x}(k-i+1|k-i+1)$ in a similar fashion. Let $y(k-i), i \in [0, D-1]$ be the oldest measurement received by the estimator at time k, then $\hat{x}(k|k)$ is computed by $i+1$ **KF**s as

$$\begin{aligned}
&(\hat{x}(k-i|k-i), P(k-i|k-i)) \\
&= \mathbf{KF}(\hat{x}(k-i-1|k-i-1), P(k-i-1|k-i-1), 1, y(k-i), u(k-i-1)) \\
&(\hat{x}(k-i+1|k-i+1), P(k-i+1|k-i+1)) \\
&= \mathbf{KF}(\hat{x}(k-i|k-i), P(k-i|k-i), \gamma(k-i+1), y(k-i+1), u(k-i)) \\
&\vdots \\
&(\hat{x}(k-1|k-1), P(k-1|k-1)) \\
&= \mathbf{KF}(\hat{x}(k-2|k-2), P(k-2|k-2), \gamma(k-1), y(k-1), u(k-2)) \\
&(\hat{x}(k|k), P(k|k)) \\
&= \mathbf{KF}(\hat{x}(k-1|k-1), P(k-1|k-1), \gamma(k), y(k), u(k-1))
\end{aligned} \tag{8.14}$$

In order to compensate for the network transmission time delay and data dropout in the feedback channel, a buffer is set in the controller to store the new data from the sensor and recalculate the $\hat{x}(k-i|k-i)$ to get the new $\hat{x}(k|k)$. With the new $\hat{x}(k|k)$, the controller can give out the control signal $u(k|k)$ and the predictive control sequences $u(k+1|k), \cdots, u(k+N|k)$ and send it to the actuator through network. In the controller, if the controller received the new data $y(k-i)$ at time k, where $i \in [0, D-1]$, the controller will store the new data corresponding to the cell of the buffer and set the $\gamma(k-i)$ to 1. Then the controller will find the oldest measurement stored in the buffer with $\gamma(k-i) = 1$ and calculate the $\hat{x}(k|k)$ according to equations (8.14). At last. the controller can calculate the predictive state sequences $x(k+1|k), x(k+2|k), \cdots, x(k+N|k)$ according to equations (8.6) and gets the predictive signal sequence $u(k|k), u(k+1|k), \cdots, u(k+N|k)$, which is sent to the actuator to control the system. After the actuator received the predictive control sequences, the compensator will choose the best control signal from the sequences according to the law which have been proposed in 8.2.3. Using this method, we can compensate for the time delay and data dropout, which happen in the both forward and feedback channels, and optimize the performance of the system.

8.3 Choose Model of System Structure

In the MPC schemes for NCS, we use a full nonlinear model and its linearized model to denote the inverted pendulum, and it would be accomplished by

the control loop with the network simulation, in which the Markov model is used.

8.3.1 Inverted Pendulum Model

Consider a single inverted pendulum, which contains a vertical level of the inverted pendulum and a cart. The structure of the inverted pendulum is shown as Fig. 8.2. The pendulum angle, the cart position, the inverted pendulum angular velocity and the cart velocity are denoted by ϕ, x, $\dot{\phi}$ and $\dot{x}$, respectively.

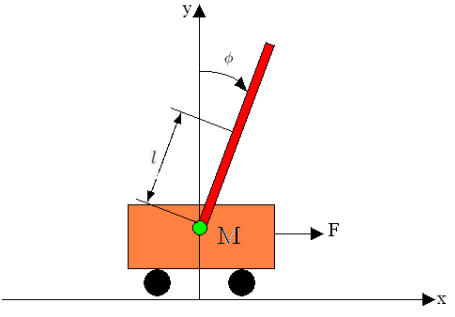

Fig. 8.2 Structure of the linear inverted pendulum.

We can obtain the nonlinear dynamics equations (8.15) of the inverted pendulum through the mechanical analysis of the inverted pendulum.

Table 8.1 Parameters used in the linear inverted pendulum model

Symbol	Value	Meaning
m	0.109 Kg	Mass of the pendulum rod
M	1.096 Kg	Mass of the cart
l	0.25 m	Length from the pendulum axis to its centroid
b	0.1 $N/m/sec$	The friction coefficient of the cart
I	$0.0034kg*m*m$	Inertia of the rod
g	$9.81m/s^2$	Gravitational constant

1. Nonlinear Model

$$\begin{aligned}(M+m)\ddot{x}+b\dot{x}+ml\ddot{\phi}\cos\phi-ml\dot{\phi}^2\sin\phi&=F\\-(I+ml^2)\ddot{\phi}+mgl\sin\phi&=ml\ddot{x}\cos\phi\end{aligned}\tag{8.15}$$

   where, F means the force, which can drive the cart moving to keep the pendulum rod in the vertical upward.
2. Linear Model
   Linearize the nonlinear dynamics equations, let $\cos\phi=-1, \sin\phi=\phi, (\frac{d\phi}{dt})^2=0$ and use u instead of F, we can get

$$\begin{aligned}-(I+ml^2)\ddot{\phi}+mgl\phi&=ml\ddot{x}\\(M+m)\ddot{x}+b\dot{x}+ml\ddot{\phi}&=u\end{aligned}\tag{8.16}$$

Let $X^T=[x,\dot{x},\phi,\dot{\phi}], u=-\ddot{x}$ and $I=\frac{1}{3}ml^2$, we can obtain the state-space model:

$$\dot{X}=\begin{bmatrix}0&1&0&0\\0&0&0&0\\0&0&0&1\\0&0&\frac{3g}{4l}&0\end{bmatrix}X+\begin{bmatrix}0\\-1\\0\\\frac{3}{4l}\end{bmatrix}u\tag{8.17}$$

$$y=\begin{bmatrix}x\\\phi\end{bmatrix}=\begin{bmatrix}1&0&0&0\\0&0&1&0\end{bmatrix}\begin{bmatrix}x\\\dot{x}\\\phi\\\dot{\phi}\end{bmatrix}+\begin{bmatrix}0\\0\end{bmatrix}u\tag{8.18}$$

By using the plant parameters of the TABLE 8.1 and discretize the system dynamics with the sample time 0.01s, we have

$$\begin{aligned}&X(k+1)=A_dX(k)+B_du(k)\\&=\begin{bmatrix}1&0.01&0&0\\0&1&0&0\\0&0&1.0015&0.01\\0&0&0.2941&1.0015\end{bmatrix}X(k)+\begin{bmatrix}-0.0001\\-0.01\\0.0002\\0.03\end{bmatrix}u(k)\end{aligned}\tag{8.19}$$

8.3.2 Random Network Time Delay Model

As described in 8.2.2, in this chapter, the network with time delay and data dropout are simulated by the Markov model. Let each of states of the Markov chain represents the different random time delay and data dropout. According to the state jump in the Markov chain, the time delay of the network is variable. In this example, we assume a 5 states Markov chain with $N=4$, which means that the maximum number of steps of time delay is 4 in the both forward and feedback channels. Thus the maximum number of steps of

time delay in the control loop is 8 steps and the state transition probability matrix of the forward and feedback channel is shown in the following:

$$P_{forward} = P_{feedback} = \begin{bmatrix} 0.3\ 0.2\ 0.2\ 0.2\ 0.1 \\ 0.2\ 0.3\ 0.2\ 0.2\ 0.1 \\ 0.1\ 0.2\ 0.4\ 0.2\ 0.1 \\ 0.1\ 0.2\ 0.2\ 0.3\ 0.2 \\ 0.1\ 0.1\ 0.2\ 0.2\ 0.4 \end{bmatrix} \tag{8.20}$$

where $P_{forward}$ is the state transition probability matrix of the forward channel and the $P_{feedback}$ is the state transition probability matrix of the feedback channel.

8.3.3 Structure of the Controller

Through the discrete LQR state feedback control law, the linearized model (8.19) could be used to derive a controller with the form

$$u = -LX \tag{8.21}$$

Design a discrete LQR state feedback control law for state regulation, then it can be obtained by minimizing the cost function:

$$J = \int_0^\infty (X^T Q X + u^T R u) dt \tag{8.22}$$

8.4 Simulation Results

In order to demonstrate the effectiveness of the proposed predictive control scheme (8.11) and the optimal estimation method (8.14) in the feedback channel, numerical simulations have been performed and presented comparing with the control method without any compensation in this section. The plant is chosen as the linear inverted pendulum model (8.17) and the pendulum parameter values are selected in Table 8.1. This section gives the trajectory curves of the pendulum angle ϕ and the cart position x with different control methods when the pendulum angle ϕ reaches stable from the initial state $\phi = 0.2$ ($X = [0\ 0\ 0.2\ 0]'$).

8.4.1 Control the Inverted Pendulum without Network

Consider the model of the inverted pendulum (8.19) and LQR state feedback control law (8.21) without data dropouts and noises. The parameters in cost function (8.22) are selected as

$$Q = \begin{bmatrix} 1000 & 0 & 0 & 0 \\ 0 & 0 & 0 & 0 \\ 0 & 0 & 500 & 0 \\ 0 & 0 & 0 & 0 \end{bmatrix}, \qquad R = 1 \tag{8.23}$$

which yields the feedback gain

$$L = [-31.6228 \ -20.8404 \ -77.0990 \ -13.6080] \tag{8.24}$$

The trajectory of the pendulum angle reaches at zero from the initial position and keeps the pendulum stability. The trajectory of the cart position is depicted in Fig. 8.3, which indicates that, without networks, the pendulum stability can be guaranteed under the LQR state feedback control law.

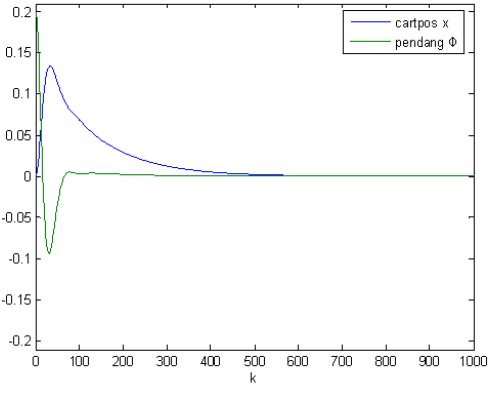

Fig. 8.3 Control the inverted pendulum without network.

From Fig. 8.3, we can see that the cart position and the pendulum angle reach stability before $k = 600$ and the overshoot of the pendulum angle is smaller than 0.1. The curve of the cart position shows that the cart doesn't leave far away from the center position $x = 0$, which tells us that the performance of the system is good when the controller control the pendulum and keep it stable.

8.4.2 Control the Inverted Pendulum through Network without Compensation of the Time Delay and Data Dropout

In this part, we will consider the NCSs with time delay and data dropouts. In order to construct a NCS with random time delay and packet loss, which

is depicted by Markov chains, the transition probability matrix is selected as the Markov model (8.20). System performances of the control without any compensation are shown when the time delay and data dropout happen in both the forward and feedback channels.

The method of controlling the system without any compensation means that if the signals of control and feedback, which are transited through network, are delayed or discarded when the network is busy, the actuator will give out a zero signal to control the plant. Because of the time delay and data dropout, the closed-loop system will become the open-loop system and the performances of the system will be worse than the system without network. As Fig. 8.4 shown, we can see that the curves of the pendulum angle and cart position are divergence because time delay and data dropout are bad for the performances of the system. Time delay and data dropout are added to the channel of the transition, which will lead the inverted pendulum out of control.

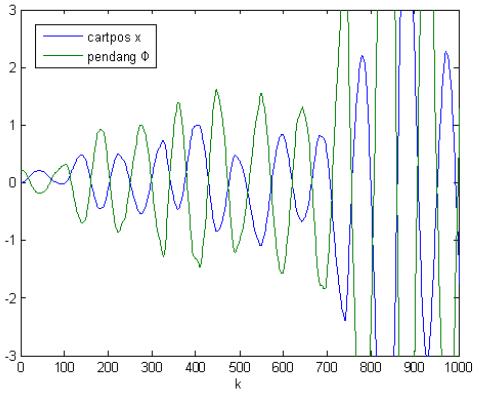

Fig. 8.4 Control the inverted pendulum through network without compensation.

8.4.3 Predictive Control Scheme and Optimal Estimation Method for NCSs

In the following, we firstly consider that only the predictive control is applied in the NCSs. Fig. 8.5 shows the curves of the pendulum angle and cart position with predictive control used to compensate for the time delay and data dropout. From the figure, we can get that the pendulum angle is well stabilized in the equilibrium position when there are time delay and data dropout in both forward and feedback channels. Compared with Fig. 8.4, the pendulum angle and the cart position are stable at the position of equilibrium

in Fig. 8.3 although the curve of the cart position has larger overshoot and the time delay and data dropout happen in both the forward and feedback channels with network. Because the predictive control is introduced to control the system, the pendulum angle can be stabilized in the vertical position but the performance of the system is not good and the cart position is far away from the center position shown as Fig. 8.4 and Fig. 8.5.

Fig. 8.6 shows the curve of the pendulum angle and the cart position with predictive control and optimal estimation. As we expect, the performance of the system is improved after introducing both the predictive control and optimal estimation method to the controller. Compared Fig. 8.6 with Fig. 8.5, it is obvious that the curve of cart position in Fig. 8.6 has smaller overshoot and settling time than the one in Fig. 8.5.

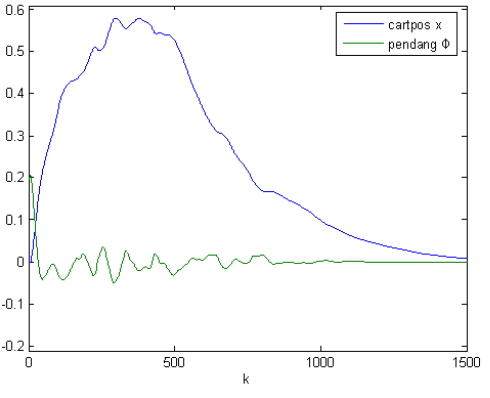

Fig. 8.5 Control the inverted pendulum through network with predictive control.

The control behavior of LQR state feedback control with network and without network have been shown, and we have also discussed the control behavior of the predictive control and optimal estimation method in the front of this part. In this simulation, the predictive control can guarantee the stability of inverted pendulum system with time delay and data dropout while the system is unstable without any compensation for the time delay and data dropout. Both the predictive control and optimal estimation method are introduced into the controller, which can not only guarantee the inverted pendulum system stable but also the curve of the cart position with smaller overshoot. In this part, the result of the simulation shows that the predictive control and optimal estimation method can compensate for the time delay and data dropout in the network and improve the performance of the NCSs.

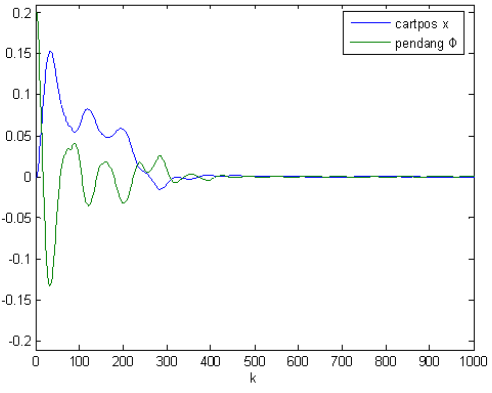

Fig. 8.6 Control the inverted pendulum through network with predictive control and optimal estimation.

8.5 Summary

A new networked predictive control scheme and an optimal estimation method, which is based on the Kalman filter, have been proposed for MIMO networked distributed control systems with random network time delay and data dropout. The controller uses the optimal estimate to compute a set of future control predictions satisfying the system performance requirements. The compensator chooses the best control signal to compensate for the random network transmission time delay and packet loss. Simulation results have been presented to illustrate the effectiveness of the proposed predictive control and the optimal estimation method based on Kalman filter strategy via comparing with the control scheme without any compensation.

Part IV
Fault Detection over Networks

Chapter 9
Robust Fault Detection of Systems over Networks with Packet Loss

9.1 Introduction

It is clear that fault diagnosis (including fault detection and isolation, FDI) has been becoming an important subject in modern control theory and practice. Since the beginning of 1970s, research in fault diagnosis has been gaining increasing consideration world-wide in both theory and application [134, 47]. This development was mainly stimulated by the trend of automation towards more complexity and the growing demand for higher availability and security of control systems. However, a strong impetus also comes from the side of modern control theory estimation and parameter identification that have been made feasible by the spectacular progresses of computer technology [26].

Generally speaking, a fault detection (FD) process is to construct a residual signal which can then be compared with a predefined threshold. When the residual signal exceeds the threshold, the fault is detected and an alarm is generated [26, 38]. During last three decades, many methods have been proposed, for example: Clark, and co-workers proposed observer-based FDI approach [31] and the parity relation schemes for FDI were later developed by Mironovski [120]. Leininger [95] pointed out the impact of modeling errors on FDI performance. The first attempt of improving robustness of observer-based FDI approaches is attributed to Frank and Keller [48]. It should be pointed out that, in all the aforementioned schemes, it has been implicitly assumed that data transmission is without time delay and packet loss. Since network cables are involved in control systems in today's world, a seemingly natural problem is to study FDI problems for networked control systems (NCSs) in the presence of network-induced delays or with data packet loss [68, 193, 149, 198, 16]. Fang et al [44] proposed an overview of main ideas and results on fault diagnosis of NCSs, including the fundamentals of fault diagnosis for NCSs with information scheduling, fault diagnosis approaches based on the simplified time-delay system models, and the quasi T-S fuzzy model and fault diagnosis for linear and nonlinear NCSs with long delay.

Y. Xia, M. Fu, and G.-P. Liu: Analysis and Synthesis of NCSs, LNCIS 409, pp. 143–158.
springerlink.com

However, in the most of the aforementioned methods, it is assumed that the fault detection center is located at the same node with the controller. In this chapter, we focus our attention on a more general case that the FD center is neither located at the controller node nor located at the plant node, all the input data and measurement data is transmitted from the actuator node and the sensor node to the FD center, respectively, over unreliable networks with bounded packet loss. The bounded packet loss is modeled in two ways: arbitrary packet loss process and Markovian packet loss process. The stability analysis of the error system and the design of fault detection filter (FDF) gains are also given to satisfy some performance constraints.

The rest of this chapter is organized as follows. In Section 9.2, the FD model taking into account the packet transmission loss and main assumptions are presented. The stability analysis and FDF design are given, which satisfies the given constraits in Section 9.3. In Section 9.4, the FD algorithm is proposed according to the trade-off design of robustness and sensitivity. An illustrative example is presented in Section 9.5 to show the effectiveness of the result. The chapter is concluded in Section 9.6.

9.2 Description of Fault Detection over Networks

Consider a monitored system described by

$$\begin{cases} \dot{x}(t) = A_c x(t) + B_c u(t) + E_{dc} d(t) + E_{fc} f(t) \\ y(t) = C_c x(t) \end{cases} \tag{9.1}$$

where $x \in \mathbb{R}^n$, $u \in \mathbb{R}^p$ and $y \in \mathbb{R}^m$ are the system's state, reference inputs and measurements, respectively, $d \in \mathbb{R}^{n_d}$ and $f \in \mathbb{R}^{n_f}$ are disturbance and the latent fault in the system. Matrices A_c, B_c, C_c, E_{dc}, and E_{fc} are of appropriate dimensions. For data acquisition, it is supposed that the sensor and the actuator are time-driven with an constant sampling period h. Discretization of the monitored system (9.1) according to the sampling period h will then give

$$\begin{cases} x(k+1) = Ax(k) + Bu(k) + E_d d(k) + E_f f(k) \\ y(k) = Cx(k) \end{cases} \tag{9.2}$$

where

$$A = e^{A_c h},\ C = C_c,\ B = \int_0^h e^{A_c s} B_c ds,$$
$$E_d = \int_0^h e^{A_c s} E_{dc} ds,\ E_f = \int_0^h e^{A_c s} E_{fc} ds$$

Remark 9.1. The monitored system is shown in Fig. 9.1, the inputs and outputs of the plant are $u_R(t)$ and $y_R(t)$, respectively. However, $u_R(t)$ are not

available for measurement, we have to use the reference command $u(k)$ and the measured output $y(k)$ in FDI. Hence, the model of the monitored system involves the actuator and the sensor additionally.

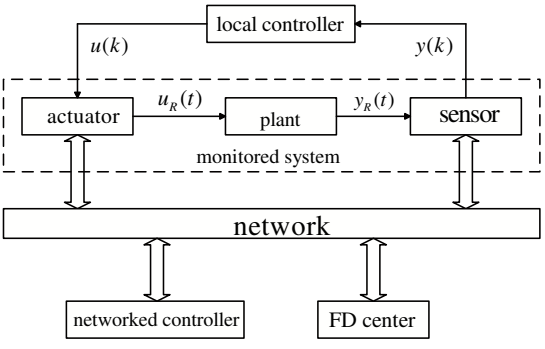

Fig. 9.1 The structure of FD over networks.

The structure of fault detection over networks discussed in this chapter is shown in Fig. 9.1. The inputs of monitored system, $u(k)$, and the measurements of the monitored system, $y(k)$, are transmitted to the FD center node from the actuator and the sensor in a single packet at each time step without time delay, respectively. However, the networks are not reliable, the data packets may be lost during the transmission. Note that the structure considered in this chapter is not as same as structures in most literature, this structure is a more general case, namely, the fault detection center is located neither at the controller node nor plant node, and the controller considered in this structure is also not limited in topology. Some researchers focus on the scheme that the controller is remote, and fault detection center is with the remote controller at a same network node. On the other side, local controllers is generally used in distributed control systems (DCS). For example, in most thermal power plant DCS, every controlled object is with a local stabilizing controller, which ensures the plant stable. This plant-controller pair is called subsystem. The entire system of controllers and objects is connected by networks to a center node for communication and monitoring. The fault detection algorithm can be applied in this center to diagnose the latent faults of every subsystem. The aforementioned two schemes are special cases of the structure considered in this chapter.

We define $\lambda_k = \{0, 1\}$ for data packets transmitted from the actuator to the FDI node at time instant k, if the FDI node receives the data packet successfully, then $\lambda_k = 1$, if the data packet losses, then $\lambda_k = 0$. Similarly, We define $\gamma_k = \{0, 1\}$ for data packets transmitted from the sensor to the FDI node in the same way. Let $\mathbb{F} = \{i|1, 2, 3, \cdots\}$ denote the sequence of time

points of successful data transmission from the sensor to the FDI node. We define a function $g(x)$, $x \in \{k|\gamma_k = 1\}$

$$i = g(k) = \sum_{j=0}^{k} \gamma_j - 1 \tag{9.3}$$

which denotes the map from index k to the index i, see Fig. 9.2. The following concept and mathematical models are introduced to capture the nature of packet losses.

Definition 9.2. Packet-loss process is defined as

$$\{N_i \triangleq g^{-1}(i+1) - g^{-1}(i)\} \tag{9.4}$$

where $g^{-1}(\cdot)$ denotes the inverse function of $g(\cdot)$, which takes values in the finite state space $\mathbb{N} \triangleq \{1, 2, \cdots, s\}$. Note that the $N(i)$ is duration between two successful transmissions.

Definition 9.3. Packet-loss process (9.4) is said to be arbitrary if it take values in $\mathbb{N}$ arbitrarily.

Definition 9.4. Packet-loss process (9.4) is said to be Markovian if it is a discrete-time homogeneous Markov chain on a complete probability space $(\Omega, \mathbb{N}, P)$, and takes values in $\mathbb{N}$ with known transition probability matrix $\Pi \triangleq (\pi_{ij}) \in \mathbb{R}^{s \times s}$, where

$$\pi_{ij} \triangleq Pr\left(N_{i+1} = j | N_i = i\right) \geq 0 \tag{9.5}$$

for all $i, j \in \mathbb{N}$, and $\sum_{j=1}^{s} \pi_{ij} = 1$ for each $i \in \mathbb{N}$.

We further impose an assumption on the design as follows:

Assumption 9.1. *The data from the controller to each actuator are restricted to belong to a small and fixed finite set of scalars* $\mathbb{U}$.

Remark 9.5. The information used for FDI in this chapter is the measured outputs from sensor and the inputs to the actuators. The case that the controller is placed at the plant's node is same as the case that the controller is placed at another node which is connected with networks.

The principle of model-based FD is to reconstruct the outputs of the monitored system and compare them with real measurements [38]. Therefore, only the time instants when new measurement data packets arrive are of concern. Let $\bar{u}(k)$ and $\bar{y}(k)$ denote the data available at the FDI node:

$$\bar{u}(k) = \lambda_k u(k) \tag{9.6}$$

$$\bar{y}(k) = \gamma_k y(k) \tag{9.7}$$

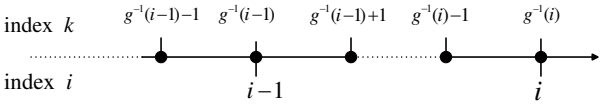

Fig. 9.2 Double index.

Therefore, system (9.2) can be rewritten as

$$\begin{cases} x(i+1) = A(i)x(i) + \bar{B}(i)\bar{U}(i) + \breve{B}(i)U(i) + \bar{E}_d(i)\bar{d}(i) + \bar{E}_f(i)\bar{f}(i) \\ y(i) \quad = Cx(i) \end{cases} \tag{9.8}$$

where

$$A(i) = A^{N_i} \in \mathbb{A} \triangleq \{A_i | A_i \triangleq A^{N_i} i \in \mathbb{N}\} \tag{9.9}$$

$$\bar{B}(i) = \left[A^{N_i-1}B \; A^{N_i-2}B \cdots B \right]$$

$$\breve{B}(i) = \bar{B}(i) \left(diag\{\bar{\lambda}_{g^{-1}(i)}\bar{\lambda}_{g^{-1}(i)+1}, \cdots, \bar{\lambda}_{g^{-1}(i+1)-1}\} \bigotimes I_p \right) \tag{9.10}$$

$$\bar{E}_f(i) = A^{N_i-1}E_f, \; \bar{E}_d(i) = A^{N_i-1}E_d$$

$$\bar{U}(i) = \begin{bmatrix} \bar{u}(g^{-1}(i)) \\ \bar{u}(g^{-1}(i)+1) \\ \vdots \\ \bar{u}(g^{-1}(i+1)-1) \end{bmatrix}, U(i) = \begin{bmatrix} u(g^{-1}(i)) \\ u(g^{-1}(i)+1) \\ \vdots \\ u(g^{-1}(i+1)-1) \end{bmatrix}$$

where $\bar{\lambda}_k = 1 - \lambda_k$ and $I_p \in \mathbb{C}^{p\times p}$ is a unit matrix.

Remark 9.6. $\bar{f}(i)$ and $\bar{d}(i)$ are not the sampled value of fault signal $f(t)$ and noise signal $d(t)$ at time instant i. According to Chen and Francis [27], the inter-sample behavior of $d(t)$ and $f(t)$ is omitted in the system described by equation (9.8), the virtual signals $\bar{f}(i)$ and $\bar{d}(i)$ are equivalent to the effect of real signals, they have a relation as follows:

$$A^{N_i-1}E_f\bar{f}(i) = \sum_{l=0}^{N_i-1} f(g^{-1}(i)+l) \tag{9.11}$$

$$A^{N_i-1}E_d\bar{d}(i) = \sum_{l=0}^{N_i-1} d(g^{-1}(i)+l) \tag{9.12}$$

Note that, the vector $\breve{B}(i)U(i)$ is unknown for the FD center, but this term can be regarded as a random disturbance according to Assumption 9.1, thus we rewrite system (9.8) as

$$\begin{cases} x(i+1) = A(i)x(i) + \bar{B}(i)\bar{U}(i) + B_m(i)\omega_m(i) + \bar{E}_f(i)\bar{f}(i) \\ y(i) \quad = Cx(i) \end{cases} \tag{9.13}$$

where

$$B_m(i) = [I \ \bar{E}_d(i)], \quad \omega_m(i) = [U^T(i)\breve{B}^T(i) \ \bar{d}^T(i)]^T \tag{9.14}$$

we can also rewrite system (9.8) as

$$\begin{cases} x(i+1) = A(i)x(i) + \bar{B}(i)\bar{U}(i) + B_a(i)\omega_a(i) + \bar{E}_f(i)\bar{f}(i) \\ y(i) \quad = Cx(i) \end{cases} \tag{9.15}$$

where

$$B_a(i) = [\breve{B}(i) \ \bar{E}_d(i)] \tag{9.16}$$

$$\omega_a(i) = [U^T(i) \ \bar{d}^T(i)]^T \tag{9.17}$$

Remark 9.7. If system (9.1) is with the Markovian packet-loss process (9.4), the parameter matrix $A(i) \triangleq A^{N_i} \in \mathbb{A} \triangleq \{A_i | A_i \triangleq A^{N_i}\}$ and $B_m(i)$ are Markovian jump matrices [32], [210]. Meanwhile, if system (9.1) is with the arbitrary packet-loss process (9.4), the parameter matrices $A(i)$ and $B_a(i)$ are arbitrary matrices. For a measurements transmission mode i, there are $\sum_{h=0}^{i} A_i^h$ submodes for inputs transmission, so $B_a(i)$ has $\sum_{i=1}^{s}\sum_{h=0}^{i} A_i^h$ modes totally in system (9.15), where A_i^h denotes the permutation of h elements in i elements.

9.3 Observer Based Residual Generation and Evaluation

In this section, a fault detection filter (FDF) will be designed to achieve residual generation and evaluation over networks with bounded packet loses.

The FDF to be designed is

$$\begin{cases} \hat{x}(i+1) = A(i)\hat{x}(i) + \bar{B}(i)\bar{U}(i) + K(i)\left(y(i) - C\hat{x}(i)\right) \\ r(i) \quad = L\left(y(i) - C\hat{x}(i)\right) \end{cases} \tag{9.18}$$

where $\hat{x}(i)$ is the estimate of the state $x(i)$, $r(i)$ is residual, and $K(i)$, L are design parameters matrices. In this chapter, the FDF gain $K(i)$ is designed to be time variant, and the matrix L is the risidual weighting factor which,

in this chapter, is static. Let the state estimation error $e(i) = \hat{x}(i) - x(i)$ and the residual $r(i)$ propagate as

$$P_a : \begin{cases} e(i+1) = (A(i) - K(i)C)\, e(i) + B_a(i)\omega_a(i) + \bar{E}_f(i)\bar{f}(i) \\ r(i) \quad\;\; = LCe(i) \end{cases} \tag{9.19}$$

or

$$P_m : \begin{cases} e(i+1) = (A(i) - K(i)C)\, e(i) + B_m(i)\omega_m(i) + \bar{E}_f(i)\bar{f}(i) \\ r(i) \quad\;\; = LCe(i) \end{cases} \tag{9.20}$$

In order to guarantee a satisfactory FD performance, $K(i)$ and L should be designed such that the residual $r(i)$ is sensitive to the fault $\bar{f}(i)$ and robust to disturbance $\omega_a(i)$ or $\omega_m(i)$.

Rest of the aim of the chapter is then to design the FDF parameters satisfying the constrains as:

C1: For the monitored system (9.1) with arbitrary packet-loss process (9.4), the H_∞-norm of system P_a is less than a prescribed scalar $\gamma > 0$, namely:

$$\|P_a\|_\infty := \sup_{N_i \in \mathbb{N}} \sup_{0 \neq \omega_a \in l_2} \frac{\|\omega_a\|_2}{\|r\|_2} < \gamma \tag{9.21}$$

C2: For the monitored system (9.1) with Markovian packet-loss process (9.4), the H_∞-norm of system P_m is less than a prescribed scalar $\gamma > 0$, namely:

$$\|P_m\|_\infty := \sup_{N_i \in \mathbb{N}} \sup_{0 \neq \omega_m \in l_2} \frac{\|\omega_m\|_2}{\|r\|_2} < \gamma \tag{9.22}$$

C3: For the monitored system (9.1) with arbitrary packet-loss process (9.4) or with Markovian packet-loss process (9.4), the H_--norm of system P_a or system P_m is greater than a prescribed scalar $\beta > 0$, namely:

$$\|P_a\|_-(\|P_m\|_-) := \inf_{N_i \in \mathbb{N}} \frac{\|\bar{f}\|_2}{\|r\|_2} > \beta \tag{9.23}$$

9.3.1 FDF Stability Analysis with Packet Loss

In this subsections, we analyze the stability property of the FDF. For the monitored system (9.1) with the arbitrary packet-loss process (9.4), a sufficient condition is derived by adopting a packet-loss dependent Lyapunov function approach. For the monitored system (9.1) with the Markovian packet-loss process (9.4), a necessary and sufficient condition is established by using the theory from Markovian jump systems. The conditions are given in terms of LMIs.

Definition 9.8. Let $e(l; e_0)$ be the trajectory of system (9.19) with initial state e_0. System (9.19) with arbitrary packet-loss process (9.4) is said to be

stable if for any $\varepsilon > 0$ there exists a $\delta \triangleq \delta(\varepsilon) > 0$ such that $\| e_0 \| < \delta$ implies $\| e(l; e_0) \| < \varepsilon$ for $l \in \mathbb{Z}^+$. Furthermore, it is said to be asymptotically stable if it is stable and $\lim_{l\to\infty} \| e(l; e_0) \|^2 = 0$ for any initial state $e_0 \in \mathbb{R}^n$.

Theorem 9.9. *System (9.19) with arbitrary packet-loss process asymptotically stable if there exist matrices $P_i \in \mathbb{S}^+$, $i \in \mathbb{N}$, such that*

$$(A_j - K_j C)^T P_j (A_j - K_j C) - P_i < 0 \tag{9.24}$$

holds for all $i, j \in \mathbb{N}$, where $A_j \in \mathbb{A}$.

Proof. The initial state of system (9.19) is $e(1) = (A(0) - K(0)C)e_0$, and let $i \triangleq N_{i-1}$, $j \triangleq N_i$, we take the packet-loss Lyapunov function as

$$V(i) = e^T(i) P_{(g^{-1}(i) - g^{-1}(i-1))} e(i) = e^T(i) P_i e(i), \tag{9.25}$$

so we have

$$V(i+1) = e^T(i)(A_j - K_j C)^T P_j (A_j - K_j C) e(i) \tag{9.26}$$

Therefor, $V(i+1) - V(i) < 0$ for any $e(i) \neq 0$ if inequality (9.24) holds. Hence, $\lim_{i\to\infty} V(i) = 0$.

Furthermore, let $\beta_1 \triangleq \max_{l\in\mathbb{N}} \|P_l\|$, $\beta_2 \triangleq \min_{l\in\mathbb{N}} \{1/\|P_l^{-1}\|\}$, $\beta_3 \triangleq \max\{\max_{l\in\mathbb{N}} \|A_l - KC\|^2, 1\}$, and $\beta = \sqrt{(\beta_1\beta_2)/\beta_3}$. Then given any $\varepsilon < 0$, we prove that $\|e_0\| < \beta\varepsilon$ implies $\|e(l, e_0)\| < \varepsilon$ for $l \in \mathbb{Z}_+$ in the following.

For $l > 1$, we have $\beta_2 \|e(l, e_0)\|^2 < V(l)$ according to the definition of Lyapunov function, and $V(l) < V(1) \leq \beta_1 \|e(1)\|^2 \leq \beta_1\beta_3 \|e_0\|^2$. So $\|e(l, e_0)\| < \sqrt{(\beta_1\beta_2)/\beta_3}\|e_0\| < \sqrt{(\beta_1\beta_2)/\beta_3}\beta\varepsilon \leq \varepsilon$. Thus we conclude that $\|e(l, e_0)\| < \varepsilon$ for all $l \in \mathbb{Z}_+$ if $\|e_0\| < \delta$ with $\delta = \beta\varepsilon$. According to Definition 9.8, system (9.19) is asymptotically stable.

Definition 9.10. System (9.20) with Markovian packet-loss process (9.4) is said to be mean square stable if $\lim_{l\to\infty} E(\|e(l, e_0)\|^2) = 0$ for any initial state $e_0 \in \mathbb{R}^n$

Theorem 9.11. *System (9.20) with Markovian packet-loss process (9.4) is mean square stable if, and only if, there exist matrices $P_i \in \mathbb{S}^+$, $i \in \mathbb{N}$, such that*

$$\sum_{j=1}^{s} \left[\pi_{ij} (A_j - K_j C)^T P_j (A_j - K_j C)\right] - P_i < 0 \tag{9.27}$$

holds for all $i \in \mathbb{N}$.

Proof. (*Sufficiency*) Because $\{N_i : i \in \mathbb{N}\}$ is a discrete-time homogeneous Markov chain, system (9.20) is a discrete-time Markovian jump linear system with s operation modes. Now take a Lyapunov function as follows:

$$V(i) = e^T(i) P_{(g^{-1}(i) - g^{-1}(i-1))} e(i) = e^T(i) P_i e(i) \tag{9.28}$$

we have

$$\begin{aligned} &E\left(V(i+1|N_{i-1}=i)-V(i)\right) \\ &=e^T(i)\left(\sum_{j=1}^{s}[\lambda_{ij}(A_j-K_jC)^TP_j(A_j-K_jC)]-P_i\right)e^T(i)<0 \end{aligned}$$

for any $e(i)\neq 0$ if inequality (9.27) holds. Hence, $\lim_{i\to\infty}E(V(i))=0$ and $\lim_{i\to\infty}E(\|e(i;e(1))\|^2)=0$. That is, system (9.20) is mean square stable.

(*Necessity*) Suppose system (9.20) is mean square stable. Because system (9.20) is a Markovian jump system, according to the stability results from Markovian jump systems, there exist matrices $P_i\in\mathbb{S}^+$, $i\in\mathbb{N}$, such that (9.27) holds.

9.3.2 Robust Design of FDF

With the stability results developed in subsection 9.3.1, the robust FDF design techniques are provided in this subsection. We introduce two lemmas as follows

Lemma 9.12. *For a given scalar $\gamma>0$ and a system as follows:*

$$P:\begin{cases} x(k+1)=A_{\theta_k}x(k)+B_{\phi_k}\omega(k) \\ z(k)=Cx(k)+D\omega(k) \end{cases} \tag{9.29}$$

where $\theta_k\in\mathbb{N}_1\triangleq\{1,2,\cdots,s_1\}$ and $\phi_k\in\mathbb{N}_2\triangleq\{1,2,\cdots,s_2\}$, the following conditions are equivalent:

(i) system P is asymptotically stable and the H_∞-norm denoted as

$$\|P\|_\infty\triangleq\sup_{\theta_0\in\mathbb{N}_1,\phi_0\in\mathbb{N}_2}\sup_{0\neq\omega\in l_2}\frac{\|z\|_2}{\|\omega\|_2} \tag{9.30}$$

satisfies $\|P\|_\infty<\gamma$.

(ii) there exist matrices $P_{ij}>0$, $\forall i\in\mathbb{N}_1$, $\forall j\in\mathbb{N}_2$ that satisfy

$$\begin{bmatrix} A_i & B_j \\ C & D \end{bmatrix}^T\begin{bmatrix} P_{ij} & 0 \\ 0 & I \end{bmatrix}\begin{bmatrix} A_i & B_j \\ C & D \end{bmatrix}-\begin{bmatrix} P_{hg} & 0 \\ 0 & \gamma^2I \end{bmatrix}<0 \tag{9.31}$$

(iii) there exist matrices $P_{ij}>0$ and G_{ij} , $\forall i\in\mathbb{N}_1$, $\forall j\in\mathbb{N}_2$ that satisfy

$$\begin{bmatrix} G_{ij}A_i & G_{ij}B_j \\ C & D \end{bmatrix}^T\begin{bmatrix} G_{ij}+G_{ij}^T-P_{ij} & 0 \\ 0 & I \end{bmatrix}^{-1}\begin{bmatrix} G_{ij}A_i & G_{ij}B_j \\ C & D \end{bmatrix}-\begin{bmatrix} P_{hg} & 0 \\ 0 & \gamma^2I \end{bmatrix}<0 \tag{9.32}$$

Proof. (ii) $\Leftrightarrow$ (i). If there exist matrices $P_{ij}>0$ such that inequality (9.31) holds, so there exist a proper scalar ϵ, $0<\epsilon<1$ such that

$$\begin{bmatrix} P_{hg} & 0 \\ 0 & (1-\epsilon)\gamma^2 I \end{bmatrix} > \begin{bmatrix} A_i & B_j \\ C & D \end{bmatrix}^T \begin{bmatrix} P_{ij} & 0 \\ 0 & I \end{bmatrix} \begin{bmatrix} A_i & B_j \\ C & D \end{bmatrix} \tag{9.33}$$

holds. According to inequality (9.31), we have

$$P_{hg} - A_i^T P_{ij} A > 0 \tag{9.34}$$

so, system (9.29) is asymptotically stable, and

$$V(k) = x^T(k) P x(k) \tag{9.35}$$

is a Lyapunov function of system (9.29). Now we prove that $\gamma^2\|\omega\|_2^2$ is an upper bound of $\|z\|_2^2$, consider a function:

$$J_k = \|z\|^2 - (1-\epsilon)\gamma^2\|\omega\|^2. \tag{9.36}$$

Let $\Delta V(k) = V(k+1) - V(k)$, we have

$$\begin{aligned} J_k = & \left[\|z\|^2 - (1-\epsilon)\gamma^2\|\omega\|^2 + \Delta V(k)\right] \\ & -\Delta V(k) \\ = & \begin{bmatrix} x(k) \\ \omega(k) \end{bmatrix}^T \left([C\ D]^T [C\ D] - \begin{bmatrix} P_{hg} & 0 \\ 0 & (1-\epsilon)\gamma^2 I \end{bmatrix} \right. \\ & \left. + [A_i\ B_j]^T P_{ij} [A_i\ B_j] \right) \begin{bmatrix} x(k) \\ \omega(k) \end{bmatrix} \\ & -\Delta V(k) \\ = & \begin{bmatrix} x(k) \\ \omega(k) \end{bmatrix}^T \left(\begin{bmatrix} A_i & B_j \\ C & D \end{bmatrix}^T \begin{bmatrix} P_{ij} & 0 \\ 0 & I \end{bmatrix} \begin{bmatrix} A_i & B_j \\ C & D \end{bmatrix} - \begin{bmatrix} P_{hg} & 0 \\ 0 & (1-\epsilon)\gamma^2 I \end{bmatrix} \right) \begin{bmatrix} x(k) \\ \omega(k) \end{bmatrix} \\ & -\Delta V(k) \end{aligned}$$

According to inequality (9.33), we have $J_k < -\Delta V(k)$, that is

$$\|z(k)\|^2 < (1-\epsilon)\gamma^2\|\omega\|^2 - \Delta V(k) \tag{9.37}$$

sum both side of inequality (9.37) from $k = 0$ to $k = n$, since the disturbance $w(k) \in l_2$, we have

$$\sum_{k=0}^{n} \|z(k)\|^2 < (1-\epsilon)\gamma^2 \sum_{k=0}^{n} \|w(k)\|^2 - V(n+1) \tag{9.38}$$

$$\leq (1-\epsilon)\gamma^2\|w(k)\|_2^2 - V(n+1), \tag{9.39}$$

because of $\lim_{n\to\infty} x(n) = 0$, we have

$$\|z(k)\|_2^2 \leq (1-\epsilon)\gamma^2\|\omega\|_2^2 < \gamma^2\|\omega\|_2^2 \tag{9.40}$$

(ii)→ (iii). We choose $G_{ij} = G_{ij}^T = P_{ij}$, that is (ii) implies (iii).

(iii)→ (ii). By Schur compement, an LMI can be obtained from (iii) as follows

$$\begin{bmatrix} -P_{hg} & 0 & A_i^T G_{ij}^T & C^T \\ 0 & -\gamma^2 I & B_j^T G_{ij}^T & 0 \\ G_{ij}A_i & G_{ij}B_j & P_{ij} - G_{ij} - G_{ij}^T & 0 \\ C & 0 & 0 & -I \end{bmatrix} < 0 \tag{9.41}$$

and pre-multiplying and post-multiplying $\begin{bmatrix} I & \bar{A} \end{bmatrix}$ and its transpose to (9.41) will yield (ii), where

$$\bar{A} = \begin{bmatrix} A_i & B_j \\ C & D \end{bmatrix}$$

Lemma 9.13. *[149] For a given scalar $\gamma > 0$ and a system as follows:*

$$P : \begin{cases} x(k+1) = A_{\theta_k} x(k) + B_{\theta_k} \omega(k) \\ z(k) = Cx(k) + D\omega(k) \end{cases} \tag{9.42}$$

where $\theta_k \in \mathbb{N} \triangleq \{1, 2, \cdots, s\}$ and we define that $\pi_{ij} = Pr\{\theta_{k+1} = j | \theta_k = i\} \geq 0$ is Markovian jump probability, the following conditions are equivalent:

(i) system (9.42) is square stable and the H_∞-norm denoted as

$$\|P\|_\infty \triangleq \sup_{\theta_0 \in \mathbb{N}_1, \phi_0 \in \mathbb{N}_2} \sup_{0 \neq \omega \in l_2} \frac{\|z\|_2}{\|\omega\|_2} \tag{9.43}$$

satisfies $\|P\|_\infty < \gamma$.

(ii) there exist matrices $P_i > 0$ that satisfy

$$\begin{bmatrix} A_i & B_i \\ C & D \end{bmatrix}^T \begin{bmatrix} \bar{P}_i & 0 \\ 0 & I \end{bmatrix} \begin{bmatrix} A_i & B_i \\ C & D \end{bmatrix} - \begin{bmatrix} P_i & 0 \\ 0 & \gamma^2 I \end{bmatrix} < 0 \tag{9.44}$$

where $\bar{P}_i = \sum_{j=1}^s \pi_{ij} P_j$ and $i = \theta_k \in \mathbb{N}$

(iii) there exist matrices $P_i > 0$ and G_i that satisfy

$$\begin{bmatrix} G_i A_i & G_i B_i \\ C & D \end{bmatrix}^T \begin{bmatrix} G_i + G_i^T - \bar{P}_i & 0 \\ 0 & I \end{bmatrix}^{-1} \begin{bmatrix} G_i A_i & G_i B_i \\ C & D \end{bmatrix} - \begin{bmatrix} P_i & 0 \\ 0 & \gamma^2 I \end{bmatrix} < 0 \tag{9.45}$$

where $\bar{P}_i = \sum_{j=1}^s \pi_{ij} P_j$ and $i = \theta_k \in \mathbb{N}$

Based on Lemma 9.12 and Lemma 9.13, two theorems can be obtained easily to design the FDF gain as follows:

Theorem 9.14. *For given scalar $\gamma > 0$, if there exist matrices $P_{ij} = P_{ij}^T > 0$, G_{ij} and Y_{ij}, $\forall i \in \mathbb{N}, j \in \mathbb{N}_f$ such that*

$$\begin{bmatrix} -P_{hg} & 0 & A_i^T G_{ij}^T - C^T Y_{ij}^T & C^T L^T \\ 0 & -\gamma^2 I & B_{aj}^T G_{ij}^T & 0 \\ G_{ij} A_i - Y_{ij} C & G_{ij} B_{aj} & P_{ij} - G_{ij} - G_{ij}^T & 0 \\ LC & 0 & 0 & -I \end{bmatrix} < 0 \tag{9.46}$$

where $K_{ij} = G_{ij}^{-1} Y_{ij}$, then system (9.19) with arbitrary packet-loss process (9.4) is asymptotically stable and ensures the constraint C1.

Proof. If there exist matrices $P_{ij} = P_{ij}^T > 0$, G_{ij} and $Y_{ij} = G_{ij} K_{ij}$ such that LMI (9.46) holds, we obtain

$$\begin{bmatrix} -P_{hg} & 0 & \bar{A}_i^T G_{ij}^T & \bar{C}^T \\ 0 & -\gamma^2 I & \bar{B}_j^T G_{ij}^T & 0 \\ G_{ij} \bar{A}_i & G_{ij} \bar{B}_j & P_{ij} - G_{ij} - G_{ij}^T & 0 \\ \bar{C} & 0 & 0 & -I \end{bmatrix} < 0 \tag{9.47}$$

where $\bar{A}_i = A_i - K_{ij} C$, $\bar{B}_j = B_{aj}$ and $\bar{C} = LC$. By Schur complement, we obtain that (9.47) implies (9.32). Hence, the FDF gain $K_{ij} = G_{ij}^{-1} Y_{ij}$ ensures system (9.19) asymptotically stable and the constraint C1.

Theorem 9.15. *For given scalar $\gamma > 0$, if there exist matrices $P_i = P_i^T > 0$, G_i and Y_i, $\forall i \in \mathbb{N}, j \in \mathbb{N}_f$ such that*

$$\begin{bmatrix} -P_j & 0 & A_i^T G_i^T - C^T Y_i^T & C^T L^T \\ 0 & -\gamma^2 I & B_{mi}^T G_i^T & 0 \\ G_i A_i - Y_i C & G_i B_{mi}^T & \bar{P}_i - G_i - G_i^T & 0 \\ LC & 0 & 0 & -I \end{bmatrix} < 0 \tag{9.48}$$

where $\bar{P}_i = \sum_{j=1}^{s} \pi_{ij} P_j$ and $K_i = G_i^{-1} Y_i$, then system (9.20) with Markovian packet-loss process (9.4) is square stable and ensures the constraint C2.

Proof. If there exist matrices $P_i = P_i^T > 0$, G_i and $Y_i = G_i K_i$ such that LMI (9.48) holds, we obtain

$$\begin{bmatrix} -P_i & 0 & \bar{A}_i^T G_i^T & \bar{C}^T \\ 0 & -\gamma^2 I & \bar{B}^T G_i^T & 0 \\ G_i \bar{A}_i & G_i \bar{B} & \bar{P}_i - G_i - G_i^T & 0 \\ \bar{C} & 0 & 0 & -I \end{bmatrix} < 0 \tag{9.49}$$

where $\bar{A}_i = A_i - K_i C$, $\bar{B} = B_{mi}$, $\bar{C} = LC$ and $\bar{P}_i = \sum_{j=1}^{s} \pi_{ij} P_j$. By Schur complement, we obtain that (9.49) implies (9.45). Hence, the FDF gain $K_{ij} = G_{ij}^{-1} Y_{ij}$ ensures system (9.20) asymptotically stable and the constraint C2.

Remark 9.16. In Theorem 9.14, we can substitute a positive matrix P, a symmetric matrix G and a matrix Y for the positive matrices P_{ij}, symmetric matrices G_{ij} and matrices Y_{ij}, respectively, then a conservative FDF gain is given by $K = G^{-1} Y$. Same result can be obtained in Theorem 9.15.

9.3.3 Sensitivity Constraint of FDF

First, we look at the minimum (i.e., worst-case) fault sensitivity requirement:

$$\|P_a\|_-(\|P_m\|_-) := \inf_{N_i \in \mathbb{N}} \frac{\|\bar{f}\|_2}{\|r\|_2} > \beta, \tag{9.50}$$

similarly, we have the following two lemmas from Lemma 9.12:

Lemma 9.17. *For a given scalar $\beta > 0$ and an asymptotically stable system as follows:*

$$P : \begin{cases} x(k+1) = A_{\theta_k} x(k) + B_{\theta_k} f(k) \\ z(k) = Cx(k) + Df(k) \end{cases} \tag{9.51}$$

where $\theta_k \in \mathbb{N} \triangleq \{1, 2, \cdots, s\}$, the following conditions are equivalent:

(i) the H_--index of system (9.54) denoted as

$$\|P\|_- \triangleq \inf_{\theta_k \in \mathbb{N}} \frac{\|f\|_2}{\|z\|_2} \tag{9.52}$$

satisfies $\|P\|_- > \beta$.

(ii) there exist symmetric matrices P_i that satisfy

$$\begin{bmatrix} A_i & B_i \\ C & D \end{bmatrix}^T \begin{bmatrix} P_i & 0 \\ 0 & -I \end{bmatrix} \begin{bmatrix} A_i & B_i \\ C & D \end{bmatrix} - \begin{bmatrix} P_j & 0 \\ 0 & -\beta^2 I \end{bmatrix} < 0 \tag{9.53}$$

where $i = \theta_k \in \mathbb{N}$.

Lemma 9.18. *For a given scalar $\beta > 0$ and a square stable system as follows:*

$$P : \begin{cases} x(k+1) = A_{\theta_k} x(k) + B_{\theta_k} f(k) \\ z(k) = Cx(k) + Df(k) \end{cases} \tag{9.54}$$

where $\theta_k \in \mathbb{N} \triangleq \{1, 2, \cdots, s\}$ and we define that $\pi_{ij} = Pr\{\theta_{k+1} = j | \theta_k = i\} \geq 0$ is Markovian jump probability, the following conditions are equivalent:

(i) the H_--index of the system (9.54) denoted as

$$\|P\|_- \triangleq \inf_{\theta_k \in \mathbb{N}} \frac{\|f\|_2}{\|z\|_2} \tag{9.55}$$

satisfies $\|P\|_- > \beta$.

(ii) there exist symmetric matrices P_i that satisfy

$$\begin{bmatrix} A_i & B_i \\ C & D \end{bmatrix}^T \begin{bmatrix} \bar{P}_i & 0 \\ 0 & -I \end{bmatrix} \begin{bmatrix} A_i & B_i \\ C & D \end{bmatrix} - \begin{bmatrix} P_i & 0 \\ 0 & -\beta^2 I \end{bmatrix} < 0 \tag{9.56}$$

where $\bar{P}_i = \sum_{j=1}^{s} \pi_{ij} P_j$ and $i = \theta_k \in \mathbb{N}$.

Proof. The proofs of these Lemmas are similar to Lemma 9.12.

9.4 Fault Detection Algorithm Design

According to Chen and Patton [26], the combined constraints C1/C2 with C3 such as in the way of

$$\frac{\|G_{rf}\|_-}{\|G_{rf}\|_\infty} > \alpha_2$$

can, of course, be chosen and this combination also makes sense. However, this is not recommended. The reason are as follows. First, the problem formulation in C1/C2 has clear physical meaning. The constraints C1/C2 and C3 provide directly quantitative measures for robustness and sensitivity of a fault detection observer. The value γ is very useful for threshold selection in detection decision-making. The ratio β/γ indicates how good a designed fault detection observer is and therefore can be used for evaluation of fault detection observers. Secondly, the present problem formulation enables the direct time-domain solution of the robust fault detection observer problem by using the LMI approach. Finally, as will be shown, the robust fault detection is equivalent to a constrained H_∞ estimation problem, the latter can be further reformulated as standard problem of constrained optimization, thus we give the following algorithms:

Algorithm 9.1. *Given a scalar β, the search problem of the lowest possible value of γ and make system (9.1) with arbitrary packet-loss process (9.4) asymptotically stable can be formulated as the following convex optimization problem:*

$$\min \gamma \quad s.t. \quad LMI\ (9.46)\ (9.53) \tag{9.57}$$

which can be effectively solved by the existing Matlab LMI toolbox [54].

Algorithm 9.2. *Given a scalar β, the search problem of the lowest possible value of γ and make system (9.1) with Markovian packet-loss process (9.4) square stable can be formulated as the following convex optimization problem:*

$$\min \gamma \quad s.t. \quad LMI\ (9.48)\ (9.56) \tag{9.58}$$

which can be effectively solved by the existing Matlab LMI toolbox [54].

9.5 Numerical Example and Simulations

In this section, in order to validate the proposed method, a servo motor control system [110] that consists of a DC motor, load plate, speed, and angle sensors is considered. The model of the motor control plant at sampling period $h = 0.04s$ was identified to be

$$G(z^{-1}) = \frac{0.05409z^{-2} + 0.115z^{-3} + 0.001z^{-4}}{1 - 1.12z^{-1} - 0.213z^{-2} + 0.335z^{-3}} \tag{9.59}$$

The system can also be written as the state space form with the following system matrices

$$A = \begin{bmatrix} 1.12 & 0.213 & -0.335 \\ 1 & 0 & 0 \\ 0 & 1 & 0 \end{bmatrix}, B = \begin{bmatrix} 1 \\ 0 \\ 0 \end{bmatrix}, E_f = E_d = \begin{bmatrix} 1\ 0\ 0 \\ 0\ 1\ 0 \\ 0\ 0\ 1 \end{bmatrix}$$

$$C = \begin{bmatrix} 0.0541\ 0.1150\ 0.0001 \end{bmatrix}$$

The state feedback matrix Ku is designed to be

$$Ku = \begin{bmatrix} 0.027\ 0.575\ 0.0001 \end{bmatrix}$$

which ensures that the close-loop system is stable. A state jump fault

$$f(k) = \begin{bmatrix} 1 \\ 0 \\ 0 \end{bmatrix}$$

occurs when $k \geq 60$, and the disturbance $d(k)$ is assumed to be white noise, $d(k) \in N(0, 0.1)$. The outputs of controller $u(k)$ and the measurements from sensor $y(k)$ are transmitted to the FD center over networks with packet loss.

For arbitrary packet loss process simulation, we assume that packet loss is a random process, and let $\beta = 10$, and weighting matrix $L = 0.001[100\ 50\ 5000]$, then the optimal value of γ is $\gamma^* = 1.8177$, thus the conservative filter gain

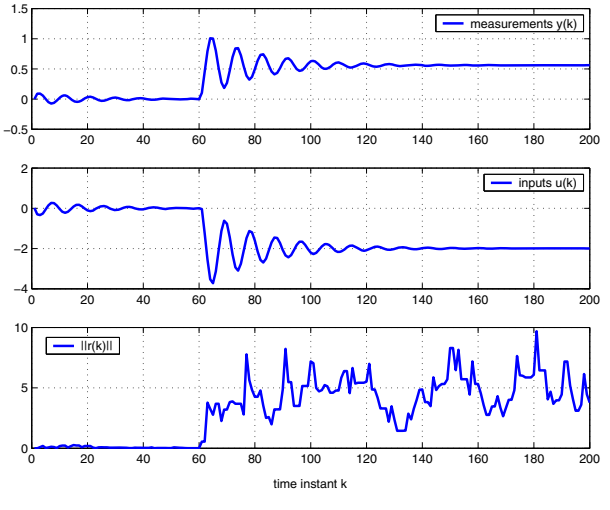

Fig. 9.3 The simulation results of proposed methods in arbitrary packet loss process situation.

is designed to be $K = [8.4400\ 8.1843\ 7.5937]^T$, Fig. 9.3 shows the results of this simulation.

For Markovian packet loss process simulation, we assume that the transition probability matrix

$$\Pi = \begin{bmatrix} 0.6 & 0.3 & 0.1 \\ 0.8 & 0.1 & 0.1 \\ 0.7 & 0.2 & 0.1 \end{bmatrix}$$

and let $\beta = 10$, then the optimal value of γ is $\gamma^* = 2.5310$, thus the filter gain is designed to be $K_1 = [7.4890\ 6.3995\ 5.6861]^T$, $K_2 = [8.0768\ 7.7909\ 6.1123]^T$, $K_2 = [0.1791\ 0.3511\ -0.0415]^T$. Fig. 9.4 shows the results of this simulation.

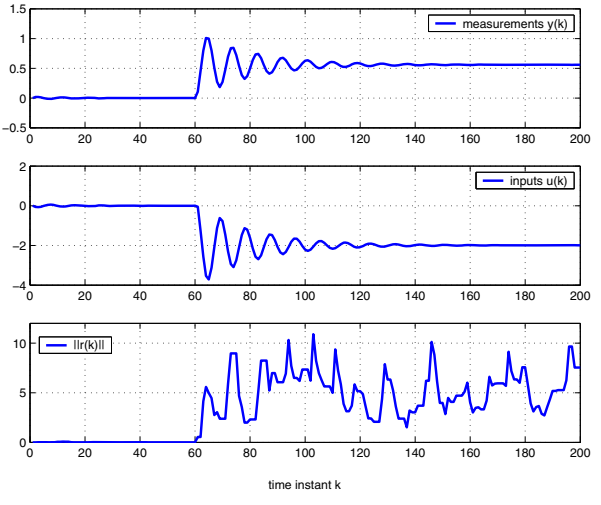

Fig. 9.4 The simulation results of proposed methods in Markovian packet loss process situation.

9.6 Summary

A problem of fault detection over unreliable networks is considered in this chapter, the missing data of actuator is treated as noise, and the fault detection filter updates at every time instant when the measurements arrive at the fault detection center successfully. The stability analysis and filter gain design method are proposed, a numerical example is also given to illustrate the proposed scheme.

Chapter 10
Fault Detection over Networks Subject to Delay and Clock Asynchronism

10.1 Introduction

The research of fault detection (FD) stems from its practical application to a variety of industries such as aerospace, energy systems, and process control to name a few. The main function of a FD scheme is to detect a fault when it happens, which may then be acted on by sending alarm signals, taking protection measures, or reconfiguring a running control scheme [135] [176]. The observer based FD scheme is currently receiving much attention [227], Generally speaking, an observer based FD system consists of an observer based residual generator and a residual evaluator. It is the state of the art that problems related to the observer based FD system design are mainly addressed in the context of improving system robustness against unknown disturbances and simultaneously enhancing system sensitivity to faults. Study on solving such problems builds the recent research which focus on designing observer based FD systems [69], [82].

Networked control system (NCS) has many advantages over a traditional point-to-point control system includes low cost of installation, ease of maintenance, low cost and greater flexibility. For these reasons the networked control architecture has been already used many applications, particularly where weight and volume are of consideration, for example in automobiles and aircraft [198], [110], [108]. However, there are many fundamental questions regarding stable operation of an interconnected hard real-time system, such as signal coding and control information flow, peer-to-peer networking, effects of the network on the performance of the system, etc. Different control methods for NCS have been reported (see, for example, [232], [80], [186]). The network-induced time delay and data packet dropout cannot be ignored in fault detection and isolation [231]. There are some important achievements in the fault detection and isolation (FDI) for NCS (see, for example, [192], [59], [68]). The theory and practice of fault diagnosis and fault-tolerant control for NCS are different from the ones for traditional control systems in many aspects. For example, it is apparent that networked-induced delay,

Y. Xia, M. Fu, and G.-P. Liu: Analysis and Synthesis of NCSs, LNCIS 409, pp. 159–181.
springerlink.com

packet dropout and other characteristics of networks could influence the performance of a fault diagnosis system designed without taking them into account [44]. With some assumptions, the NCS was modeled as a simplified delay system, then many existing methods, such as state observer, filtering algorithm, etc., developed originally for ordinary time-delay systems could be used for or extended to fault diagnosis of NCS. Further, new algorithms dedicated to NCS have been presented based on these models.

In control systems, faults are defined as a kind of latent disordered dynamics, which may occur at any part of control systems. Usually, sensor and actuator faults as a sudden offset or drift can all be modeled as additive changes in state (for example, see [36], [22]) or as unknown nonlinear functions (for example, see [184, 234, 93]). In addition, disturbances are traditionally modeled as additive state changes. In the current chapter, we model faults as abrupt changes in system states with unknown occurrence time and jump magnitude. Hence, the fault detection problem in this chapter becomes estimation of the changes. Maximum likelihood (ML) estimation is a powerful tool for estimating the unknown parameters by maximizing the likelihood of given measurements. However, it is more popular to use the ratio of likelihoods under different hypotheses to estimate the unknown parameter [63]. As for estimating the occurrence time and magnitude of an unknown abrupt state change for linear systems, Willsky and Jones [196] proposed the generalized likelihood ratio test algorithm in time domain. In their method, a Kalman filter is applied to estimate the states under the hypothesis that there is no any state change occur, meanwhile the innovations of the Kalman filter are refiltered under the hypothesis that a change occurs at the hypothetical time instant with unknown magnitude to obtain the estimate of magnitude, then the estimate of occurrence time is solved by maximizing the likelihood ratio.

This chapter proposes a fault detection and compensation scheme based likelihood ratios for networked predictive control systems with random time delay and clock asynchronism. A predictive control scheme based on state observer is designed to compensate the network time delay. Two schemes are proposed to update the fault estimation. One of them is conservative and it need a buffer to keep the data packet's sequence. The other one is without buffer, and the observer processes the packets in sequence, and it discard others. Hence, the likelihood ratios of fault are computed, and if a fault is detected and identified, the estimate of the fault is sent to the controller to compensate the fault. A numerical simulation is also given to validate the proposed method.

10.2 Networked Predictive Control for Systems with Network Delay

This chapter considers the case where the controller at the local node is far away from the plant and the manipulated variables and measured outputs of

plant are transmitted through networks with random time delay and clock asynchronism. The network delay in the feedback channel and forward channel is bounded. The plant studied in this chapter is described by

$$x(k+1) = A(k)x(k) + B(k)u(k) + v(k) + \sigma_{k-k'}\nu \tag{10.1}$$

$$y(k) = C(k)x(k) + e(k) \tag{10.2}$$

where $x \in R^n$, $y \in R^l$ and $u \in R^m$ represent the state variables, measured outputs and manipulated inputs, respectively. The additive fault $\nu \in R^n$ enters at time k' as a step jump, where σ_k denotes the unit step function. $v(k)$ and $e(k)$ are noises. Here $v(k)$, $e(k)$ and $x(0)$ are assumed to be independent Gaussian variables:

$$v(k) \in N(0, Q(k)),\ e(k) \in N(0, R(k)),\ x(0) \in N(0, \Pi(0)) \tag{10.3}$$

Furthermore, they are assumed to be mutually independent. For the simplicity of stability analysis, it is assumed that the reference input of the system is zero. Also, the following assumptions are made.

Assumption 10.1. *The pair $(A(k), B(k))$ is completely controllable, and the pair $(A(k), C(k))$ is completely observable.*

Assumption 10.2. *The sum of the upper bound of the network delay in the forward channel and the feedback channel is not greater than N_1, where N_1 is a positive integer.*

Assumption 10.3. *A buffer is set at the local node with length of N_2, which is to gather the measured outputs transmitted from the sensors, where N_2 is the upper bound of the network delay in the feedback channel. Note that if GLR with intermittent observation (proposed in Section 10.5) is applied, this buffer is not needed.*

Assumption 10.4. *Clock asynchronism exists between the local clock and the remote clock.*

In the rest part of this section, we present a predictive control scheme considering the clock asynchronism and random time delay. Liu et al proposed a predictive control method to compensate for the network-induced time delay [107] [108], but their method is not suitable for the system in this chapter since there is clock asynchronism exists.

First, we explain why the predictive control method proposed by Liu et al [107] [108] can not be applied in the current chapter. The predictive controller gives predictive control signals based on the measurements and the controlled plants model. Assume that at time instant k the clock of the controller (at the local node) reads k', there is a constant shift, denoted by δ, exists between k and k', i.e., $k' + \delta = k$, and the shift $\delta = \pm 1, \pm 2, \cdots$ is unknown and can not be obtained easily since the time delay between the local node and the remote node is random. There are two cases needed to be considered: $\delta > 0$

and $\delta < 0$. First, if $\delta > 0$, then the local node receives the measured outputs with time stamp k at time instant $k + \Delta_b$, but the clock at local node reads $k + \Delta_b - \delta$, where Δ_b denotes the time delay in the feedback channel of this transmission. As for the case $\Delta_b \geq \delta$, the controller treats the delay as $\Delta_b - \delta$, which is shorter than its real value. Thus the controller gives the predictive control signals not based on k, but k', i.e., $u_{k'+i|k'}$, $i = 0, 1, \cdots$. This set of control signal does not guarantee that the controlled plant is stabilized. On the other hand, if $\Delta_b < \delta$, then a serious logical error occurs since the controller receives the measured outputs before it is transmitted according to its clock. As for another case that $\delta < 0$, the analysis is very similar. In summary, the existence of clock asynchronism may incur some drawback even serious error in predictive control systems.

Due to the latent asynchronism between the local clock and the remote clock and the existence of random delay in the feedback channel, we present a scheme that the controller and observer generate the estimates and predictive manipulated variables based on the remote clock time, namely, all the time information subscripts in this chapter denote the time shown by remote clock, thus the asynchronism can be ignored. See Fig. 10.1, a data packet with time stamp k is transmitted to the local node at time instant k (remote node clock time), and it arrives at the local node at time instant $k + \Delta_b$ (remote node clock time). Then the controller at the local node gives a set of predictive manipulated variables which is put into a forward data packet with time stamp k, and sends it to the remote node. The remote node receives the same packet at time instant $k + \Delta_b + \Delta_f$, where Δ_f is the time delay in the forward channel. According to the assumptions, we have $\Delta_b + \Delta_f \leq N_1$, the time delay compensator at the remote node chooses the newest $\hat{u}_{k+\Delta_b+\Delta_f|h}$, where h is anyone available, as the input of the plant, thus the time asynchronism is canceled.

Based on the scheme and analysis above, the networked control system considered in the current chapter is equal to a system, in which the data packets are transmitted from the remote node to local node without any time delay, and the data packets are transmitted from the local node to the remote node with random time delay $\Delta_b + \Delta_f$.

Since the networks time delay is random, the data packet transmitted may be out of sequence. As aforementioned Assumption 10.3, a buffer of length N_2 is set at local node and the measured outputs arrived at local node are stored in the buffer. The observer chooses the measured observations from the buffer according to the sequence in which the measured outputs are sampled by sensors. For example, after the measured output $y(k)$ is processed, the buffer deletes the same measured output, and the observer searches the next measured output $y(k + 1)$ from the buffer, if $y(k + 1)$ is not available in the buffer, then the observer holds on, and searches the same one at the next step, and if $y(k + 1)$ is available, then the observer uses it to update. This kind of application is to ensure the observations are processed by their intrinsic

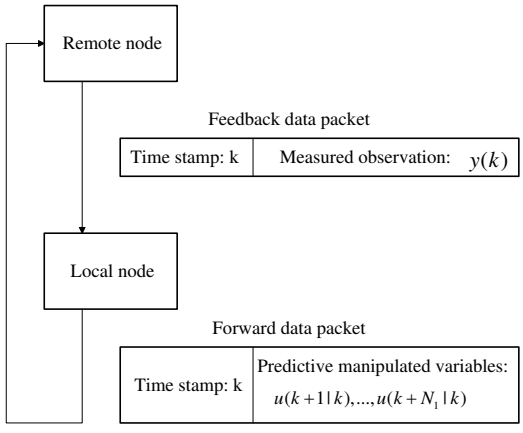

Fig. 10.1 Both feedback and forward data packets are with a same time stamp.

order. However, an alternative method does not process those observations out of sequence.

First, the state observer is designed as

$$\hat{x}(k+1|k) = A(k)\hat{x}(k|k-1) + B(k)u(ok) + L(k)\varepsilon(k) \tag{10.4}$$

where $\hat{x}(k+1|k) \in R^n$ and $u(ok) \in R^m$ are the one-step ahead state prediction and the input of the observer at time k, respectively. $\varepsilon(k) = y(k) - C(k)\hat{x}(k|k-1)$ is innovation. The matrix $L(k) = A(k)M(k) \in R^{n\times l}$ can be designed using observer design approaches.

The estimator of the state is

$$\hat{x}(k|k) = \hat{x}(k|k-1) + M(k)\varepsilon(k) \tag{10.5}$$

where $M(k)$ is filter gain, and it can be obtained by

$$S(k) = C(k)P(t|t-1)C(k)^T + R(k) \tag{10.6}$$

$$M(k) = P(k|k-1)C(k)^T S(k)^{-1} \tag{10.7}$$

$$P(k+1|k) = A(k)[P(k|k-1) - M(k)C(k)P(k|k-1)]A(k)^T + Q(k) \tag{10.8}$$

where $P(k+1|k)$ is covariance of estimate before the measurement $y(k+1)$ is processed, and (10.5)-(10.8) is obtained easily from the famous Kalman filter equations.

Following the state observer described by (10.4), based on the output data up to k, the state predictions from time $k+1$ to $k+N_1$ are constructed as

$$\begin{aligned}
\hat{x}(t+1|t) &= A(k)\hat{x}(k|k-1) + B(k)u(ok) + L(k)(y(k) - C(k)\hat{x}(k|k-1)) \\
\hat{x}(k+2|k) &= A(k+1)\hat{x}(k+1|k) + B(k+1)\hat{u}(k+1|k) \\
&\vdots \\
\hat{x}(k+N_1|k) &= A(k+N_1-1)\hat{x}(k+N_1-1|k) \\
&\quad + B(k+N_1-1)\hat{u}(k+N_1-1|k)
\end{aligned} \tag{10.9}$$

The gain of feedback controller, K_k, can be designed based on the modern control theory in the case of no delay, for example, Linear Quadratic Gaussian (LQG), eigenstructure or pole assignment, H_2 and H_∞ in the presence of disturbance, etc. The predictive manipulated variables are calculated by

$$\hat{u}(k+i|k) = K(k+i)\hat{x}(k+i|k), i = 0, 1, ..., N_1 \tag{10.10}$$

and it follows from equation (10.9) that

$$\hat{u}(k+i|k) = K(k+i) \prod_{h=k}^{k+i-1} (A(h) + B(h)K(h))\hat{x}(k|k), \quad i = 1, 2, ..., N_1 \tag{10.11}$$

At every step, the controller sends a set of predictive manipulated variables in a data packet:

$$\{\hat{u}(k+i|k) \mid i = 0, 1, ..., N_1\}$$

while at the remote node, a compensator is designed to choose a predictive manipulated variables to plant as the actual manipulated input from it's receiving buffer:

$$u(k) = \hat{u}(k|k-i) \tag{10.12}$$

where

$$i = \min\{i \mid \hat{u}(k|k-i) \text{ has arrived at the remote node buffer.}\}$$

From the above, it is shown that in the case of no network delay in the communication channel, the input to the plant actuator is the output of the controller. In the case of a delay iT, where T is the sampling period, the control input to the actuator is the ith-step ahead control prediction received in the current sampling period.

10.3 Stability Analysis of Closed-Loop Systems

In the fault free and disturbance free case, namely, $v(k) = 0$ and $\nu = 0$, the stability of closed-loop system will be proved in this section. Use predicted value as the control input to actuator:

$$u(k) = K(k)\hat{x}(k|k-i) \tag{10.13}$$

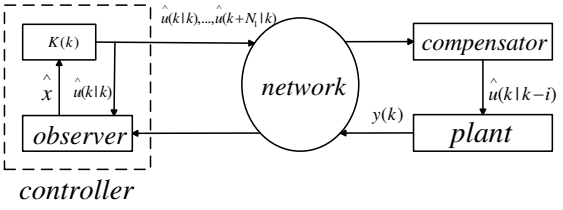

Fig. 10.2 Structure of proposed control method for networked predictive control systems.

while the control input to the observer is

$$u(ok) = \hat{u}(k|k) = K(k)\hat{x}(k|k) \tag{10.14}$$

where $K(k) \in R^{m\times n}$ is the state feedback control matrix to be determined using modern control theory. Fig. 10.2 shows the structure of proposed control method for networked predictive control systems.

Remark 10.1. In some research works, the actual inputs $u(k)$ of plant are assumed to be sent back to the local node without time delay, thus the actual inputs and outputs of plant are available for observer. However, this scheme can not be easily applied in practice, so it is assumed in this chapter that the actual inputs $u(k)$ of plant can not be sent back to the local node, and are also not available for observer.

Thus, it follows from equation (10.4)? that

$$\hat{x}(k+i|k) = \prod_{h=k+1}^{k+i} (A(h) + B(h)K(h))\hat{x}(k+1|k) \tag{10.15}$$

Based on equations (10.1), (10.2) and (10.4), it can be shown that

$$\begin{aligned}
&\hat{x}(k+i|k)\\
&= \prod_{h=k+1}^{k+i} (A(h) + B(h)K(h)) \left(B(k)K(k)M(k)C(k) + L(k)C(k)\right) x(k)\\
&\quad + \prod_{h=k+1}^{k+i} (A(h) + B(h)K(h))\\
&\quad \times (A(k) + B(k)K(k) - L(k)C(k) - B(k)K(k)M(k)C(k))\\
&\quad \times \hat{x}(k|k-1)
\end{aligned} \tag{10.16}$$

and

$$\begin{aligned}
&\hat{u}(k+i|k)\\
&= K(k+i)\prod_{h=k+1}^{k+i}(A(h)+B(h)K(h))(B(k)K(k)M(k)C(k)+L(k)C(k))x(k)\\
&\quad +K(k+i)\prod_{h=k+1}^{k+i}(A(h)+B(h)K(h))\\
&\quad \times(A(k)+B(k)K(k)-L(k)C(k)-B(k)K(k)M(k)C(k))\\
&\quad \times\hat{x}(k|k-1)
\end{aligned} \tag{10.17}$$

Theorem 10.2. *For the networked predictive control systems with random network delay, the closed-loop system described by (10.4), (10.11) and (10.12) is stable if there exists a positive definite matrix* $P \in R^{(2N_1+2)n\times(2N_1+2)n}$ *such that*

$$\overline{A}^T(i)P\overline{A}(i)-P<0 \tag{10.18}$$

for $i=0,1,2,\cdots,N_1$, where

$$\overline{A}(i)=\begin{bmatrix}
A & 0\cdots & M_1(i) & 0\cdots & 0 & 0 & 0 & \cdots & M_2(i) & 0 & \cdots & 0 & 0\\
I & 0\cdots & 0 & 0\cdots & 0 & 0 & 0 & \cdots & 0 & 0 & \cdots & 0 & 0\\
\vdots & \vdots\cdots & \vdots & \vdots\cdots & \vdots & \vdots & \cdots & \vdots & \vdots & \cdots & \vdots & \vdots & \\
0 & 0\cdots & I & 0\cdots & 0 & 0 & 0 & \cdots & 0 & 0 & \cdots & 0 & 0\\
0 & 0\cdots & 0 & I\cdots & 0 & 0 & 0 & \cdots & 0 & 0 & \cdots & 0 & 0\\
\vdots & \vdots\cdots & \vdots & \vdots\cdots & \vdots & \vdots & \cdots & \vdots & \vdots & \cdots & \vdots & \vdots & \\
0 & 0\cdots & 0 & 0\cdots & I & 0 & 0 & \cdots & 0 & 0 & \cdots & 0 & 0\\
M_3(i) & 0\cdots & 0 & 0\cdots & 0 & 0 & M_4(i) & \cdots & 0 & 0 & \cdots & 0 & 0\\
0 & 0\cdots & 0 & 0\cdots & 0 & 0 & I & \cdots & 0 & 0 & \cdots & 0 & 0\\
\vdots & \vdots\cdots & \vdots & \vdots\cdots & \vdots & \vdots & \vdots & \cdots & \vdots & \vdots & \cdots & \vdots & \vdots\\
0 & 0\cdots & 0 & 0\cdots & 0 & 0 & 0 & \cdots & I & 0 & \cdots & 0 & 0\\
0 & 0\cdots & 0 & 0\cdots & 0 & 0 & 0 & \cdots & 0 & I & \cdots & 0 & 0\\
\vdots & \vdots\cdots & \vdots & \vdots\vdots & \cdots & \vdots & \vdots & \cdots & \vdots & \vdots & \cdots & \vdots & \vdots\\
0 & 0\cdots & 0 & 0\cdots & 0 & 0 & 0 & \cdots & 0 & 0 & \cdots & I & 0
\end{bmatrix} \tag{10.19}$$

with $i\in\{1,2,\cdots,N_1\}$, $A(i)\in R^{2(N_1+1)n\times 2(N_1+1)n}$,

$$\begin{aligned}
M_1(i) &= B(k)K(k)\prod_{h=k-i+1}^{k}(A(h)+B(h)K(h))\\
&\quad\times(B(k-i)K(k-i)M(k-i)C(k-i)+L(k-i)C(k-i))
\end{aligned}$$

$$
\begin{aligned}
M_2(i) &= B(k)K(k)\prod_{h=k-i+1}^{k}(A(h)+B(h)K(h)) \\
&\quad\times(A(k-i)+B(t-i)K(t-i)-L(t-i)C(t-i) \\
&\quad-B(t-i)K(t-i)M(t-i)C(t-i)) \\
M_3(i) &= B(k)K(k)M(k)C(k)+L(k)C(k) \\
M_4(i) &= A(k)+B(k)K(k)-L(k)C(k)-B(k)K(k)M(k)C(k)
\end{aligned}
$$

$$
\overline{A}(0)=\begin{bmatrix}
M_1(0) & 0\cdots 0 & 0\cdots 0 & 0 & M_2(0) & \cdots 0 & 0 & \cdots 0 & 0 \\
I & 0\cdots 0 & 0\cdots 0 & 0 & 0 & \cdots 0 & 0 & \cdots 0 & 0 \\
\vdots & \vdots\cdots\vdots & \vdots\cdots\vdots & \vdots & \cdots & \vdots & \vdots\cdots & \vdots & \vdots \\
0 & 0\cdots I & 0\cdots 0 & 0 & 0 & \cdots 0 & 0 & \cdots 0 & 0 \\
0 & 0\cdots 0 & I\cdots 0 & 0 & 0 & \cdots 0 & 0 & \cdots 0 & 0 \\
\vdots & \vdots\cdots\vdots & \vdots\cdots\vdots & \vdots & \cdots & \vdots & \vdots\cdots & \vdots & \vdots \\
0 & 0\cdots 0 & 0\cdots I & 0 & 0 & \cdots 0 & 0 & \cdots 0 & 0 \\
M_3(0) & 0\cdots 0 & 0\cdots 0 & 0 & M_4(0) & \cdots 0 & 0 & \cdots 0 & 0 \\
0 & 0\cdots 0 & 0\cdots 0 & 0 & I & \cdots 0 & 0 & \cdots 0 & 0 \\
\vdots & \vdots\cdots\vdots & \vdots\cdots\vdots & \vdots & \vdots & \cdots\vdots & \vdots & \cdots\vdots & \vdots \\
0 & 0\cdots 0 & 0\cdots 0 & 0 & 0 & \cdots I & 0 & \cdots 0 & 0 \\
0 & 0\cdots 0 & 0\cdots 0 & 0 & 0 & \cdots 0 & I & \cdots 0 & 0 \\
\vdots & \vdots\cdots\vdots & \vdots\cdots\vdots & \vdots & \cdots\vdots & \vdots & \cdots\vdots & \cdots\vdots & \vdots \\
0 & 0\cdots 0 & 0\cdots 0 & 0 & 0 & \cdots 0 & 0 & \cdots I & 0
\end{bmatrix} \tag{10.20}
$$

$$
\begin{aligned}
M_1(0) &= A(k)+B(k)K(k)M(k)C(k) \\
M_2(0) &= B(k)K(k)-B(k)K(k)M(k)C(k) \\
M_3(0) &= B(k)K(k)M(k)C(k)+L(k)C(k) \\
M_4(0) &= A(k)+B(k)K(k)-L(k)C(k)-B(k)K(k)M(k)C(k)
\end{aligned}
$$

Proof. Since the control input to the actuator of the plant is $u(k) = K(k)\hat{x}(k|k-i)$, then, based on (10.17), the closed-loop system can be written as

$$
\begin{aligned}
x(k+1) &= A(k)x(k)+B(k)u(k) \\
&= A(k)x(k)+B(k)\hat{u}(k|k-i) \\
&= A(k)x(k)+M_1(i)x(k-i) \\
&\quad+M_2(i)\hat{x}(k-i|k-i-1)
\end{aligned} \tag{10.21}
$$

Since the control input to the observer is $u(ok) = u(k|k) = K\hat{x}(k|k)$, then, based on (10.4), the state observer has the following form

$$\begin{aligned}\hat{x}(k+1|k) &= A(k)\hat{x}(k|k-1) + B(k)u(k|k) \\ &\quad + L(k)(C(k)x(k) - C_t\hat{x}(k|k-1)) \\ &= (A(k) - L(k)C(k))\hat{x}(k|k-1) + L(k)C(k)x(k) \\ &\quad + B(k)K(k)(\hat{x}(k|k-1) + M_t(y(k) - C(k)\hat{x}(k|k-1))) \\ &= M_4(i)\hat{x}(k|k-1) + M_3(i)x(k)\end{aligned} \tag{10.22}$$

Let

$$\begin{aligned}\overline{x}^T(k) = [&x^T(k)\ x^T(k-1)\ \cdots\ x^T(k-i)\ x^T(k-(i+1))\ \cdots \\ &\cdots\ x^T(k-N)\ \ \hat{x}^T(k|k-1)\ \hat{x}^T(k-1|k-2)\cdots \\ &\cdots\ \hat{x}^T(k-i|k-i-1)\ \cdots\ \hat{x}^T(k-N|k-N-1)]\end{aligned} \tag{10.23}$$

then, the augmented system can be expressed as

$$\overline{x}(k+1) = \overline{A}(i)\overline{x}(k)$$

When $i = 0$, based on (10.16), the augmented system can be expressed as

$$\bar{x}(t+1) = \overline{A}(0)\overline{x}(k) \tag{10.24}$$

It follows that the closed-loop system is a switched system which is composed of $N_1 + 1$ discrete-time subsystems, i.e.,

$$\overline{x}(k+1) = \overline{A}(i)\overline{x}(k) \tag{10.25}$$

where $i = 0, 1, \cdots, N_1$. The switched system can be described as

$$\overline{x}(t+1) = \overline{A}_{\delta(k)}\overline{x}(k) \tag{10.26}$$

where $\delta(k) : \{0, 1, \cdots\} \to \{0, 1, 2, \cdots, N_1\}$, $\delta(k)$ is switching signal.

Let $V(k) = \overline{x}^T(k)P\overline{x}(k)$, then

$$\begin{aligned}V(k+1) - V(k) &= \overline{x}^T(k+1)P\overline{x}(k+1) - \overline{x}^T(k)P\overline{x}(k) \\ &= \overline{x}^T(k)[\overline{A}_{\delta(k)}^T P\overline{A}_{\delta(k)} - P]\overline{x}^T(k)\end{aligned} \tag{10.27}$$

From (10.18), it follows that $V(k+1) - V(k) < 0$, for $\delta(k)$. Therefore, system (10.26) is stable for all switching sequences $\delta(k)$.

10.4 Fault Detection and Identification Based on Likelihood Ratios

The likelihood ratios (LR) test is a multiple hypotheses test, where the different fault hypotheses are compared to the no fault hypotheses pairwise. In the LR test, the fault magnitude is assumed to be known. The hypotheses under consideration are

H_0: no fault
$H_1(k', \nu)$: a fault of magnitude ν at time k'.

The log likelihood ratio for the hypotheses as the test statistic:

$$l_N(k', \nu) := 2log\frac{p(y^N|H_1(k', \nu))}{p(y^N|H_0)} = 2log\frac{p(y^N|k', \nu)}{p(y^N|k' = N)} \tag{10.28}$$

where the factor 2 is for notational convenience, and y^N denotes the set of measurements $y(1), y(2), ..., y(N)$. In this chapter, we use the convention that $H_1(N, \nu) = H_0$, so again, $k' = N$ means no fault. Then the LR estimate can be expressed as

$$\hat{k'}^{ML} = \arg\max_{k'} l_N(k', \nu) \tag{10.29}$$

when fault magnitude ν is known. However, the fault magnitude ν is assumed to be unknown in this chapter, so a double maximization over k' and ν called Generalized Likelihood Ratio (GLR) proposed by Willsky and Jones [196] is given to estimate the fault:

$$\hat{\nu}(k') = \arg\max_{\nu} 2log\frac{p(y^N|k', \nu)}{p(y^N|k' = N)} \tag{10.30}$$

$$\hat{k'} = \arg\max_{k'} 2log\frac{p(y^N|k', \hat{\nu}(k'))}{p(y^N|k' = N)} \tag{10.31}$$

where $\hat{\nu}(k')$ is the maximum likelihood estimate of ν, given a fault at time k'. The fault candidate $\hat{k'}$ in the GLR test is accepted if

$$l_N(\hat{k'}, \hat{\nu}(\hat{k'})) > h,$$

where the threshold h is a parameter to be tuned. The key point of GLR test is that the innovation from the state observer can be expressed as a linear regression in ν,

$$\varepsilon_{k'}(k) = \varphi_{k'}^T(k)\nu + \varepsilon(k) \tag{10.32}$$

where $\varepsilon_{k'}(k)$ is the actual innovation from the state observer if ν and k' are known, $\varepsilon(k)$ is the virtual innovation of system (10.1) without additive fault. Before the fault occurs, the actual innovation is equal to the virtual innovation:

$$\varepsilon_{k'}(k) = \varepsilon(k)$$

and the innovations get a bias,

$$\varepsilon(k) \in N(0, S(k))$$

that means

$$\varphi_{k'}(k) = 0, \ k' = 0, 1, ..., k$$

However, given a fault ν at time k', the innovations get a bias,

$$\varepsilon_{k'}(k) \in N(\varphi_{k'}(k)\nu, S(k)),$$

and the regressors $\varphi_{k'}(k)$ can be computed using

$$\varphi_{k'}^T(k) = C(k)\left[\prod_{i=k}^{t-1} A(h) - A(k-1)\mu_{k'}(k)\right] \tag{10.33}$$

$$\mu_{k'}^T(k+1) = A(k)\mu_{k'}(k) + M(k+1)\varphi_{k'}^T(k), \tag{10.34}$$

initialized by zeros at time $k = k'$. Here $\varphi(k) \in R^n$ and $\mu(k) \in R^{n\times n}$.

At the time $k' = N$, the test statistic is given by

$$l_N(k', \hat{\nu}(k')) = f_{k'}^T(N) R_{k'}^{-1}(N) f_{k'}(N) \tag{10.35}$$

where the linear regression quantities are

$$R_{k'}(k) = \sum_{i=1}^{k} \varphi_{k'}(i) S(i)^{-1} \varphi_{k'}^T(i) \tag{10.36}$$

$$f_{k'}(k) = \sum_{i=1}^{k} \varphi_{k'}(i) S(i)^{-1} \varepsilon(i) \tag{10.37}$$

for each k', $1 \le k' \le k$. A change candidate is given by

$$\hat{k'} = \arg\max l_N(k', \hat{\nu}(k'))$$

It is accepted if $l_N(k', \hat{\nu}(k'))$ is greater than some threshold h (otherwise $\hat{k'} = N$) and the corresponding estimate of the change magnitude is given by

$$\hat{\nu}_N(\hat{k'}) = R_{\hat{k'}}^{-1}(N) f_{\hat{k'}}(N).$$

The formulation (10.35) is off-line. Since the test statistic involves a matrix inversion of $R(N)$, a more efficient on-line method is as follows,

$$l_k(k', \hat{\nu}(k')) = f_{k'}^T(k) \hat{\nu}_{k'}(k)$$

where k is used as time index instead of N. $\hat{\nu}_{k'}(k)$ can be updated recursively, eliminating the matrix inversion of $R_{k'}(k)$.

However, in real applications, because of the observed signal is too large, the memories required to restore the computed data is square increasing, and computation time increases step by step, so setting a suitable data structure becomes important. In this chapter, we recommend a trade-off windowed on-line GLR method if the FDI system is with limited computation capacity:

$$l_k(k-W, \hat{\nu}(k-W)) = f_{k-W}^T(k) \hat{\nu}_{k-W}(k) \tag{10.38}$$

where W is the length of data window. Better performance of estimate can be obtained if a larger W is chosen, however, a larger W means that much time is needed for detecting a fault after it occurs. Computing $\hat{\nu}_{k-W}(k)$ recursively needs data from step $k-W$ to k, so that the computing time of every step is fixed.

From (10.32), we can know that the innovations from the state observer are the linear combinations of fault ν, so that the Recursive Least Squares (RLS) algorithm can be used to estimate the fault ν for each time k':

$$\hat{\nu}_{k'}(k) = \hat{\nu}_{k'}(k-1) + K^{\nu}(k)[\varepsilon(k) - \varphi_{k'}^{T}(k)\hat{\nu}_{k'}(k-1)] \tag{10.39}$$

$$K(k)^{\nu} = \frac{P(k-1)\varphi_{k'}(k)}{\lambda + \varphi_{k'}^{T}(k)P(k-1)\varphi_{k'}(k)} \tag{10.40}$$

$$\begin{aligned} P(k) = \frac{1}{\lambda}[P(k-1) - \frac{P(k-1)}{\varphi_{k'}(k)\varphi_{k'}^{T}(k)P(k-1)}\lambda \\ +\varphi_{k'}^{T}(k)P(k-1)\varphi_{k'}(k)] \end{aligned} \tag{10.41}$$

where the design parameter λ is called the forgetting factor.

If the windowed likelihood ratios estimate $\hat{\nu}_{k-W}(k)$ is greater than the threshold, the fault detection

$$\left(\hat{\nu}(\hat{k'}), \hat{k'}\right) = (\hat{\nu}_{k-W}(k), k-W)$$

is sent to the predictive state observer to compeansate the fault. From the time k', the predictive state observer (10.4) is modified to:

$$\hat{x}(k+1|k) = A(k)\hat{x}(k|k-1) + B(k)u(ok) + L(k)\varepsilon(k) + \hat{\nu}(\hat{k'}), \tag{10.42}$$

and the state predictive equation and predictive manipulated variables equation are modified as follows

$$\begin{aligned} \hat{x}(k+1|k) &= A(k)\hat{x}(k|k-1) + B(k)u(ok) + L(k)\varepsilon(k) + \hat{\nu}(\hat{k'}) \\ \hat{x}(k+2|k) &= A(k+1)\hat{x}(k+1|k) + B(k+1)\hat{u}(k+1|k) + \hat{\nu}(\hat{k'}) \\ &\vdots \\ \hat{x}(k+N_1|k) &= A(k+N_1-1)\hat{x}(k+N_1-1|k) \\ &\quad +B(k+N_1-1)\hat{u}(k+N_1-1|k) + \hat{\nu}(\hat{k'}) \end{aligned} \tag{10.43}$$

and the predictive manipulated variables are as follows,

$$\hat{u}(k+i|k) = K(k+i)\hat{x}(k+i|k),\ i = 0, 1, ..., N_1$$

From the above, the recursive computing equations of predictive states and predictive manipulated variables are given as follows

$$
\begin{aligned}
&\hat{x}(k+i|k) \\
&= \prod_{h=k}^{k+i-1}(A(h)+B(h)K(h))\hat{x}(k|k) + \left[\prod_{h=k+1}^{k+i-1}(A(h)+B(h)K(h))\right. \\
&\quad + \prod_{h=k+2}^{k+i-1}(A(h)+B(h)K(h)) + \ldots + \left.\prod_{h=k+i-1}^{k+i-1}(A(h)+B(h)K(h)) + I\right]\hat{\nu}(\hat{k}') \\
&= \prod_{h=k}^{k+i-1}(A(h)+B(h)K(h))\hat{x}(k|k) + \sum_{m=1}^{i-1}\left[\prod_{h=k+m}^{k+i-1}(A(h)+B(h)K(h))\right]\hat{\nu}(\hat{k}') \\
&\quad + \hat{\nu}(\hat{k}')\hat{u}(k+i|k) \\
&= K(k+i)\hat{x}(k+i|k) \qquad (10.44)
\end{aligned}
$$

Fig. 10.3 shows the structure of proposed FDI method for networked predictive control system. The likelihood ratios are computed according to (10.38)-(10.41) step by step. When the log likelihood ratio is greater than a given threshold, the estimate of the fault is sent to the controller, the state observer compensates the fault immediately.

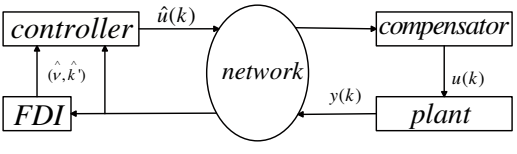

Fig. 10.3 Structure of proposed FDI method for networked predictive control system.

Remark 10.3. Note that after a fault is detected, the controller compensates the fault according to (10.44). If the fault estimate converges at its true value, the state estimates converge at their true value. However, since the existence of network time delay and the data window size W, the additive fault keeps its effect on the system state for a period of time after compensation, the states and the measured outputs converge at another stable points after fault compensation.

10.5 GLR with Intermittent Observations

In the previous section, a buffer is set at the local node to save the observation packets which are out of sequence. The observer processes the observations according to the sequence in which the remote node sends the packets. This method is easy to be applied, but with some drawbacks. First, though an observation is available for the observer, it is not processed until all the

previous observations have arrived at the local node and been processed. It costs much more time to detect a fault after it occurs. Secondly, if there is no any observation packet need to be processed at some time instants, the observer is idle. On the contrary, the computation burden is heavy at some time instants when there are many packets need to be processed. Thirdly, the additional buffer increase the hardware cost.

An alternative scheme for the local node is to process the observations without buffer. In this case, when an observation packet arrives at the local node, the observer checks the time stamp of this packet, if this time stamp is greater than every time stamp of the packets which has already arrived at the local node, the observer processes it; if the time stamp is not the newest at the present time instant, the observer discards it and treats the observation as zero. First, the state observer is designed as

$$\hat{x}(k+1|k) = A(k)\hat{x}(k|k-1) + B(k)u(ok) + \gamma(k)L(k)\varepsilon(k) \tag{10.45}$$

where $\gamma(k) = \{0,\ 1\}$ denotes whether the observation with time stamp k is processed or is discarded, which is with probability distribution $p_{\gamma(k)}(1) = \lambda$. Note that a similar description of $\gamma(k)$ is presented in much literature to denote whether the data is transmitted successfully. The meanings of these two descriptions of $\gamma(k)$ are different from each other, but same in mathematical analysis.

Now we give the convergence analysis of GLR with intermittent observations. However, the work of this section is limited to LTI (linear time-invariant) systems. First, by minimizing the following loss function,

$$V_k(\nu) = \sum_{t=1}^{k} \gamma(t) \left(\varepsilon(t) - \varphi(t)^T\nu\right)^T S(t)^{-1} \left(\varepsilon(t) - \varphi(t)^T\nu\right) \tag{10.46}$$

we have the least square estimate with intermittent observations:

$$\hat{\nu}(k) = \hat{\nu}(k-1) + \gamma(k)(R^{\varphi}(k))^{-1}\varphi(k)S(k)^{-1}\left(\varepsilon(k) - \varphi(k)^T\hat{\nu}(k-1)\right) \tag{10.47}$$

where $R^{\varphi}(k) = \sum_{t=1}^{k} \varphi(t)S(t)^{-1}\varphi(t)^T$. This is the recursive update for estimate, we also can obtain the update of $R^{\varphi}(k)$:

$$R^{\varphi}(k) = R^{\varphi}(k-1) + \gamma(k)\varphi(k)S(k)^{-1}\varphi(k)^T \tag{10.48}$$

Let $P(k)$ denotes the covariance matrix of $\hat{\nu}$, according to [63], we have $P(k) = (R^{\varphi}(k))^{-1}$. The famous matrix inversion lemma applied to (10.48) gives

$$P(k) = P(k-1) - \gamma(k)P(k-1)\varphi(k)[\varphi(k)^T P(k-1)\varphi(k) + S(k)]^{-1}\varphi(k)^T P(k-1) \tag{10.49}$$

Now, we define a function

$$g_{\lambda,k}(X) = X - \lambda X\varphi(k)(\varphi(k)^T X\varphi(k) + S(k))^{-1}\varphi(k)^T X \tag{10.50}$$

From (10.50), we have $g_{\lambda,k}(X) \leq X$, $\forall k, X$. Now, we state some properties of function (10.50) as following lemmas:

Lemma 10.4. *For a LTI system described in (10.1), where $A(k) = A$, $B(k) = B$, $C(k) = C$, $Q(k) = Q$, $R(k) = R$, $\forall k$, let $\lambda(A)$ denote the eigenvalues of matrix A, and $\bar{M}$ denotes the solution of the following equation:*

$$\bar{M} = A\bar{M}A^T - A\bar{M}C^T(C\bar{M}C^T + R)^{-1}C\bar{M}A^T + Q \tag{10.51}$$

If $|\lambda(A)| < 1$ and $|\lambda(A - \bar{M}CA)| < 1$, then the limit of regressors $\varphi_k(t)$ exists, $k = t, t+1, \cdots$, $\forall t$, which is described as follows:

$$\varphi_k^T(t) = C\left[A^{k-t} - A\mu_k(t)\right] \tag{10.52}$$

$$\mu_{k+1}(t) = A\mu_k(t) + M(k+1)\varphi_k^T(t) \tag{10.53}$$

where $M(k)$ is Kalman filter gain, and

$$\lim_{k\to\infty} \varphi_k^T(t) = (I - \bar{M}C)(I - A)^{-1}, \tag{10.54}$$

Proof. Assume that $t = 0$ without loss of generality, we have the following equation from (10.1):

$$x(k+1) = A^{k+1}x(0) + \sum_{i=1}^{k+1} A^{k+1-i}v(i) + \sum_{i=1}^{k+1} A^{k+1-i}\nu \tag{10.55}$$

and from the Kalman filter equations, we have

$$\begin{aligned}\hat{x}(k|k) = {} & (A - M(k)CA)\hat{x}(k-1|k-1) + M(k)CA^k x(k) \\ & + M(k)C\sum_{i=1}^{k} A^{k-i}v(i) + M(k)C\sum_{i=1}^{k} A^{k-i}\nu + M(k)e(k)\end{aligned}$$

the alternative Kalman filter which is assumed to have the information of the fault gives

$$\begin{aligned}\hat{x}_0(k|k) = {} & (A - M(k)CA)\hat{x}_0(k-1|k-1) + M(k)CA^t x(0) \\ & + M(k)C\sum_{i=1}^{k} A^{k-i}v(i) + M(k)C\sum_{i=1}^{k} A^{k-i}\nu \\ & + M(k)e(k) + (I - M(k)C)\sum_{i=1}^{k} A^{k-i}\nu\end{aligned}$$

thus we define that the error between these two filters is $\tilde{x}(k)$:

$$\begin{aligned}\tilde{x}(k) &= \hat{x}_0(k|k) - \hat{x}(k|k) \\ &= (A - M(k)CA)\tilde{x}(k-1) + (I - M(k)C)\sum_{i=1}^{k} A^{k-i}\nu. \quad (10.56)\end{aligned}$$

From the concept of $\varphi_k^T(t)$ and (10.56), we have

$$\lim_{k\to\infty} \varphi_0^T(k)\nu = \lim_{k\to\infty} \tilde{x}(k) \quad (10.57)$$

Since $|\lambda(A)| < 1$, the steady state Kalman filter gain $\bar{M} = \lim k \to \infty M(k)$ exists and is found by solving:

$$\bar{M} = A\bar{M}A^T - A\bar{M}C^T(C\bar{M}C^T + R)^{-1}C\bar{M}A^T + Q$$

Because $|\lambda(A - \bar{M}CA)| < 1$, the first term of the right side of (10.56) will approach to zero when $k \to \infty$. For the second term of the right side of (10.56), we need to analyze the existence of limit of the following equation:

$$\lim_{k\to\infty} \sum_{i=1}^{k} A^{k-i}.$$

Without loss of generality, we assume that all eigenvalues of A are distinct. Then we can factorize $A = T^{-1}\Lambda T$, where Λ is a diagonal matrix with diagonal elements being the eigenvalues. Then

$$\begin{aligned}\lim_{k\to\infty} \sum_{i=1}^{k} A^{k-i} &= T^{-1}\left(\lim_{k\to\infty} \sum_{i=1}^{k} \Lambda^{k-i}\right) T \\ &= T^{-1}(I + \Lambda + \Lambda^2 + \cdots + \Lambda^t + \cdots)T \\ &= T^{-1}(I - \Lambda)^{-1}T \\ &= \left(T^{-1}(I - \Lambda)T\right)^{-1} \\ &= (I - A)^{-1}\end{aligned}$$

Then, the limit of the regressor exists

$$\lim_{k\to\infty} \varphi_k^T(t) = (I - \bar{M}C)(I - A)^{-1}$$

Lemma 10.5. *[169] Consider the function*

$$g_{\lambda,k}(X) = X - \lambda X\varphi(k)(\varphi(k)^T X\varphi(k) + S(k))^{-1}\varphi(k)^T X. \quad (10.58)$$

Assume $X, S(k) \in \mathbb{S} = \{S \in \mathbb{R}^{n\times n} | S \geq 0\}$, *and* $0 < \lambda \leq 1$. *Then, the following facts are true.*

1) If $X \leq Y$, *then* $g_{\lambda,k}(X) \leq g_{\lambda,k}(Y)$.
2) If $X \geq g_{\lambda,k}(X)$, *then* $X > 0$.
3) Let $X_{k+1} = g_{\lambda,k}(X_k)$, *if* $X_1 \geq X_0$, *then* $X_{k+1} \geq X_k$, *and if* $X_1 \leq X_0$, *then* $X_{k+1} \leq X_k$.

Now, we formally state the convergence analysis of GLR with intermittent observations as the following theorem:

Theorem 10.6. *For a LTI system described in (10.1), where* $A(k) = A$, $B(k) = B$, $C(k) = C$, $Q(k) = Q$, $R(k) = R$, $\forall k$, *let* $\lambda(A)$ *denote the eigenvalues of matrix* A, *if* $|\lambda(A)| < 1$, *then the GLR estimation covariance* $P(k)$ *with intermittent observation is bounded and for any* $P(0)$ *there exists* $\bar{P} = 0$ *independent of* $P(0)$ *such that*

$$\lim_{t\to\infty} P(k) = \bar{P} \tag{10.59}$$

Proof. From (10.49), we have

$$P(0) \geq P(1) \geq \cdots \geq P(k) \geq \cdots$$

thus, for any k, $0 \leq P(k) \leq P(0)$, that means for any initial condition $P(0) > 0$, $P(k)$ is a monotonically decreasing sequence with a lower bound 0. According to *Dedekind theorem*, the sequence converges at a finite matrix. Let $\bar{P}$ denotes the limit of $P(k)$, we have

$$\bar{P} = \lim_{k\to\infty} g^k_{\lambda,k}(P(0)) = \lim_{k\to\infty} g^k_{\lambda,k}(P(k)) \tag{10.60}$$

Substituting (10.60) to (10.59) gives

$$\bar{P}\bar{\varphi}(\bar{\varphi}^T\bar{P}\bar{\varphi} + \bar{S})^{-1}\bar{\varphi}^T\bar{P} = 0$$

where $\bar{\varphi}$ and $\bar{S}$ denote the limits of $\varphi_k(t)$ and $S(k)$, respectively, for any t, when k approaches infinity. According to Lemma 10.4, $\bar{\varphi}$ exists and does not always equal to zero. Sinopoli et al proved that if A is stable, the state covariance $P(k|k)$ is convergent when k approaches infinity [169], namely, $\bar{S}$ exists and

$$\bar{S} = CA\left(\lim_{k\to\infty} P(k|k)\right)A^TC^T + C^TQC + R > 0$$

This implies that the term

$$\bar{\varphi}(\bar{\varphi}^T\bar{P}\bar{\varphi} + \bar{S})^{-1}\bar{\varphi}^T$$

does not always equal to zero, which proves that $\bar{P} = 0$.

10.6 Numerical Simulation

In this section, in order to validate the proposed method, a servo motor control system [110] that consists of a DC motor, load plate, speed, and angle sensors is considered. The model of the motor control plant at sampling period $0.04s$ is identified to be

$$G(z^{-1}) = \frac{0.05409z^{-2} + 0.115z^{-3} + 0.001z^{-4}}{1 - 1.12z^{-1} - 0.213z^{-2} + 0.335z^{-3}} \tag{10.61}$$

The system can also be written as the state space form with the following system matrices

$$A = \begin{bmatrix} 1.12 & 0.213 & -0.335 \\ 1 & 0 & 0 \\ 0 & 1 & 0 \end{bmatrix}$$

$$B = \begin{bmatrix} 1 \\ 0 \\ 0 \end{bmatrix}, C = \begin{bmatrix} 0.0541 & 0.1150 & 0.0001 \end{bmatrix}$$

The state feedback matrix K is designed to be

$$K = \begin{bmatrix} 0.027 & 0.575 & 0.0001 \end{bmatrix}$$

which ensure that the close-loop system without time delay is stable. In this simulation, the upper bound of network time delay $N_1 = 4$ and the data window size of GLR is $W = 5$, the fault occurs at time $k' = 20$ and its magnitude is $\nu = [8\ 0\ 0]^T$.

The threshold $h = 2000$, and as Fig. 10.4 shows, the fault detected is $(\hat{\nu}(\hat{k'}),\ \hat{k'}) = (7.98, 26)$. Note that if the threshold is designed to be smaller,

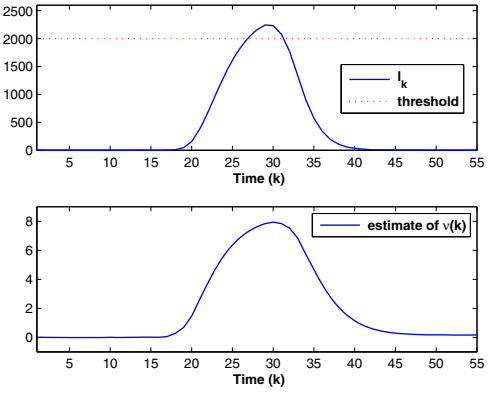

Fig. 10.4 Test statistics with fault compensation of numerical simulation in this chapter.

the $\hat{k}'$ is closer to its true value k', but the estimate of fault departure its true value, so a suitable threshold should be designed considering the trade-off between the precision of estimated k' and estimated ν. Fig. 10.5 shows the test statistics without compensation of this simulation, the log likelihood ratios do not converge at zero after the fault is detected without compensation.

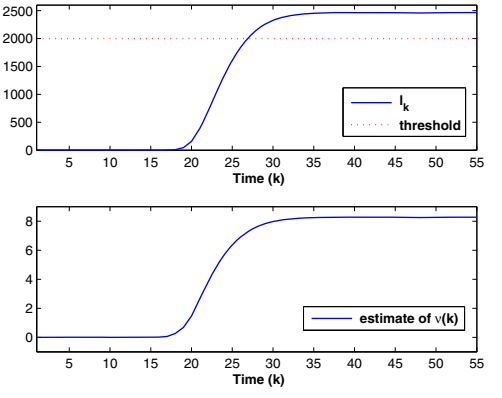

Fig. 10.5 Test statistics without fault compensation of numerical simulation in this chapter.

Fig. 10.6 shows the states and their estimates with fault compensation in this simulation, the estimates departure from their true values when the fault occurs at $k = 20$, and after the fault is detected and compensated, the estimates of states converge at their true values. Fig. 10.7 shows the actual inputs and their corresponding outputs with fault compensation.

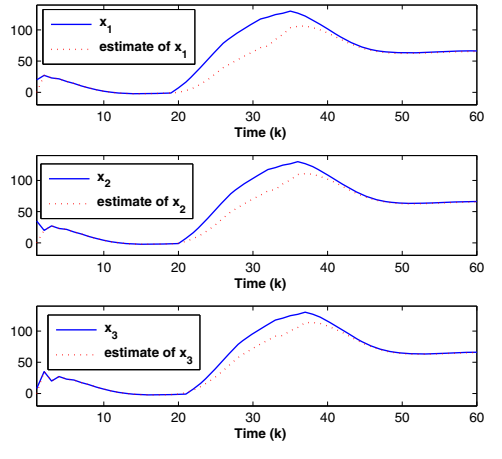

Fig. 10.6 The states and their estimates with fault compensation of this simulation.

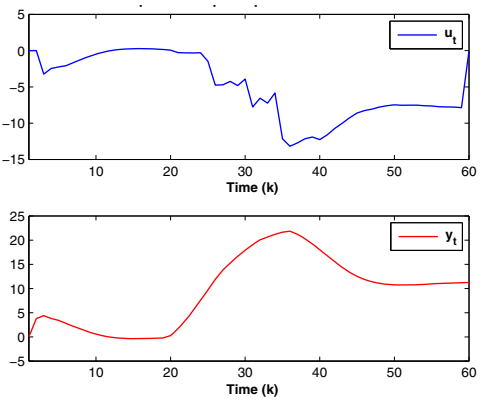

Fig. 10.7 The inputs and outputs with fault compensation of this simulation.

10.7 Discussion

Network-induced time delay is the key issue in the investigation of NCS. Generally speaking, there are two delays, sensor to controller delay (or delay in backward channel) and the controller to actuator delay (or delay in forward channel). These two delays can be combined together when the controller is linear and time-invariant. It is shown in [214], that the network-induced delay will prevent a traditional observer based fault detection system from satisfying the essential requirement of a qualified residual generator, i.e., with the delay, the residual signal of a traditional residual generator will not be able to be decoupled from the control input any longer. To solve this problem, some methods are proposed. If the network-induced time delay of an NCS is unknown and smaller than the sampling period, then the NCS with disturbance and latent fault can be described as a system without any time delay, and the affect of time delay is modeled as an unknown input item [229]. The fault diagnosis system should be robust to this term, and some schemes are developed recently. For example, traditional parity relation based low-pass post filtering residual generator for NCS with network-induced delay is proposed in [217] to reduce the influence of the unknown input item. As for the case when the delay time is greater than one sampling period, the traditional robust methods do not have good performance since the influence of the unknown input item caused by time delay is great. Huang and Nguang proposed an observer based fault detection scheme for NCSs with network-induced time delay and data packet dropout [79], wherein the lengths of delay are not limited to be smaller than sampling period, but bounded. They also treated the time delays as time-varying input delays, and developed new disturbance attenuation notation according to the H_∞ performance. There are two kinds of nuisances needed to be attenuated in the FDI systems, one is disturbance or unmodeled dynamics; the other is unknown inputs caused

by time delay. In the current chapter, the proposed predictive method faces only one nuisance, and the influence of network-induced time delay is totally compensated theoretically.

As mentioned above, predictive control is a good choice to design the FDI scheme without considering attenuating the influence of network-induced time delay, but it need the observer and controller work according to time precisely. Much literature has not paid attention to this practical problem, and its methods of predictive control have nice performance only in theory. Estimating the clock asynchronism is not easily applied in practice when the network-induce time delay is unknown and random, the proposed scheme of using the time stamps in the measurements data packets is suitable and easy to be carried out. Furthermore, it converts a NCS with time delays both in the backward channel and in the forward channel to an equivalent system with time delay in the forward channel if the controlled plant is linear. It is easy to analyze the stability of the NCS and to design controller. On the other hand, this scheme involves heavier computation burden since the controller has to extend the predictive horizon to make it longer then the sum of the maximum of time delays in two channels.

Two schemes for updating the likelihood ratios for the latent fault are also proposed in the current chapter. One is to set up a buffer at the local node to gather measurement data packets to keep them be processed in sequence, i.e., an observation is processed after all other observations are processed, which are sampled by sensors earlier than the observation. This method is conservative and easy to give an analysis of stability. The other scheme is to process the intermittent observations that are in sequence and discard the observations that are out of sequence. Based on this scheme, the NCS with random network-induced time delay is modeled as a NCS with data packet dropout. Xiao et al proposed a peak covariance stability analysis of time-varying Kalman filter with possible packet losses in transmitting measurement outputs to the filter via a packet-based network [208]. It is shown that if the observability index of the discrete-time LTI system under investigation is one, the Kalman filter is peak covariance stable under no additional condition. In the current chapter, updating likelihood ratios of the latent fault with intermittent observations is converted to the least square problem with intermittent observations. The result shows that GLR test with intermittent observations is convergent if the state transfer matrix and the covariance matrices of noise satisfy a proposed condition. However, there is still limitation exists. For example, the latent fault must be a step type function, and the convergence analysis of GLR test with intermittent observations is only for LTI systems.

10.8 Summary

A fault detection and compensation scheme based on likelihood ratios for networked predictive control systems with random network time delay and

clock asynchronism is proposed in this chapter. The networked control system is stabilized by designing a state feedback gain and sets of predictive manipulated variables. The measured outputs are sent back to the local node. The likelihood ratios of fault are computed step by step, and if a fault is detected and identified, the fault estimate is sent to the controller to compensate the fault. Two methods are proposed for the local node to update the estimates. One of them is to process the observations according to the sequence in which the observation packets are sent from the remote node. The other method is to process the observations if they are the newest, and discard the other observations. However, the convergence analysis of the second method is limited to LTI systems. A numerical simulation shows that after the fault is detected and compensated with the proposed scheme, the states estimates converge at their true value again.

References

1. Aktan, B., Bohus, C.A., Crowl, L.A., Shor, M.H.: Distance learning applied to control engineering laboratories. IEEE Transactions on Education 39, 320–326 (1996)
2. Mahdi Alavi, S.M., Walsh, M.J., Hayes, M.J.: Robust distributed active power control technique for IEEE 802.15.4 wireless sensor networks — a quantitative feedback theory approach. Control Engineering Practice 17, 805–814 (2009)
3. Almutairi, N.B., Chow, M.-Y., Tipsuwan, Y.: Network-based controlled dc motor with fuzzy compensation. In: The 27th Annual Conference of the IEEE Industrial Electronics Society, Denver CO., vol. 3, pp. 1844–1849 (2001)
4. Alouani, A.T., Gray, J.E.: Theory of distributed estimation using multiple asynchronous sensors. IEEE Trans. on Aerospace and Electronic Systems 41, 717–722 (2005)
5. Alpcan, T., Basar, T., Dey, S.: A power control game based on outage probabilities for multicell wireless data networks. IEEE Trans. Wireless Communication 5, 890–899 (2006)
6. Azuma, S.I., Sugie, T.: Optimal dynamic quantizers for discrete-valued input control. Automatica 44, 396–406 (2008)
7. Baillieul, J., Antsaklis, P.J.: Control and communication challenges in networked real-time systems. Proceedings of the IEEE 95, 9–28 (2007)
8. Bar-Shalom, Y.: Update with out-of-sequence measurements in tracking: Exact solution. IEEE Transactions on Aerospace and Electronic System 38, 769–778 (2002)
9. Bar-Shalom, Y., Chen, H.: Multisensor track-to-track association for tracks with dependent errors. In: Proceedings of the IEEE CDC, Bahamas, pp. 2674–2679 (2004)
10. Bar-Shalom, Y., Li, X.R., Kirubarajam, T.: Estimation with Application to Tracking and Navigation. John Wiley and Sons, New York (2001)
11. Basseville, M., Benveniste, A., Chou, K.C., Golden, S.A., Nikoukhah, R., Willsky, A.S.: Multiresolutional filtering using wavelet transform. IEEE Trans. on Information Theory 38, 766–784 (1992)
12. Benveniste, A., Nikoukhah, R., Willsky, A.S.: Multiscale system theory. In: Proceeding of the 29th IEEE Conference on Decision and Control, Hawaii, USA, pp. 2484–2487 (1990)

13. Besada-Portas, E., Lopez-Orozco, J.A., Besada, J.A., de la Cruz, J.M.: Multisensor out of sequence data fusion for estimating the state of discrete control systems. IEEE Transactions on Automatic Control 54, 1728–1732 (2009)
14. Bi, Z.: Stabilization of linear systems over networks with quantization and packet dropout. In: 34th Annual Conference of the IEEE-Industrial-Electronics-Society, Orlando, pp. 2951–2954 (2008)
15. Boers, Y., Driessen, H., Zwaga, J.: The modified Riccati equation in target tracking: some recent results. In: International Conference on Information Fusion, Philadelphia, USA, pp. 25–29 (2005)
16. Boukas, E.-K., Xia, Y.: Descriptor discrete-time systems with random abrupt changes: Stability and stabilisation. International Journal of Control 81(8), 1311–1318 (2008)
17. Brockett, R.W., Liberzon, D.: Quantized feedback stabilization of linear systems. IEEE Transactions on Automatic Control 45, 1279–1289 (2000)
18. Bullo, F., Liberzon, D.: Quantized control via locational optimization. IEEE Transactions on Automatic Control 51, 2–13 (2006)
19. Calafiore, G., Abrate, F.: Distributed linear estimation over sensor networks. International Journal of Control 82(5), 868–882 (2009)
20. Carlson, N.A.: Federated square root filter for decentralized parallel processes. IEEE Transactions on Aerospace and Electronic Systems 26, 517–525 (1990)
21. Ceragioli, F., Persis, C.D.: Discontinuous stabilization of nonlinear systems: quantized and switching control. Systems and Control Letters 56, 461–473 (2007)
22. Chan, C.W., Song, H., Zhang, H.Y.: Application of fully decoupled parity equation in fault detection and identification of dc motors. IEEE Transactions on Industrial Electronics 53, 1277–1284 (2006)
23. Chang, K.C., Saha, R.K., Bar-Shalom, Y.: On optimal track-to-track fusion. IEEE Trans. on Aerospace and Electronic Systems 33, 1271–1276 (1997)
24. Chang, K.C., Tian, Z., Mon, S.: Performance evaluation for map state estimate fusion. IEEE Transactions on Aerospace and Electronic Systems 40(2), 706–714 (2004)
25. Che, W., Wang, J., Yang, G.: Quantized H_∞ control for networked control systems with packet dropouts. In: Decision and Control and Chinese Control Conference 2009, pp. 4087–4092 (2009)
26. Chen, J., Patton, R.J.: Robust model-based fault diagnosis for dynamic systems. Kluwer Academic Publishers, Dordrecht (1999)
27. Chen, T.W., Francis, B.: Optimal Sampled-Data Control Systems. Springer, Heidelberg (1995)
28. Chong, C.Y., Chang, K.C.: Architectures and algorithms for track association and fusion. IEEE AES Systems Magazine, 5–13 (2000)
29. Chow, M.Y., Tipsuwan, Y.: Network-based control systems: A tutorial. In: 27th Annu. Conf. IEEE Industrial Electronics Soc., pp. 1593–1602 (2001)
30. Chui, C.K., Chen, G.: Kalman Filtering: with Real-time Applications. Springer, New York (1999)
31. Clark, R.N., Fosth, D.C., Walton, V.M.: Detection instrument malfunctions in control systems. IEEE Transactions on Aerospace and Electronic Systems 11, 465–473 (1975)
32. Costa, O.L.V., Fragoso, M.D., Marques, R.P.: Discrete-Time Markov Jump Linear Systems. Springer, Heidelberg (2005)

33. Coutinho, D.F., Fu, M., de Souza, C.E.: Input and output quantized feedback linear systems. IEEE Transactions on Automatic Control 55, 761–766 (2010)
34. Cushing, M.: Process control across the Internet. In: Chemical Engineering, pp. 80–82 (2000)
35. Munoz de la Pena, D., Christofides, P.D.: Lyapunov-based model predictive control of nonlinear systems subject to data losses. IEEE Transactions on Automatic Control 53(9), 2076–2089 (2009)
36. Deshpande, A.P., Patwardhan, S.C., Narasimhan, S.S.: Intelligent state estimation for fault tolerant nonlinear predictive control. Journal of Process Control 19, 187–204 (2009)
37. Dey, S., Leong, A.S., Evans, J.S.: Kalman filtering with faded measurements. Automatica 45, 2223–2233 (2009)
38. Ding, S.X.: Model-based fault diagnosis techniques-design schemes, algorithms and tools. Springer, Berlin (2008)
39. Edward, W., James, L.: Multisensor Data Fusion. Artech House, Boston (1990)
40. Elia, N., Mitter, S.K.: Stabilization of linear systems with limited information. IEEE Transactions on Automatic Control 46, 1384–1400 (2001)
41. Evans, R., Krishnamurthy, V., Nair, G., Sciacca, L.: Networked sensor management and data rate control for tracking maneuvering targets. IEEE Trans. Signal Processing 53, 1979–1991 (2005)
42. Fabrizio, A., Luciano, A.: Filterbanks design for multisensor data fusion. IEEE Signal Processing Letters 7, 100–103 (2000)
43. Fagnani, F., Zampieri, S.: Quantized stabilization of linear systems: complexity versus performance. IEEE Transactions on Automatic Control 49, 1534–1548 (2004)
44. Fang, H., Ye, H., Zhong, M.: Fault diagnosis of networked control systems. Annual Reviews in Control 31, 55–68 (2007)
45. Fletcher, K.A., Goyal, V.K.: Estimation from lossy sensor data: Jump linear modeling and kalman filtering. In: Proceedings of the 3rd ACM/IEEE International Symposium on Information Processing in Sensor Networks, pp. 251–258 (2004)
46. Francesco, B., Liberzon, D.: Quantized control via locational optimization. IEEE Transactions on Automatic Control 51, 2–13 (2006)
47. Frank, P.M., Ding, X.: Survay of robust residual generation and evaluation method in observer-based fault detection systems. Journal of Process Control 7(6), 403–424 (1997)
48. Frank, P.M., Keller, L.: Sensitivity discriminating observer design for instrument failure detection. IEEE Transactions on Aerospace and Electronic Systems 16, 460–476 (1981)
49. Franklin, J.N.: Matrix Theory. Dover Publications, Mineola (2000)
50. Fridman, E., Dambrine, M.: Control under quantization, saturation and delay: An LMI approach. Automatica 45, 2258–2264 (2009)
51. Fu, M., Xie, L.: The sector bound approach to quantized feedback control. IEEE Transactions on Automatic Control 50, 1698–1711 (2005)
52. Fu, M., Xie, L.: Finite-level quantized feedback control for linear system. IEEE Transactions on Automatic Control 54, 1165–1170 (2009)

53. Gafvert, M.: Modeling the furuta pendulum. In: Lund Institute of Technology, Department of Automatic Control, technical report ISRN LUTFD2/TFRT-7574-SE (1998)
54. Gahinet, P., Apkarian, P.: A linear matrix inequality approach to H_∞ control. International Journal of Robust Nonlinear Control 4, 421–448 (1994)
55. Gao, H., Chen, T.: A new approach quantized feedback control systems. Automatica 44, 534–542 (2008)
56. Gao, H., Chen, T., James, L.: A new delay system approach to network-based control. Automatica 44, 39–52 (2008)
57. Gao, H., Meng, X., Chen, T., Lam, J.: Stabilization of networked control systems via dynamic output-feedback controllers. SIAM J. Control Optim. 48, 3643–3658 (2010)
58. Garcia-Rivera, M., Barreiro, A.: Analysis of networked control systems with drops and variable delays. Automatica 43, 2054–2059 (2007)
59. Ghantasala, S., El-Farra, N.H.: Robust diagnosis and fault-tolerant control of distributed processes over communication networks. International Journal of Adaptive Control and Signal Processing 23, 699–721 (2009)
60. Goktas, F.: Distributed control of systems over communicaiton networks PH. D dissertation. University of Pennsylvania (2000)
61. Guo, Y., Li, S.: Stability and stabilization of discrete-time linear systems over networks with control input quantization. In: Proceedings of the 26th Chinese Control Conference, Zhangjiajie, Hunan, China, pp. 137–140 (2007)
62. Guo, Y., Li, S.: H_∞ control for discrete-time systems with limited communication channel. In: 27th Chinese Control Conference, pp. 160–164 (2008)
63. Gustafsson, F.: Adaptive filtering and change detection. John Wiley and Sons, West Sussex (2000)
64. Halevi, Y., Ray, A.: Integrated communication and control systems: Part 1-analysis. Journal of Dynamic Systems, Measurement, and Control 110, 367–373 (1988)
65. Halley, A., Gauld, P.: Integration where java meets process control. Control and Instrumentation 31, 57–58 (1999)
66. Hayakawa, T., Ishii, H., Tsumura, K.: Adaptive quantized control for linear uncertain discrete-time systems. Automatica 45, 692–700 (2009)
67. Hayakawa, T., Ishii, H., Tsumura, K.: Adaptive quantized control for nonlinear uncertain systems. Systems and Control Letters 58, 625–632 (2009)
68. He, X., Wang, Z., Zhou, D.H.: Robust diagnosis and fault-tolerant control of distributed processes over communication networks. International Journal of Adaptive Control and Signal Processing 23, 737–756 (2009)
69. Henry, D., Zolghadri, A.: Design and analysis of robust residual generators for systems under feedback control. Automatica 41, 251–264 (2005)
70. Hespanha, J.P., Naghshtabrizi, P., Xu, Y.: A survey of recent results in networked control systems. Proceedings of the IEEE 95, 138–162 (2007)
71. Hitz, B.E., Anderson, B.D.O.: Discrete positive-real functions and their application to system stability. Proceedings of the IEE 116(2), 153–155 (1969)
72. Hong, L.: Multiresolutional filtering using wavelet transform. IEEE Trans. on Aerospace and Electronic Systems 29, 769–778 (1993)
73. Hong, S.H.: Scheduling algorithm of data sampling times in the integrated communication and control systems. IEEE Transactions on control systems technology 3, 225–230 (1995)

74. Horn, R.A., Johnson, C.R.: Matrix analysis. The Press Syndicate of the University of Cambridge (1999)
75. Hou, M., Patton, R.J.: An LMI approach to H_-/H_∞ fault detection observers. In: Proceedings of UKACC International Conference on Control, pp. 305–310 (1996)
76. Hu, L., Huang, B., Cao, Y.: Robust digital model predictive control for linear uncertain systems with saturations. IEEE Transactions on Automatic Control 49(5), 792–796 (2004)
77. Hu, S., Yan, W.: Stability of networked control systems under a multiple-packet transmission policy. IEEE Transactions on Automatic Control 53(7), 1706–1711 (2008)
78. Hu, W., Liu, G.-P., Rees, D.: Event-driven networked predictive control. IEEE Transactions on Industrial Electronics 54, 1603–1613 (2007)
79. Huang, D., Nguang, S.K.: Robust fault estimator design for uncertain networked control systems with random time delays: An LMI approach. Information Sciences 180, 465–480 (2010)
80. Huang, J., Wang, Y., Yang, S., Xua, Q.: Robust stability conditions for remote SISO DMC controller in networked control systems. Journal of Process Control 19, 743–750 (2009)
81. Huang, M.Y., Dey, S.: Stability of Kalman filtering with Markovian packet losses. Automatica 43, 598–607 (2007)
82. Li, Z., Jaimoukha, I.M., Papakos, V.: A matrix factorization solution to the H_∞/H_- fault detection problem. Automatica 42, 1907–1912 (2006)
83. IEEE. Special issue on systems and control methods for communication networks. IEEE Transactions on Automatic Control 47 (2002)
84. IEEE. Special issue on networked control systems. IEEE Transactions on Automatic Control 49 (2004)
85. Imer, C.O., Yüksel, S., Basar, T.: Optimal control of LTI systems over unreliable communication links. Automatica 42, 1429–1439 (2006)
86. Ishii, H., Başar, T.: Remote control of LTI systems over networks with state quantization. Systems and Control Letters 54, 15–31 (2005)
87. Izadi, I., Zhao, Q., Chen, T.: An optimal scheme for fast rate fault detection based on multirate sampled data. Journal of Process Control 15, 307–319 (2005)
88. Jaimoukha, I.M., Li, Z., Papakos, V.: A matrix factorization solution to the H_- and H_∞ fault detection problem. Automatica 42(11), 1907–1912 (2006)
89. Kawka, P.A., Alleyne, A.G.: Stability and feedback control of wireless networked systems. In: Proceedings of the American Control Conference, pp. 2953–2959 (2005)
90. Kawka, P.A., Alleyne, A.G.: Robust wireless servo control using a discrete-time uncertain Markovian jump linear model. IEEE Transactions on Control Systems Technology 19, 733–742 (2009)
91. Kim, D.S., Choi, D.H., Mohapara, P.: Real-time scheduling method for networked discrete control systems. Control Engineering Practice 17, 564–570 (2009)
92. Kim, J.G., Krunz, M.M.: Delay analysis of selective repeat ARQ for a Markovian source over a wireless channel. IEEE Transactions on Vehicular Technology 49, 1968–1981 (2000)
93. Kim, T.J., Lee, W.C., Hyun, D.S.: Detection method for open-circuit fault in neutral-point-clamped inverter systems. IEEE Transactions on Industrial Electronics 56, 2754–2763 (2009)

94. Kothare, M.V., Balakrishnan, V., Morari, M.: Robust constrained model predictive control using linear matrix inequalities. Automatica 32, 1361–1379 (1996)
95. Leininger, G.G.: Model degradation effects on sensor failure detection. In: Proceedings of the 1981 Joint Amer. Control Conf., pages Paper FP–3A, Charlottesville, VA (1981)
96. Li, D., Fei, S.: Robust stabilization for delta operator based systems. Fuzzy Systems and Mathematics 19(2), 140–145 (2005)
97. Li, X., Zhou, K.: A time domain approach to robust fault detection of linear time-varying systems. Automatica 45, 94–102 (2009)
98. Liang, J., Wang, Z., Liu, Y., Liu, X.: Global synchronization control of general delayed discrete-time networks with stochastic coupling and disturbances. IEEE Transactions on Systems, Man, and Cybernetics: Part B 38, 1073–1083 (2008)
99. Liang, Y., Chen, T.W., Pan, Q.: Multi-rate optimal state estimation. International Journal of Control 82(11), 2059–2076 (2009)
100. Liberzon, D.: Hybrid feedback stabilization of systems with quantized signals. Automatica 39, 1543–1554 (2003)
101. Liberzon, D.: Input-to-state stabilization of linear systems with quantized state measurements. IEEE Transactions on Automatic Control 52, 767–781 (2007)
102. Limon, D., Alamo, T., Alvarado, I., Camacho, E.F.: MPC for tracking piecewise constant references for constrained linear systems. Automatica 44(9), 2382–2387 (2008)
103. Liu, B.S., Yan, L.P., Shi, H.: State fusion estimation with missing measurements. In: American Control Conference, New York City, USA, pp. 899–902 (2007)
104. Liu, B.S., Zhou, D.H.: The modeling and estimation of asynchronous multirate multisensor dynamic systems. Aerospace Science and Technology 10, 63–71 (2006)
105. Liu, G.-P., Mu, J., Rees, D.: Networked predictive control of systems with random communication delays. In: Proceedings of UKACC International Conference on Control, UK, p. ID–015 (2004)
106. Liu, G.-P., Mu, J., Rees, D., Chai, S.C.: Design and stability of networked control systems with random communication time delay using the modified MPC. International Journal of Control 79, 288–297 (2006)
107. Liu, G.-P., Xia, Y., Chen, J., Rees, D., Hu, W.: Networked predictive control of systems with random network delays in both forward and feedback channels. IEEE Transactions on Industrial Electronics 54, 1282–1297 (2007)
108. Liu, G.-P., Xia, Y., Rees, D., Hu, W.: Design and stability criteria of networked predictive control systems with random network delay in the feedback channel. IEEE Transaction on Systemsms, man and Cybernetic-Part C: Applications and Reviews 37, 173–184 (2007)
109. Liu, G.-P., Xia, Y., Rees, D.: Networked predictive control of systems with random network with delays in both forward and feedback channels. In: Proceedings of the 16th IFAC World Congress, Prague (2005)
110. Liu, G.-P., Xia, Y., Rees, D., Hu, W.: Design and stability criteria of networked predictive control systems with random network delay in the feedback channel. IEEE Transaction on Systems, Man, and Cybernetics-Part C 37, 173–184 (2007)

111. Liu, X., Liu, G.-P., Xia, Y., Rees, D.: Stability criteria for a class of MIMO networked control systems with network constraints. In: Proceedings of the 2009 IEEE International Conference on Systems, Man, and Cybernetics, San Antonio, pp. 4853–4857 (2009)
112. Liu, X., Liu, G.-P., Xia, Y., Rees, D.: Stability criteria and output feedback controller design for MIMO networked control systems with network constraints. In: Proceedings of the 22nd Chinese Control and Decision Conference (2010)
113. Lu, L., Xie, L., Fu, M.: Optimal control of networked systems with limited communication: a combined heuristic and convex optimization approach. In: 42nd IEEE Conf. Decision and Control, Maui, Hawaii USA, pp. 1194–1199 (2003)
114. Luck, R., Ray, A.: Experimental verification of a delay compensation algorithm for integrated communication and control systems. International Journal of Control 59, 1357–1372 (1994)
115. Magni, L., Scattolini, R.: Model predictive control of continuous-time nonlinear systems with piecewise constant control. IEEE Transactions on Automatic Control 49(6), 900–906 (2004)
116. Mahmoud, M., AL-Sunni, F., Xia, Y.: Interconnected switched discrete-time systems: Robust stability and stabilization. IMA Journal of Mathematical Control and Information (2010)
117. Mahmoud, M., Shi, P.: Methodologies for control of jump time-delay systems. Kluwer Academic Publishers, Dordrecht (2003)
118. Mallick, M., Coraluppi, S., Carthel, C.: Advances in asynchronous and decentralized estimation. In: Proceedings of the 2001 IEEE Aerospace Conference, USA, pp. 1873–1888 (2001)
119. Matveev, A.S., Savkin, A.V.: An analogue of Shannon information theory for networked control systems: State estimation via a noisy discrete channel. In: 43rd IEEE Conference Decision and Control, CDC, vol. 4, pp. 4485–4490 (2004)
120. Mironovski, L.A.: Function diagnosis of linear dynamic systems. Automn Remote Control 41, 1122–1143 (1980)
121. Montestruque, L.A., Antsaklis, P.J.: On the model-based control of networked systems. Automatica 39, 1837–1843 (2003)
122. Montestruque, L.A., Antsaklis, P.J.: Static and dynamic quantization in model-based networked control systems. International Journal of Control 80, 87–101 (2007)
123. Mostofi, Y., Murray, R.M.: Kalman filtering over wireless fading channelshow to handle packet drop. International Journal of Robust and Nonlinear Control 19, 1993–2015 (2008)
124. Mudumbai, R., Barriac, G., Madhow, U.: On the feasibility of distributed beamforming in wireless networks. IEEE Transactions on Wireless Communications 6, 1754–1763 (2007)
125. Nair, G.N., Evans, R.J.: Stabilizability of stochastic linear systems with finite feedback data rates. SIAM Journal on Control and Optimization 43, 413–436 (2004)
126. Nair, G.N., Fagnani, F., Zampieri, S., Evans, R.J.: Feedback control under data rate constraints: an overview. Proceedings of the IEEE 95, 108–137 (2007)
127. Naylor, J.: Online data transfer standard. The Chemical Engineers 24 (2002)

128. Necoara, I., van den Boom, T.J.J., Schutter, B.D., Hellendoorn, H.: Stabilization of max-plus-linear systems using model predictive control: The unconstrained case. Automatica 44(4), 971–981 (2008)
129. Nemoto, Y., Hamamoto, N., Suzuki, R., Ikegami, T., Hashimoto, Y., Ide, T., Ohta, K., Mansfield, G., Kato, N.: Construction and utilizaiton experiment of multimedia education system using satelite ETS-V and internet. IEICE Transaction on Information and Systems 80, 162–169 (1997)
130. Nilsson, J.: Real-time control systems with delays. Ph.D. dissertation, Lund Institute of Technology (1998)
131. Nilsson, J., Bernhardsson, B., Wittenmark, B.: Stochastic analysis and control of real-time systems with random time delays. Automatica 34, 57–64 (1998)
132. Niu, Y., Jia, T., Wang, X., Yang, F.: Output-feedback control design for NCSs subject to quantization and dropout. Information Sciences 179, 3804–3813 (2009)
133. Overstreet, J.W., Tzes, A.: An internet-based real-time control engineering laboratory. IEEE Control Systems Magazine 19, 19–34 (1999)
134. Patton, R.J., Chen, J.: Proceedings of IFAC Symposium on Fault Detection, Supervision and Safty for Technical Processes. In: SAFEPROSS 1997, Pergamon (1998)
135. Patwardhan, S.C., Manuja, S., Narasimhan, S., Shah, S.L.: From data to diagnosis and control using generalized orthonormal basis filters, part II: Model predictive and fault tolerant control. Journal of Process Control 16, 157–175 (2006)
136. Pena, D.M., Christofides, P.D.: Lyapunov-based model predictive control of nonlinear systems subject to data losses. IEEE Transactions on Automatic Control 53(9), 2076–2089 (2008)
137. Peng, C., Tian, Y.: Networked H_∞ control of linear systems with state quantization. Information Sciences 177, 5763–5774 (2007)
138. Peng, C., Yue, D., Gu, Z., Xia, F.: Sampling period scheduling of networked control systems with multiple-control loops. Mathematics and Computers in Simulation 79(5), 1502–1511 (2009)
139. Persis, C.D.: Robust stabilization of nonlinear systems by quantized and ternary control. Systems and Control Letters 58, 602–608 (2009)
140. Plarre, K., Bullo, F.: On Kalman filtering for detectable systems with intermittent observations. IEEE Transactions on Automatic Control 54, 386–390 (2009)
141. Ploplys, A.: Wireless feedback control of mechanical systems. Masters Thesis, Department of Mechanical Engineering, University of Illinois, Champaign, IL (2003)
142. Qiang, L., Lemmon, M.D.: Stability of quantized control systems under dynamic bit assignment. IEEE Transactions on Automatic Control 50, 734–740 (2005)
143. Quevedo, D.E., Stergaard, J.: Quantized predictive control over erasure channels. In: Decision and Control and Chinese Control Conference, pp. 2076–2081 (2009)
144. Raisch, J.: Control of continuous plants by symbolic output feedback. In: Hybrid Systems II. lecture notes in computer science, vol. 999, pp. 370–390 (2008)
145. Ranasingha, M.C., Murthi, M.N., Premaratne, K., Fan, X.: Transmission rate allocation in multisensor target tracking over a shared network. IEEE Transactions on Systems, Man, and Cybernetics: Part B 39, 348–362 (2009)

146. Richter, H., Misawa, E.A.: Stability of discrete-time systems with quantized input and state measurements. IEEE Transactions on Automatic Control 48, 1453–1458 (2003)
147. Ryu, M., Hong, S.: Toward automatic synthesis of schedulable real-time controllers. Integrated Computer-Aided Engineering 5, 261–277 (1988)
148. Edwards, D.W., Yang, S., Chen, X., Alty, J.L.: Design issues and implementation of Internet based process control. Control Engineering Practices 11(6), 709–720 (2003)
149. Sauter, D.: Robust fault diagnosis of networked control systems. International Journal of Adaptive Control and Signal Processing 23, 722–736 (2009)
150. Sauter, D., Hamelin, F.: Frequency domain optimization for robust fault detection and isolation in dynamic systems. IEEE Transaction on Automatic Control 44(4), 878–882 (1999)
151. Savkin, A.V.: Analysis and synthesis of networked control systems: Topological entropy, observability, robustness and optimal control. Automatica 42, 51–62 (2006)
152. Savkin, A.V.: Detectability and output feedback stabilizability of nonlinear networked control systems. IEEE Transactions on Automatic Control 52, 730–735 (2007)
153. Savkin, A.V., Petersen, I.R.: Set-valued state estimation via a limited capacity communication channel. IEEE Transactions on Automatic Control 48, 676–680 (2003)
154. Schenato, L.: Optimal sensor fusion for distributed sensors subject to random delay and packet loss. In: Proceedings of the 46th IEEE Conference on Decision and Control, pp. 1547–1552 (2007)
155. Schenato, L.: Optimal estimation in networked control systems subject to random delay and packet drop. IEEE Transactions on Automatic Control 53(5), 1311–1317 (2008)
156. Schenato, L.: To zero or to hold control inputs with lossy links? IEEE Transactions on Automatic Control 54, 1099–1105 (2009)
157. Scholte, E., Campbell, M.E.: Robust nonlinear model predictive control with partial state information. IEEE Transactions on Control Systems Technology 16(4), 636–651 (2008)
158. Scokaert, P.O.M., Mayne, D.Q.: Min-max feedback model predictive control for constrained linear systems. IEEE Transactions on Automatic Control 43(8), 1136–1142 (1998)
159. Scokaert, P.O.M., Mayne, D.Q., Rawlings, J.B.: Suboptimal model predictive control (feasibility implies stability). IEEE Transactions on Automatic Control 44(3), 648–654 (1999)
160. Seiler, P., Raja, S.: An H_∞ approach to networked control. IEEE Transactions on Automatic Control 50, 356–364 (2005)
161. Seiler, P., Sengupta, R.: An H_∞ approach to networked control. IEEE Trans. Autom. Control 50, 356–364 (2005)
162. Seto, D., Lehoczky, J.P., Sha, L., Shin, K.G.: On task schedulability in real-time control systems. In: Proceedings of the 17th IEEE Real-Time Systems Symposium, Washington, DC, USA, pp. 13–21 (1996)
163. Shen, X.J., Song, E.B., Zhu, Y.M., Luo, Y.T.: Globally optimal distributed Kalman fusion with local out-of-sequence-measurement updates. IEEE Transactions on Automatic Control 54, 1928–1934 (2009)

164. Shen, X.J., Song, E.B., Zhu, Y.M., Luo, Y.T.: Optimal centralized update with multiple local out-of-sequence measurements. IEEE Transactions on Singal Processing 57, 1551–1562 (2009)
165. Shi, L.: Kalman filtering over graphs: Theory and applications. IEEE Transactions on Automatic Control 54(9), 2230–2234 (2009)
166. Shi, L., Xie, L.H., Murray, R.M.: Kalman filtering over a packet-delaying network: A probabilistic approach. Automatica 45, 2134–2140 (2009)
167. Simon, D.: Optimal State Estimation: Kalman, H_∞, and Nonlinear Approaches. John Wiley and Sons, New Jersey (2006)
168. Sinha, A., Chen, H., Danu, D.G., Kirubarajan, T., Farooq, M.: Estimation and decision fusion: A survey. Neurocomputing 71, 2650–2656 (2008)
169. Sinopoli, B., Schenato, L., Franceschetti, M., Poolla, K., Jordan, M.I., Sastry, S.S.: Kalman filtering with intermittent observations. IEEE Trans. on Automatic Control 49, 1453–1464 (2004)
170. Sinopoli, B., Schenato, L., Franceschetti, M., Poolla, K., Sastry, S.: An LQG optimal linear controller for control systems with packet losses. In: 44th IEEE Conf. Decision Control/Eur. Control Conf., pp. 458–463 (2005)
171. Smith, C.S., Seiler, P.: Estimation with lossy measurements: Jump estimator for jump systems. IEEE Transaction on Automatic Control 48, 2163–2171 (2003)
172. Speranzon, A., Fischione, C., Johansson, K.H., Sangiovanni-Vincentelli, A.L.: A distributed minimum variance estimator for sensor networks. IEEE Journal on Selected Areas in Communications 26(4), 609–621 (2008)
173. Subhrakanti, D., Alex, S.L., Jamie, S.E.: Kalman filtering with faded measurements. Automatica 45 (2009)
174. Sun, S.L., Deng, Z.L.: Multi-sensor optimal information fusion Kalman filter. Automatica 403, 1017–1023 (2004)
175. Tabbara, M., Nesic, D.: Input-output stability of networked control systems with stochastic protocols and channels. IEEE Transactions on Automatic Control 53, 1160–1175 (2008)
176. Tan, C.P., Crusca, F., Aldeen, M.: Extended results on robust state estimation and fault detection. Automatica 44, 2027–2033 (2008)
177. Tarn, T.J., Xi, N.: Planning and control of internet-based teleoperation. In: Proceedings of SPIE: Telemanipulator and Telepresence Technologies V, Boston, MA, vol. 3524, pp. 189–193 (1998)
178. Tatikonda, S., Mitter, S.: Control under communication constraints. IEEE Transactions on Automatic Control 49, 1056–1068 (2004)
179. Taylor, K., Dalton, B.: Internet robots: A new robotics niche. IEEE Robotics and Automation Magazine 7, 27–34 (2000)
180. Thomopoulos, S.C.A., Zhang, L.: Distributed filtering with random sampling and delay. In: Proceedings of the American Control Conference, Chicago, pp. 1327–1331 (2000)
181. Tian, E., Yue, D., Peng, C.: Quantized output feedback control for networked control systems. Information Sciences 178, 2734–2749 (2008)
182. Tian, E., Yue, D., Zhao, X.: Quantised control design for networked control systems. IET Control Theory and Applications 1, 1693–1699 (2007)
183. Tipsuwan, Y., Chow, M.Y.: Gain adaptation of networked mobile robot to compensate QoS deterioration. In: The 28th Annual Conference of the IEEE Industrial Electronics Society (IECON 2002), Spain, vol. 4, pp. 3146–3151 (2002)

184. Tortora, G., Kouvaritakis, B., Clarke, D.W.: Simultaneous optimization of tracking performance and accommodation of sensor faults. Journal of Control 75, 163–176 (2002)
185. Tsumura, K., Ishii, H., Hoshina, H.: Tradeoffs between quantization and packet loss in networked control of linear systems. Automatica 45, 2963–2970 (2009)
186. Vaccarini, M., Longhi, S., Katebi, M.R.: Unconstrained networked decentralized model predictive control. Journal of Process Control 19, 328–339 (2009)
187. Wada, N., Saito, K., Saeki, M.: Model predictive control for linear parameter varying systems using parameter dependent Lyapunov function. IEEE Transactions on Circuits and Systems II: Express Briefs 53(12), 1446–1450 (2006)
188. Walsh, G.C., Beldiman, O., Bushnell, L.: Asymptotic behavior of nonlinear networked control systems. IEEE Trans. Automatic Control 46, 1093–1097 (2001)
189. Walsh, G.C., Ye, H., Bushnell, L.: Stability analysis of networked control systems. In: Proceedings of the 1999 American Control Conference, vol. 4, pp. 2876–2880 (1999)
190. Wang, H., Yang, G.-H.: A finite frequency domain approach to fault detection for linear discrete-time systems. International Journal of Control 81(7), 1162–1171 (2008)
191. Wang, H., Yang, G.-H.: A finite frequency domain approach to fault detection observer design for linear continuous-time systems. Asian Journal of Control 10(5), 1–10 (2008)
192. Wang, Y., Ding, S.X., Ye, H., Wei, L., Zhang, P., Wang, G.: Fault detection of networked control systems with packet based periodic communication. International Journal of Adaptive Control and Signal Processing 23, 682–698 (2009)
193. Wang, Y., Ye, H., Ding, S.X., Wang, G., Zhou, D.H.: Residual generation and evaluation of networked control systems subject to random packet dropout. Automatica 45(10), 2427–2434 (2009)
194. Wang, Z.D., Ho, D.W.C., Liu, X.H.: Variance-constrained filtering for uncertain stochastic systems with missing measurements. IEEE Trans. on Automatic Control 48, 1254–1258 (2003)
195. Wen, C.L., Zhou, D.H.: Multiscale Estimation Theory and Application. Publishing House of Tsinghua University, Beijing (2002)
196. Willsky, A.S., Jones, H.L.: A generalized likelihood ratio approach to the detection and estimation of jumps in linear systems. IEEE Transaction on Automatic Control 21, 108–112 (1976)
197. Wong, W.S., Brockett, R.W.: Systems with finite communication bandwidth constraints. II. stabilization with limited information feedback. IEEE Transactions on Automatic Control 44, 1049–1053 (1999)
198. Xia, Y., Chen, J., Liu, G.-P., Rees, D.: Stability analysis of networked predictive control systems with random network delay. In: 2007 IEEE International Conference on Networking, Sensing and Control, Longdon, pp. 815–820 (2007)
199. Xia, Y., Chen, J., Zhou, L.: Networked control systems with different control inputs. In: Chinese Control Conference, Zhangjiajie, pp. 539–543 (2007)
200. Xia, Y., Fu, M., Liu, B., Liu, G.-P.: Design and performance analysis of networked control systems with random delay. Journal of Systems Engineering and Electronics 20, 807–822 (2009)

201. Xia, Y., Fu, M., Shi, P.: Analysis and Synthesis of Dynamical Systems with Time-Delays. Springer, Heidelberg (2009)
202. Xia, Y., Liu, G.-P., Fu, M., Rees, D.: Predictive control of networked systems with random delay and data dropout. IET Control Theory Applications 3, 1476–1486 (2009)
203. Xia, Y., Liu, G.-P., Rees, D.: Predictive control of networked systems with random delay and data dropout. In: 2006 IEEE International Conference on Networking, Sensing and Control, Ft. Lauderdale, Florida, USA, pp. 643–648 (2006)
204. Xia, Y., Liu, G.-P., Shi, P., Chen, J., Rees, D.: Robust constrained model predictive control based on parameter-dependent lyapunov functions. Circuits Syst. Signal Process 27(4), 429–446 (2008)
205. Xia, Y., Shang, J., Chen, J., Liu, G.-P.: Data fusion over network. In: 27th Chinese Control Conference, pp. 452–456 (2008)
206. Xia, Y., Shang, J., Chen, J., Liu, G.-P.: Networked data fusion with packet losses and variable delays. IEEE Transactions on Systems, Man, and Cybernetics: Part B 39, 1107–1120 (2009)
207. Xia, Y., Zhu, Z., Mahmoud, M.: H_2 control for networked control systems with Markovian data losses and delays. ICIC Express Letters 3(3), 271–276 (2009)
208. Xiao, N., Xie, L., Fu, M.: Kalman filtering over unreliable communication networks with bounded Markovian packet dropouts. International Journal of Robust and Nonlinear Control 19, 1770–1786 (2009)
209. Xiao, N., Xie, L.H., Fu, M.Y.: Kalman filtering over unreliable communication networks with bounded Markovian packet dropouts. International Journal of Robust and Nonlinear Control 19, 1770–1786 (2009)
210. Xiong, J., Lam, J.: Stabilization of linear systems over networks with bounded packet loss. Automatica 43, 80–87 (2007)
211. Yan, L.P., Liu, B.S., Zhou, D.H.: An asynchronous multirate multisensor information fusion algorithm. IEEE Trans. on Aerospace and Electronic Systems 43, 1135–1146 (2007)
212. Yang, L., Guan, X., Luo, X., Ye, C.: The high performance controller design for networked control systems with multi-packet transmission. In: 27th Chinese Control Conference, pp. 511–515 (2008)
213. Yang, S.H., Chen, X., Edwards, D.W., Alty, J.L.: Design issues and implementation of internet based process control. Control Engineering Practices 11, 709–720 (2003)
214. Ye, H., Ding, S.X.: Fault detection of networked control systems with network-induced delay. In: Proceedings of the 8th International Conference on Control, Automation, Robotics and Vision (ICARCV 2004), pp. 654–659 (2004)
215. Ye, H., Ding, S.X., Wang, G.: Integrated design of fault detection systems in time-frequency domain. IEEE Transactions on Automatic Control 47(2), 384–390 (2002)
216. Ye, H., Walsh, G.C., Bushnell, L.: Real-time mixed-traffic wireless networks. IEEE Transactions on Industrial Electronics 48, 883–890 (2001)
217. Ye, H., Zhang, P., Ding, S.X., Wang, G.: A time-frequency domain fault detection approach based on parity ralation and wavelet transform. In: Proceedings of the 39th IEEE Conference on Control and Decision (IEEE CDC 2000), pp. 4156–4161 (2000)

218. You, K., Xie, L.: Minimum data rate for mean square stabilization of discrete LTI systems over lossy channels. IEEE Transactions on Automatic Control (2010)
219. Yu, M., Wang, L., Xie, G., Chu, T.: Stabilization of networked control systems with data packet dropout via switched system approach. In: IEEE Int. Symp. Comput. Aided Control Syst. Design, pp. 362–367 (2004)
220. Yue, D., Han, Q., Lam, J.: Network-based robust H_∞ control of systems with uncertainty. Automatica 41, 999–1007 (2005)
221. Yue, D., Han, Q., Peng, C.: State feedback controller design of networked control systems. IEEE Trans. Circuits Syst. II, Exp. Briefs 51, 640–644 (2004)
222. Yue, D., Lam, J., Wang, Z.: Persistent disturbance rejection via state feedback for networked control systems. Chaos, Solitons and Fractals 40, 382–391 (2009)
223. Yue, D., Peng, C., Tang, G.: Guaranteed cost control of linear systems over networks with state and input quantizations. IEE Proceedings: Control Theory and Applications 153, 658–664 (2006)
224. Zhang, J., Xia, Y.: Design of H_∞ fuzzy controllers for nonlinear systems with random data dropouts. Optimal Control, Applications and Methods (2010)
225. Zhang, L., Shi, Y., Chen, T.: A new method for stabilization of networked control systems with random delays. IEEE Transaction on Automatic Control 50, 1177–1181 (2005)
226. Zhang, L., Wu, X.L., Pan, Q., Zhang, H.C.: Multiresolution modeling and estimation of multisensor data. IEEE Trans. on Signal Processing 52, 3170–3182 (2004)
227. Zhang, P., Ding, S.X.: An integrated trade-off design of observer based fault detection systems. Automatica 44, 1886–1894 (2008)
228. Zhang, P., Ding, S.X., Wang, G.Z., Zhou, D.H.: A frequency domain approach to fault detection in sampled-data systems. Automatica 39(7), 1303–1307 (2003)
229. Zhang, W., Branicky, M.S., Phillips, S.M.: Stability of networked control systems. IEEE Control Syst. Mag. 21, 84–99 (2001)
230. Zhang, W., Yu, L.: Output feedback stabilization of networked control systems with packet dropouts. IEEE Transactions on Automatic Control 52, 1705–1710 (2007)
231. Zhang, Y., Chen, Y., Sheng, J., Hesketh, T.: Fault detection and diagnosis of networked control system. International Journal of Systems Science 39, 1017–1024 (2008)
232. Zhang, Y., Li, S.: Networked model predictive control based on neighbourhood optimization for serially connected large-scale processes. Journal of Process Control 17, 37–50 (2007)
233. Zhang, Y., Meng, Q.: Stability of networked control system with quantization. In: Decision and Control and Chinese Control Conference, pp. 559–564 (2009)
234. Zhang, Y., Qin, S.J.: Adaptive actuator fault compensation for linear systems with matching and unmatching uncertainties. Journal of Process Control 19, 985–990 (2009)
235. Zhao, Y.B., Liu, G.-P., Rees, D.: A predictive control-based approach to networked Hammerstein systems: Design and stability analysis. IEEE Transactions on Systems, Man, and Cybernetics: Part B 38, 700–708 (2008)

236. Zhivoglyadov, P.V., Middleton, R.H.: Networked control design for linear systems. Automatica 39, 743–750 (2003)
237. Zhou, B., Duan, G., Lam, J.: On the absolute stability approach to quantized feedback control. Automatica 46, 337–346 (2010)
238. Zhou, L., Lu, G.: Detection and stabilization for discrete-time descriptor systems via a limited capacity communication channel. Automatica 45, 2272–2277 (2009)
239. Zhu, X., Yang, G.: New H_∞ controller design method for networked control systems with quantized state feedback. In: American Control Conference Hyatt Regency Riverfront, St. Louis, MO, USA (2009)

Index

Lecture Notes in Control and Information Sciences

Edited by M. Thoma, F. Allgöwer, M. Morari

Further volumes of this series can be found on our homepage:
springer.com

Vol. 409: Xia, Y., Fu, M., Liu, G.-P.;
Analysis and Synthesis of
Networked Control Systems
198 p. 2011 [978-3-642-17924-2]

Vol. 408: Richter, J.H.;
Reconfigurable Control of
Nonlinear Dynamical Systems
291 p. 2011 [978-3-642-17627-2]

Vol. 407: Lévine, J., Müllhaupt, P.:
Advances in the Theory of Control,
Signals and Systems with
Physical Modeling
380 p. 2010 [978-3-642-16134-6]

Vol. 406: Bemporad, A., Heemels, M.,
Johansson, M.:
Networked Control Systems
appro. 371 p. 2010 [978-0-85729-032-8]

Vol. 405: Stefanovic, M., Safonov, M.G.:
Safe Adaptive Control
appro. 153 p. 2010 [978-1-84996-452-4]

Vol. 404: Giri, F.; Bai, E.-W. (Eds.):
Block-oriented Nonlinear System Identification
425 p. 2010 [978-1-84996-512-5]

Vol. 403: Tóth, R.;
Modeling and Identification of
Linear Parameter-Varying Systems
319 p. 2010 [978-3-642-13811-9]

Vol. 402: del Re, L.; Allgöwer, F.;
Glielmo, L.; Guardiola, C.;
Kolmanovsky, I. (Eds.):
Automotive Model Predictive Control
284 p. 2010 [978-1-84996-070-0]

Vol. 401: Chesi, G.; Hashimoto, K. (Eds.):
Visual Servoing via Advanced
Numerical Methods
393 p. 2010 [978-1-84996-088-5]

Vol. 400: Tomás-Rodríguez, M.;
Banks, S.P.:
Linear, Time-varying Approximations
to Nonlinear Dynamical Systems
298 p. 2010 [978-1-84996-100-4]

Vol. 399: Edwards, C.; Lombaerts, T.;
Smaili, H. (Eds.):
Fault Tolerant Flight Control
appro. 350 p. 2010 [978-3-642-11689-6]

Vol. 398: Hara, S.; Ohta, Y.;
Willems, J.C.; Hisaya, F. (Eds.):
Perspectives in Mathematical System
Theory, Control, and Signal Processing
appro. 370 p. 2010 [978-3-540-93917-7]

Vol. 397: Yang, H.; Jiang, B.;
Cocquempot, V.:
Fault Tolerant Control Design for
Hybrid Systems
191 p. 2010 [978-3-642-10680-4]

Vol. 396: Kozlowski, K. (Ed.):
Robot Motion and Control 2009
475 p. 2009 [978-1-84882-984-8]

Vol. 395: Talebi, H.A.; Abdollahi, F.;
Patel, R.V.; Khorasani, K.:
Neural Network-Based State
Estimation of Nonlinear Systems
appro. 175 p. 2010 [978-1-4419-1437-8]

Vol. 394: Pipeleers, G.; Demeulenaere, B.;
Swevers, J.:
Optimal Linear Controller Design for
Periodic Inputs
177 p. 2009 [978-1-84882-974-9]

Vol. 393: Ghosh, B.K.; Martin, C.F.;
Zhou, Y.:
Emergent Problems in Nonlinear
Systems and Control
285 p. 2009 [978-3-642-03626-2]

Vol. 392: Bandyopadhyay, B.;
Deepak, F.; Kim, K.-S.:
Sliding Mode Control Using Novel Sliding
Surfaces
137 p. 2009 [978-3-642-03447-3]

Vol. 391: Khaki-Sedigh, A.; Moaveni, B.:
Control Configuration Selection for
Multivariable Plants
232 p. 2009 [978-3-642-03192-2]

Vol. 390: Chesi, G.; Garulli, A.; Tesi, A.; Vicino, A.: Homogeneous Polynomial Forms for Robustness Analysis of Uncertain Systems 197 p. 2009 [978-1-84882-780-6]

Vol. 389: Bru, R.; Romero-Vivó, S. (Eds.): Positive Systems 398 p. 2009 [978-3-642-02893-9]

Vol. 388: Jacques Loiseau, J.; Michiels, W.; Niculescu, S-I.; Sipahi, R. (Eds.): Topics in Time Delay Systems 418 p. 2009 [978-3-642-02896-0]

Vol. 387: Xia, Y.; Fu, M.; Shi, P.: Analysis and Synthesis of Dynamical Systems with Time-Delays 283 p. 2009 [978-3-642-02695-9]

Vol. 386: Huang, D.; Nguang, S.K.: Robust Control for Uncertain Networked Control Systems with Random Delays 159 p. 2009 [978-1-84882-677-9]

Vol. 385: Jungers, R.: The Joint Spectral Radius 144 p. 2009 [978-3-540-95979-3]

Vol. 384: Magni, L.; Raimondo, D.M.; Allgöwer, F. (Eds.): Nonlinear Model Predictive Control 572 p. 2009 [978-3-642-01093-4]

Vol. 383: Sobhani-Tehrani E.; Khorasani K.; Fault Diagnosis of Nonlinear Systems Using a Hybrid Approach 360 p. 2009 [978-0-387-92906-4]

Vol. 382: Bartoszewicz A.; Nowacka-Leverton A.; Time-Varying Sliding Modes for Second and Third Order Systems 192 p. 2009 [978-3-540-92216-2]

Vol. 381: Hirsch M.J.; Commander C.W.; Pardalos P.M.; Murphey R. (Eds.) Optimization and Cooperative Control Strategies: Proceedings of the 8th International Conference on Cooperative Control and Optimization 459 p. 2009 [978-3-540-88062-2]

Vol. 380: Basin M. New Trends in Optimal Filtering and Control for Polynomial and Time-Delay Systems 206 p. 2008 [978-3-540-70802-5]

Vol. 379: Mellodge P.; Kachroo P.; Model Abstraction in Dynamical Systems: Application to Mobile Robot Control 116 p. 2008 [978-3-540-70792-9]

Vol. 378: Femat R.; Solis-Perales G.; Robust Synchronization of Chaotic Systems Via Feedback 199 p. 2008 [978-3-540-69306-2]

Vol. 377: Patan K. Artificial Neural Networks for the Modelling and Fault Diagnosis of Technical Processes 206 p. 2008 [978-3-540-79871-2]

Vol. 376: Hasegawa Y. Approximate and Noisy Realization of Discrete-Time Dynamical Systems 245 p. 2008 [978-3-540-79433-2]

Vol. 375: Bartolini G.; Fridman L.; Pisano A.; Usai E. (Eds.) Modern Sliding Mode Control Theory 465 p. 2008 [978-3-540-79015-0]

Vol. 374: Huang B.; Kadali R. Dynamic Modeling, Predictive Control and Performance Monitoring 240 p. 2008 [978-1-84800-232-6]

Vol. 373: Wang Q.-G.; Ye Z.; Cai W.-J.; Hang C.-C. PID Control for Multivariable Processes 264 p. 2008 [978-3-540-78481-4]

Vol. 372: Zhou J.; Wen C. Adaptive Backstepping Control of Uncertain Systems 241 p. 2008 [978-3-540-77806-6]

Vol. 371: Blondel V.D.; Boyd S.P.; Kimura H. (Eds.) Recent Advances in Learning and Control 279 p. 2008 [978-1-84800-154-1]

Vol. 370: Lee S.; Suh I.H.; Kim M.S. (Eds.) Recent Progress in Robotics: Viable Robotic Service to Human 410 p. 2008 [978-3-540-76728-2]

Vol. 369: Hirsch M.J.; Pardalos P.M.; Murphey R.; Grundel D. Advances in Cooperative Control and Optimization 423 p. 2007 [978-3-540-74354-5]

Vol. 368: Chee F.; Fernando T. Closed-Loop Control of Blood Glucose 157 p. 2007 [978-3-540-74030-8]